The strecker reaction of benzaldehyde, amines and cyanide: some mechanistic and synthetic studies

Christophe Grosjean

The Strecker Reaction of Benzaldehyde, Amines and Cyanide: Some Mechanistic and Synthetic Studies

Christophe Grosjean B.Sc.(Hons)

(Ustinov College)

Thesis submitted for the qualification Doctor of Philosophy

University of Durham

Department of Chemistry

October 2004

Contents

Abstract

The Strecker reaction involves the formation of aminonitriles by the reaction of an aldehyde with an amine in the presence of cyanide ions. In this work kinetic, equilibrium and synthetic measurements have been made using benzaldehyde, or 4-nitrobenzaldehyde, as the aldehyde and benzylamine or allylamine as the amine.

A side reaction involves the formation of a cyanohydrin from benzaldehyde and cyanide ion. The equilibria involved in the reaction and their pH dependence have been examined. For comparison values for the equilibrium constants for the reaction of benzaldehyde with sulfite are also reported. The syntheses and structural characterisations of N-benzylidene benzylamine, N-benzylidene allylamine and N-(4-nitro)-benzylidene benzylamine are reported.

A major part of the thesis is concerned with the kinetics and equilibria involved in the reaction of N-benzylidene benzylamine and N-benzylidene allylamine with cyanide in aqueous solutions. The results are compatible with the rate-determining step involving reaction of the corresponding iminium ions with cyanide ions. The pH profile is bell-shaped with a plateau between pH = 6.5 and 8.5 defined by the pK_a values of the iminium ions and hydrogen cyanide. pK_a values of 6.14 ± 0.1 and 6.05 ± 0.1 have been calculated for N-benzylidene benzyliminium and N-benzylidene allyliminium ions respectively. Rate constants for reaction of cyanide ion with these cations are 6.70×10^3 and 1.03×10^4 $dm^3mol^{-1}s^{-1}$ respectively. The hydrolysis reactions of imines to yield benzaldehyde have also been quantitatively investigated. The relatively low reactivity found for those iminium ions may be attributed to charge delocalisation in the aromatic ring.

An important aspect of the Strecker reaction is the possibility of forming enantiomerically pure products. The asymmetric catalysis by Salen metal complexes of the reaction of the imines with trimethylsilyl cyanide in organic solvents has been investigated. Various methods for the determination of the enantiomeric excess were tested and the most reliable was found to be use of camphorsulfonic acid. The reaction carried out in the presence of a Salen V(V) complex was optimised to yield aminonitriles in a 80% e.e. at -30°C and 69% e.e. at room temperature.

Trifluoroacetic anhydride (TFFA) has been reported in the literature as a reagent for reaction with aminonitriles to allow the separation of enantiomers. Here the reaction of imines with TFAA in acetonitrile and in benzene has been investigated In each solvent there are strong reactions yielding trifluoroacetylated derivatives which are thought to exist in both ionic and covalently-bound forms.

Acknowledgments

First, I would like to thank most dearly my supervisor Dr M. Crampton. Mike, I owe you my PhD and 3 years of the most enjoyable collaboration on a fascinating project. Thank you for your kindness and your help. My gratitude also extends to Alison and I would like to thank you both for welcoming me to your house whenever I was invited.

I must also thank greatly Avecia and Syngenta for fundings. More significantly, I would like to thank John Atherton and John Blacker from Avecia for being my most attentive industrial supervisors. To both John's I want to express my gratitude for those always enjoyable quarterly meetings and for making me feel at home during my stays at Huddersfield. My thanks to Avecia for the good times I had at Huddersfield must be extended to the guys in the lab. So, thanks to: Ernest, Louise, Paul, Andy, Nick, Pete, Deirdre, Jody, Matt and more especially Neil who has looked so well after me both in the lab and outside!!

Not to be forgotten is EPSRC who provided me with a grant to pay for my tuition fees.

Now moving onto a more personal side of my acknowledgments, I have to make the best of use of the *cliché*: 'I would like to thank my parents without whom...'!!!! Well, Mum, Dad, thank you ever so much for everything, most of all for all your support during my PhD and more generally throughout my long (very long indeed!) student life both in England and back home. To my brother, Séverine and their little Elisa I must be thankful too. You guys have been so supportive that you made me a Godfather before even knowing if I would be a doctor. Cheers!!!

Back to England now, where I have got so many to thank! First of all, a big thank you to my fellow physical organic chemists in Lab 54: Ian, Dave, Chucks and Basim. Smithy, thanks for your friendship and all those hours spent in the New Inn and in all of the other public houses Durham has to offer. Oh! And thank you for the sofas at Gladstone Villas!!!! Dave, cheers for teaching me how to play mini golf (☺) and for being a cheerful chap to be around with. Chucks, cheers mate! See, I shall be a doctor soon too!!! Basim, thank you. Good luck with the PhD but anyway it is going to be alright you have the best supervisor ever!

To be complete with the Chemistry department I would like to thank, in no preferential order whatsoever: Romain, Jordan, Ste, Dave H., Ian H., Jitendra, Stèph, Alessandra and all those whose name escape me right now! A special mention to Romain who has been here with and for me for quite a while now and will hopefully be for many more years to come! Kisses to Jenny and baby Luke!

How could I write this page... oops I meant these pages (!) without thanking all my friends from GradSoc. And yes it will always be GradSoc to me even if my title page denies it by using the name of the great man I had the chance to meet shortly before he passed away. From the pool club (Dave D., Greig, Rich, Ian V., Phil, Adam and all the others) to the bar (Jeff, Jon, Ana, Michael, Keith, Frankie, Nui and many more) via my social secretary duties everything and everybody made me feel great at Parsons Field. Nevertheless some of you guys must be singled out for being special friends throughout. So here it is to you: George S., Matthias, Christine, George T., John A. and D.D.. Please tell me if it is ironic or atavistic[1] (this one is for you Romain Crispini!!) that I am writing those words down in Parsons Field bar during a pool match!!!!!

It is often that one keeps the best for the end. I do not know if it is appropriate or not but there is one person I need to thank and whom I want to be singled out from the others.

To All of the above I will eternally be thankful for contributing in one way or another to produce those two hundred and sixty something pages. Nevertheless I would have never been able to produce all of this (and almost on time!!) without the incommensurable support of the one person who had to live with me for the past 14 months (and it is not easy. Trust me!!). So there you are Amel!!!!! Thank you so much for everything you are and everything you have done for me! Thank you for comforting me, texting me, making me laugh, helping me, teasing me, pushing me to work, laughing at me, and for all those other little things which kept me sane!!! I have already told you many times but I'll say it one more time: you're the best! This thesis is definitely partly yours. THANK YOU!!!!

[1]. Atavistic: happening because of a very old natural and basic habit from the distant past, not because of a conscious decision or present need or usefulness.

Remerciements

Note informative: ceci est une traduction révisée de la page officielle de remerciements écrite en anglais.

Tout d'abord, je tiens à remercier le plus chaleureusement possible mon superviseur Dr M. Crampton. Mike, je vous dois mon doctorat et 3 années d'une collaboration des plus agréables sur un projet fascinant. Merci pour votre gentillesse et votre aide. Ma gratitude s'étend également à Alison et je voudrais vous remercier tous deux pour m'avoir si bien accueilli chez vous à chaque fois que j'y étais invité.

Je me dois également de remercier mes mécènes industriels : Avecia et Syngenta. J'adresse tout particulièrement un grand merci à John Atherton et John Blacker qui furent de merveilleux superviseurs industriels et avec qui nous eûmes des réunions trimestrielles des plus intéressantes. Je tiens également à remercier tous ceux qui ont permit que mon séjour à Huddersfield soit des plus agréables: Ernest, Louise, Paul, Andy, Nick, Pete, Deirdre, Jody, Matt et surtout Neil qui a tant veillé sur moi dans le labo mais aussi en dehors!

Je remercie également EPSRC pour la bourse finançant mes frais d'inscription.

Maintenant place à la cérémonie de remise des Oscars et à l'utilisation de cette petite phrase si célèbre: "Je tiens à remercier mes parents sans qui...". Eh bien, Maman, Papa, merci du plus profond de mon coeur pour tout ce que vous avez fait, et surtout pour tout le soutien dont vous avez fait preuve vis à vis de moi durant ma thèse et toutes mes longues (très longues, trop longues?) années étudiantes que cela soit en Angleterre ou en France. Evidemment je dois aussi remercier mon frère, Séverine et leur petite Elisa! Les enfants vous avez été d'un support incroyable pour moi et en plus vous avez décidé de faire de moi un Parrain avant même de savoir si je serais Docteur! Merci!

En Angleterre j'ai tant de personnes à remercier que lorsque je rédigeai la version anglaise de ces remerciements je n'ai su par où commencer! Je ne vais pas renommer ici tous ceux qui ont déjà été cités dans la langue de Shakespeare. L'intérêt en est de plus limité si l'on considère que c'est en anglais que nous avons lié amitié et que la majorité d'entre vous ne font

que balbutier le français ! La liste suivante n'est donc que nominative et est loin d'être exhaustive. Merci à: Ian, Dave P., George S., Matthias, Christine, George T., John A., Greig, Phil, Adam et tous les autres!!!

Une petite mention particulière pour les Français d'Angleterre. Merci à tous, que ce soit à Durham ou ailleurs. Vous avez tous joué votre rôle dans la rédaction de cette thèse donc merci à vous : Jordan, Stèph, Manue, Damien, Arnaud et surtout à Romain qui m'a fait l'honneur de m'inviter à son mariage et de me laisser y prendre une part importante en tant que "usher". Merci à toi et que tout se passe bien pour ta thèse ainsi que pour ta petite famille à laquelle je fais de grosses bises.

J'en arrive à un point de ma rédaction où il me semble être frappé d'un mélange d'amnésie et de paranoïa. Il ne me faut oublier personne ! Et pourtant je suis persuadé que cela va se produire... Je demande donc à tous ceux qui ne trouvent par leur nom sur les présentes pages de bien vouloir me pardonner.

Vient le moment où je dois remercier mes chers amis de France qui, de par leurs appels téléphoniques, emails ou quelqu'autres moyens de communication m'ont soutenu pendant toute la durée de ma thèse. Merci donc à Greg (Boulou), Lena, Jean-Pierre, Doudou, Victor, Romain, Dara, Pascal, Christelle, Fred, Angèle, Gorian, Vero, Damien, Julie, Bea, Greg (cousin), Caro, Ingrid, Xavier, Lolo et tous les autres que j'aime à revoir quand je regagne mes Vosges natales.

Encore une fois et tout comme dans la version originale le dernier paragraphe est réservé a quelqu'un dont la contribution et le support moral me sont inestimables, quelqu'un sans qui je n'aurais pu mener à bien la rédaction de ce long épître de deux cent soixante et quelques pages. Amel, ceci est ta spéciale dédicace de la part de Cali, Bozo, Mr Tof, Gaston et tous les autres!!!!! Merci pour tout. Merci d'avoir été là pour moi durant les 14 derniers mois. Merci de ton soutien, de ta patience, de ton humour, de tes rires, de ton épaule, de tes texts, de ta maman et de ta confiance. Bref merci d'avoir été une petite fée bienveillante!!!!! Sans toi je n'y serais jamais arrivé, honnêtement ! Je te dédie en partie ma thèse Amel et te remercie de tout mon cœur. MERCI!

Declaration

The work in this thesis was carried out in the Department of Chemistry at the University of Durham between 1st October 2001 and 30th September 2004. It has not been submitted for any other degree and is the author's own work, except where acknowledged by reference.

Copyright

Abbreviations/Definitions

A	Absorbance
A_0	Initial absorbance
A∞	Absorbance at reaction completion
B:	Base
C	Concentration
cat.	Catalyst
C_6D_6	d-6 Benzene
$CDCl_3$	d Chloroform
CD_3CN	d-3 Acetonitrile
CH_3CN	Acetonitrile
CN^-	Cyanide ion
δ / ppm	Chemical shift / parts per million
δ^+	Partial positive charge
δ^-	Partial negative charge
d	Doublet
dd	Double doublet
deg.	Degrees
DMSO	Dimethyl sulfoxide
DNP	Dinitrophenylhydrazine
ε	Extinction coefficient
e. e. / %	Enantiomeric excess / %
EI	Electronic ionisation
eq.	Equivalent
Et	Ethyl group, CH_3CH_2
EtOH	Ethanol
$Eu(fod)_3$	Europium(6,6,7,7,8,8,8-heptafluoro-2,2-dimethyl-3,5-octanedionate)
GC	Gas chromatography
GC/MS	Gas chromatography/ Mass spectrometer

H^+	Hydrogen ion or proton
H_-	Acidity function in water
H_M	Acidity function in methanol
HA	Solvent or acid
HCl	Hydrochloric acid
HCN	Hydrogen cyanide
HMS	Hydroxymethane sulfonate, $CH_2(OH)(SO_3Na)$
HPMS	Hydroxyphenylmethane sulfonate, $(C_6H_5)CH(OH)SO_3Na$
HSO_3^-	Bisulfite ion
I	Ionic strength
Im	Imine
$ImineH^+$	Iminium ion
^iPr	Isopropyl, $CH(CH_3)_2$
IR	Ionisation ratio
J / Hz	Coupling constant / Hertz
k	Rate constant
K	Equilibrium constant
K_a	Acid dissociation constant
k_b	Rate constant of reverse reaction
KCN	Potassium cyanide
k_f	Rate constant of forward reaction
k_{obs}	Observed rate constant
K_{obs}	Observed equilibrium constant
K_w	Dissociation constant of water = $1x10^{-14}$ mol dm^{-3}
λ / nm	Wavelength / nanometer
λ_{max}	Wavelength of peak of maximum absorbance
LSR	Lanthanide shift reagent
m	Multiplet
M^+	Molecular ion
Me	Methyl group, CH_3
MeOH	Methanol
MeONa	Sodium methoxide
MS	Mass spectrometer

m.p.	Melting point
m/z	Relative molar mass
NMR	Nuclear magnetic resonance
Nu	Nucleophile
OH^-	Hydroxide ion
Ph	Phenyl group, C_6H_5
pH	$-Log_{10}[H^+]$
pK_a	$-Log_{10} K_a$
pK_w	$-Log_{10} K_w$
$Pr(hfc)_3$	Praseodymium(3-(heptafluoropropylhydroxymethylene)-(+)-camphorate)
(R)	Rectus configuration
$R_2C=O$	Aldehyde or ketone
Ref.	Reference
RNH_2	Primary amine
ROH	Alcohol
RR'NH	Secondary amine
R.T.	Room temperature
s	Singlet
(S)	Sinister configuration
stoich	Stoichiometric
Salen	N,N'-bis(salicylaldehydo)ethylene diamine
SO_3^{2-}	Sulfite ion
t	Triplet
T	Temperature
^tBu	Tertio-butyl group, $C(CH_3)_3$
TFAA	Trifluoroacetic anhydride, $CF_3C(O)OC(O)CF_3$
THF	Tetrahydrofuran
TMS	Trimethylsilyl group, $(CH_3)_3Si$
TMSCN	Trimethylsilyl cyanide, $(CH_3)_3SiCN$
TMSOH	Trimethylsilanol, $(CH_3)_3SiOH$
TMS-O-TMS	Hexamethyldisiloxane, $((CH_3)_3Si)_2O$
UV	Ultraviolet

Vis	Visible
$[X]_{stoich}$	Total X concentration

Chapter One: Introduction

Chapter one: Introduction

1.1 Background

Nucleophilic addition to carbonyl compounds may lead to potentially useful synthetic intermediates. Thus compounds such as cyanohydrins are widely used to synthesise α-hydroxy-carboxylic acids, α-amino acids and β-amino alcohols.

Of even more interest are the products formed from condensation reactions between carbonyl compounds, amines and a nucleophile. The overall process is shown in Scheme 1.1. Probably one of the best-known examples is the Mannich reaction[1], which leads to Mannich bases that are important reactants in the pharmaceutical and polymer industries:

Scheme 1.1

$$RNH_2 + R'CHO + HZ \longrightarrow RNHCHR'Z + H_2O$$

A particular application of the Mannich reaction is the use of hydrogen cyanide as the nucleophile (HZ). This constitutes the first step of the Strecker reaction[2] that leads to the formation of α-aminonitriles which may be hydrolysed to give amino acids.

The Strecker reaction, although known since the 1850's, was not investigated in detail until the 1970's. Commeyras and Taillades[3] showed that several steps were involved and that an important intermediate was the imine resulting from the addition of the amine to the carbonyl compound. Formation of the cyanohydrin was a side-reaction which did not lead directly to the product.

Detailed kinetic work by Jencks[4] and co-workers has provided a considerable amount of information on the formation and the hydrolysis of imines. It appeared that both reactions are pH dependent displaying bell shaped curves.

The Strecker synthesis is a very useful general method to form amino acids, however it usually results in formation of the product in racemic form. Industries are generally interested in
only one of the active forms. Therefore it is important to be able to be stereoselective and get the largest enantiomeric excesses possible.

This is why in more recent years there has been a growing interest in the asymmetric Strecker synthesis and the screening of various catalysts[5] has been reported. The present work, after presenting kinetic aspects of the uncatalysed reaction, focuses on the asymmetric Strecker reaction.

1.2 Reactions of carbonyl compounds with nucleophiles

Addition on carbonyl compounds is made possible by the electronegative character of the oxygen atom which polarises the double bond and results in an electron deficient carbon atom. The intermediate formed is approximately tetrahedral (sp^3 hybridisation) due to the attack of the nucleophile at an angle of ca 107° on the sp^2 hybridised (planar) carbonyl group[6] (Scheme 1.2).

Scheme 1.2

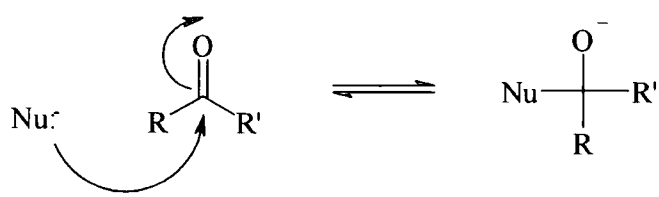

In some cases an unstable intermediate is formed which can not be isolated. This is the case when R and/or R' lead to the formation of good leaving groups such as PhO^-. Here the oxygen-carbon double bond is re-formed and one of the R groups is substituted by the nucleophile (Scheme 1.3). However for carbonyls such as ketones and aldehydes the R^- and H^- are too strong bases and can not be eliminated. The reaction therefore is an addition rather

than a substitution (Scheme 1.4). In this case rate of reaction and equilibrium constants are subject to steric, resonance and inductive effects with acid-base catalysis playing an important role.

Scheme 1.3

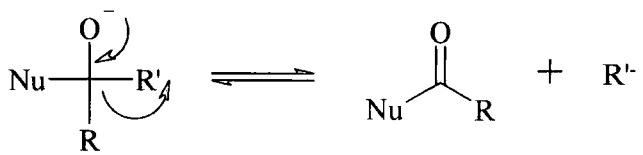

Scheme 1.4

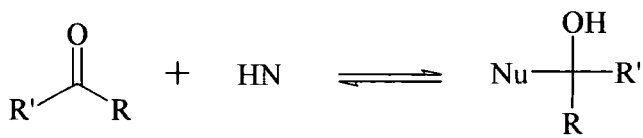

1.2.1 Addition of sulfite

Sulfite simply adds to aldehydes and unhindered ketones to form so called bisulfite addition compounds. Early studies[7] proved that it is the sulphur atom which bonds to the carbonyl carbon rather than the harder oxygen atom leading to the formation of hydroxy sulfonic acids, rather than hydroxy sulfite esters, shown in Scheme 1.5.

Scheme 1.5

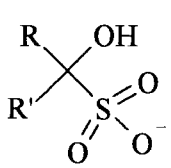

Hydroxy sulfonic acid

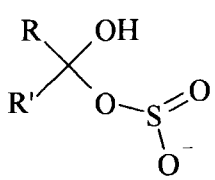

Hydroxy sulfite ester

In neutral and alkaline conditions the addition of the sulfite dianion (SO_3^{2-}) is favoured and is diffusion controlled[8]. In the acidic region Stewart and Donally[9] also accounted for a slow catalysed pathway for the mechanism (Scheme 1.6).

Scheme 1.6

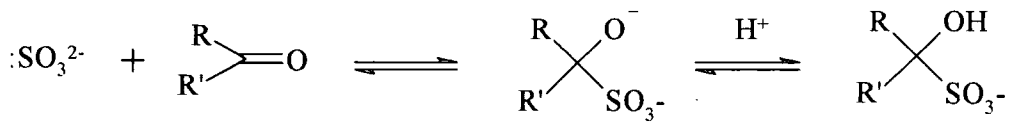

Jencks and Young[10], studied the reaction in acidic media by investigating the decomposition of bisulfite addition compounds There is evidence for general acid catalysis and the proposed mechanism, shown in Scheme 1.7, involves slow acid assisted expulsion of hydrogen sulfite, followed by rapid deprotonation. In the reverse direction this involves rate-limiting attack of hydrogen sulfite in the protonated carbonyl compound.

Scheme 1.7

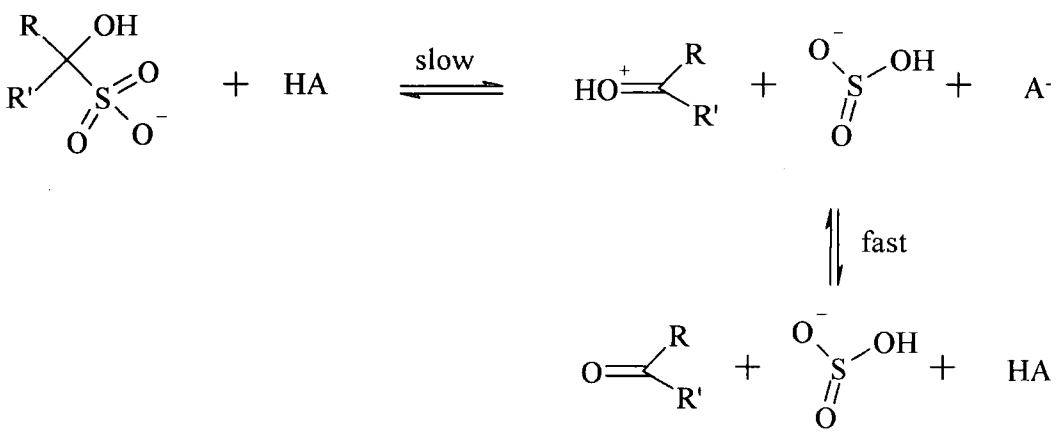

Equilibrium studies[11] indicate that addition of sulfite/bisulfite is generally more favourable in the case of aldehydes compared to ketones (Table 1.1). This is attributable to the lower steric requirement for the sulfite adduct when one of the groups R or R' is hydrogen.

Table 1.1 Equilibrium constants for the addition of bisulfite to aldehydes and ketones, RR'CO

R	R'	K (dm^3mol^{-1})
H	CH_3	800
H	C_6H_5	6400 [11b]
CH_3	CH_3	200
CH_3	C_2H_5	40
CH_3	*i*-C_3H_7	8
CH_3	*i*-C_4H_9	1.6

Conditions: 11a): 50% ethanol solutions, T = 0°C; 11b) aqueous buffers, T=25°C, I = 1.0 M

1.2.2 Addition of cyanide

The reaction of carbonyl compounds with hydrogen cyanide forms cyanohydrins. Similarly to most additions on carbonyls the reaction involving cyanide is pH dependent. Indeed cyanide must be in the, CN^-, basic form in order to attack the carbonyl (Scheme 1.8). Lapworth[12] and, later, Roth and Svirbely[13] commented on the reaction and showed that the rate is dependent on the concentration of the cyanide ion but that no, or little, acid catalysis is required.

Scheme 1.8

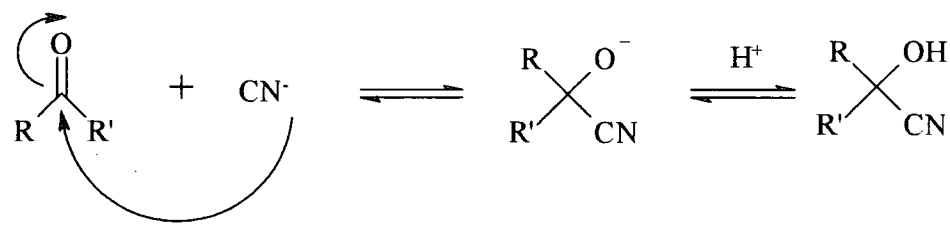

The general mechanism[14] can be represented as in Scheme 1.9.

Scheme 1.9

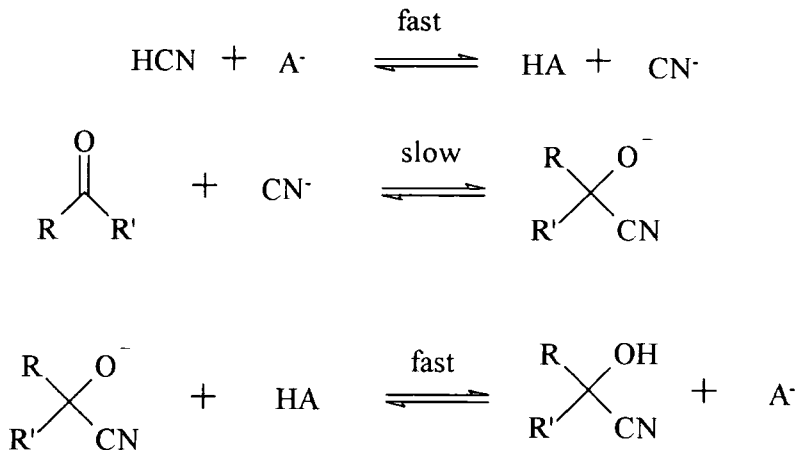

The carbon-carbon bond formation is therefore the rate-determining step as confirmed by Ching and Kallen[15].

It is of interest to note studies[16] showing a strong solvent dependence on the rate of formation of the cyanohydrin.

The reverse process in Scheme 1.9 shows that decomposition of the cyanohydrin involves elimination of cyanide from the deprotonated form. Direct elimination from the neutral cyanohydrin is less favourable since it would lead to the protonated carbonyl compound.

As described previously in the addition of sulfite compounds to carbonyls, the equilibrium for the addition of cyanide to aldehydes and ketones lies essentially to the right; with cyanohydrins formed from the former being more favoured (Table 1.2).

Table 1.2 Equilibrium constants for the addition of HCN to aldehydes and ketones, RR'CO

R	R'	K (dm^3mol^{-1})
C_6H_5	H	236[15]
p-CH_3-C_6H_5	H	114[15]
p-CH_3O-C_6H_5	H	32.7[15]
p-NO_2-C_6H_5	H	1820[15]
C_6H_5	CH_3	0.77[17]
CH_3	CH_3	33[17]
CH_3	C_2H_5	38[17]
CH_3	*i*-C_3H_7	65[17]
CH_3	*i*-C_4H_9	32[17]

Conditions: Ref 15: aqueous solution, T = 25°C, I = 1.0 M; Ref 17: 96% ethanol solutions, T = 20°C

Cyanohydrins are synthetically useful since they can react further to give α-hydroxy-carboxylic acids, α-amino acids and β-amino alcohols.

A classic example is the synthesis of mandelic acid which proceeds through the formation of mandelonitrile from benzaldehyde[18]. The cyanohydrin is then hydrolysed in acidic conditions[19] to lead the desired hydroxyl carboxylic acid (Scheme 1.10).

Scheme 1.10: Synthesis of mandelic acid

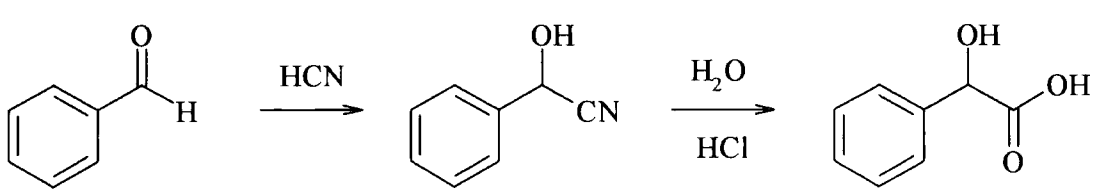

Mandelonitrile Mandelic acid

1.2.3 Addition of amines

The addition of amines to carbonyl compounds, namely aldehydes and ketones has been widely studied[20]. However it is worth noting the difference in the end products depending on the amine type (primary, secondary or tertiary).

1.2.3.1 Primary amines

The reaction between carbonyls and primary amines (RNH_2), or ammonia derivatives (NH_2-Z) forms imines (Scheme 1.11).

Scheme 1.11

The product formed using primary amines is sometimes known as a Schiff base since Schiff first discovered the reaction[21].

The addition reaction of amines to carbonyls involves two steps, the first of which is the attack on the carbonyl by the amine to form a carbinolamine intermediate. Dehydration of that compound, via the iminium ion leads to the imine as shown in Scheme 1.12.

Scheme 1.12

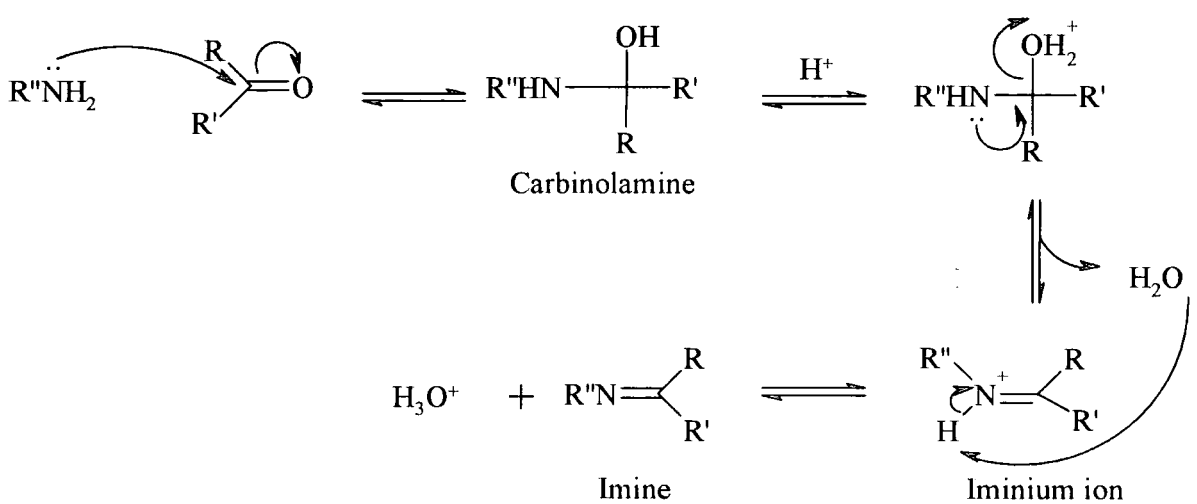

Formation of the carbinolamine is favourable and providing that the reactants are sufficiently concentrated the conversion is virtually complete[4]. Studies[22] of the reaction of aldehydes with various amines showed that the equilibrium constant value is dictated by the pK_a value for the amine and by steric properties. It is worth noting that when formaldehyde reacts with a range of amines the pK_a value for the resulting carbinolamine is two to three units lower than for the parent amine[23]. This phenomenon can be accounted for by the fact that one of the amines protons is substituted by a hydroxymethyl group which lowers the ability of the solvent to stabilise the cation.

Similarly to the sulfite and cyanide additions the two steps involved in the imine formation may be subject to acid and base catalysis as will be described in section 1.3.1.

Industrially imines are used in many enzymatic and synthetic processes[24]. Although since imines are not always readily isolable alternative syntheses have been developed such as solvent-less synthesis on alumina surfaces[25].

1.2.3.2 Secondary amines

The reaction between a carbonyl compound and a secondary amine again proceeds through a carbinolamine intermediate but now forms an iminium ion[26] (Scheme 1.13). As there is no proton on the nitrogen atom it is not possible to get the imine.

Scheme 1.13

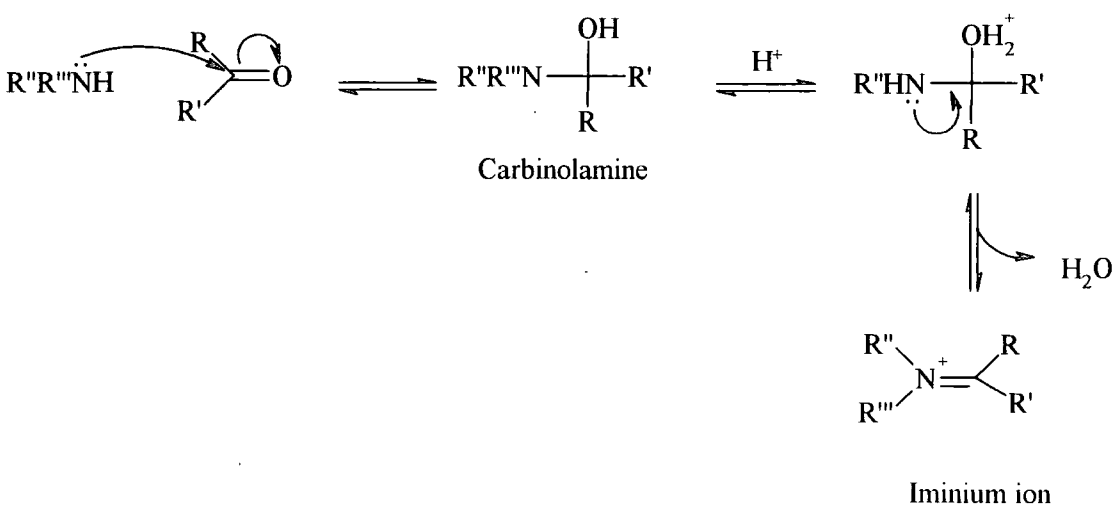

However if there is a α-hydrogen on the molecule it then can be lost to form an enamine[27] (Scheme 1.14).

Scheme 1.14

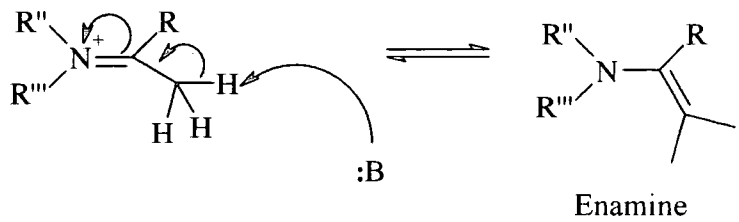

Enamine

It is worth noting that imines with α-hydrogens can undergo imine-enamine tautomerism[28].

1.2.3.3 Tertiary amines

The addition of a tertiary amine to a carbonyl compound leads to the formation of a zwitterionic carbinolamine that is not very stable and generally decomposes back to the starting materials.

However for molecules bearing both carbonyl and amino groups at the same time the reaction can form a ring making the resulting carbinolamine more stable. A typical example is the case of 3,3-dimethyl-4-dimethylaminobutanal[29] (Scheme 1.15).

Scheme 1.15

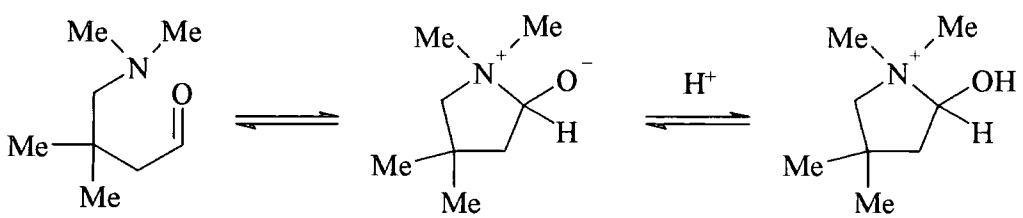

1.3 Reactions of imines

Depending on the nature of the R, R' and R'' substituents, imines bear different names[30] (Table 1.3).

It is worth noting that imines are not very stable and can be isolated only if having one or more aryl substituents on the carbon or nitrogen as steric hindrance prevents further reaction[31]. The presence of a hydroxyl group or second nitrogen on the nitrogen atom also enhances stability (as is the case for oximes, hydrazones and semicarbazones).

Table 1.3 Nomenclature of imines depending on the carbonyl and amino groups

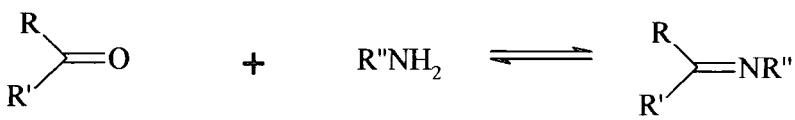

Aldehyde	Amine	Aldimine	R = H; R' = Alkyl or Aryl; R" = Alkyl or H
Ketone	Amine	Ketimine	R = Alkyl or Aryl; R' = Alkyl or Aryl; R" = Alkyl or H
Aldehyde/Ketone	Amine	Anil	R = Alkyl or Aryl or H; R' = Alkyl or Aryl or H; R" = Aryl
Aldehyde/Ketone	Semicarbazide	Semicarbazone	R = Alkyl or Aryl or H; R' = Alkyl or Aryl or H; R" = -$NHCONH_2$
Aldehyde/Ketone	Hydroxylamine	Oxime	R = Alkyl or Aryl or H; R' = Alkyl or Aryl or H; R" = -OH
Aldehyde/Ketone	Hydrazine	Hydrazone	R = Alkyl or Aryl or H; R' = Alkyl or Aryl or H; R" = -NHR

1.3.1 Imine formation

The pH dependence of the rate constant for the formation of imines has been well established[32]. A plot of the rate constant against pH usually displays a bell-shaped curve with a maximum slightly below the pK of the reacting amine.

Early mechanistic investigations led by Conant and Bartlett[32b] and later by Hammett[33] argued that the shape was due to the opposing effects of general catalysis and of the protonation of the parent amine at low pH.

Further studies[34] proved that the pH dependence exhibited by the bell-shaped curve was the result of a change in the rate-determining step. Below the maximum (i.e. below the amine pK_a) the rate-determining step is the addition of the amine on the carbonyl group. At those pH values the amine is significantly protonated and the concentration of free amine relatively low. Above the maximum the acid catalysed dehydration of the carbinolamine is rate limiting.

1.3.1.1 Carbinolamine formation

Depending on the nature of the amine, the carbonyl compound and pH carbinolamine formation can be stepwise with the zwitterionic form of the carbinolamine being present as an intermediate. However another possible pathway is a 'concerted mechanism'.

a) 'Concerted' pathway:

This process involves proton transfer to the carbonyl oxygen concerted with the formation of the carbon-nitrogen bond. The phenomenon is subject to both general acid catalysis (Scheme 1.16) and general base catalysis[35] (Scheme 1.17).

Scheme 1.16: Acid catalysis

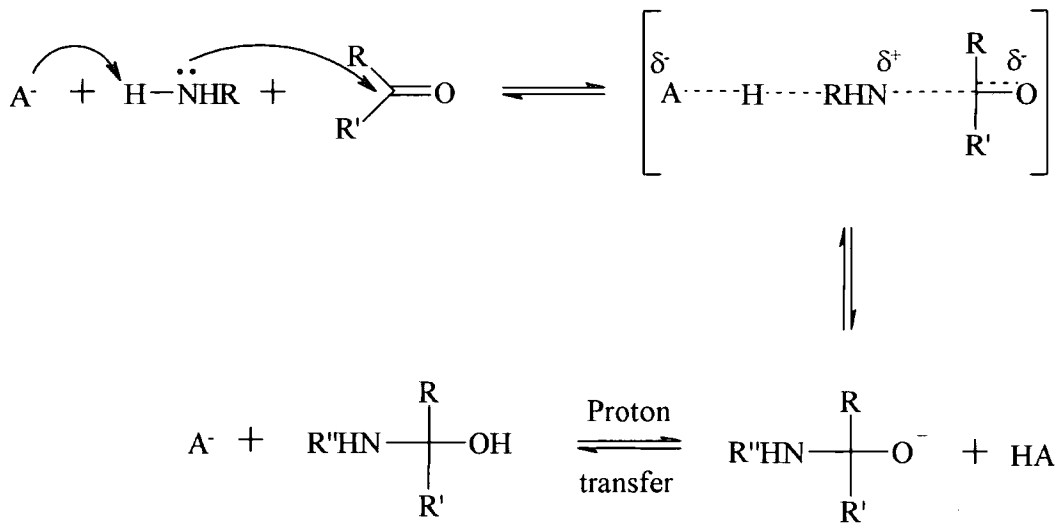

Scheme 1.17: Base catalysis

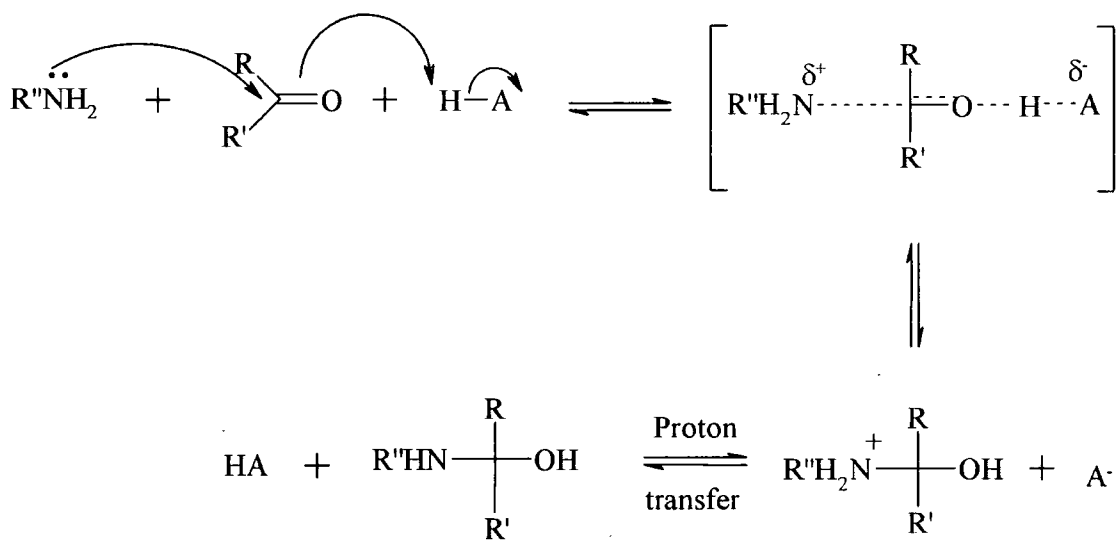

b) Stepwise pathway

Carbinolamine formation involves the intermediacy of an unstable zwitterionic species, which breaks down rapidly unless it is trapped by a proton transfer process (Scheme 1.18). It is worth noting some theoretical studies[36] suggesting that the conversion from the zwitterionic species to carbinolamine involves two molecules of water.

Scheme 1.18

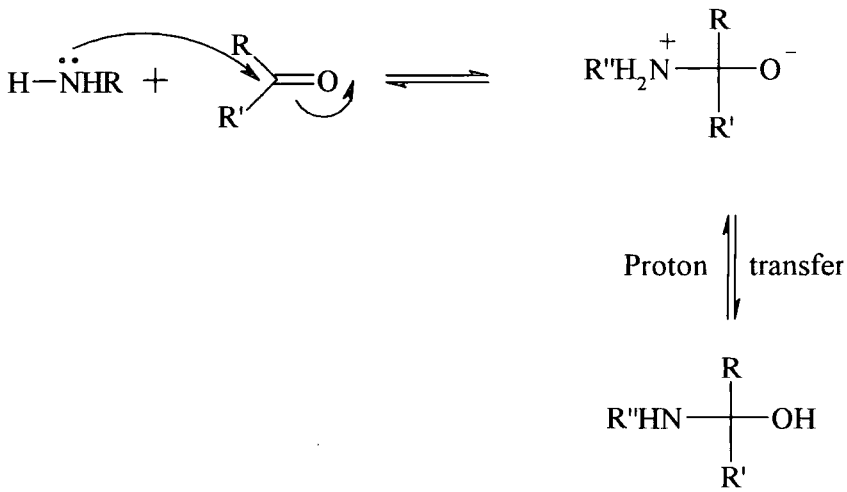

At acidic pH values carbinolamine formation is the rate-determining step. The amine pK_a as well as the equilibrium affinity for the carbonyl compound decide which pathway (general acid catalysed concerted pathway or stepwise mechanism) is favoured. The two pathways are summarised in Scheme 1.19.

Scheme 1.19

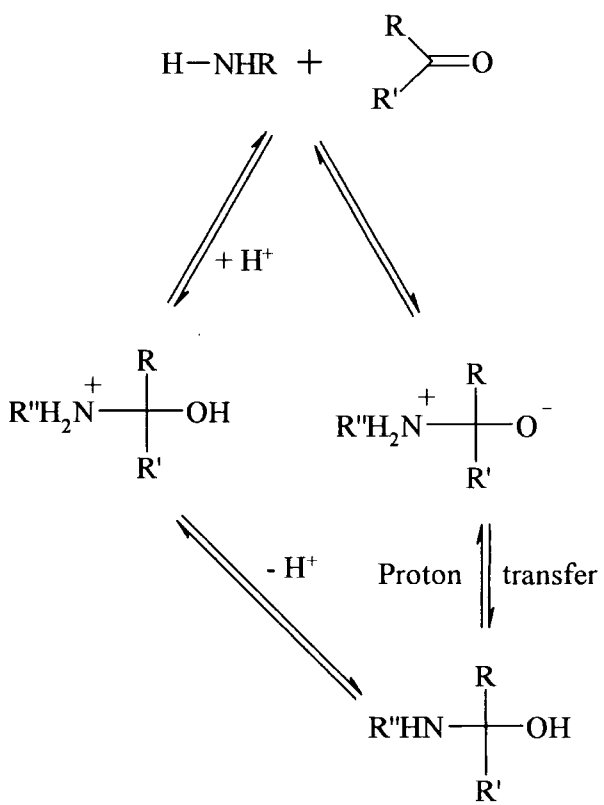

For amines of moderate basicity and with a large equilibrium constant for carbinolamine formation the zwitterionic intermediate is relatively stable. The stepwise mechanism is therefore favoured. It is worth mentioning that as the pH decreases there is a change in the rate-determining step. The proton transfer becomes faster than the attack of the amine onto the carbinolamine and a break in the profile is noticed for pH's values between 0 and 2[37]. At even lower pH's values the concerted pathway is favoured.

For weakly basic amines and reactions for which the formation of the carbinolamine is unfavoured (small equilibrium constants for addition to the carbonyl) the zwitterion is less stable and the pathway of choice is the acid catalysed concerted one.

It is worth noting that for pH values around 4-5 the pH independent addition of both types of amines (basic and weakly basic) to the carbonyl becomes significant. The rate determining step then becomes the solvent mediated 'proton switch' between the nitrogen and oxygen atoms of the zwitterion.

1.3.1.2 Carbinolamine dehydration

Carbinolamines formed from strongly basic amines can be dehydrated by direct expulsion of hydroxide ion (Scheme 1.20).

Scheme 1.20

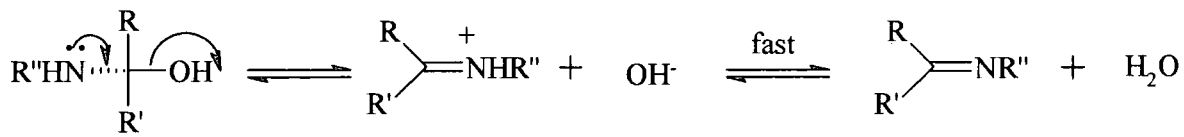

Carbinolamine dehydration is also subject to general acid catalysis and Kallen[38] calculated the rate constant for the proton catalysed dehydration of the carbinolamine formed from formaldehyde and cysteine (Scheme 1.21).

Scheme 1.21

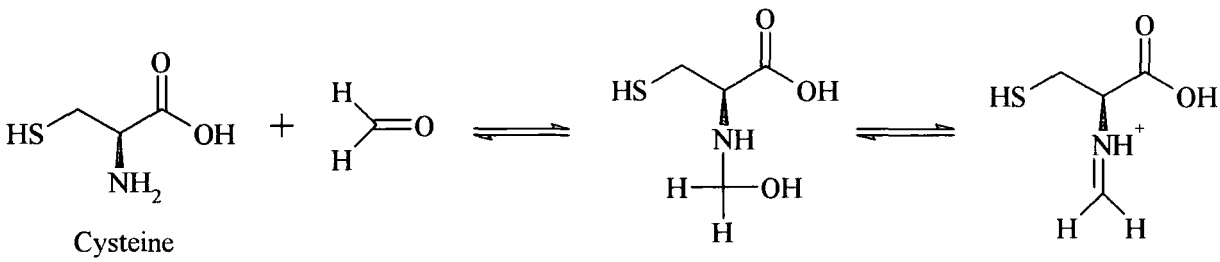

Cysteine

$$k_{dehydration} = 1.4 \times 10^{8}\,dm^{3}mol^{-1}s^{-1};\ T = 25°C;\ I = 1.0M$$

Also of interest are Jencks[39] studies on the catalysis by aniline and substituted anilines of the formation of semicarbazones and oximes. It was shown that, compared to acid catalysis by acids of comparable acid strength, anilinium ion catalysis is more efficient. The reaction involves the formation of a first imine (product of the reaction between aniline and the carbonyl compound) which then reacts with the semicarbazide or hydroxylamine to yield the final product as shown in Scheme 1.22.

Scheme 1.22

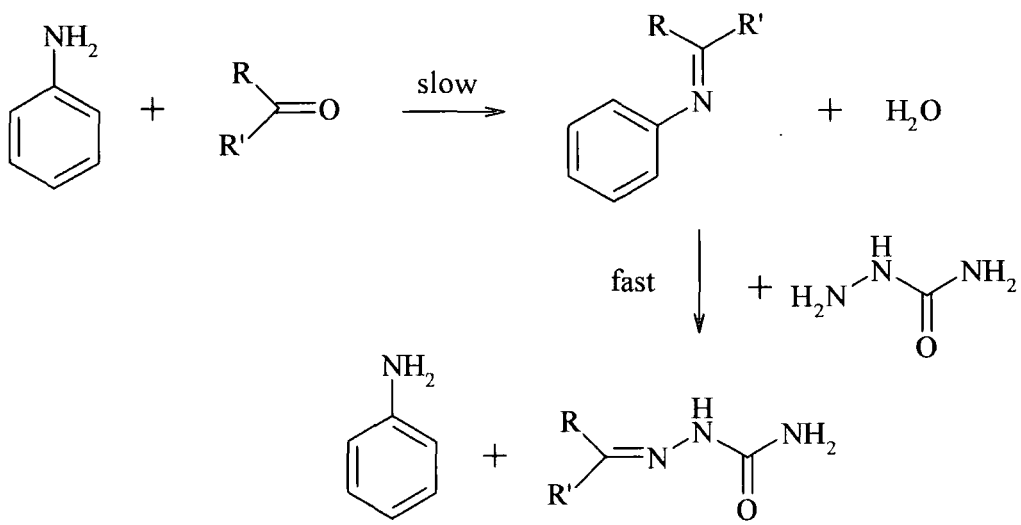

It is worth mentioning that although the bell shape pH profile is noticed in most cases for imine formation there are systems which do not display this particular profile.

Indeed the rate determining step for formation of some semicarbazones, oximes and hydrazones formation is the carbinolamine dehydration even at very low pH levels[40]. In those

cases the reaction can occur intramolecularly within an aromatic ring. The transition state contains a cationic site which increases the rate of amine attack relative to dehydration and because this can happen at very low pH values dehydration becomes the rate-determining step at all pHs.

1.3.2 Hydrolysis of imines

Because of the reversibility of all the steps in the imine synthesis, hydrolysis back to starting amine and carbonyl is possible.

The results are consistent with reaction occurring via the iminium ion. The rate is dependent on steric factors and the nature of the groups present on the imine[41]. The principle of microscopic reversibility states that forward and backward reactions must occur by the same mechanism. Therefore, similarly to the one accounting for the formation of imines, the plot of the hydrolysis rate constant against pH is bell-shaped[42] and is representative of a change in rate determining step[43].

The mechanism of imine hydrolysis[44] is shown in Scheme 1.23. In alkaline media the rate determining step is likely to be hydroxide attack on the iminium ion (Scheme 1.23 a). As the pH is reduced attack of water rather than by the hydroxide ion predominates as shown in Scheme 1.23 b.

Scheme 1.23

a) Alkaline medium

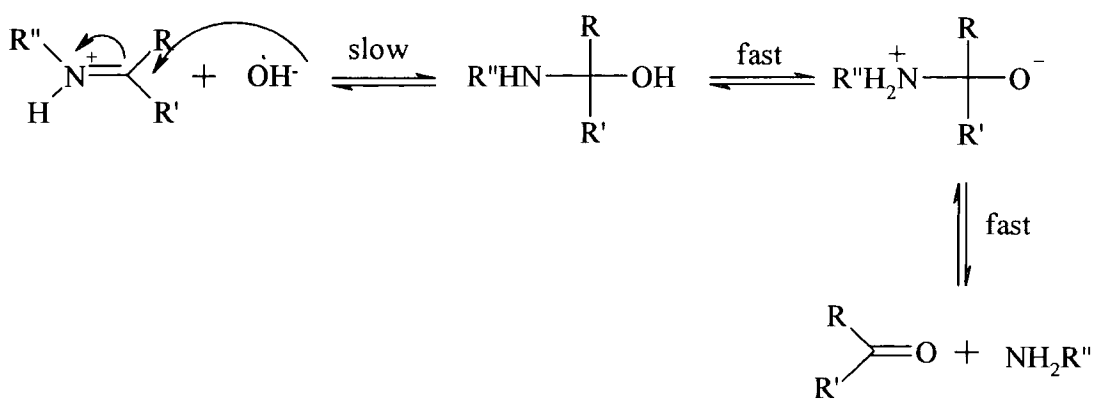

b) Acidic medium

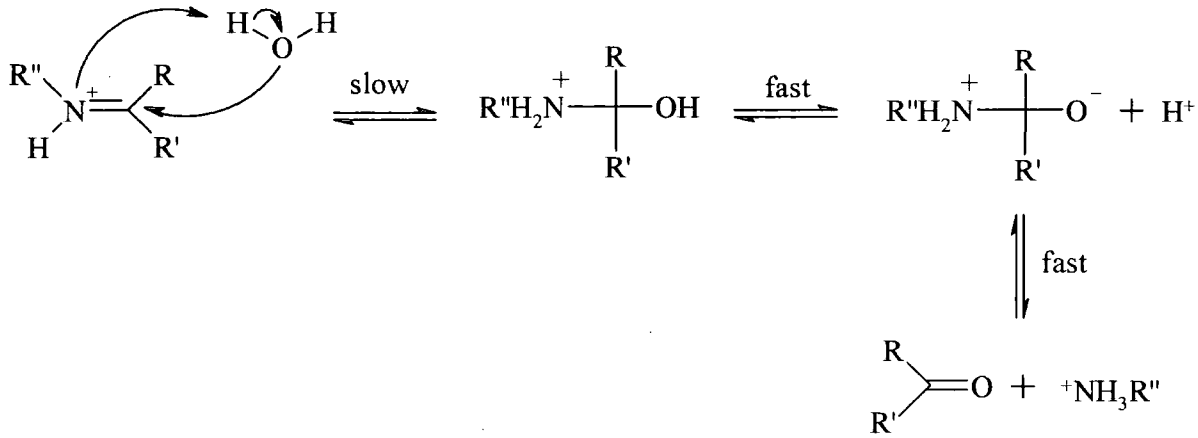

c) Highly acidic conditions

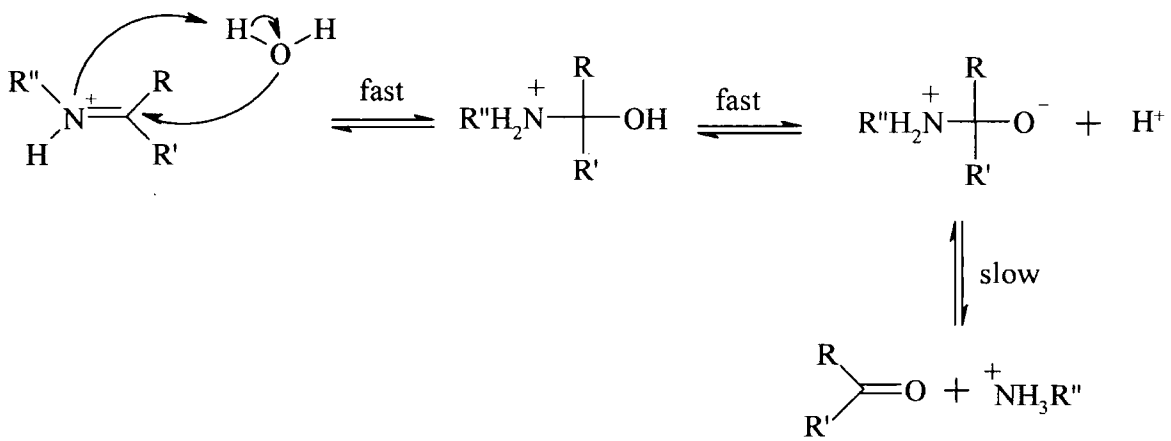

In more acidic conditions the cleavage of the carbinolamine may become rate limiting, as shown in Scheme 1.23 c.

This reaction is slow at low pH values, as a proton has to be removed from the oxygen atom of the carbinolamine in order to obtain a sufficient driving force for amine expulsion.

Values have been reported for the rate constants of the reaction of iminium ions with water. Eldin[45] reported a value of 1.8×10^7 s^{-1} for the reaction of the iminium ion $H_2C{=}N^+(CH_3)(CH_2CF_3)$ with water at 25°C. Jencks studied the hydrolysis of iminium ions formed from formaldehyde and N-methylaniline derivatives[46] and reported rate constants ranging from 3.1×10^6 to 1.0×10^8 s^{-1}.

1.3.3 The Mannich reaction

The Mannich synthesis is the reaction between an aldehyde (most often formaldehyde), an amine and a compound with an acidic, easily removable, hydrogen. In practice the latter is generally an enolizable aldehyde or ketone. They react together to form what is known as a Mannich base (Scheme 1.24).

Generally the carbonyl compound is heated with formaldehyde and an amine in a protic solvent.

The reaction has been thoroughly studied[47] and the mechanism discussed. Kinetic studies[48] suggest that the mechanism could be represented as follows.

Scheme 1.24

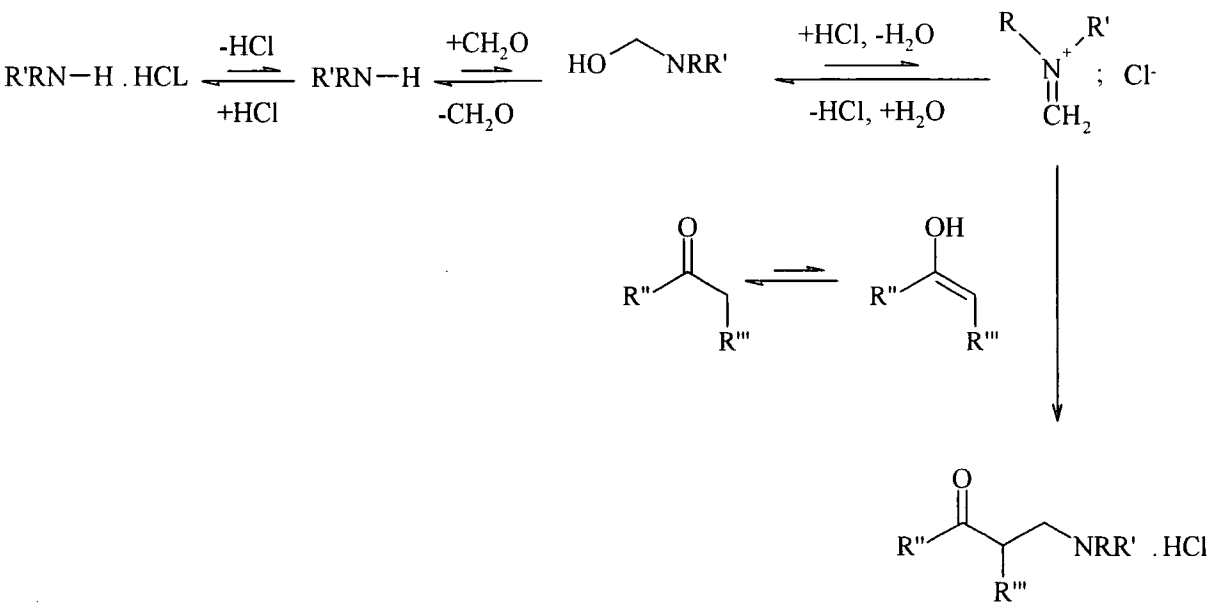

Depending on the acidity of the medium the mechanism for the electrophilic attack of the iminium ion on the carbonyl can be represented differently.

a) In acidic conditions, the enol form of the substrate (cyclohexanone in the following example[49]) is attacked by the iminium ion.

Scheme 1.25: Acidic medium

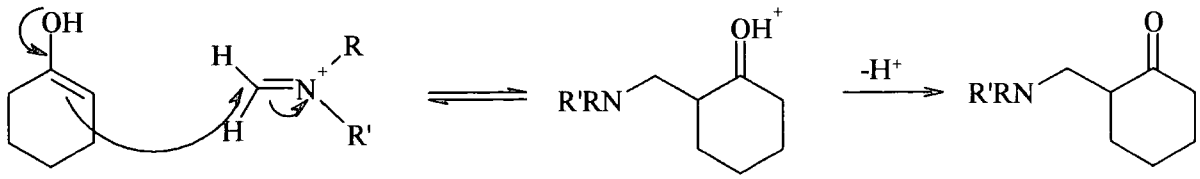

b) In alkaline conditions it is the enolate form that is attacked by the iminium ion (Scheme 1.26).

Scheme 1.26: Basic medium

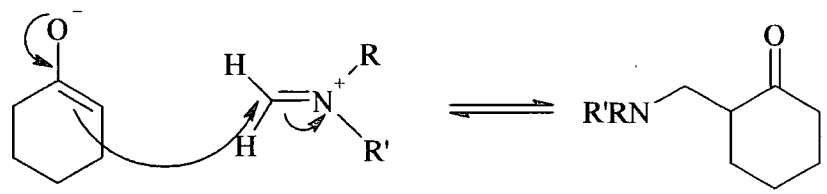

Mannich bases are useful intermediates and can be converted to various derivatives such as Michael acceptors, 1,3-amino alcohols or other functionalised carbonyl compounds. They find applications in the polymer chemistry and paint manufacture[50] and probably most importantly in the pharmaceutical industry[51].

However it is worth mentioning that the Mannich reaction presents some major synthetic challenges as side reactions can take place. There is also no control of the region-selectivity and mainly only aldehydes and ketones can be used as the acidic substrate. Recently preformed Mannich reagents have been synthesised to overcome those problems. Typical examples for those reagents are imines[52], aminals and N,O-acetals[53] and perhaps more commonly iminium salts[54].

1.3.4 The Strecker reaction

The Strecker synthesis is a particular case of the Mannich reaction with hydrogen cyanide, HCN, being used as the RH compound. It was developed in 1850[2] and leads to an α-aminonitrile that is then hydrolysed in very acidic conditions to form an α-amino acid[55] (Scheme 1.27).

Early studies[56] suggested that the cyanohydrin was an intermediate in the reaction and the imine and/or the iminium ion were not involved. Later Ogata and Kawasaki[57] suggested the contribution of the imine in the reaction but it was not until the mid 1970s and the work of Taillades and Commeyras[58] that the mechanism for the Strecker reaction was entirely explained.

Scheme 1.27

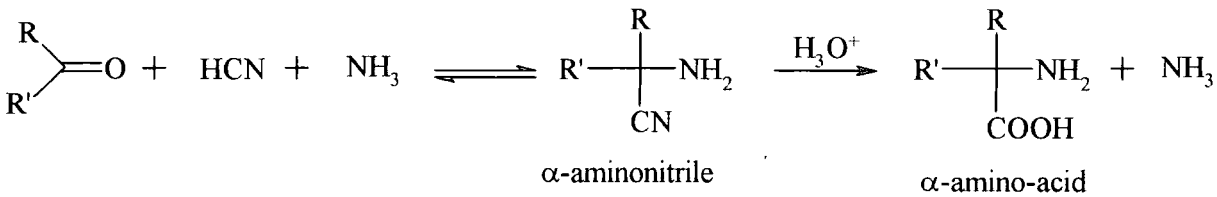

Their kinetic studies[3b] showed that the formation of α-aminoisobutyronitrile from acetone, cyanide and amine in aqueous solution proceeds through two successive steps. The fast formation of cyanohydrin and its decomposition were evident. The cyanohydrin is not, however, an intermediate in the reaction. It is a competition product between the cyanide and the amine towards acetone. The aminonitrile is then slowly formed and is more stable than the cyanohydrin.

The slow step of the reaction is the formation of the imine intermediate, which then reacts quickly to form the α-aminonitrile (Scheme 1.29).

Scheme 1.28

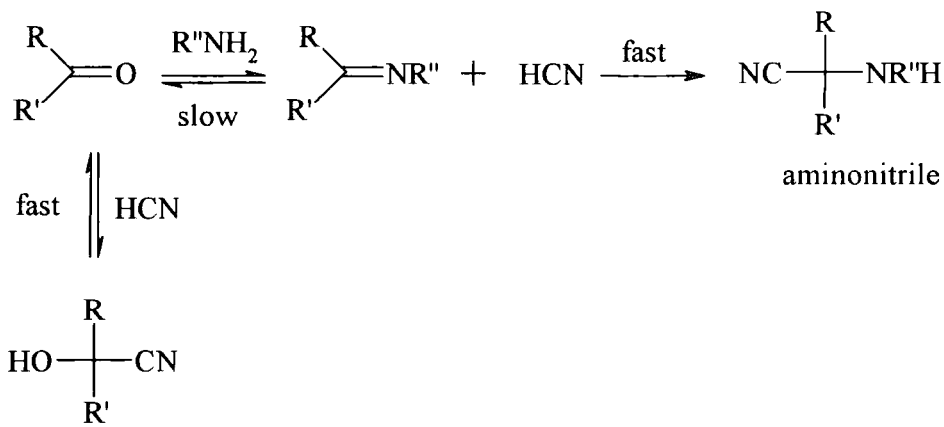

The value of the equilibrium constant for the formation of α-aminoacetonitrile from free formaldehyde, ammonia and hydrogen cyanide at 25°C has been reported[59] as $1x10^7$ $mol^{-2}dm^6$.

In recent years a lot of work focused on the asymmetric Strecker reaction and the understanding of the catalysed process. This will be discussed further in the next part.

1.4 Asymmetric Catalysis

1.4.1 Asymmetric catalysis

Many naturally occurring products are constituted of asymmetric molecules however the synthesis of these compounds often leads to the formation of mixtures of enantiomers. Furthermore in most cases the biological properties of the two substances will be different and there is a need for isolating only the interesting species. Examples of pharmaceutical enantiomers and their properties are shown below:

Scheme 1.29[60]

Thalidomide

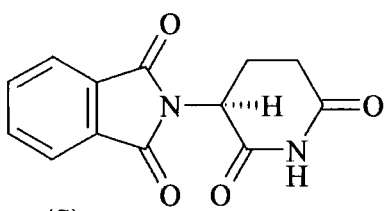

(S)

Causes foetal abnormalities

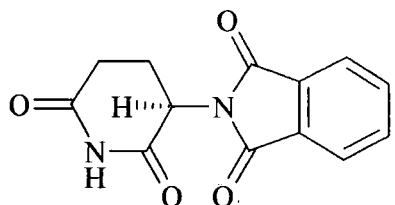

(R)

Sedative and anti-nausea drug

Ibuprofen

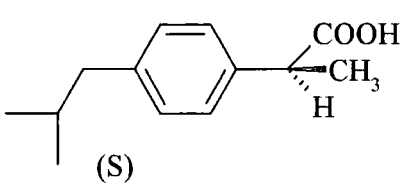

(S)

Anti inflammatory agent

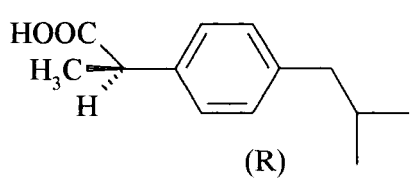

(R)

Non toxic but inactive

It is therefore important to be able to either separate the enantiomers or ensure that the synthesis will lead to pure products.

Methods used to obtain enantio-pure products include:

- Optical resolution using derivatisation (diastereoisomers)
- Separation using chiral chromatography
- Enzymatic resolution
- Kinetic resolution
- Asymmetric synthesis

In 1904 Marckwald[61] gave a definition for asymmetric synthesis:

"Asymmetric syntheses are those reactions which produce optically active substances from symmetrically constituted compounds with the intermediate use of optically active materials but with the exclusion of all analytical processes"

Later Morrison and Mosher[62] gave a broader definition for the process:

"An asymmetric synthesis is a process which converts a prochiral unit so that unequal amounts of stereoisomeric products result"

Various natural asymmetric compounds such as alkaloids, sugars, amino acids or terpenoids have been used to induce chirality. They are used as chiral auxiliaries and connect to the molecule at a critical stage to induce asymmetry. Once this is completed they can be disconnected and recycled. However the need for high yields, rates, stereoselectivity and, more importantly for industry, reasonable costs mean that asymmetric synthesis using stoichiometric amounts of chiral precursors is not convenient when the reaction is scaled up.

A more efficient use of the chiral source is to incorporate it into a catalyst, which can be recovered after the reaction is over. Catalytic asymmetric synthesis has been widely studied for the past 40 years.

In 1966 Noyori and Nozaki[63] reported for the first example of asymmetric catalysis using a chiral transition-metal complex. They used a copper complex in the asymmetric cyclopropanation of styrene with ethyl diazoacetate and produced 10 and 6% enantiomeric excess for the synthesis of the *Cis*- and *Trans*-cyclopropanecarboxylates respectively.

Scheme 1.30

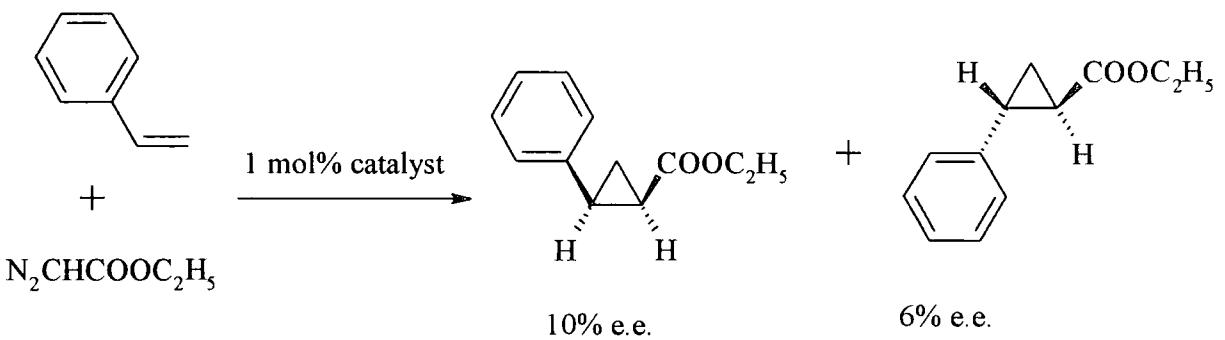

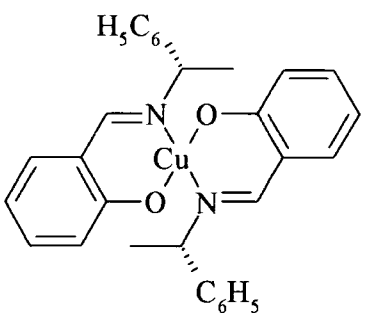

Chiral Cu Catalyst

In 1968 Knowles and Horner[64] developed the first homogeneous catalysed asymmetric hydrogenation of olefins. Later, in 1974, the "Monsanto process" developed by Knowles and co-workers[65] was the first commercialised catalytic asymmetric synthesis employing a chiral transition metal complex (Scheme 1.31).

In 2001, Knowles alongside Noyori and Sharpless received the Nobel Prize[66] in chemistry for their work on chirally catalysed hydrogenation and oxidation reduction.

Scheme 1.31: The Monsanto process: synthesis of L-DOPA

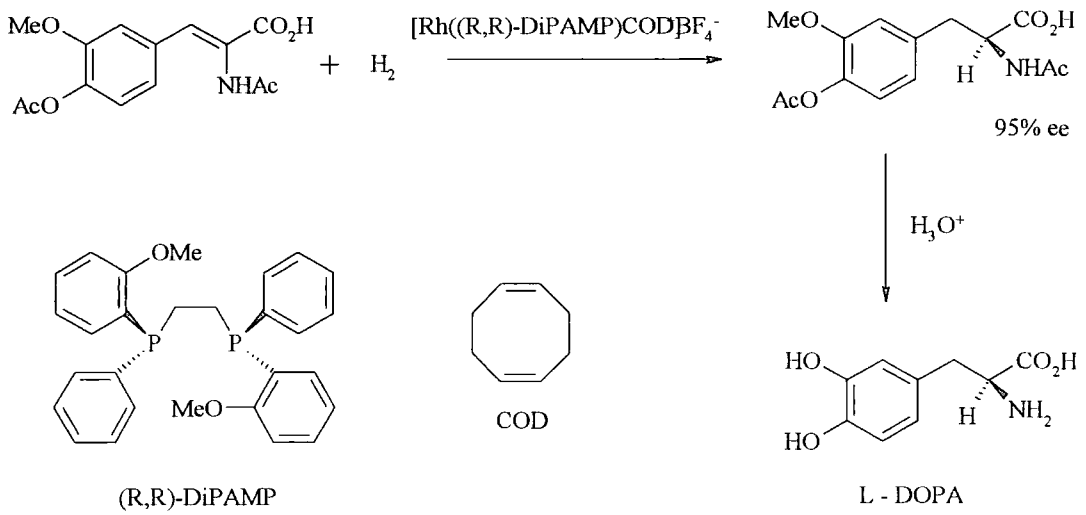

Asymmetric catalysis has been applied to many reactions in recent years. Of particular interest here are the asymmetric catalysed reactions of the addition of nucleophiles to carbonyls and imines in the cyanohydrin, Mannich and Strecker syntheses.

1.4.2 Catalytic asymmetric cyanohydrin synthesis

As seen in Part 1.2.2 cyanohydrins are very important synthetic intermediates and there is a need for optically pure cyanohydrins.

The use of enzymes[67] and polymers[68] as catalysts has been recorded. However the use of organometallic reagents and peptides[69] (especially cyclic dipeptides) has been the main focus point for the past 15 years

Various organometallic reagents have been found to lead to optically active cyanohydrins. In the late 1980s Narasaka[70] use a complex formed from a tartaric acid derivative and dichlorodiisopropoxytitanium (IV) (Scheme 1.32) to add trimethylsilyl cyanide (TMSCN) to aromatic and aliphatic aldehydes in good yields up to 96% and satisfactory enantiomeric excesses with values ranging from 56 to 97% e.e..

In a similar method Oguni[71] reported the asymmetric addition of TMSCN to aromatic aldehydes using a modified version of the Sharpless catalyst (Scheme 1.33).

Scheme 1.32

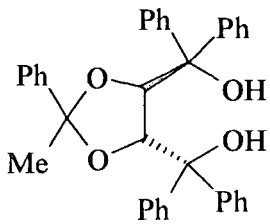

+ $TiCl_2(O^iPr)_2$

Narasaka catalyst

Scheme 1.33

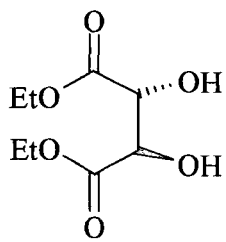

+ $Ti(O^iPr)_4$ + t-BuOOH

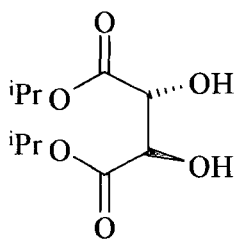

+ $Ti(O^iPr)_4$

Sharpless Catalyst

Oguni Catalyst

Several examples of organometallic compounds used in the asymmetric synthesis of cyanohydrin are available in the literature[72]. However of most interest for our work is the use of the salen ligand, shown in Scheme 1.34.

Extensive work by North and Belokon[73] showed that metal complexes of the ligand shown above were good catalysts for the asymmetric formation of cyanohydrins.

Most of the studies have been carried out using Ti (IV) as the metal core. Full investigation on the mechanism[74] of the reaction indicated the formation of a dinuclear complex (Scheme 1.35) which is the active form of the catalyst in the proposed cycle for trimethylsilylcyanation (TMSCN) of benzaldehyde below (Scheme 1.36).

Scheme 1.34: Salen Ligand

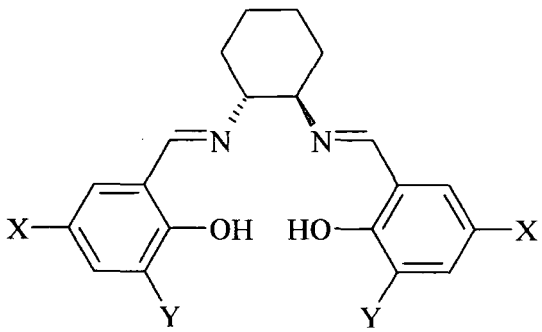

Scheme 1.35: Salen titanium catalyst

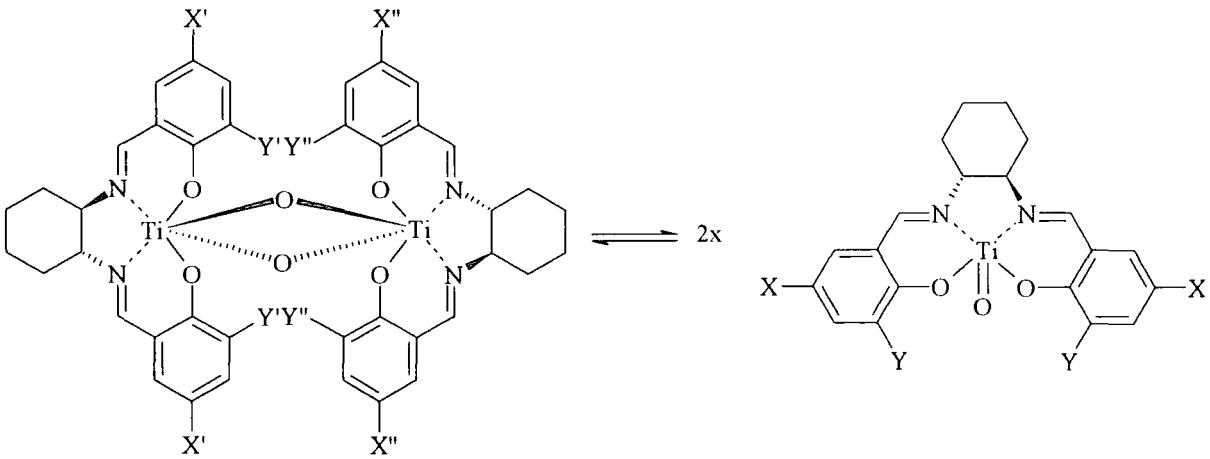

a) X'=X"=Y'=Y"=H
b) X'=X"=Y'=Y"=^{t}Bu
c) X'=X"=NO_2; Y'=Y"=^{t}Bu
d) X'=NO_2; X"=Y'=Y"=^{t}Bu

A dinuclear complex, **1**, is formed by the interaction between TMSCN and the salen structure. However the structure is unstable and decomposes to form a dicyano-complex, **2**. In the presence of benzaldehyde the salen structure interact with the aldehyde to form complex **3**.

Scheme 1.36

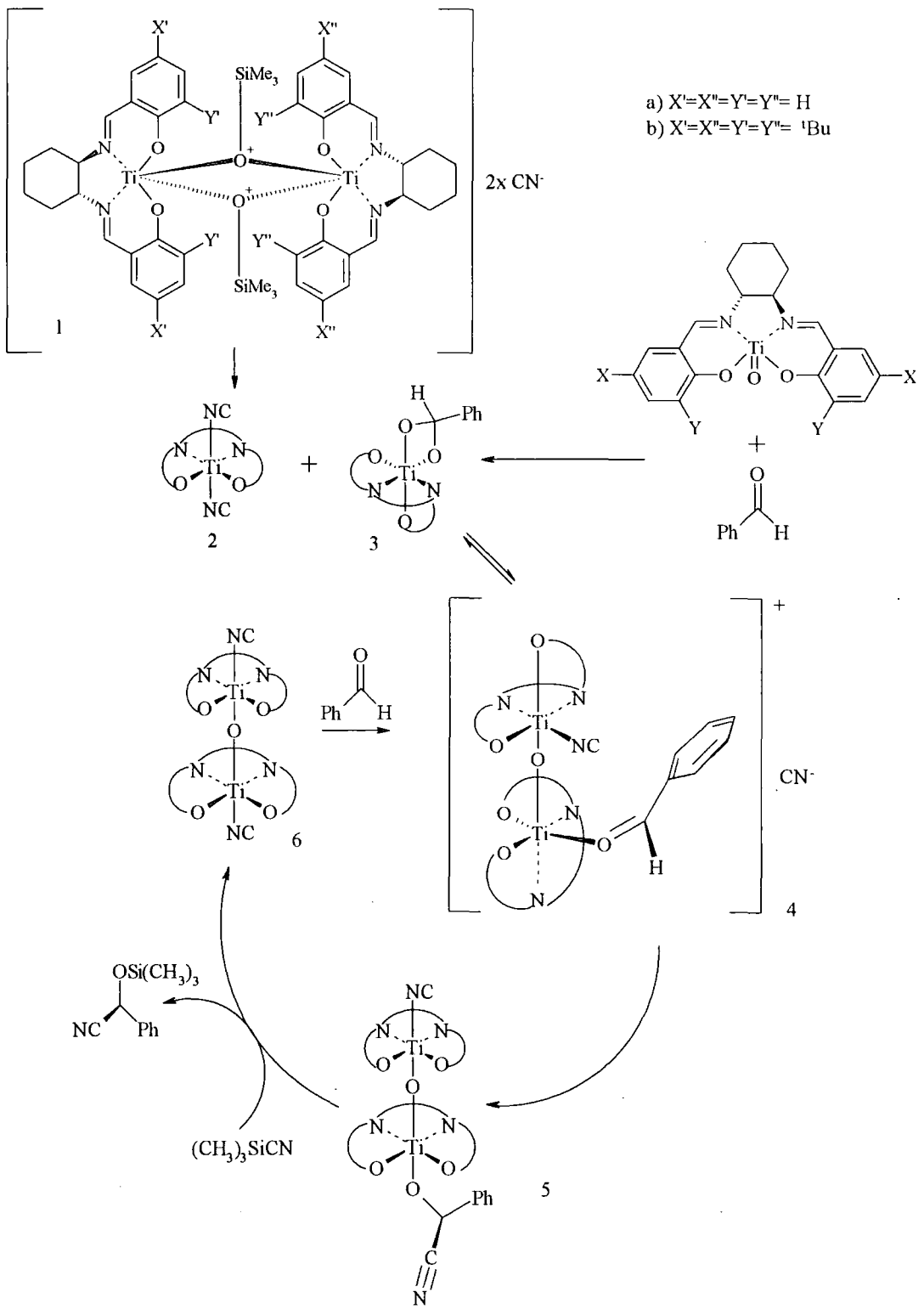

Combination of **2** and **3** leads to a product, **4**, a binuclear complex, featuring an activated aldehyde and a titanium-cyanide bond. Intramolecular rearrangement adds the cyanide onto the aldehyde to form a new structure, **5**, bearing a cyanohydrin bound to the titanium

Reaction with TMSCN generates the product and regenerates a dinuclear cyanide complex, **6**, which on reaction with benzaldehyde can re-form directly the 'activated aldehyde' structure, **4**.

It is worth mentioning that a vanadium (IV)[75] derivative has also been used and proved to be more enantioselective than the titanium based complex.

1.4.3 Catalytic asymmetric Mannich reaction

Several studies have reported asymmetric syntheses of Mannich bases, using chiral auxiliaries[76] and catalysts[77], for the addition of preformed enolates and enamines to preformed imines. However the preformed enolates are not always readily synthesisable and can be unstable. Therefore a catalysed direct approach (carbonyl + amine + acidic substrate) to the reaction is generally preferred.

The catalysts used can be either organometallic complexes[78] or metal-free organic compounds[79]. Examples are shown in Scheme 1.37.

Scheme 1.37

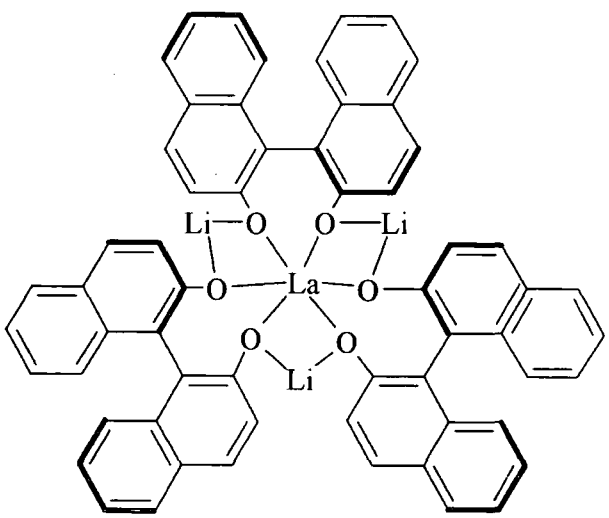

$LaLi_3$tris(binaphthoxide) LLB[80]

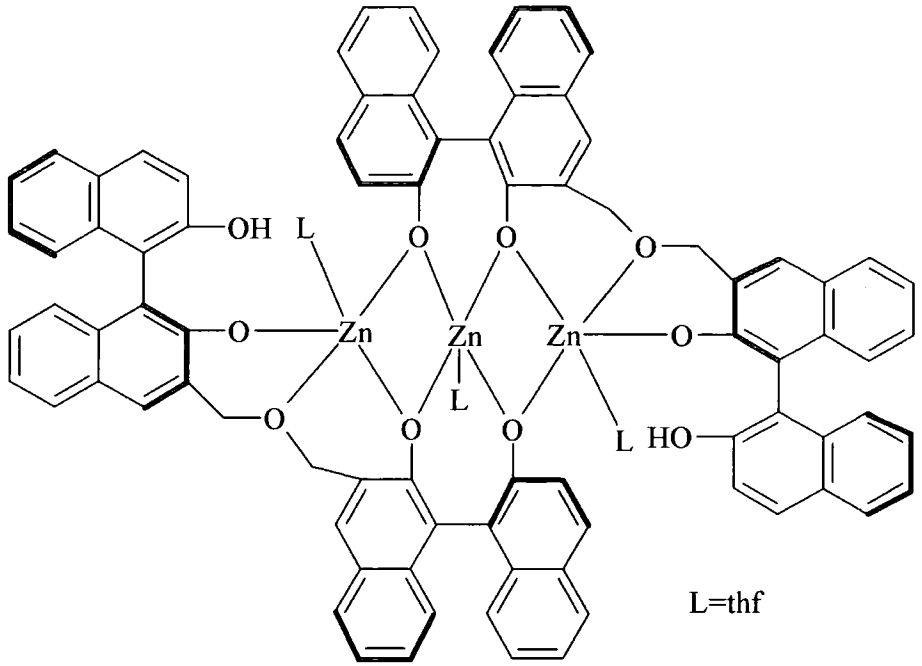

Et_2Zn/linked-BINOL complex[81]

Shibasaki et al. investigated the mechanism for the direct Mannich reaction using the BINOL complex and N-diphenylphosphinoyl-protected imines. The transition state below was proposed.

Scheme 1.38

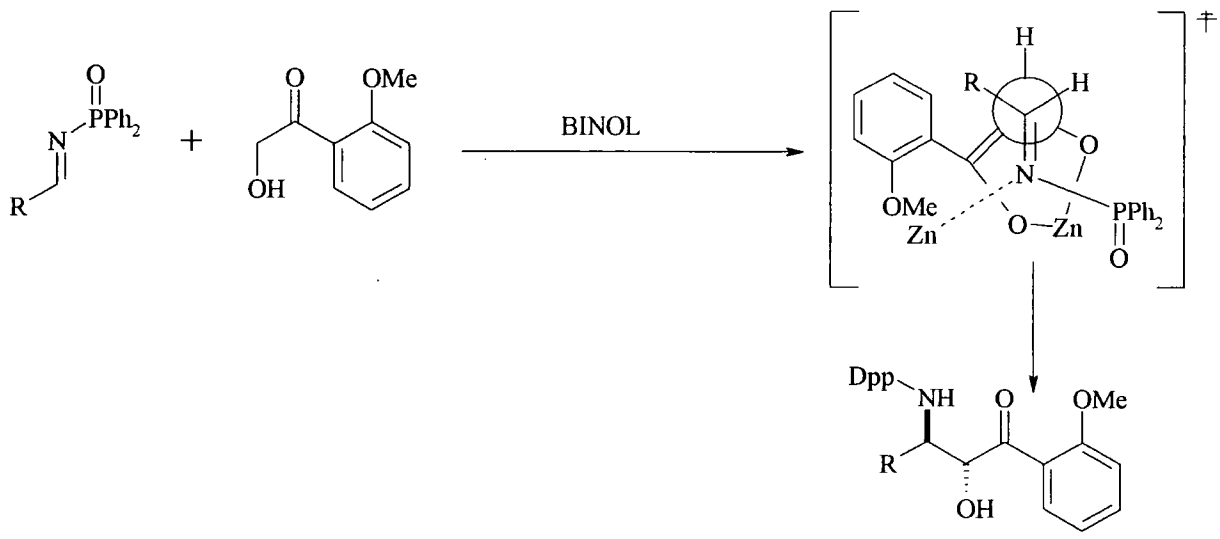

1.4.4 Catalytic asymmetric Strecker reaction

There have been several investigations of the catalytic asymmetric Strecker reaction in the past ten years. In 1996 Lipton and co-workers[82] adapted Inoue's catalyst[69a,d] for the asymmetric formation of cyanohydrin shown in Scheme 1.39 to the addition of cyanide to imines.

Scheme 1.39

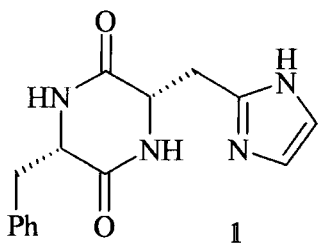

1

Cyanohydrin catalyst

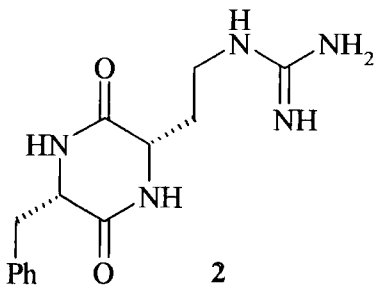

2

Strecker catalyst

It is worth noting that the imidazole catalyst, **1**, did not exhibit any catalytic effect towards the Strecker reaction but derivatisation to structure **2,** which bears a more basic guanidine function, yielded an efficient catalyst.

Using 2 mol% of the catalyst, **2**, Lipton et al. reported the addition of hydrogen cyanide onto N-Benzhydrylimines derived from aromatic aldehydes. The catalyst was used with the preformed imine since the direct reaction with the aldehyde, the amine and cyanide yields a racemic mixture. Results for the conversion to benzhydryl-α-aminonitriles showed good enantiomeric excesses. However reactions of imines derived from aliphatic aldehydes and from electron deficient (namely 3-nitro and 3-pyridyl) aromatic aldehydes only afforded racemic products.

Corey[83] also used a guanidine derivative to catalyse the addition of cyanide to preformed imines. His C_2-symmetric structure yielded high conversion and enantiomeric excess. The catalytic cycle includes only 3 steps and the mechanism may also apply to Lipton's catalyst (Scheme 1.40).

In a first step the hydrogen cyanide binds to the catalyst. The imine is then added by hydrogen bonding to the guanidine structure leading to a reactive structure where attack by the cyanide ion affords the products.

Scheme 1.40

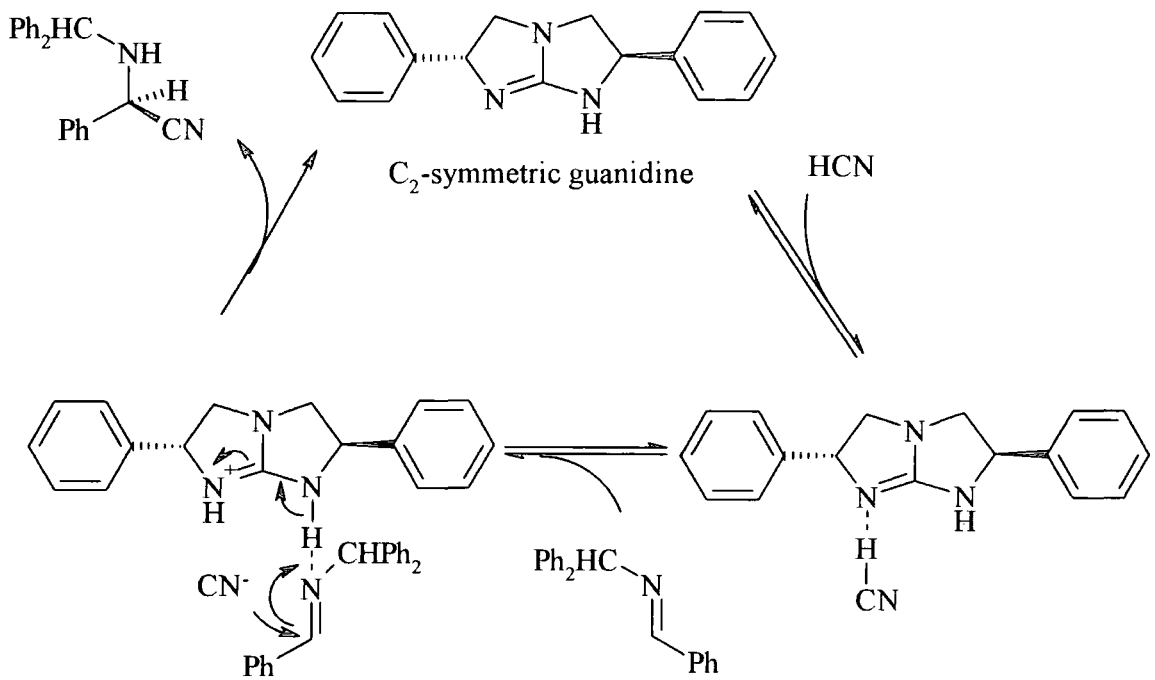

The three-dimensional arrangement in the transition state is such that cyanide is positioned to attack the *re* face of the imine allowing the major formation of the (R) enantiomer. Although this is true for the benzhydryl derivatives, imines formed from aliphatic aldehydes exhibit a different spatial arrangement and the main enantiomer is (S).

Schiff bases can also be used as catalysts. Sigman and Jacobsen used a salicylimine catalyst for the reaction of aromatic and aliphatic imines with cyanide (Scheme 1.41). The reaction gives good yields and significant enantiomeric excesses. Moreover the Schiff base can be bound to a polystyrene resin making the extraction of the products easier.

Here the enantioselectivity can be accounted for by the presence of the bulky ter-butyl groups.

As with other asymmetric reactions, organometallic catalysts have also been used to enhance the Strecker reaction and the formation of aminonitriles.

Scheme 1.41

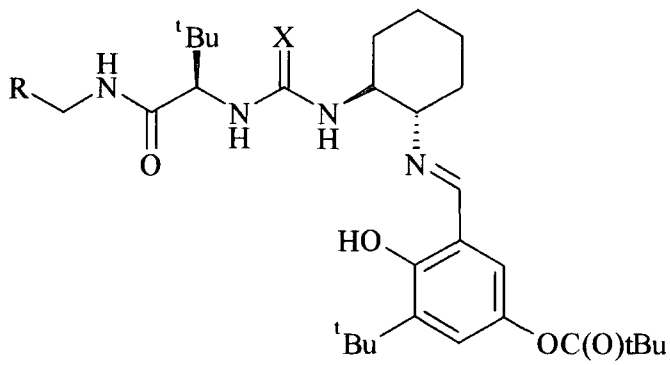

a) R = Ph and X = O
b) R = Polystyrene and X = S

Sigman and Jacobsen first reported a metal-based catalyst for the Strecker reaction[84]. They used the Salen ligand previously mentioned in the asymmetric synthesis of cyanohydrins (Part 1.4.2).

After screening different metals it appeared that the Al (III) complex was the best catalyst for the reaction of HCN with N-allyl imines affording yields between 91 and 99% with enantiomeric excesses ranging from 35 to 99% (Scheme 1.42).

Scheme 1.42

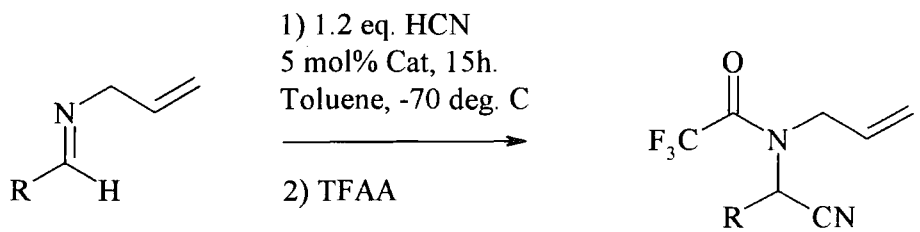

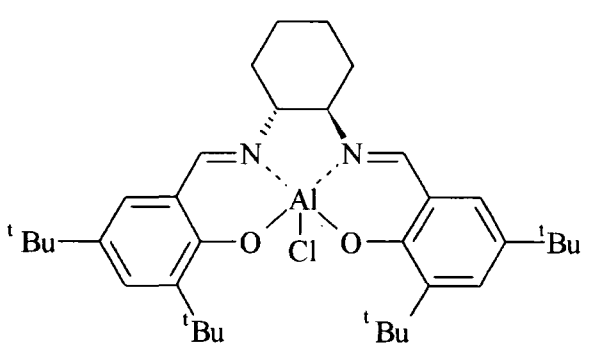

Salen Al(III) catalyst

Snapper and Hoveyda[85] used a salicylimine Schiff base ligand together with titanium isopropoxide to catalyse the cyanilation of imines as shown in Scheme 1.43. Interestingly they found that when using TMSCN as the cyanide source, both the yields and the enantioselectivity were enhanced by the slow addition of an alcohol. This suggests that HCN, formed from the slow reaction between the alcohol and TMSCN, is involved in the reaction.

Scheme 1.43

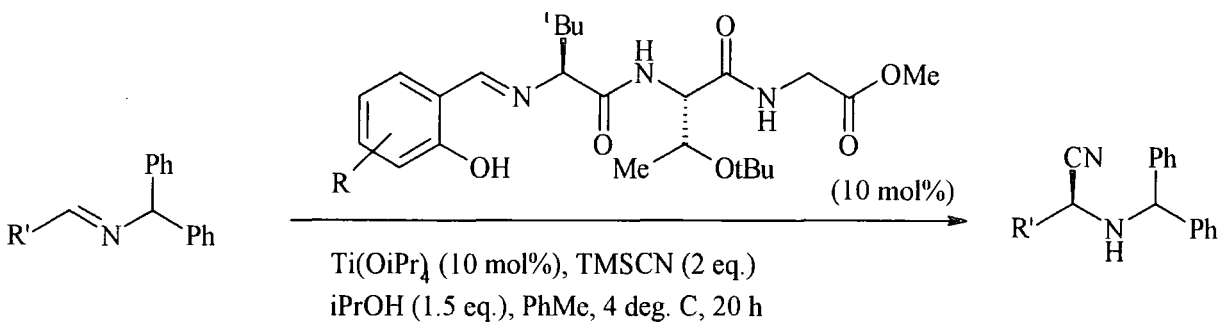

Also of interest for the asymmetric catalysis of the Strecker reaction are a zirconium catalyst developed by Kobayashi and co-workers[86] (Scheme 1.44) and a scandium $(BINOL)_2Li$ complex[87] (Scheme 1.45).

Scheme 1.44

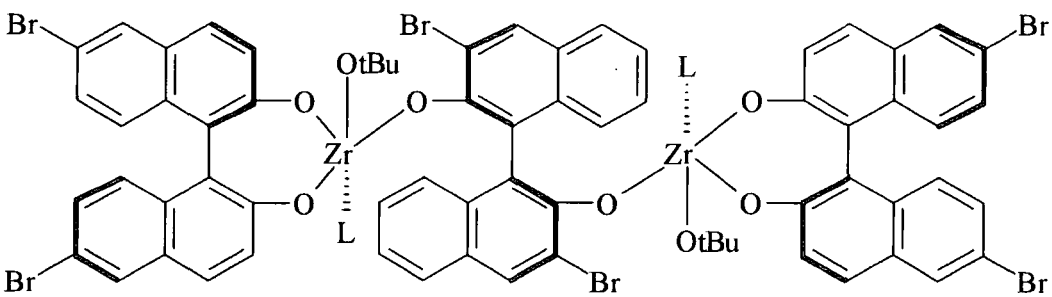

Scheme 1.45

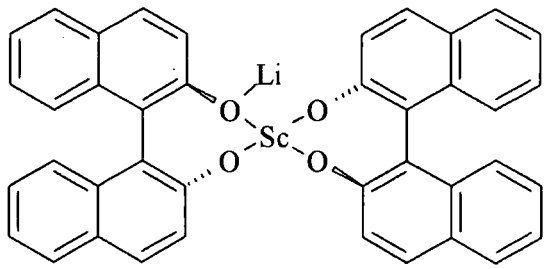

Finally it is worth mentioning Shibasaki's bifunctional Lewis acid-Lewis base catalyst (Scheme 1.46) for the reactions of N-fluorenylimines with TMSCN[88]. Here the enantioselective catalysis appears to be due to the simultaneous activation of imines by the Lewis acid and the activation of the trimethylsilyl group by the oxygen atom of the phosphane oxide.

Scheme 1.46

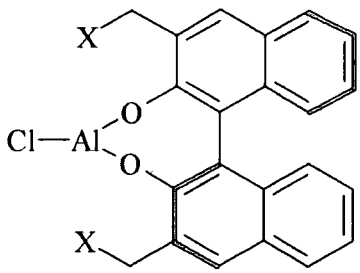

1. X = $P(O)Ph_2$
2. X = $CHPh_2$

1.5 Aims

A major aim of the project is to obtain mechanistic understanding of the catalysis of the Strecker reaction, so that asymmetric products may be obtained.

The three basic constituents for the formation of an α-aminonitrile are a carbonyl group, an amine and cyanide. For the purpose of this work benzaldehyde has been chosen as our carbonyl compound since it absorbs strongly in the ultraviolet region hence facilitating spectrophotometric measurements. Sources of cyanide included potassium cyanide (KCN) and trimethylsilyl cyanide (TMSCN). As for the amines benzylamine and allylamine were preferred.

Taillades and Commeyras[3b] showed that α-aminonitriles formation proceeds through two successive steps with the iminium ion being the main intermediate. The cyanohydrin is also formed although it is just a product of competition between the cyanide and the amine for the carbonyl compound.

This study therefore aims to report on various aspects of the Strecker reaction:

- 1) The addition reaction on benzaldehyde: namely the formation of cyanohydrin but also the addition of bisulfite so the equilibrium constants for the two nucleophiles can be compared.

- 2) The cyanilation of the imine: a kinetic study of the addition of cyanide (from potassium cyanide in aqueous buffers) onto the two preformed imines mentioned above. This enables the calculation of the equilibrium constant for the formation of aminonitriles as well as the acid dissociation constant for the respective iminium ions and aminonitriles.

- 3) The hydrolysis of the imine: as this is an important side-reaction, kinetics were measured so that the pH profile for the decomposition of the imines in water can be

drawn and another estimate of the acid dissociation constant for the iminium ions calculated.

- 4) The addition product of the reaction of trifluoroacetic anhydride (TFAA) with imines: TFAA has been used to derivatise α-aminonitriles[84]. Incidentally it proves a useful tool for separating the enantiomers in chiral gas chromatography. However reaction with the imines is possible. The interaction between the Schiff base and the anhydride will be considered and the adduct questioned as to whether it promotes the addition of cyanide or not.

- 5) The catalysed asymmetric addition of cyanide to imines: the asymmetric Strecker reaction will be studied using a salen complex as catalyst. Various methods for the separation of the enantiomers will be discussed. The reaction parameters (concentrations, time, and temperature) will be reviewed and discussed.

1.6 References

1. M. Tramontini and L. Angiolini, *Tetrahedron*, 1990, **46**, 1791

2. A. Strecker, *Liebigs Ann. Chem.*, 1850, **75**, 27

3. (a) J. Taillades and A. Commeyras, *Tetrahedron*, 1974, **30**, 127; (b) J. Taillades and A. Commeyras, *Tetrahedron*, 1974, **30**, 2493; (c) A. Commeyras, J. Taillades L. Mion and M. Béjaud, *Informations chimie*, 1976, **158**, 199

4. W. P. Jencks, *Progr. Phys. Org. Chem.*, 1964, **2**, 63

5. L. Yet, *Angew. Chem. Int. Ed.*, 2001, **40**, 875

6. (a) H. B. Bürgi, J. D. Dunitz and E. Shefter, *J. Am. Chem. Soc.*, 1973, **95**, 5065; (b) H. B. Bürgi, J. D. Dunitz, J. M. Lehn and G. Wipff, *Tetrahedron*, 1974, **30**, 1563

7. (a) W. A. Sheppard and A. N. Bourns, *Can. J. Chem.*, 1954, **32**, 4; (b) C. N. Caughlan and H. V. Tarter, *J. Am. Chem. Soc.*, 1941, **63**, 1265; (c) R. L. Shriner and A. H. Land, *J. Org. Chem.*, 1941, **6**, 888; (d) W. M. Lauer and C. M. Langkammerer, *J. Am. Chem. Soc.*, 1935, **57**, 2360

8. P. R. Young and W. P. Jencks, *J. Am. Chem. Soc.*, 1977, **9**, 8238

9. T. D. Stewart and L. H. Donally, *J. Am. Chem. Soc.*, 1932, **54**, 3559

10. P. R. Young and W. P. Jencks, *J. Am. Chem. Soc.*, 1978, **100**, 1228

11. (a) T. H. Lowry and K. S. Richardson, *Mechanism and Theory in Organic Chemistry*, Harper & Row, New York, 2nd Ed., 1981, p. 614; (b) F. C. Kokesh and R. E. Hall, *J. Org. Chem.*, 1975, **40**, 1632

12. A. Lapworth, *J. Chem. Soc.*, 1903, **83**, 995

13. W. J. Svirbely and J. F. Roth, *J. Am. Chem. Soc.*, 1953, **75**, 3106

14. (a) V. Prelog and M. Wilhelm, *Helv. Chim. Acta*, 1954, **37**, 1634; (b) H. Hustedt and E. Pfeil, *Justus Liebigs Ann Chem.*, 1961, **640**, 15

15. W.-M. Ching and R. G. Kallen, *J. Am. Chem. Soc.*, 1978, **100**, 6119

16. (a) J. P. Kuebrich, R. L. Schowen, M. S. Wang and M. E. Lupes, *J. Am. Chem. Soc.*, 1971, **93**, 1214; (b) Ref 13(b)

17. A. Lapworth and R. H. F. Manske, *J. Chem. Soc.*, 1930, 1976

18. (a) Naquet and V. Louguinine, *Ann.*, 1866, **139**, 299; (b) Wallach, *Ann.*, 1878, **193**, 38; (c) Spiegel, *Ber.*, 1881, **14**, 239; (d) Ultee, *Rec. Trav. Chim.*, 1909, **28**, 254; (e) Rule, *J. Chem. Soc.*, 1918, **113**, 12

19. Wood and Lilley, *J. Chem. Soc.*, 1925, **127**, 95

20. (a) B. Capon, *Org. React. Mech.*, 1975, 1; (b) M. M. Sprung, *Chem. Rev.*, 1940, **26**, 297; (c) Ref. 4; (d) R. Bonnet, *The Chemistry of the Carbon Nitrogen Double Bond*, Ed. S. Patai, Interscience, London, 1970, p. 64

21. H. Schiff, *Ann.*, 1864, **131**, 118

22. (a) R. G. Kallen, R. O. Viale and L. K. Smith, *J. Am. Chem. Soc.*, 1972, **94**, 576; (b) L. M. C. Brighente, L. R. Vottero, A. J. Terezani and R. A. Yunes, *J. Phys. Org. Chem.*, 1991, **4**, 107; (c) I. M. C. Brighente and R. A. Yunes, *J. Braz. Chem. Soc.*, 1997, **8**, 549; (d) R. Wolfenden and W. P. Jencks, 1961, **83**, 2763; (e) J. M. Sayer, B. Pinsky, A. Schonbrunn, and W. Washtien, 1974, **96**, 7998

23. R. G. Kallen and W. P. Jencks, *J. Biol. Chem.*, 1966, **241**, 5864

24. (a) E. E. Snell and W. T. Jenkins, *J. Cell. Comp. Physiol.*, 1959, **54**, 161; (b) D. E. Metzler, M. Ikawa and E. E. Snell, *J. Am. Chem. Soc.*, 1954, **76**, 648; (c) G. A. Hamilton and F. H. Westheimer, *J. Am. Chem. Soc.*, 1959, **81**, 6332; (d) W. P. Jencks, *Catalysis in Chemistry and Enzymology*, Dover, New York, 1987; (e) A. E. Braunstein, *The Enzymes*, Vol. 2, Eds P. D. Boyer, H. Lardy and K. Myrback, Academic Press, Inc., New York, 1960, p.113; (f) E. E. Snell, *The Mechanism of Action of Water-soluble Vitamins*, Little, Brown and Co., Boston, Mass., 1961, p.18; (g) I. Fridovich and F. H. Westheimer, *J. Am. Chem. Soc*, 1962, **84**, 3208; (h) E. Grazi, T. Cheng and B. L. Horecker, *Biochem. Biophys. Res. Comm.*, 1962, 7, 250; (i) E. Grazi, P. T. Rowley T. Cheng, O. Tchola and B. L. Horecker, *Biochem. Biophys. Res. Comm.*, 1962, **9**, 38; (j) R. A. Morton and G. A. J. Pitt, *Progr. Chem. Org. Nat. Prod.*, 1957, **14**, 244; (k) R. Hubbard, *Proc. Natl. Phys. Lab.*, London, *Symp. No. 8*, 1958, 151

25. F. Texier-Boullet, *Synthesis*, 1985, 679

26. (a) S. J. Benkovic, P. A. Benkovic and D. R. Comfort, *J. Am. Chem. Soc.*, 1969, **91**, 1860; (b) J. W. Stanley, J. G. Beansley and I. W. Mathison, *J. Org. Chem.*, 1972, **37**, 3746

27. S. F. Dyke, *The Chemistry of Enamines*, Cambridge University Press, London, 1973

28. (a) D. Craig, L. Schaefgen and W. P. Tyler, *J. Am. Chem. Soc.*, 1948, **70**, 1624; (b) G. O. Dudek and R. H. Holm, *J. Am. Chem. Soc.*, 1961, **83**, 3914; (c) T. M. Patrick, Jr., *J. Am. Chem. Soc.*, 1952, **74**, 2984; (d) M. Saunders and E. H. Gold, *J. Org. Chem.*, 1962, **27**, 1439

29. R. Mc Crindle and A. J. Mc Alees, *J. Chem. Soc., Chem. Comm.*, 1983, 61

30. R. W. Layer, *Chem. Rev.*, 1963, **63**, 489

31. F. Sachs and P. Steinert, *Chem. Ber.*, 1904, **37**, 1733

32. E. Barrett and A. Lapworth, *J. Chem. Soc.*, 1908, **93**, 85; (b) J. B. Conant and P. D. Bartlett, *J. Am. Chem. Soc.*, 1932, **54**, 2881; (c) A. Ölander, *Z. Physik. Chem. (Leipzig)*, 1927, **129**, 1; (d) F. H. Weistheimer, *J. Am. Chem. Soc.*, 1934, **56**, 1962; (e) J. Hine, J. P. Ziegler and

M. Johnson, *J. Org. Chem.*, 1979, **44**, 3540; (f) W. P. Jencks, *J. Am. Chem. Soc.*, 1959, **81**, 475; (g) B. M. Anderson and W. P. Jencks, *J. Am. Chem. Soc.*, 1960, **82**, 1773; (h) E. H. Cordes and W. P. Jencks, *J. Am. Chem. Soc.*, 1962, **84**, 832; (i) Ref 4

33. L. P. Hammett, *Physical Organic Chemistry*, McGraw-Hill, New York, 1940, p.331

34. (a) Ref. 31f-i; (b) A. S. Stachissini and L. do Amaral, *J. Org. Chem.*, 1991, **56**, 1419; (c) J. E. Reimann and W. P. Jencks, *J. Am. Chem. Soc.*, 1966, **88**, 3973

35. (a) Ref. 31a, b, f, h; (b) L. do Amaral, W. A. Sandstrom and E. H. Cordes, *J. Am. Chem. Soc.*, 1966, **88**, 2225; (c) A. Williams and L. Bender, *J. Am. Chem. Soc.*, 1966, **88**, 2508; (d) E. H. Cordes and W. P. Jencks, *J. Am. Chem. Soc.*, 1962, **84**, 4319; (e) D. H. R. Barton, R. E. O'Brien and S. Sternhall, *J. Chem. Soc.*, 1962, 470

36. (a) N. E. Hall and B. J. Smith, *J. Phys. Chem.*, 1998, **102A**, 4930; (b) I. H. Williams, *J. Am. Chem. Soc.*, 1987, **109**, 6299; (c) M. Eigen, *Disc. Faraday Soc.*, 1965, **39**, 7; (d) R. P. Bell, *Advances in Physical Organic Chemistry*, Vol. 4, Ed. V. Gold, Acad Press, London, 1966

37. (a) Ref 21e; (b) S. Rosenberg, S. M. Silver, J. M. Sayer and W. P. Jencks, *J. Am. Chem. Soc.*, 1974, **96**, 7986; (c) J. Hine, F. A. Via, J. K. Gotkis and J. C. Craig, Jr., *J. Am. Chem. Soc.*, 1970, **92**, 5186; (d) J. M. Sayer and W. P. Jencks, *J. Am. Chem. Soc.*, 1972, **94**, 3262; (e) H. Diebler and R. N. F. Thorneley, *J. Am. Chem. Soc.*, 1973, **95**, 896

38. R. G. Kallen, *J. Am. Chem. Soc.*, 1971, **93**, 6236

39. E. H. Cordes and W. P. Jencks, *J. Am. Chem. Soc.*, 1962, **84**, 826

40. (a) M. Calzadilla, A. Malpica and P. M. Diaz, *Int. J. Chem. Kinetics*, 1996, **28**, 687; (b) A. Malpica, M. Calzadilla, J. Baumrucker, J. Jimenez, L. Lopez, G. Escobar and C. Montes, *J. Org. Chem.*, 1994, **59**, 3398; (c) P. Sojo, F. Viloria, L. Malave, R. Possamai, M. Calzadilla, J. Baumrucker, A. Malpica, R. Moscovici, L. Doamaral, *J. Am. Chem. Soc.*, 1976, **98**, 4519

41. (a) Ref 37; (b) Ref 4; (c) J. M. Sayer, M. Peskin and W. P. Jencks, *J. Am. Chem. Soc.*, 1973, **95**, 4277; (d) J. M. Sayer and W. P. Jencks, *J. Am. Chem. Soc.*, 1973, **95**, 5637; (e) E. H. Cordes and W. P. Jencks, *J. Am. Chem. Soc.*, 1963, **85**, 2843

42. (a) Ref. 31 h; (b) Ref 40 d; (c) Ref 4; (d) K. Koehler, W. Sandstrom and E. H. Cordes, *J. Am. Chem. Soc.*, 1964, **86**, 2413

43. (a) Ref 31 h; (b) Ref 40 e; Ref 41 d; (d) W. P. Jencks, *Catalysis in Chemistry and Enzymology*, Dover, New York, 1987, p.460; (e) M. A. E. D. El Taher, *J. Solution. Chem.*, 1996, **25**, 401; (f) M. Brault, R. M. Pollack and C. L. Bevins, *J. Org. Chem.*, 1976, **41**, 346

44. (a) Ref 40 d; (b) R. L. Reeves, *J. Am. Chem. Soc.*, 1962, **84**, 3332

45. S. Eldin, J. A. Digits, S.-T. Huang and W. P. Jencks, *J. Am. Chem. Soc.*, 1995, **117**, 6631

46. S. Eldin and W. P. Jencks, *J. Am. Chem. Soc.*, 1995, **117**, 4851

47. (a) Ref 1; (b) F. F. Blicke, *Organic Reactions*, Wiley, New York, 1942, **1**, p. 303; (c) H. O. House, *Modern Synthetic Reactions*, 2nd Ed., W. A. Benjamin, New York, 1972, p. 654; (d) K. Bodendorf and G. Koralewski, *Arch. Pharm.*, 1933, **271**, 101; (e) S. V. Lieberman and E. C. Wagner, *J. Org. Chem.*, 1949, **14**, 1001; (f) M. Tramontini, *Synthesis*, 1973, 703; (g) M. Arend, B. Westermann and N. Risch, *Angew. Chem. Int. Ed.*, 1998, **37**, 1044

48. (a) E. R. Alexander and E. J. Underhill, *J. Am. Chem. Soc.*, 1949, **71**, 4014; (b) J. E. Fernandez and J. S. Fowler, *J. Org. Chem.*, 1964, **29**, 402; (c) M. Masui, K. Fujita and H. Ohmori, *Chem. Comm.*, 1970, **13**, 182; (d) H. Volz and H. H. Kiltz, *Tetrahedron Lett.*, 1970, **22**, 1917

49. T. F. Cummings and J. R. Shelton, *J. Org. Chem.*, 1960, **25**, 419

50. (a) Ref 1; (b) M Tramontini, L. Angiolini and N. Ghedini, *Polymer*, 1988, **29**, 771

51. (a) H. Bungaard, *Methods in Enzymology*, 1985, **112**, 347; (b) J. R. Dimmock, S. K. Raghavan, B. M. Logan and G. E. Bigam, *Eur. J. Med. Chem.*, 1983, **18**, 249; (c) P. Traxler, U. Trinks et al., *J. Med. Chem.*, 1995, **38**, 2441; (d) J. R. Dimmock, K. K. Sidhu, M. Chen, R. S. Reid, T. M. Allen, G. Y. Kao and G. A. Truitt, *Eur. J. Med. Chem.*, 1993, **28**, 313

52. (a) H. Kunz and W. Pfrengle, *Angew. Chem.*, 1989,**101**, 1041; (b) L. S. Liebeskind, M. E. Welker and R. W. Fengl, *J. Am. Chem. Soc.*, 1986, **108**, 6328; (c) L. S. Liebeskind, M. E. Welker and V. Goedken, *J. Am. Chem. Soc.*, 1984, **106**, 441; (d) K Broadley and S. G. Davies, *Tetrahedron Lett.*, 1984, **25**, 1743

53. (a) D. Enders, D. Ward, J. Adam and G. Raabe, *Angew. Chem. Int. Ed.*, 1996, **108**, 1059; (b) H. J. Bestmann and G. Wölfel, *Angew. Chem.*, 1984, **23**, 53; (c) K. Okano, T. Moritomo and M. Sekiya, *J. Chem. Soc. Chem. Commun.*, 1984, 883

54. (a) E. F. Kleinman, *Comprehensive Organic Synthesis*, Pergamon, Oxford, 1991, p.893; (b) E. Winterfeldt, *J. Prakt. Chem.*, 1994, **336**, 91; (c) R. P. Polniaszek and S. J. Bell, *Tetrahedron Lett.*, 1996, **37**, 575; (d) S. K. Panday, D. Griffart-Brunet and N. Langlois, *Tetrahedron Lett.*, 1994, **35**, 6673

55. (a) M. Béjaud, L. Mion, J. Taillades and A. Commeyras, *Tetrahedron*, 1975, **31**, 403; (b) R. M. Williams, *Synthesis of Optically Active α-Amino Acids*, Pergamon Press, New York, 1989, p.208

56. (a) D. T. Mowry, *Chem. Rev.*, 1948, **42**, 326; (b) T. D. Stewart and C. H. Li, *J. Am. Chem. Soc.*, 1938, **60**, 2782; (c) K. Harada and S. W. Fox, *Naturwiss*, 1964, **51**, 6

57. Y. Ogata and A. Kawasaki, *J. Chem. Soc. B*, 1971, 325

58. (a) Ref 3; (b) J. Taillades and A. Commeyras, *Tetrahedron*, 1974, **30**, 3407; (c) M. Béjaud, L. Mion and A. Commeyras, *Bull. Soc. Chim.*, 1976, 1425

59. G. Moutou, J. Taillades, S. Benefice-Malouet, A. Commeyras, G. Messina and R. Mansani, *Phys. Org. Chem.*, 1995, **8**, 721

60. G. Blaschke, H. P. Kraft, K. Fickentscher and F. Köhler, *Arzneim. Forsch.*, 1979, **29**, 1640

61. W. Marckwald, *Ber.*, 1904, **37**, 1368

62. S. Mosher and J. D. Morrison, *Asymmetric Organic Reactions*, Prentice Hall, ACS Washington DC, 1971, p.1

63. (a) H. Nozaki, S. Moriuti, H. Takaya and R. Noyori, *Tetrahedron Lett.*, 1966, 5239; (b) H. Nozaki, H. Takaya, S. Moriuti and R. Noyori, *Tetrahedron*, 1968, **24**, 3655

64. W. S. Knowles and M. J. Sabacky, *Chem. Commun.*, 1968, 1445

65. W. S. Knowles, *Acc. Chem. Res.*, 1983, **16**, 106

66. P. Ahlberg, *Advanced Information on the Nobel Prize in Chemistry 2001*, http://www.nobel.se/chemistry/laureates/2001/chemadv.pdf

67. (a) W. Becker and E. Pfeil, *Angew. Chem. Int. Ed. Engl.*, 1965, **4**, 1079; (b) U. Niedermeyer and M.-R. Kula, *Angew. Chem. Int. Ed. Engl.*, 1990, **29**, 386; (c) F. Effenberger, B. Horsh, S. Forster and T. Ziegler, *Tetrahedron Lett.*, 1990, **31**, 1249

68. (a) S. Tsuboyama, *Bull. Chem. Soc. Jpn.*, 1962, **35**, 1004; (b) S. Tsuboyama, *Bull. Chem. Soc. Jpn.*, 1965, **38**, 354; (c) H. Danda, K. Chino and S. Wake, *Chem. Lett.*, 1991, 731; (d) H. J. Kim and W. R. Jackson, *Tetrahedron Asymmetry*, 1992, **3**, 1421

69. (a) J. Oku, N. Ito and S. Inoue, *Makromol. Chem.*, 1979, **180**, 1089; (b) W. R. Jackson, G. S. Jayatilake, B. R. Matthews and C. Wilshire, *Aust. J. Chem.*, 1988, **41**, 203; (c) B. R. Matthews, W. R. Jackson, G. S. Jayatilake, C. Wilshire and H. A. Jacobs, *Aust. J. Chem.*, 1988, **41**, 1697; (d) A. Mori, Y. Ikeda, K. Kinoshita and S. Inoue, *Chem. Lett.*, 1989, 2119

70. K. Narasaka, T. Yamada and H. Minamikawa, *Chem. Lett.*, 1987, 2073

71. M. Hayashi, T. Matsuda and N. Oguni, *J. Chem. Soc, Chem. Comm.*, 1990, 1364

72. Examples include: (a) M. T. Reetz, S.-H. Kyung C. Bolm and T. Zierke, *Chem. Ind.*, 1986, 824; (b) H. Nitta, D. Yu, M. Kudo, A. Mori and S. Inoue, *J. Am. Chem. Soc.*, 1992, **14**, 7969; (c) S. Kobayashi, Y. Tsuchiya and T. Mukaiyama, *Chem. Lett.*, 1991, 541; (d) Y. Jiang, L. Z. Gong, X. M. Feng, W. H. Hu, W. D. Pan, Z. Li and A. Q. Mi, *Tetrahedron*, 1997, **53**, 14327; (e) Z.–H. Yang, L. X. Wang, Z. H. Zhou, Q. L. Zhou and C.-C. Tang, *Tetrahedron Asymmetry*, 2001, **12**, 1579; (f) Y. Hamashima, M. Kanai and M. Shibasaki, *Tetrahedron Lett.*, 2001, **42**, 691; (g) Y. Hamashima, M. Kanai and M. Shibasaki, 2000, **122**, 7412

73. (a) Y. Belokon, M. Flego, N. Ikonnikov, M. Moscalenko, M. North, C. Orizu, V. Tararov and M. Tasinazzo, *J. Chem. Soc., Perkin Trans. 1*, 1997, 1293; (b) V. I. Tararov, D. E. Hibbs, M. B. Hursthouse, N. S. Ikonnikov, K. M. A. Malik, M. North, C. Orizu and Y. Belokon, *Chem. Commun.*, 1998, 387; (c) Y. N. Belokon, B. Green, N. S. Ikonnikov, M. North, and V. Tararov, *Tetrahedron Lett.*, 1999, **40**, 8147; (d) Y. N. Belokon, S. Caveda-Cepas, B. Green, N. S. Ikonnikov, V. N. Krustalev, V. S. Larichev, M. A. Moscalenko, M. North, C. Orizu, V. I. Tararov, M. Tasinazzo, G. I. Timofeeva and L. V. Yashkina, *J. Am. Chem. Soc.*, 1999, **121**, 3968; (e) Y. Belokon, B. Green, N. S. Ikonnikov, M. North, T. Parsons and V. I. Tararov, *Tetrahedron*, 2001, **57**, 771; (f) Y. Belokon, P. Carta, A. V. Gutnov, V. Maleev, M. A. Moskalenko, L. V. Yashkina, N. S. Ikonnikov, N. V. Voskoboev, V. N. Khrustalev and M. North, *Helvetica Chimica Acta*, 2002, **85**, 3301

74. Y. Belokon, B. Green, N. S. Ikonnikov, V. S. Larichev, B. V. Lokshin, M. A. Moscalenko, M. North, C. Orizu, A. S. Peregudov and G. I. Timofeeva, *Eur. J. Org. Chem.*, 2000, 2655

75. Y. Belokon, M. North and T. Parsons, *Org. Lett.*, 2000, **2**, 1617

76. (a) D. Seebach and M. Hoffmann, *Eur. J. Org. Chem.*, 1998, 1337; (b) Y. Aoyagi, R. P. Jain and R. M. Williams, *J. Am. Chem. Soc.*, 2001, **123**, 3472; (c) D. A. Evans, F. Urpi, T. C. Somers, J. S. Clark and M. T. Bilodeau, *J. Am. Chem. Soc*, 1990, **112**, 8215; (d) C. Palomo,

M. Oiarbide, A. Landa, M. C. Gonzalez-Rego, J. M. Garcia, A. Gonzalez, J. M. Odriozola, M. Martin-Pastor and A. Linden, *J. Am. Chem. Soc.*, 2002, **124**, 8637

77. (a) H. Ishitani, S. Ueno and S. Kobayashi, *J. Am. Chem. Soc.*, 2000, **122**, 8180; (b) A. Fujii, E. Hagiwara and M. Sedona, *J. Am. Chem. Soc.*, 1999, **121**, 545; (c) D. Ferraris, B. Young, C. Cox, T. Dudding, W. J. Drury, L. Ryzhkov, A. E. Taggi and T. Lectka, *J. Am. Chem. Soc.*, 2002, **124**, 67; (d) G. A. Wenzel and E. N. Jacobsen, *J. Am. Chem. Soc.*, 2002, **124**, 12964

78. (a) B. M. Trots and H. Ito, *J. Am. Chem. Soc.*, 2000, **122**, 12003; (b) K. Juhl, N. Gathergood and K. A. Jørgensen, *Angew. Chem. Int. Ed.*, 2001, **40**, 2995

79. (a) B. List, *J. Am. Chem. Soc.*, 2000, **122**, 9336; (b) B. List, P. Pojarliev, W. T. Biller and H. J. Martin, *J. Am. Chem. Soc.*, 2002, **124**, 827; (c) W. Notz, K. Sakthivel, T. Bui, G. F. Zhong and C. F. Barbas, *Tetrahedron Lett.*, 2001, **42**, 199; (d) C. F. Barbas, S. Watanabe, F. Tanaka, W. Notz and A. Córdova, *J. Am. Chem. Soc.*, 2002, **124**, 1866

80. S. Yamasaki, T. Iida and M. Shibasaki, *Tetrahedron Lett.*, 1999, **40**, 307

81. (a) S. Matsunaga, N. Kumagai, S. M. Harada and M. Shibasaki, *J. Am. Chem. Soc.*, 2003, **125**, 4712; (b) N. Kumagai, S. Matsunaga, T. Kinoshita, S. Harada, S. Okada, S. Sakamoto, K. M. Yamaguchi and M. Shibasaki, *J. Am. Chem. Soc.*, 2003, **125**, 2169

82. (a) M. S. Iyer, K. M. Gigstad, N. D. Namdev and M. Lipton, *J. Am. Chem. Soc.*, 1996, **118**, 4910; (b) M. S. Iyer, K. M. Gigstad, N. D. Namdev and M. Lipton, *Amino Acids*, 1996, **11**, 259

83. E. J. Corey and M. J. Grogan, *Org. Lett.*, 1999, **1**, 157

84. M. S. Sigman and E. N. Jacobsen, *J. Am. Chem. Soc.*, 1998, **120**, 5315

85. (a) C. A. Krueger, K. W. Kuntz, C. D. Dzierba, W. G. Wirschun, J. D. Gleason, M. L. Snapper and A. H. Hoveyda, *J. Am. Chem. Soc.*, 1999, **121**, 4284; (b) J. R. Porter, W. G. Wirschun, K. W. Kuntz, M. L. Snapper and A. H. Hoveyda, *J. Am. Chem. Soc.*, 2000, **122**, 2657; (c) N. S. Josephsohn, K. W. Kuntz, M. L. Snapper and A. H. Hoveyda, *J. Am. Chem. Soc.*, 2001, **123**, 11594

86. (a) H. Ishitani, S. Komiyama and S. Kobayashi, *Angew. Chem. Int. Ed.*, 1998, **37**, 3186; (b) H. Ishitani, S. Komiyama, Y. S. Hasegawa and Kobayashi, *J. Am. Chem. Soc.*, 2000, **122**, 762

87. M. Chavarot, J. J. Byrne, P. Y. Chavant and Y. Vallée, *Tetrahedron: Asymmetry*, 2001, **12**, 1147

88. (a) M. Takamura, Y. Hamashima, H. Usuda, M. Kanai and M. Shibasaki, *Angew. Chem. Int. Ed.*, 2000, **39**, 1650; (b) H. Nogami, S. Matsunaga, M. Kanai and M. Shibasaki, *Tetrahedron Lett.*, 2001, **42**, 279

Chapter Two: Addition reactions on benzaldehyde

Chapter two: Addition reactions on benzaldehyde

2.1 Introduction

Reactions of nucleophiles with carbonyl compounds initially yield tetrahedral intermediates. Depending on the nature of the R groups the reaction will be either an addition (poor leaving R groups) or a substitution (good leaving groups), as shown in Scheme 2.1.

Scheme 2.1

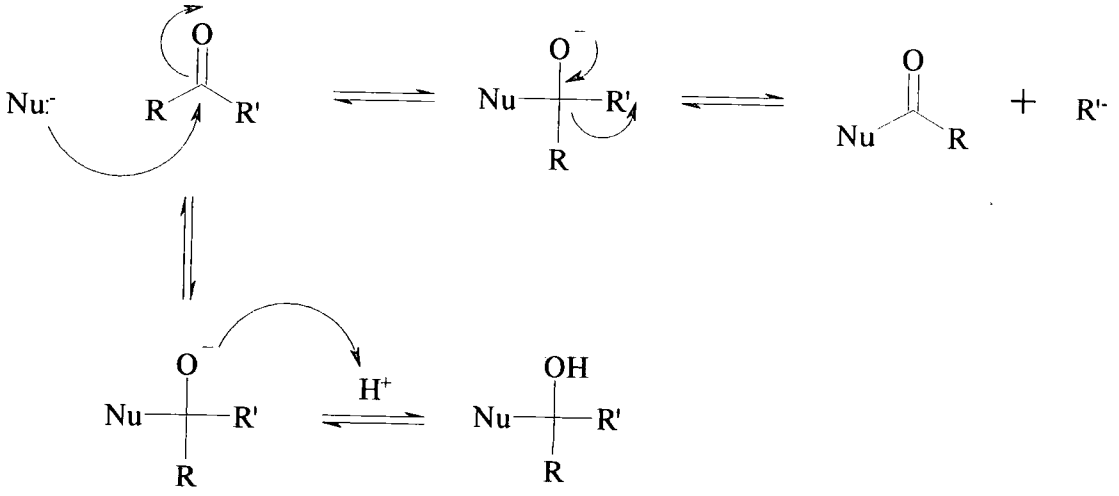

2.1.1 Addition of sulfite

The addition of sulfite on carbonyl compounds has been reported[1] and the literature provides data for the reaction with formaldehyde and various other carbonyl compounds.

In acidic solutions the addition of sulfite to formaldehyde leads to hydroxymethanesulfonate (HMS), as shown in scheme 2.2

Scheme 2.2

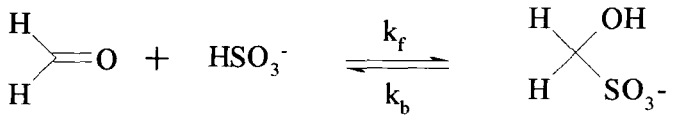

Values of the rate and/or equilibrium constants have been measured by iodine titration[2] and UV spectrophotometry[3], leading to the values in Table 2.1.

Table 2.1 Rate and equilibrium constants for the addition of bisulfite to formaldehyde

	k_f ($dm^3mol^{-1}s^{-1}$)	k_b (s^{-1})	$K=k_f/k_b$ (dm^3mol^{-1})	pH
a)	/	/	$8.5x10^6$	4.0
b)	1.94	$4.8x10^{-7}$	$4.0x10^6$	4.0
c)	/	$5.5x10^{-6}$	/	5.0
d)	12.6	$3.5x10^{-6}$	$3.6x10^6$	5.0
e)	42	$1.1x10^{-5}$	$3.8x10^6$	5.6

a) Ref. 2d, T = 20°C; b) Ref. 3a, T = 25°C; c) Ref. 3b, T = 20°C; d) Ref. 3a, T = 25°C; e) Ref. 2a-c, T = 25°C

It is worth noting that the reported values do not take account of the hydration of formaldehyde. Since the equilibrium constant for the hydration of formaldehyde is ca. 2000, values of the equilibrium constant for sulfite addition would be correspondingly higher if written in terms of the free formaldehyde concentration.

Clearly the values of k_f and k_b in Table 2.1 increase with increasing pH. This is compatible with the major processes involving attack of the sulfite dianion on formaldehyde in the forward direction and sulfite expulsion from the dianion of the adduct in the reverse direction.

The overall picture is represented in Scheme 2.3.

Scheme 2.3

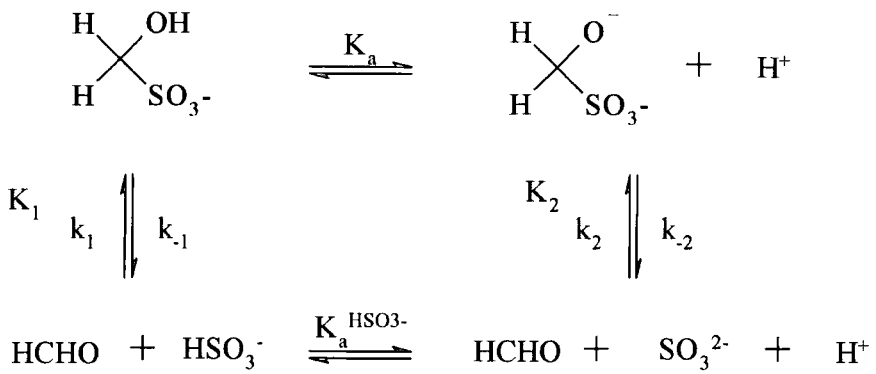

Note: $\frac{k_1}{k_{-1}} = K_1$ = equilibrium constant for the formation of $CH_2(OH)SO_3^-$

$\frac{k_2}{k_{-2}} = K_2$ = equilibrium constant for the formation of $CH_2(O^-)SO_3^-$

Values for pK_a, relating to the acid dissociation of the adduct, have been reported as 11.7 by Sørensen and Andersen[4], and 11.0 by Boyce and Hoffmann[5].

Overall it appears that the expulsion of sulfite is more favourable from the dianionic species rather than the monoanionic one as k_{-2} is significantly higher than k_{-1}. Similarly k_2 was found to be bigger than k_1 showing a greater affinity of the sulfite ion compared to bisulfite for the aldehyde. Only in fairly acidic solutions, pH < 3, can the bisulfite reaction compete effectively. This process is likely to involve sulfite addition on the protonated aldehyde, as shown in Scheme 2.4.

Scheme 2.4

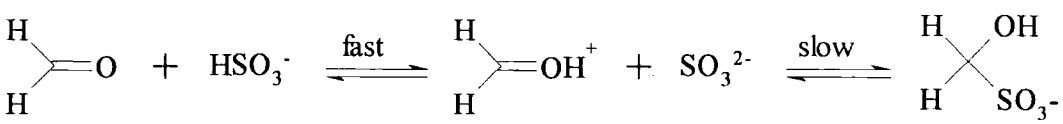

Kinetic and equilibrium studies of other bisulfite addition compounds have been carried out. Notably Gubareva[2d] reported values for K_1 calculated at 20°C using iodometric

titration. More recently Smith[6] used a spectrophotometric method to account for the reactions of propanal, propanone and chloro-propanone with bisulfite.

The values for the equilibrium constants, according to Scheme 2.3, are collected in Table 2.2.

Table 2.2 Equilibrium and acid dissociation constants for the reaction of carbonyl compounds with sulfite /bisulfite

	K_1 (dm^3mol^{-1})	K_2 (dm^3mol^{-1})	$pK_a^{Bisulfite\ adduct}$
Acetone[a]	290	/	/
2-Butanone[a]	54.6	/	/
Ethyl acetoacetate[a]	91.3	/	/
Propanal[a]	3000	/	/
Propanal[b]	$3.3x10^5$	95	10.7
Propanone[b]	240	0.03[c]	11[c]
Chloro-propanone[b]	1650	21	9

a) M. A. Gubareva, Ref. 2d, T = 20°C, Water; b) I. J. Smith, Ref 6, T = 25°C, Water;
c) Calculation of pKa was not possible experimentally therefore the value was assumed to be 11 and K_2 calculated accordingly

It is worth noting the discrepancy between results gained from iodometric titration and a spectrophotometric method (namely for propanal).

Of particular interest to this thesis is the reaction of benzaldehyde. In 1986 Hoffmann and co-workers reported a value of 4800 dm^3mol^{-1} for K_1 and compiled various values found in the literature prior to their study, as shown in Table 2.3. As can be seen there is a considerable spread in the values obtained.

Kokesh and Hall[3a] calculated the equilibrium constant for the addition of bisulfite to benzaldehyde using a spectrophotometric method and found a value of 6400 dm^3mol^{-1}. The

results were compared to the ones of Stewart and Donally in an attempt to check the validity of the iodometric method. They found that titration tool was not accurate at high pH values as rapid dissociation of the complex can occur. Kokesh and Hall have accounted for the variation of the overall equilibrium constant with pH with values of 0.9 dm^3mol^{-1} and $2x10^{-11}$ mol dm^{-3} for K_2 and K_a respectively.

Table 2.3 Equilibrium constant for the formation of $PhCH(OH)SO_3^-$

K_1 (dm^3mol^{-1})	Conditions	Ref.
11300	20.9 °C, pH=5.21	2b-c
4700	23 °C	7
10000	15-17 °C, μ~0.1 M	8
440	30 °C	2d
1270	20 °C, pH=4.3	9
6400	21 °C, μ~0.1 M, pH 3.5-5.3	3a

Decomposition of the benzaldehyde-bisulfite adduct proved a useful tool in the understanding of the reaction. The early works of Stewart and Donally[2a-c] and Blackadder and Hinshelwood[10] showed a linear increase in the rate of decomposition at increasing pH values. At around pH=2 the values levelled off. Stewart and Donally suggested a catalysed decomposition in more acid solutions. Jencks and Young[11] later made a detailed study of the decomposition reaction of the acetophenone adduct in acidic conditions (pH<2). They suggested general acid catalysis in a mechanism which involves the rate limiting donation of a proton to the leaving sulfite group as shown on Scheme 2.5.

Scheme 2.5

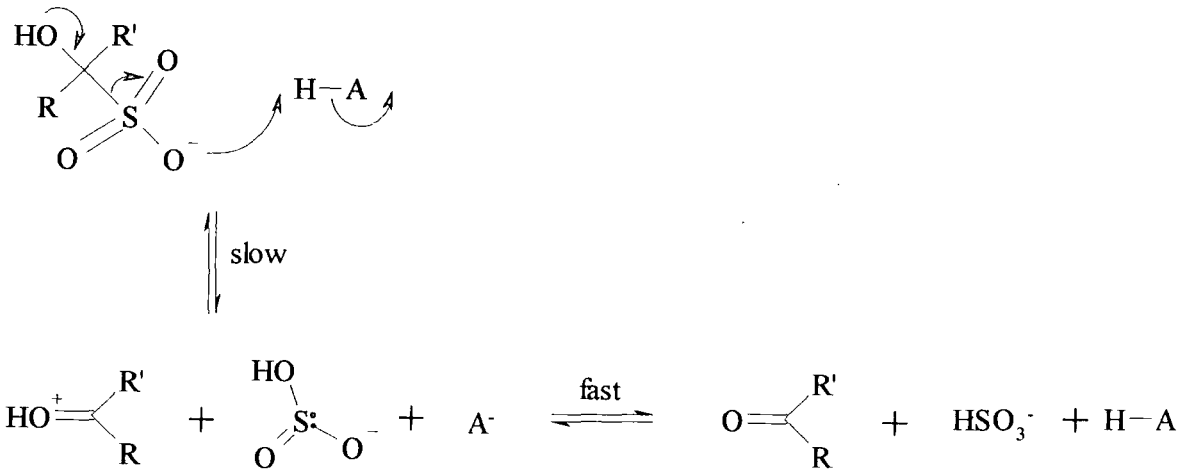

When considering the reverse process it implies that in strongly acidic solutions the rate-limiting step is the attack of bisulfite on the protonated carbonyl compound.

Hoffmann and co-workers[3b-c] studied the influence of substituents on the addition of bisulfite to a series of benzaldehyde derivatives (Table 2.4).

Table 2.4 Rate constants for the addition of sulfite/bisulfite to benzaldehyde derivatives, T = 25°C, I = 1.0 M

Substituent	$k_{bisulfite}$ ($mol^{-1}dm^3s^{-1}$)	$k_{sulfite}$ ($mol^{-1}dm^3s^{-1}$)
p-OH	/	$5.8x10^3$
p-OCH_3	/	$7.8x10^3$
p-CH_3	0.68	$1.6x10^4$
p-Cl	1.05	$5.5x10^4$
p-NO_2	5.31	$5.7x10^4$

Note: $k_{bisulfite}$ corresponds to the rate constant for bisulfite addition; $k_{sulfite}$ corresponds to the rate constant for sulfite addition

2.1.2 Addition of cyanide

Addition of cyanide to carbonyl compounds leads to cyanohydrins, as shown on Scheme 2.6.

Scheme 2.6

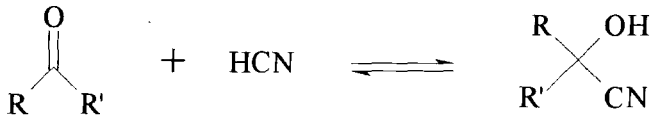

At the turn of the last century Lapworth[12] showed that addition of potassium cyanide (KCN) to a mixture of camphorquinone and hydrogen cyanide (HCN) increased significantly the rate of reaction. He concluded that it was the cyanide ions that were involved in the addition reaction rather than HCN and postulated that the formation of cyanohydrins involved the slow addition of cyanide ions to the carbonyl compound followed by a very rapid protonation of the anionic intermediate as represented in Scheme 2.7.

Scheme 2.7

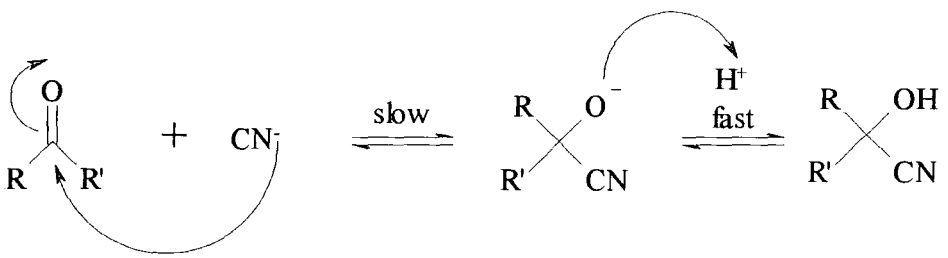

Lapworth also suggested that, if using water as a proton source, potassium cyanide itself should be able to convert carbonyl compounds to cyanohydrins.

Ching and Kallen[13] determined that the formation of the cyanohydrin involving the cyanide ion must proceed through a stepwise pathway (Scheme 2.7). Based on Jencks' statement that the pK_a value of a proton donating catalyst must be intermediate between the pK_a values of the conjugate acid of the starting material and products for a general acid catalysed pathway to be concerted, they showed that this process is unlikely in the case of the reaction of cyanide with a carbonyl compound in the presence of water.

Scheme 2.8: Concerted addition of cyanide ion to the carbonyl compound

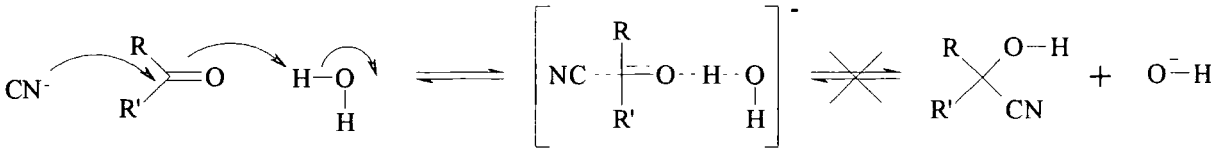

Lapworth and Manske[14] reported values of the equilibrium constants for the dissociation process in 96% ethanol. They particularly showed the influence of the substituent on benzaldehyde on the stability of the cyanohydrin. Data are presented in table 2.5.

Table 2.5 Equilibrium constant, K, for the dissociation of some cyanohydrins

Carbonyl compound	K (mol dm^{-3})
Benzaldehyde	$4.7x10^{-3}$
o-nitro benzaldehyde	$7.0x10^{-4}$
p-nitro benzaldehyde	$1.81x10^{-2}$
o-chloro benzaldehyde	$1.0x10^{-3}$
p-chloro benzaldehyde	$4.9x10^{-3}$
o-methoxy benzaldehyde	$2.6x10^{-3}$
p-methoxy benzaldehyde	$3.1x10^{-2}$
Acetone	$3.1x10^{-2}$
Methyl Ethyl ketone	$2.7x10^{-2}$
n-propyl methyl ketone	$3.6x10^{-2}$
Acetophenone	1.3
Ethyl phenone	0.6
Cyclopentanone	$1.5x10^{-2}$

It is worth noting that, in the case of substituted benzaldehydes, ortho substituents apparently stabilise the cyanohydrin whereas the group in para position favours the dissociation products.

As in the case of bisulfite addition compounds, cyanohydrins formed from aldehydes are more stable than the ones from the reaction of ketones. This is mainly due to the conformational change at the carbonyl carbon where going from a trigonal sp^2 hybridisation, the bond angles are reduced from 120° to 109° in the sp^3 tetrahedral configuration. In this case the steric hindrance caused by the two R groups is greater than that between one hydrogen and one R group.

Ching and Kallen[13] also investigated the influence of substituents on benzaldehyde for the formation of cyanohydrins. They showed that the reaction is promoted by the electron withdrawing nature of the substituent which increases the electrophilicity of the carbonyl group. Considering both the neutral and anionic species involved in the mechanism, as shown in Scheme 2.9, they accounted for the values of the equilibrium and dissociation constants (Table 2.6).

Scheme 2.9

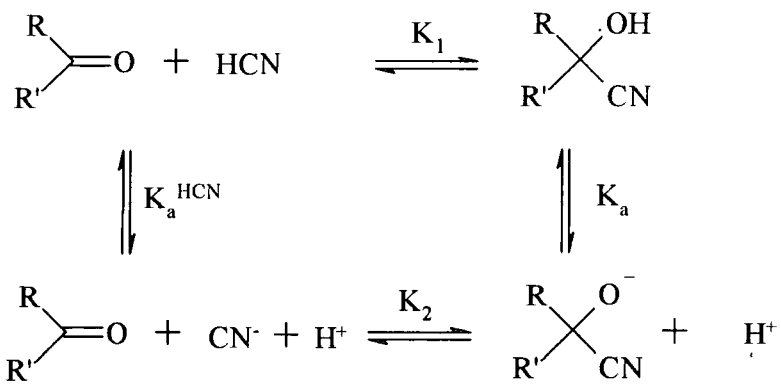

Table 2.6 Equilibrium constants for the reaction of HCN/CN⁻ with benzaldehyde derivatives, T = 25°C, I = 1.0 M

Substituent	K_1 ($mol.dm^{-3}$)	K_2 ($mol.dm^{-3}$)	K_a (dm^3mol^{-1})
p-$(CH_3)_2N$	4.85	0.02	$3.27x10^{-12}$
p-CH_3O	32.7	0.47	$1.14x10^{-11}$
p-CH_3	114	1.68	$1.17x10^{-11}$
H	236	5.47	$1.85x10^{-11}$
p-Cl	308	7.18	$1.85x10^{-11}$
p-NO_2	1820	140.9	$6.15x10^{-11}$

It is clear that the data in Tables 2.5 and 2.6 are not consistent. For example in Table 2.5 the effect of a p-NO_2 group is to increase the dissociation constant while in Table 2.6 the effect is to increase the association constant.

2.1.3 Addition of amines

The reaction of a carbonyl compound with a primary amine yields an imine. In the synthesis of imines Dean-Stark traps or molecular sieves are generally used to remove the water produced as a by-product and therefore drive the equilibrium in favour of the product.

The reaction of benzaldehyde with various primary amines has been reported. Of particular interest for this work are the reactions of benzaldehyde with benzylamine, allylamine and 4-nitrobenzaldehyde.

Reports for the formation of benzylidene benzylamine, resulting from the addition of benzylamine to benzaldehyde, show quite high yields in various solvents (CH_2Cl_2, Et_2O) [15]. Recently Tashiro[16] and co-workers studied the feasibility of carrying out imine formation in water without any buffer or catalyst. They reported the formation of benzylidene benzylamine in aqueous medium in a 85% yield.

Scheme 2.10

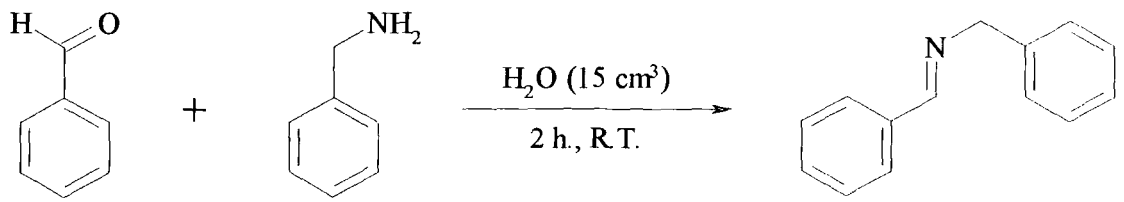

10 mmol 10 mmol

The product was extracted with dichloromethane. The organic layers were then dried over magnesium sulfate ($MgSO_4$) and the organic solvent evaporated off.

Also of interest for environmental issues is the solvent-free green synthesis of Kaupp et al[17].

The addition of allylamine to benzaldehyde yields benzylidene allylamine. Similarly to benzylidene benzylamine different synthetic methods have been described[18]. A simple method[19] giving a 100% yield is described in Scheme 2.11.

Scheme 2.11

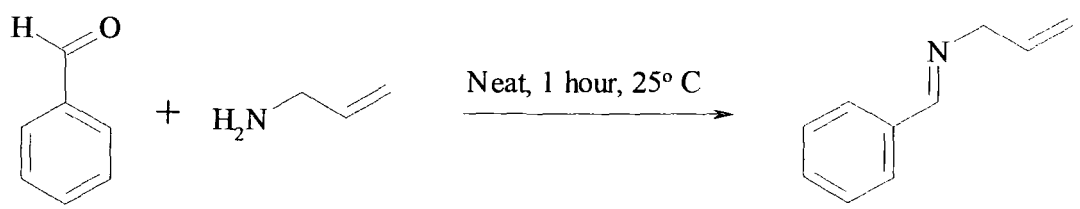

100%

Addition of benzylamine to 4-nitrobenzaldehyde has also been reported[20].

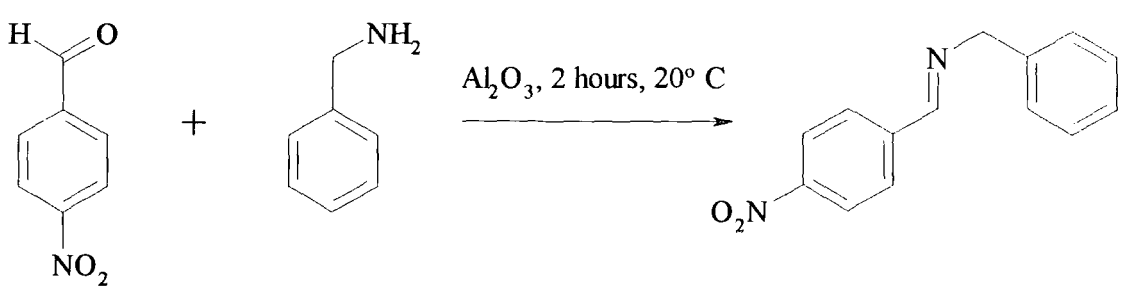

2.2 Results and discussion

Although there are values in the literature for the equilibrium constants for the addition of sulfite and of cyanide to benzaldehyde the spread in data is large. Hence data for the reactions of benzaldehyde with sulfite, cyanide, benzylamine and allylamine as well as the reaction of 4-nitro-benzaldehyde with benzylamine are reported. In the case of sulfite and cyanide the equilibrium constants for the process have been assessed. The methods for both equilibrium measurements and characterisation of products are first described and then the results are discussed.

2.2.1 Methodology

2.2.1.1 UV/Vis spectroscopy

Benzaldehyde is known to show a strong absorbance at 250nm. The bisulfite addition compound and the cyanohydrin on the other hand exhibit negligible absorbance in the region. The concentration in adduct can thus be assessed using absorbance values at $\lambda_{max} = 250$nm.

Solutions were made up so that sulfite and cyanide were added in excess to benzaldehyde. Spectra were then recorded and the values for A_{250} collected.

2.2.1.2 NMR spectroscopy

Benzaldehyde and the imines formed from benzaldehyde show a strong absorbance in the same region of the UV/Vis spectrum. Confirmation of the formation of the adducts was then determined by ^{1}H NMR where a characteristic signal for the proton, H_a, on the iminium carbon, can be seen at δ~8ppm.

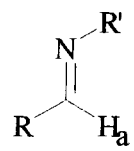

2.2.2 Sulfite addition to benzaldehyde

2.2.2.1 Equilibrium measurements

The addition of bisulfite to benzaldehyde leads α- hydroxyphenylmethanesulfonate (HPMS) and the overall equilibrium can be represented as follows:

Scheme 2.12

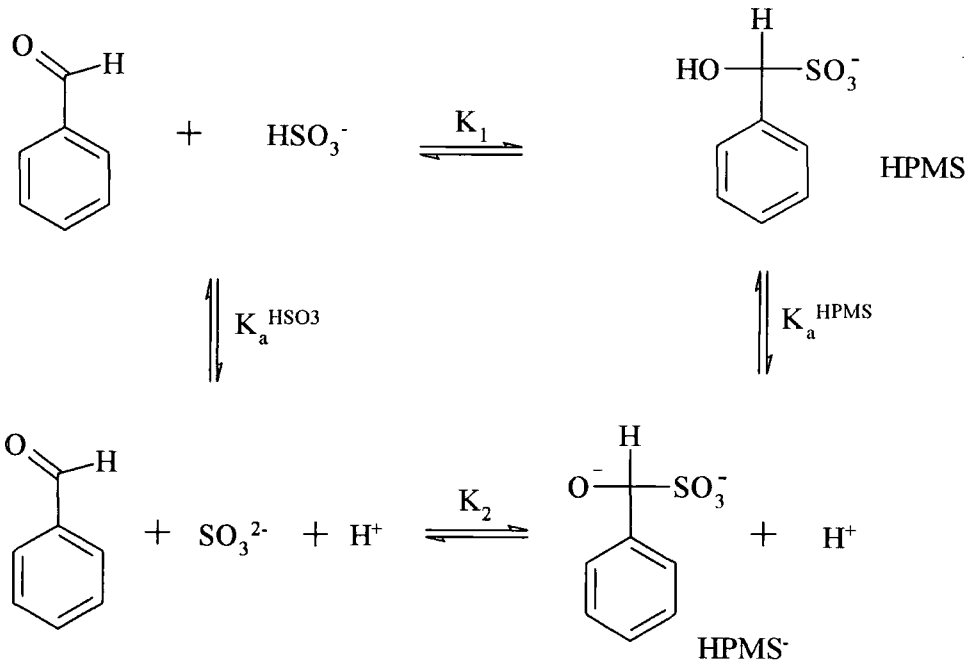

The value for the observed equilibrium constant, K_{obs}, can be expressed as equation (2.1).

$$K_{obs} = \frac{[HPMS]_{stoich}}{[Benzaldehyde][Sulfite]_{stoich}} \qquad (2.1)$$

where $[Sulfite]_{stoich} = [HSO_3^-] + [SO_3^{2-}]$

It is expected that K_{obs} will be pH dependent. Using the expressions for the dissociations constants, $K_a^{HSO_3^-}$ and K_a^{HPMS}, the observed equilibrium constant can be defined in terms of acidity dependence as given by equation (2.4).

$$K_a^{HSO_3^-} = \frac{[SO_3^{2-}][H^+]}{[HSO_3^-]} \quad (2.2)$$

$$K_a^{HPMS} = \frac{[HPMS^-][H^+]}{[HPMS]} \quad (2.3)$$

$$K_{obs} = K_1 \times \frac{([H^+] + K_a^{HPMS})}{([H^+] + K_a^{HSO_3^-})} \quad (2.4)$$

Benzaldehyde displays strong absorbance at λ = 250nm (ε = 1.5x10^4 dm^{3}mol^{-1}cm^{-1} in water) whereas HPMS absorbs negligibly. Using the Beer-Lambert law it is possible to re-express equation (2.1) in terms of absorbance:

$$K_{obs} = \frac{(A_0 - A)}{(A - A_\infty) \times ([HSO_3^-] + [SO_3^{2-}])} \quad (2.5)$$

where A_0 and A_∞ correspond to the absorbances of benzaldehyde and HPMS respectively.

2.2.2.2 Results

Experimental procedure: Stock solutions of benzaldehyde (0.01 mol dm^{-3}) were freshly prepared before each experiment using acetonitrile as a solvent.

The different aqueous buffer solutions were prepared using 0.1 mol dm^{-3} potassium dihydrogen phosphate with 0.1 mol dm^{-3} sodium hydroxide, for pH = 6.09, 6.50 and 7.00, and 0.025 mol dm^{-3} borax with 0.1 mol dm^{-3} hydrochloric acid, for pH = 8.70.

The equilibrium constants were determined by diluting benzaldehyde to a 1x10^{-4} mol dm^{-3} concentration in aqueous buffered solutions of sodium bisulfite. The spectra of the equilibrated solutions at 250nm were then recorded in 1cm silica cells.

Results:

At each pH spectra were recorded at various concentrations of bisulfite. Typical spectra are shown in Figure 2.1.

Figure 2.1: UV/Vis spectra for the reaction of $1x10^{-4}$ mol dm^{-3} benzaldehyde with various sodium bisulfite concentrations at pH=7, 25° C.

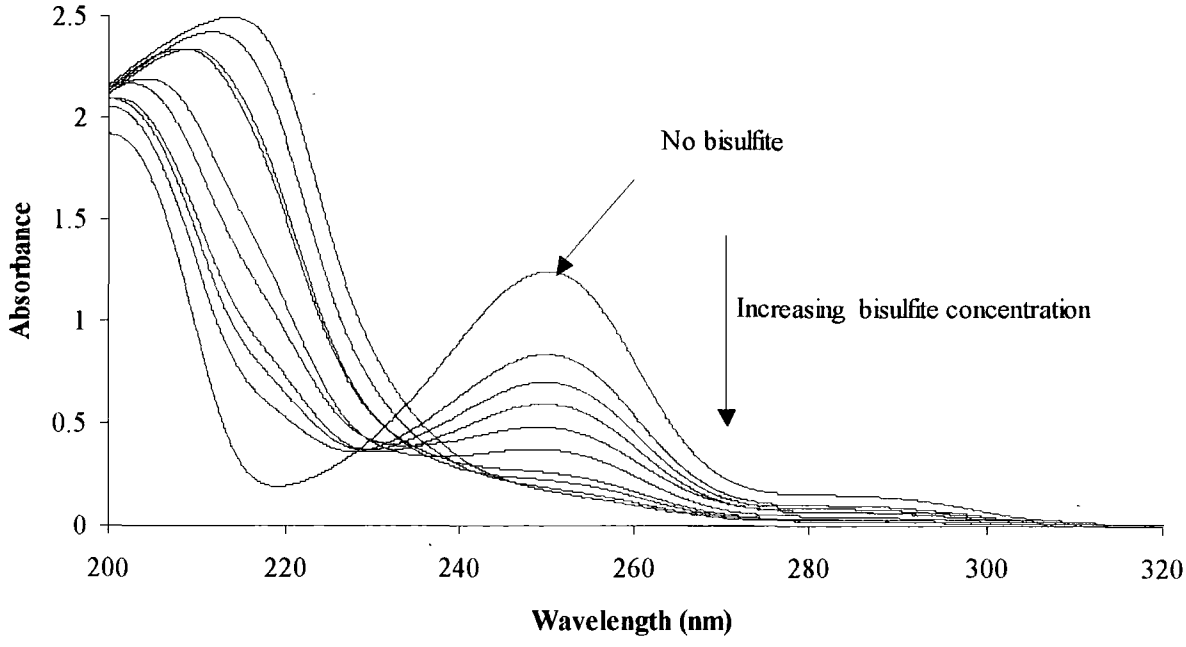

The absorbance at λ = 250nm allows the calculation of the concentration of free benzaldehyde, HPMS and free bisulfite. Sulfite absorbs at 220 nm but shows negligible absorbance at 250 nm.

Calculations corresponding to the experiment carried at pH = 7.0 are shown in Table 2.7.

Table 2.7 Equilibrium absorbances and corresponding benzaldehyde, HPMS and free sulfite concentrations measured for varying initial sulfite concentrations

$[Sulfite]_{stoich}$ (mol dm^{-3})	A (λ = 250 nm)	A_0 - A	[Benzaldehyde] (mol dm^{-3})	[HPMS] (mol dm^{-3})	$[Sulfite]_{free}$ (mol dm^{-3})
0.00	1.24	0.00	$1.00x10^{-4}$	0.00	0.00
$2x10^{-4}$	0.84	0.40	$6.51x10^{-5}$	$3.49x10^{-5}$	$1.65x10^{-4}$
$3x10^{-4}$	0.70	0.54	$5.46x10^{-5}$	$4.54x10^{-5}$	$2.55x10^{-4}$
$4x10^{-4}$	0.59	0.65	$4.64x10^{-5}$	$5.36x10^{-5}$	$3.46x10^{-4}$
$6x10^{-4}$	0.48	0.76	$3.76x10^{-5}$	$6.24x10^{-5}$	$5.38x10^{-4}$
$8x10^{-4}$	0.37	0.87	$2.91x10^{-5}$	$7.09x10^{-5}$	$7.29x10^{-4}$
$1.6x10^{-3}$	0.26	0.98	$2.04x10^{-5}$	$7.96x10^{-5}$	$1.52x10^{-3}$
$2x10^{-3}$	0.22	1.02	$1.75x10^{-5}$	$8.25x10^{-5}$	$1.92x10^{-3}$
$3x10^{-3}$	0.19	1.06	$1.46x10^{-5}$	$8.54x10^{-5}$	$2.91x10^{-3}$
$4x10^{-3}$	0.17	1.07	$1.35x10^{-5}$	$8.65x10^{-5}$	$3.91x10^{-3}$

With $A_\infty = 0.09$

The apparent equilibrium constant, K_{obs}, was then calculated according to equation (2.1). Rearranging equation (2.4) afforded K_1 with the values for $K_a^{HSO_3^-} = 6.31x10^{-8}$ mol dm^{-3} ($pK_a = 7.2$)[21] and $K_a^{HPMS} = 2.1x10^{-11}$ mol dm^{-3} ($pK_a = 10.7$)[3a].

$$K_2 = \frac{[HPMS^-]}{[Benzaldehyde][SO_3^{2-}]} \quad \textbf{(2.6)}$$

$$K_1 = \frac{[HPMS]}{[HSO_3^-][Benzaldehy\ de]} \quad \textbf{(2.7)}$$

Combining equations (2.6) and (2.7) and using the expressions for the dissociation constants of bisulfite and HPMS leads to equation (2.8):

$$K_2 = K_1 \times \frac{K_a^{HPMS}}{K_a^{HSO_3^-}} \quad \textbf{(2.8)}$$

Values for all the equilibrium constants at pH = 7.0 are shown in Table 2.8.

Table 2.8 Observed, adduct formation and adduct dissociation equilibrium constants calculated for varying sulfite concentrations

$[Sulfite]_{stoich}$ ($mol.dm^{-3}$)	K_{obs} (dm^3mol^{-1})	K_1 (dm^3mol^{-1})	K_2 (dm^3mol^{-1})
0.00	/	/	/
$2x10^{-4}$	3325	5418	1.79
$3x10^{-4}$	3504	5711	1.88
$4x10^{-4}$	3718	6058	2.00
$6x10^{-4}$	3613	5887	1.94
$8x10^{-4}$	4229	6892	2.27
$1.6x10^{-3}$	3769	6141	2.03
$2x10^{-3}$	3966	6464	2.13
$3x10^{-3}$	3729	6077	2.01
$4x10^{-3}$	3274	5336	1.76
Average:	3681	5998	1.98
St. Deviation:	300	490	$1.62x10^{-1}$

Calculations of the equilibrium constants have been carried out at four different pH values. The average values for K_{obs}, K_1 and K_2 are summarised in Table 2.9.

Table 2.9 Observed, adduct formation and adduct dissociation equilibrium constants calculated at different pH values

pH	K_{obs} (dm^3mol^{-1})	K_1 (dm^3mol^{-1})	K_2 (dm^3mol^{-1})
6.09	6162	6639	2.21
6.50	5335	6399	2.13
7.00	3681	5998	1.98
8.70	182	5867	1.95
Average:		6226	2.07
St. Deviation:		357	$1.23x10^{-1}$

A plot of K_{obs} versus pH according to equation (2.4) fitted using the Scientist© computer package is shown on Figure 2.2 and leads to a value of 6429 ± 136 dm^3mol^{-1} for K_1 and hence to a value for K_2 of 2.14 ± 0.05 dm^3mol^{-1}.

Figure 2.2 Variation of the observed equilibrium constant with pH for the reaction of sulfite/bisulfite with benzaldehyde

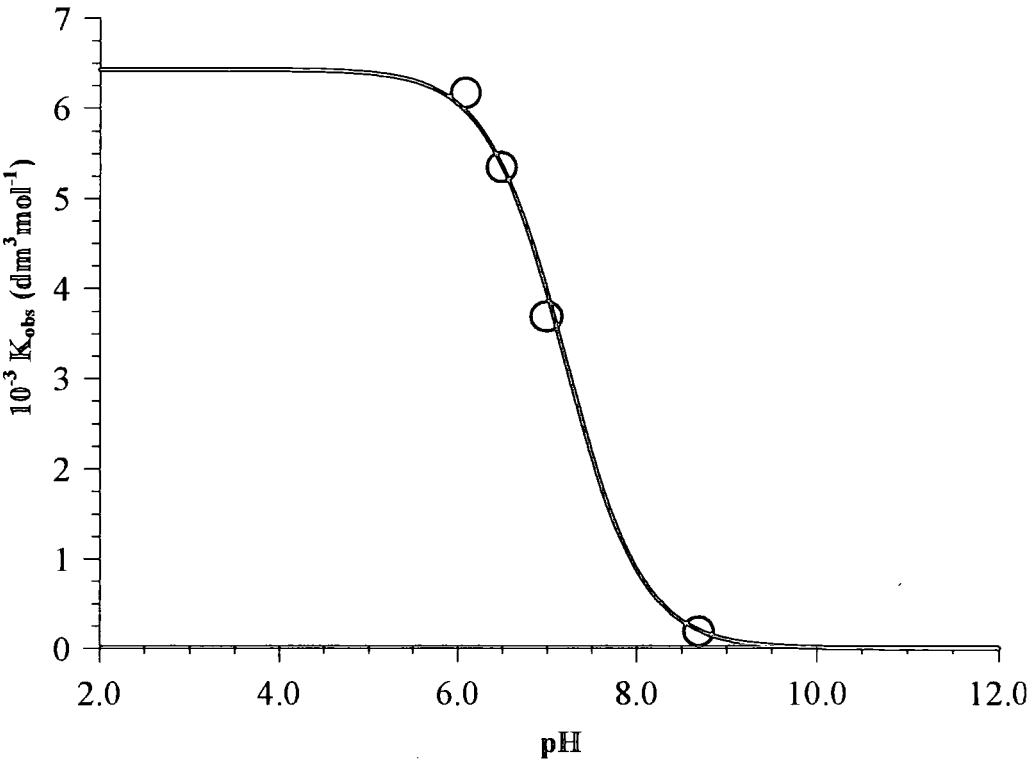

It has therefore been possible to measure the equilibrium constant for the formation of HPMS. The equilibrium constant for the formation of anionic HPMS from benzaldehyde and the bisulfite ion is significantly higher than the equilibrium constant for the formation of the di-anionic HPMS from benzaldehyde and the sulfite ion. This is a consequence of the equilibrium thermodynamic square representing the system shown in Scheme 2.12 where $K_a^{HSO_3^-}$ is larger than K_a^{HPMS}.

The value of 6430 ± 140 dm^3mol^{-1} obtained for K_1 may be compared with the literature values in Table 2.3. The value confirms that obtained by Kokesh and Hall[3a], also obtained using a spectrophotometric method.

2.2.3 Cyanide addition to benzaldehyde

2.2.3.1 Equilibrium measurements

The addition of cyanide to benzaldehyde leads to a cyanohydrin and the overall equilibrium can be represented as shown in Scheme 2.13.

Similarly to sulfite addition the observed equilibrium constant, K_{obs} is pH dependent. It can be expressed as equation (2.9).

$$K_{obs} = \frac{[\text{Cyanohydrin}]_{stoich}}{[\text{Benzaldehyde}][CN^-]_{stoich}} \quad (2.9)$$

Scheme 2.13

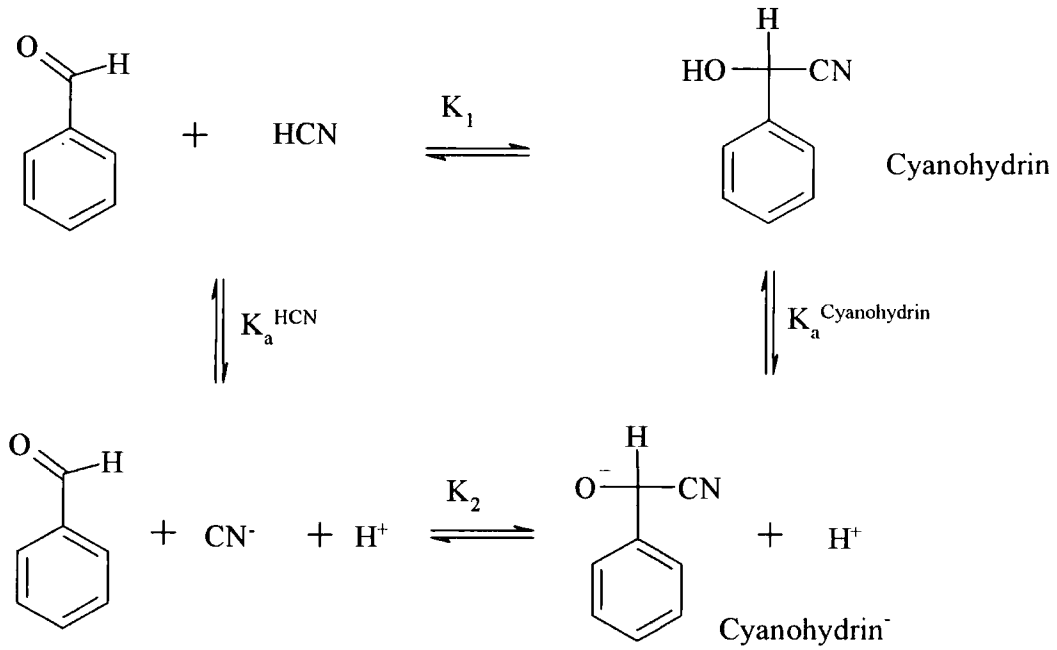

The acid dissociation constants for cyanide and cyanohydrin, K_a^{HCN} and $K_a^{Cyanohydrin}$ respectively, can be defined as:

$$K_a^{HCN} = \frac{[CN^-][H^+]}{[HCN]} \quad (2.10)$$

and

$$K_a^{Cyanohydrin} = \frac{[\text{Cyanohydrin}^-][H^+]}{[\text{Cyanohydrin}]} \quad (2.11)$$

Therefore the acidity dependence of K_{obs} can be expressed as a function of K_a^{HCN} and $K_a^{Cyanohydrin}$ (equation (2.12).

$$K_{obs} = K_2 \times \frac{(1 + \frac{[H^+]}{K_a^{Cyanohydrin}})}{(1 + \frac{[H^+]}{K_a^{HCN}})} \quad (2.12)$$

The cyanohydrin of benzaldehyde displays a negligible absorbance in the 250 nm region. It is therefore possible to determine the concentrations of free benzaldehyde and adduct using the Beer-Lambert law, in the form of equation (2.13).

$$K_{obs} = \frac{(A_0 - A)}{(A - A_\infty) \times ([HCN] + [CN^-])} \quad (2.13)$$

where A_0 and A_∞ correspond to the absorbances of benzaldehyde and cyanohydrin respectively.

2.2.3.2 Results

Experimental procedure: Stock solutions of benzaldehyde (0.01 mol dm^{-3}) were freshly prepared before each experiment using acetonitrile as a solvent.

The different aqueous buffer solutions were prepared using 0.1 mol dm^{-3} potassium dihydrogen phosphate with 0.1 mol dm^{-3} sodium hydroxide for pH = 6.87 and 0.025 mol dm^{-3} Borax with 0.1 mol dm^{-3} hydrochloric acid for pH = 10.22 whereas 0.003 mol.dm^3 NaOH was used to afford pH = 11.6.

Aqueous solutions of cyanide (using potassium cyanide) were freshly prepared under a fume hood before each experiment. The ionic strength was kept constant at 0.214 mol.dm^{-3} using freshly prepared solutions of potassium chloride.

The equilibrium constants were determined by diluting benzaldehyde to a 1×10^{-4} mol dm^{-3} concentration in aqueous buffered solutions of potassium cyanide and potassium chloride under a fume hood. The spectra of the equilibrated solutions were then recorded at 250nm in 1 cm cells.

Results:

For each pH spectra were recorded at various concentrations of cyanide. Typical spectra are shown in Figure 2.3.

Figure 2.3: UV/Vis spectral plots for the reaction of $1x10^{-4}$ mol dm^{-3} benzaldehyde with varying cyanide concentrations at pH=6.87, I = 0.21 mol.dm^3, 25° C.

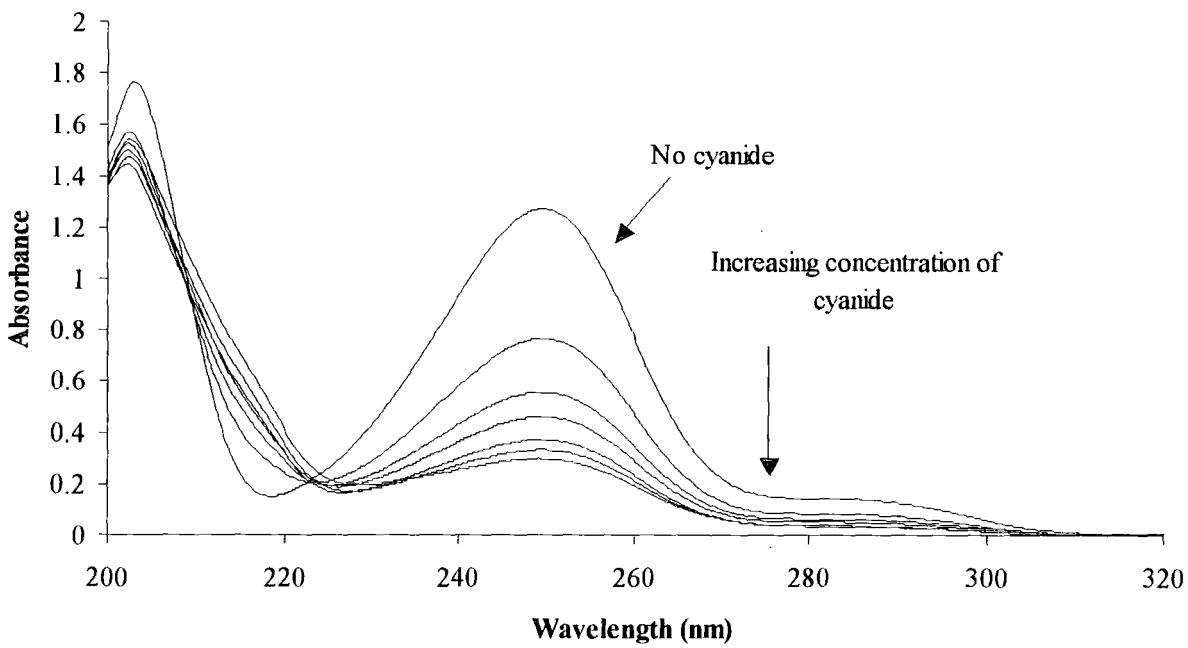

The absorbance at λ = 250nm allows the calculation of the concentration of free benzaldehyde, cyanohydrin and free cyanide.

Calculations corresponding to the experiment carried at pH = 6.87 are shown in Table 2.10.

Table 2.10 Equilibrium absorbances and corresponding benzaldehyde, cyanohydrin and free cyanide concentrations measured for varying initial cyanide concentrations

$[Cyanide]_{stoich}$ (mol dm^3)	A (λ = 250 nm)	A_0 - A	[Benzaldehyde] (mol dm^3)	[Cyanohydrin] (mol dm^3)	$[Cyanide]_{free}$ (mol dm^3)
0.00	1.27	0.00	$1.00x10^{-4}$	0.00	0.00
$2x10^{-3}$	0.77	0.50	$6.04x10^{-5}$	$3.69x10^{-5}$	$1.93x10^{-3}$
$4x10^{-3}$	0.56	0.71	$4.38x10^{-5}$	$5.62x10^{-5}$	$3.94x10^{-3}$
$6x10^{-3}$	0.46	0.81	$3.62x10^{-5}$	$6.38x10^{-5}$	$5.94x10^{-3}$
$8x10^{-3}$	0.37	0.90	$2.92x10^{-5}$	$7.08x10^{-5}$	$7.93x10^{-3}$
$1x10^{-2}$	0.33	0.94	$2.61x10^{-5}$	$7.39x10^{-5}$	$9.93x10^{-3}$

The apparent equilibrium constant, K_{obs}, was then calculated according to equation (2.9). Rearranging equation (2.12) afforded K_2 with the values for $K_a^{HCN} = 7.94x10^{-10}$ mol dm^{-3} ($pK_a = 9.1$)[13] and $K_a^{cyanohydrin} = 1.85x10^{-11}$ mol dm^{-3} [13].

$$K_2 = \frac{[\text{Cyanohydrin}^-]}{[\text{Benzaldehyde}][CN^-]} \qquad \textbf{(2.14)}$$

$$K_1 = \frac{[\text{Cyanohydrin}]}{[HCN][\text{Benzaldehyde}]} \qquad \textbf{(2.15)}$$

Combining equations (2.14) and (2.15) and using the expressions for the dissociation constants of cyanide and cyanohydrin leads to equation (2.16)

$$K_1 = K_2 \times \frac{K_a^{HCN}}{K_a^{Cyanohydrin}} \qquad \textbf{(2.16)}$$

K_1 was calculated accordingly. Values for data at pH = 6.87 are shown in Table 2.11.

Table 2.11 Observed, adduct formation and adduct dissociation equilibrium constants calculated for varying cyanide concentrations

$[Cyanide]_{stoich}$ (mol dm^3)	K_{obs} (dm^3mol^{-1})	K_2 (dm^3mol^{-1})	K_1 (dm^3mol^{-1})
0.00	/	/	/
$2x10^{-3}$	335	7.89	337
$4x10^{-3}$	326	7.68	328
$6x10^{-3}$	298	7.02	300
$8x10^{-3}$	308	7.26	310
$1x10^{-2}$	288	6.79	290
Average:	311	7.33	313
St. Deviation:	19	0.46	20

Measurements have been carried out at three different pH values (6.87, 10.22 and 11.6). In each case K_{obs}, K_1, K_2 have been calculated using the methods described above. The values obtained are summarised in Table 2.12.

Table 2.12 Observed, adduct formation and adduct dissociation equilibrium constants calculated at different pH values

pH	K_{obs} (dm^3mol^{-1})	K_2 (dm^3mol^{-1})	K_1 (dm^3mol^{-1})
6.87	311	7.33	313
10.22	28.1	7.13	305
11.60	7.73	6.84	292
Average:		7.10	303
St. Deviation:		0.25	11

A plot of K_{obs} versus pH accordingly to equation (2.12) fitted using the Scientist© computer package yields values of 7.08 ± 0.14 dm^3mol^{-1} for K_2 and 304 ± 6 dm^3mol^{-1} for K_1. The plot is shown in Figure 2.4.

Figure 2.4 Variation of the observed equilibrium constant with pH for the reaction of HCN/CN^- with benzaldehyde

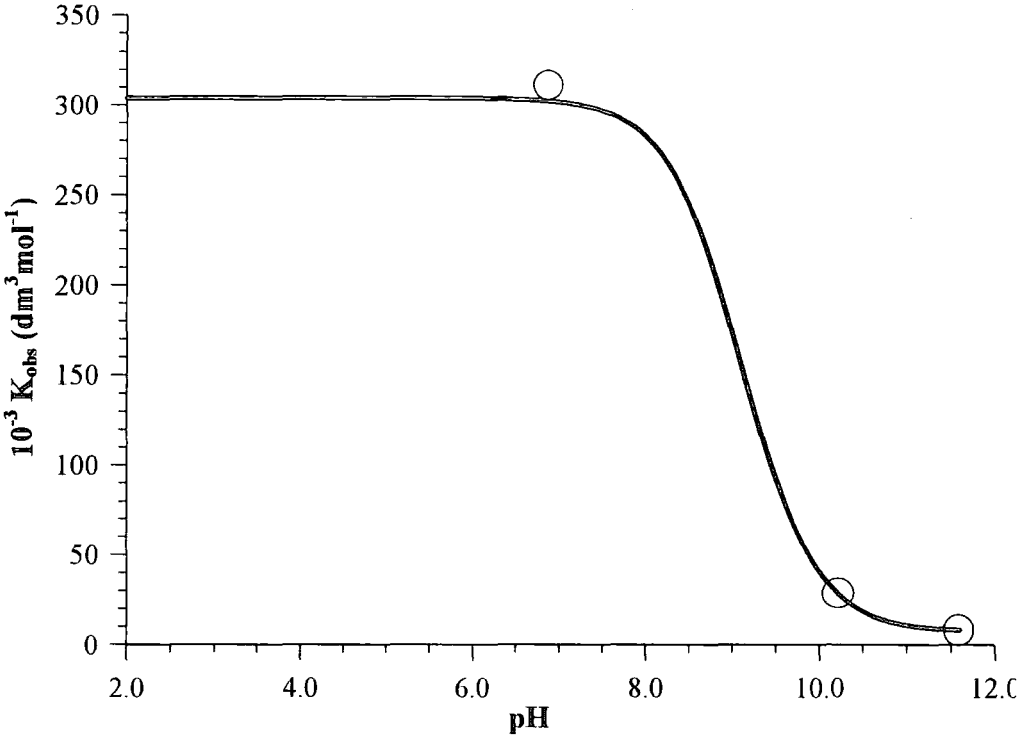

The results gained from the fit shows the reliability of both methods towards the calculation of the constants.

The experiments have been carried out in the same conditions as described by Ching and Kallen[13]. The results should therefore be comparable.

Table 2.13 Comparison of the experimental and literature values for the equilibrium constants of the reaction between benzaldehyde and HCN/CN⁻

	K_2 (dm^3mol^{-1})	K_1 (dm^3mol^{-1})
Literature	5.47 ± 0.48	236 ± 24
Experiment	7.10 ± 0.25	303 ± 11

Both the values obtained and the ones published by Ching and Kallen fall in the same range. The differences in values may be due to the difference in terms of ionic strength. Ching and Kallen worked at I = 1.0 $mol.dm^{-3}$ and the value they used for pK_a^{HCN} (= 9.1) was determined at the same strength. The present work was performed at I = 0.21 $mol.dm^{-3}$ but the same value of 9.1 for pK_a^{HCN} was used for the calculations.

The results show that the value of K_2 is considerably higher than that for K_1. In terms of Scheme 2.13 this can be attributed to the higher acidity of HCN than of the cyanohydrin.

2.2.4 Amine addition to benzaldehyde

Note: Protons labelled $H_{x'}$ in aromatic rings correspond to the other proton situated in the same position as H_x (e.g.: if H_a is ortho to the substituent $H_{a'}$ will correspond to the other ortho proton).

2.2.4.1 Formation of N-benzylidene benzylamine

It is worth noting that N-benzylidene benzylamine is commercially available (Aldrich). However the first experimental data on the addition of cyanide were collected using a stock solution of the imine produced from the reaction of benzaldehyde and benzylamine in acetonitrile. Subsequently characterisation of N-benzylidene benzylamine was limited to accounting for the formation of the desired compound.

Experimental

N-Benzylidene benzylamine

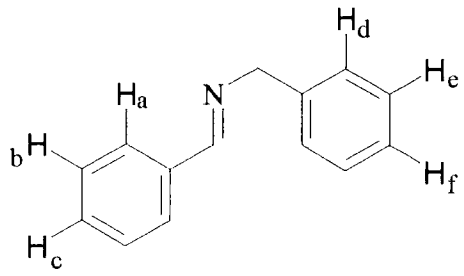

To a solution of benzaldehyde (2.54 cm^3, 25 mmol) in dry acetonitrile (50 cm^3) was added benzylamine (2.73 cm^3, 25 mmol) at room temperature. The solution was left to react overnight. ^1H NMR spectroscopy was used to check that the reaction went to completion by monitoring the disappearance of the peak characteristic of the aldehydic proton at δ = 10.0 ppm. δ_H (400 MHz, CD_3CN): 4.77 (2H, *s*, CH_2), 7.27 (1H, *m*, H_f), 7.33 (4H, *m*, $H_{d'}$, H_e and $H_{e'}$), 7.42 - 7.48 (3H, *m*, H_b, $H_{b'}$ and H_c), 7.75 – 7.80 (2H, *m*, H_a and $H_{a'}$), 8.47 (1H, *t*, J = 1.6 Hz, CHN); δ_C (400 MHz, CD_3CN): 65.6 (CH_2); 128 ($\underline{C}H_d$ and $\underline{C}H_{d'}$), 128.9 ($\underline{C}H_a$ and $\underline{C}H_{a'}$), 129 ($\underline{C}H_f$), 129.5 ($\underline{C}H_e$ and $\underline{C}H_{e'}$), 130 ($\underline{C}H_c$), 132 ($\underline{C}H_b$ and $\underline{C}H_{b'}$), 138 ($\underline{C}$-CH=N), 141 ($\underline{C}$-CH_2-N), 163 ($\underline{C}$H=N); m/z (EI): 195 (M^+, 75%), 117 (M^+ - C_6H_6, 15%), 91 (M^+ - Ph-CH=N, 100%); U.V.: λ_{max} = 244 nm (CH_3CN), λ_{max} = 249 nm (H_2O)

2.2.4.2 Formation of N-benzylidene allylamine

Experimental

N-Benzylidene allylamine

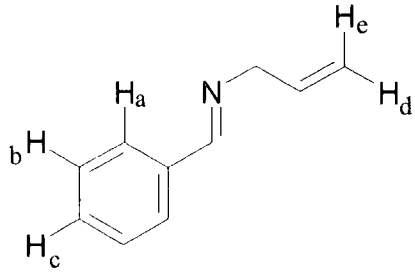

To a solution of benzaldehyde (3.5 cm^3, 34.5 mmol) in dry acetonitrile (100 cm^3) was added allylamine (2.58 cm^3, 34.5 mmol) at room temperature. The solution was left to react overnight. ^1H NMR spectroscopy was used to check that the reaction went to completion by monitoring the disappearance of the peak characteristic of the aldehydic proton at δ = 10.0 ppm. The solution was subsequently dried over molecular sieves (Type 13X, 1.6 mm pellets) and calcium hydride. The solvent was removed under reduced pressure to afford an orange oil (3.39 g, 68%). δ_H (400 MHz, CD_3CN): 4.19 (2H, *dd*, J = 5.6 Hz and 1.6 Hz, CH_2N), 5.09 (1H, *dd*, J = 10.2 Hz and 1.6 Hz, H_d), 5.19 (1H, *dd*, J = 17.1 and 1.6 Hz, H_e), 6.10 (1H, *qt*, J = 17.1 Hz, 10.2 Hz and 5.6 Hz, C<u>H</u>=CH_2), 7.38 – 7.48 (3H, *m*, $H_{b,,}$ $H_{b'}$ and H_c), 7.71 – 7.74 (2H, *dd*, J = 7.5 and 2.0 Hz, H_a and $H_{a'}$), 8.30 (1H, *s*, C<u>H</u>=N); δ_C (400 MHz, CD_3CN): 63.9 (N-CH_2), 116 (<u>C</u>H_2=CH), 129 (<u>C</u>H_a and <u>C</u>$H_{a'}$), 130 (<u>C</u>H_c), 132 (<u>C</u>H_b and <u>C</u>$H_{b'}$), 138 (<u>C</u>-CH=N), 163 (<u>C</u>H=N); m/z (EI): 145 (M^+, 30%), 144 (M^+ - H, 100%), 117 (M^+ - CH_2=CH_2, 30%), 104 (M^+ - CH_2-CH=CH_2, 24%), 91 (M^+ - N= ; m/z (CI): 146 (MH^+); U.V.: λ_{max} = 244 nm (CH_3CN), λ_{max} = 249 nm (H_2O); density = 0.926 $g.cm^{-3}$

2.2.4.3 Formation of N-(4-nitro-)benzylidene benzylamine

Experimental

N-(4-nitro-)benzylidene benzylamine

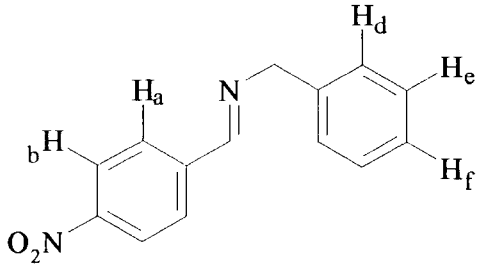

To a solution of 4-nitrobenzaldehyde (0.756 g, 5 mmol) in dry acetonitrile (50 cm^3) was added benzylamine (0.46 cm^3, 5 mmol) at room temperature. The solution was left to react overnight. ^1H NMR spectroscopy was used to check that the reaction went to completion by monitoring the disappearance of the peak characteristic of the aldehydic proton at δ = 10.0 ppm. δ_H (200 MHz, CD_3CN): 4.77 (2H, *d*, J = 1.2 Hz, CH_2), 7.33 – 7.40 (5H, *m*, H_d, $H_{d'}$, H_e, H_e and H_f), 8.00 (2H, *d*, J = 9 Hz, H_a and $H_{a'}$), 8.29 (2H, *d*, J = 9 Hz, H_b and $H_{b'}$), 8.60 (1H, *s*, CHN); U.V.: λ_{max} = 283 nm (CH_3CN), λ_{max} = 286 nm (H_2O)

2.3 Conclusions

The equilibrium constants for the formation of the bisulfite and cyanide adducts of benzaldehyde have been determined.

In both cases notable differences have been reported between the constants for the addition of bisulfite and sulfite ion in one hand and hydrogen cyanide and cyanide ion on the other hand to benzaldehyde. This phenomenon reflects the large difference between the acid dissociation constants relating to the protonated nucleophiles.

In the case of bisulfite addition $K_a^{HSO_3^-}$ is significantly higher than K_a^{HPMS} (factor of about $5x10^4$). Consequently the equilibrium constant for the addition of bisulfite to benzaldehyde is significantly higher than that of addition of sulfite to benzaldehyde.

Similarly K_a^{HCN} is higher than $K_a^{cyanohydrin}$ and addition of HCN to benzaldehyde is favoured compared to the addition of cyanide ion.

Table 2.14 Equilibrium and acid dissociation constants for HPMS and cyanohydrin formation

a)

	HPMS formation	
	HSO_3^-	HPMS
K (dm^3mol^{-1})	6429	2.14
K_a (mol dm^3)	$6.31x10^{-8}$	$2.1x10^{-11}$

b)

	Cyanohydrin formation	
	HCN	Cyanohydrin
K (dm^3mol^{-1})	303	7.08
K_a (mol dm^3)	$7.94x10^{-10}$	$1.85x10^{-11}$

Comparing the values of the equilibrium constants K_{HCN} is significantly smaller than $K_{HSO_3^-}$ whereas K_{CN^-} is larger than $K_{SO_3^{2-}}$. As for the differences within each system this reflects a difference in terms of acid dissociation constants with pK_a^{HCN} being larger than $pK_a^{HSO_3^-}$.

It is of interest that March states "In the formation of cyanohydrins it is frequently the bisulfite addition product that is treated with CN^-, in which case the reaction is actually nucleophilic substitution 2"[22]. The results found here indicate that cyanohydrin formation will only be favoured over bisulfite addition in alkaline solutions (pH > 11). Further the mechanism of this process is likely to involve a dissociation-association pathway rather than nucleophilic attack of cyanide ion on the bisulfite addition compound.

The fact that the value of K_2 for cyanide ion addition to benzaldehyde is apparently higher than the corresponding value of K_2 for sulfite addition indicates that in thermodynamic terms cyanide is the better nucleophiles in water. This behaviour contrasts with nucleophilicity parameters, n, defined in terms of rate of reaction with alkyl halide in methanol. Values of n are reported as 6.70 for cyanide and 8.53 for sulfite[23].

It may also be that the sulfite adduct (X) is destabilised relative to (Y) by the proximity of the two negative charges and also by unfavourable steric interactions.

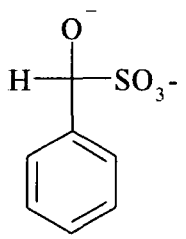

(X)

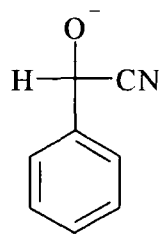

(Y)

Addition of amines to carbonyl compounds forms imines (or Schiff bases). Benzylamine and allylamine have been added to benzaldehyde to form benzylidene benzylamine and benzylidene allylamine respectively. Also 4-nitro-benzylidene benzylamine has been synthesised from the addition of benzylamine to benzaldehyde. The reaction has been

carried out in acetonitrile since benzaldehyde is not soluble in water. However it is worth mentioning the work of Tashiro et al.[15], who despite this insolubility factor successfully formed and isolated benzylidene benzylamine.

The products were characterised using NMR spectroscopy and U. V. spectrophotometry. It is worth noting that the latter displayed spectra similar to that of the reacting aldehydes with only the values for the extinction coefficients significantly different.

Table 2.15 λ_{max} and extinction coefficient values in water for the imines synthesised

	λ_{max} (nm)	ε ($dm^3mol^{-1}cm^{-1}$)
Benzylidene benzylamine	249	$1.9x10^4$
Benzaldehyde	250	$1.5x10^4$
Benzylidene allylamine	249	$1.7x10^4$
Benzaldehyde	250	$1.5x10^4$
4-Nitrobenzylidene benzylamine	286	$1.6x10^4$
4-Nitrobenzaldehyde	268	$1.3x10^4$

2.4 References

1. Raschig and Prahl, *Ann.*, 1926, **448**, 265

2. (a) T. D. Stewart and L. H. Donally, *J. Am. Chem. Soc.*, 1932, **54**, 2333; (b) T. D. Stewart and L. H. Donally, *J. Am. Chem. Soc.*, 1932, **54**, 3555; (c) T. D. Stewart and L. H. Donally, *J. Am. Chem. Soc.*, 1932, **54**, 3559; (d) M. A. Gubareva, *J. Gen. Chem. (USSR)*, 1947; **17**, 2259

3. (a) F. C. Kokesh and R. E. Hall, *J. Org. Chem.*, 1975, **40**, 1632; (b) T. M. Olson, S.D. Boyce and M. R. Hoffmann, *J. Phys. Chem.*, 1986, **90**, 2482; (c) E. A. Betterton and M. R. Hoffmann, *J. Phys. Chem.*, 1987, **91**, 3011

4. P. E. Sørensen and V. S. Andersen, *Acta Chem. Scand.*, 1970, **24**, 1301

5. S. D. Boyce and M. R. Hoffmann, *J. Phys. Chem.*, 1984, **88**, 4740

6. I. J. Smith, PhD Thesis, University of Durham, 2003

7. J. A. Sousa and J. D. Margerum, *J. Am. Chem. Soc.*, 1960, **82**, 3013

8. W. Kerp, *Chem. Zentralbl.*, 1904, **75/II**, 56

9. K. Arai, *Nippon Kagaku Zasshi*, 1962, **83**, 765

10. D. A. Blackadder and C. Hinshelwood, *J. Chem. Soc.*, 1958, 2720

11. P. R. Young and W. P. Jencks, *J. Am. Chem. Soc.*, 1978, **100**, 1228

12. A. Lapworth, *J. Chem. Soc.*, 1903, **83**, 995

13. W. M. Ching and R. G. Kallen, *J. Am. Chem. Soc.*, 1978, **100**, 6119

14 (a) A. Lapworth and R. H. F. Manske, *J. Chem. Soc.*, 1928, 2533; (b) A. Lapworth and R. H. F. Manske, *J. Chem. Soc.*, 1930, 1976

15. (a) M. J. O'Donnell, W. D. Bennett, W. A. Bruder, W. N. Jacobsen, K. Knuth, B. LeClef, R. L. Polt, F. G. Bordwell, S. R. Mrozack and T. A. Cripe, *J. Am. Chem. Soc.*, 1988, **110**, 8520; (b) A. T. Nielsen, R. A. Nissan and D. J. Vanderah, *J. Am. Chem. Soc.*, 1990, **55**, 1459; (c) C. V. Stevens, W. Vekemans, K. Moonen and T. Rammeloo, *Tetrahedron Lett.*, 2003, **44**, 1619

16. A. Simion, C. Simion, T. Kanda, S. Nagashima, Y. Mitoma, T. Yamada, K. Mimura and M. Tashiro, *J. Chem. Soc., Perkin Trans. 1*, 2001, **17**, 2071

17. G. Kaupp, *J. Chem. Soc., Perkin Trans. 2*, 1998, 989

18. (a) R. Grigg and P. J. Stevenson, *Synthesis*, 1983, **12**, 1009; (b) G. Wolf and E. -U. Würthwein, *Chemische Berichte*, 1991, **124**, 655; (c) A. Saoudi, A. Benguedach and H. Benhaoua, *Synthetic Communications*, 1995, **25**, 2349; (d) N. De Kimpe, D. De Smaele and Z. Sakonyi, *J. Org. Chem.*, 1997, **62**, 2448; (e) K. A. Tehrani, T. NguyenVan, M. Karikomi, M. Rottiers and N. De Kimpe, *Tetrahedron*, 2002, **58**, 7145

19. G. I. Georg, J. Kant, P. He, L. Y. Am and L. Lampe, *Tetrahedron Lett.*, 1988, **29**, 2409

20. F. Texier-Boullet, *Synthesis*, 1985, 679

21. (a) E. Hayon, A. Treimin and J. Wilf, *J. Am. Chem. Soc.*, 1972, **94**, 47, (b) H. V. Tartar and H. H. Garretson, *J. Am. Chem. Soc.*, 1941, **63**, 808

22 J. March, *Advanced Organic Chemistry*, Wiley

23. (a) R. G. Pearson, H. Sobel and J. Songstad, *J. Am. Chem. Soc.*, 1968, **90**, 319; (b) T. H. Lowry and K. S. Richardson, *Mechanism and Theory in Organic Chemistry*, 3rd Ed., Harper and Row, New York, 1987

Chapter Three: The reactions of imines

Chapter three: The reactions of imines

3.1 Introduction

3.1.1 The Strecker reaction

In the Strecker reaction a carbonyl compound, an amine and cyanide react together to form an α-aminonitrile. Hydrolysis may yield the corresponding α-amino acid.

Scheme 3.1

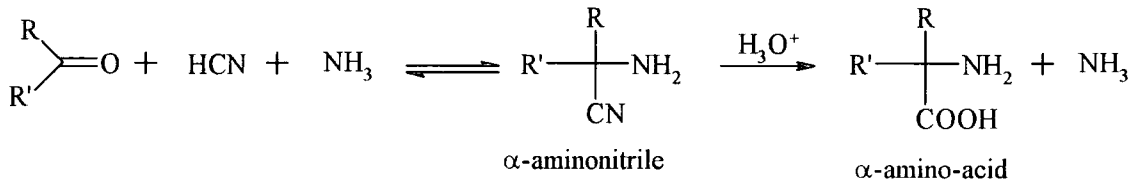

Early studies[1] considered the formation of the cyanohydrin as the rate determining step for the reaction. Sannie studied the reaction of ethanal with ammonia and hydrogen cyanide and suggested that the resulting aminonitrile decomposes to give an aminodinitrile accounting for the reformation of ammonia in the process.

Scheme 3.2

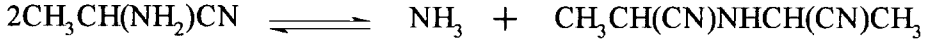

Later Stewart and Li[2] investigated the reaction of cyanohydrins with cyanide. They concluded that the cyanohydrin is in equilibrium with the carbonyl compound and the amine and that the reactive intermediate is the carbinolamine with its formation being the rate determining step.

Scheme 3.3

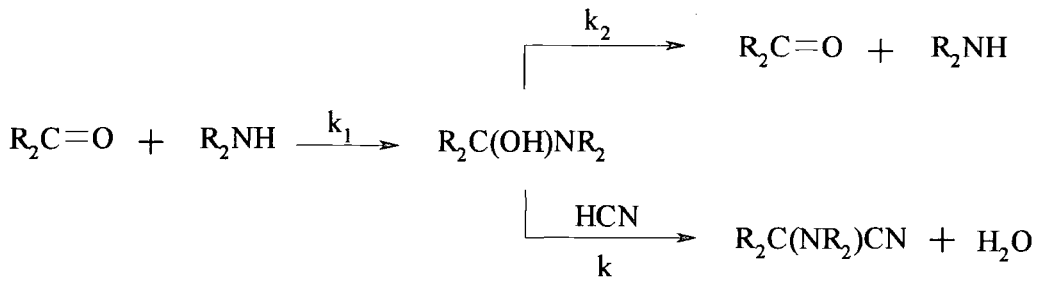

It was not until 1971 that Ogata and Kawasaki[3] offered a reliable mechanistic study of aminonitrile formation. They showed that the reaction of benzaldehyde cyanohydrin with aniline was significantly slower than that of the imine formed from benzaldehyde and aniline (benzylidene aniline) with cyanide or even than that of the three compounds mixed together.

The imine proved to be a true intermediate and the data collected fitted the following rate law:

$$\upsilon = k_2[ArCH{=}NAr'][HCN] \qquad \textbf{(3.1)}$$

Varying the cyanide concentration allowed for the calculation of $k_2 = 3.44 \times 10^{-2}$ $dm^3mol^{-1}s^{-1}$ for the addition of cyanide to benzylidene aniline.

Stanley and co-workers[4] suggested the possible intermediacy of the cationic form of the imine in aminonitrile formation. They showed that in the reaction of cyanide with secondary amines and ketones steric factors are important in formation of iminium ions.

Further, in the mid 1970's Taillades, Commeyras and co-workers investigated α-aminonitrile formation and decomposition from both ketones and aldehydes.

A study of the decomposition of α-amino, α-methylamino and α-dimethylamino-isobutyronitriles[5] indicated that an equilibrium is reached at pH values between 7 and 13. Above pH = 13 basic catalysis was noted. For pH < 7 depending on the degree of substitution on the nitrogen atom two phenomena are observed. The α-amino and α-methylamino-isobutyronitriles slowly form an intermediate which in turn reacts very quickly to form

acetone. In the case of the α-dimethylamino-isobutyronitrile accumulation of the intermediate is noticed and identified as the ketiminium ion. The presence of the two methyl groups on the nitrogen atom contributes to the stability of the intermediate.

In the formation of the aminonitrile the intermediacy of the imine or the iminium ion is implicated. Further studies[6] showed that the cyanohydrin is formed in a competitive, equilibrated and fast reaction. Thus during the formation of the aminonitrile from acetone an equilibrium between the cyanohydrin and acetone is maintained. The imine or iminium ion is a thermodynamically stable intermediate in the medium although in low concentrations.

The mechanism for the addition of cyanide involves three entities: the imine, the cyanide ion and the hydronium ion. Taillades and Commeyras considered the possibility of a concerted reaction as shown in scheme 3.4.

Scheme 3.4

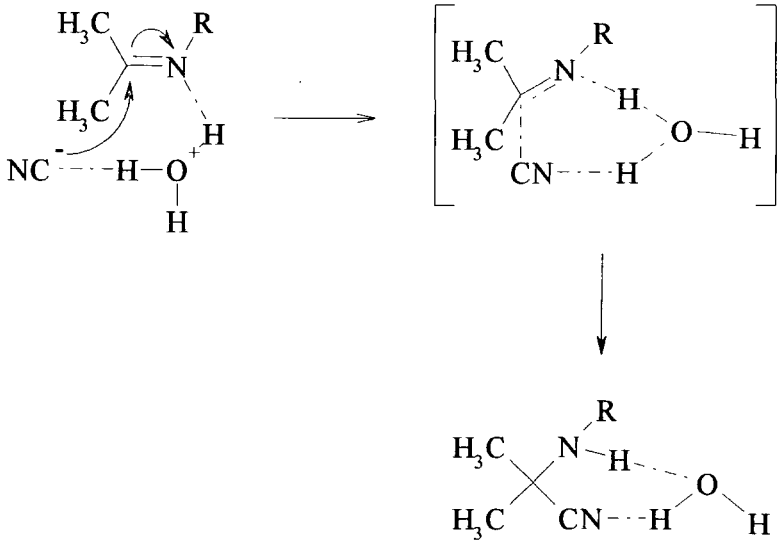

However they favoured[7] a stepwise process involving the three steps:

1. The uncatalysed attack of the basic amine yields a carbinolamine:

$$R_1R_2CO + R_3R_4NH \rightleftharpoons R_1R_2C(OH)NR_3R_4$$

2. Slow dissociation of the carbinolamine yields an iminium ion:

$$R_1R_2C(OH)NR_3R_4 \rightleftharpoons R_1R_2CN^+NR_3R_4 + OH^-$$

3. The attack of CN^- on the iminium ion yields the α-aminonitrile;

$$R_1R_2CN^+NR_3R_4 + CN^- \rightleftharpoons R_1R_2C(CN)NR_3R_4$$

A plot of the observed equilibrium constant K_{obs} for the formation of the aminonitrile against pH is a bell shaped curve. The maximum in the curve represents the pH at which the concentration of aminonitrile is optimal and $\frac{d(K_{obs})}{d(pH)} = 0$. Therefore $pH_{optimum} = \frac{1}{2}(pK_1 + pK_2)$ where K_1 and K_2 are the acidity constants of the ammonium ion and hydrogen cyanide respectively.

In the case where aldehydes are used as the carbonyl compound the formation of α-aminodinitriles is noted[8]. The α-aminonitrile then competes with the amine to react with the aldehyde as shown in Scheme 3.5.

Scheme 3.5

$$RCHO + H_2NR' \rightleftharpoons RHC(OH)NHR'$$

$$RHC(OH)NHR' \rightleftharpoons RHC{=}N^+HR' + OH^-$$

$$RHC{=}N^+HR' + CN^- \rightleftharpoons RHC(CN)NHR'$$

$$RHC(CN)NHR' + RCHO \rightleftharpoons RHC(CN)N(R')C(OH)HR$$

$$RHC(CN)N(R')C(OH)HR \rightleftharpoons RHC(CN)N^+(R'){=}CHR$$

$$RHC(CN)N^+(R'){=}CHR \rightleftharpoons RHC(CN)N(R')C(CN)HR$$

An optimum pH for the formation of the dinitriles can be expressed as $pH_{optimum} = \frac{1}{2}(pK_2 + pK_{aminonitrile})$.

3.1.2 Iminium ion reactivity

Iminium ions are known reactive intermediates in numerous chemical and biological reactions.

They result from the addition of an amine to a carbonyl compound under general acid-base catalysis reaction conditions. The iminium ion generated from a primary amine is the reactive intermediate in the reversible formation of the imine as shown in Scheme 3.6.

Scheme 3.6

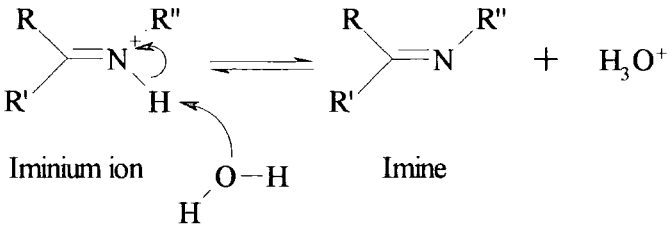

In the case of iminium ions formed from secondary amines the absence of a hydrogen atom on the nitrogen does not enable the formation of the imine. Enamine formation is however possible if an α-proton is present on the molecule (Scheme 3.7).

Scheme 3.7

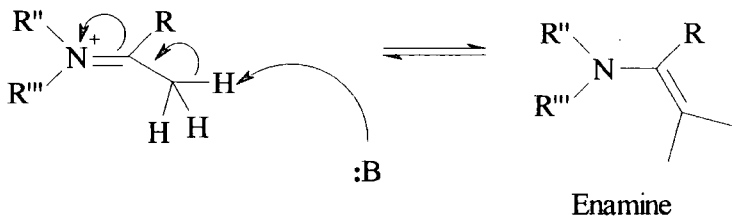

In the reverse process the hydrolysis of imines involve iminium ions as intermediates. The reaction is known and has been studied[9]. However little direct kinetic data is available for reaction of water or nucleophiles with iminium ions.

Eldin and Jencks[10] reported values for the solvolysis reaction of some anilinothioethers (1) which generate an iminium ion intermediate (2). Using added thiolate ions to trap the

iminium ions and assuming that the 'trapping reaction' was diffusion controlled, they were able to calculate the value for k_{H_2O}, rate constant for the reaction of **2** with water.

Scheme 3.8

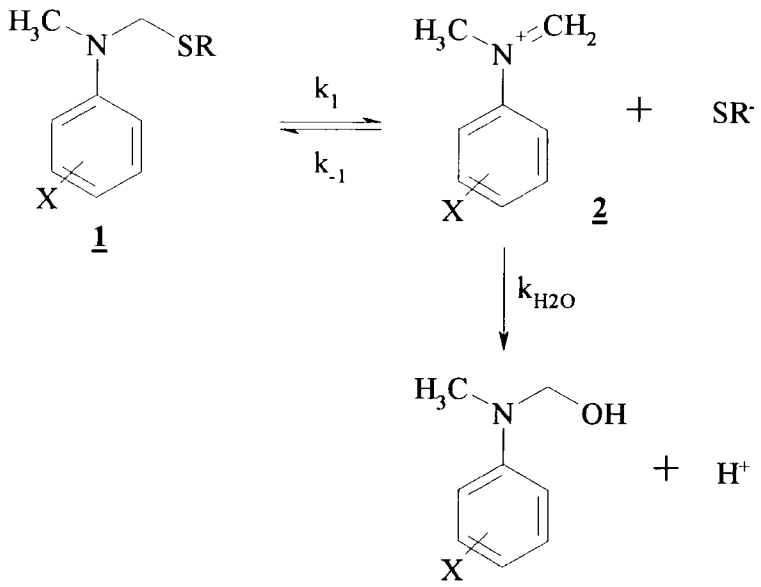

Some values for k_{H_2O} are collected in Table 3.1.

Table 3.1 Rate constants for the reaction of 2 with water, T = 25°C, I = 0.5M

X	k_{H_2O} (s^{-1})
4-NO_2	1.0×10^8
4-CN	3.1×10^7
3-NO_2	3.0×10^7
3-Cl	5.5×10^6
4-COO^-	4.5×10^6
4-Cl	3.1×10^6

Similar measurements have been recorded for other iminium ions containing aryl[11], aliphatic[12] or nitroso groups[13] as shown in Scheme 3.9.

Scheme 3.9

a)

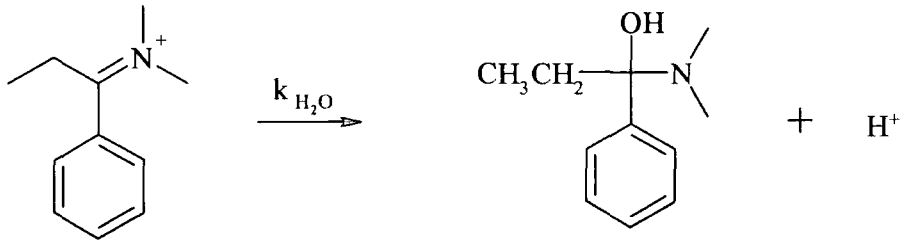

$k_{H_2O} = 2x10^{-3}\ s^{-1}$

b)

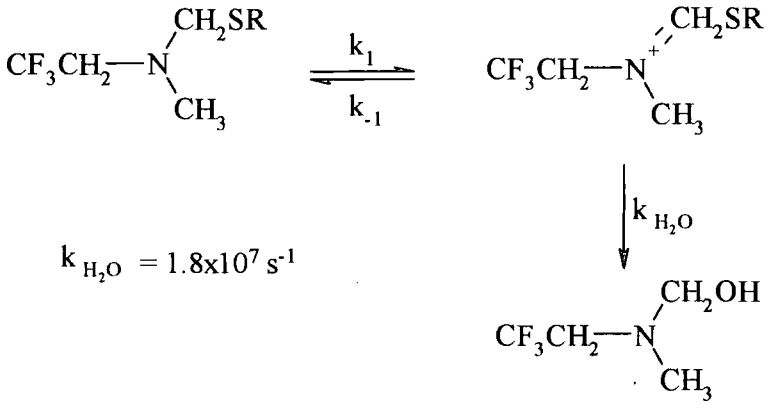

$k_{H_2O} = 1.8x10^{7}\ s^{-1}$

c)

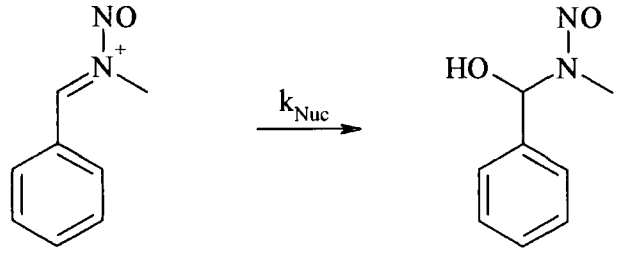

$k_{H_2O} = 7.6x10^{5}\ s^{-1}$

$k_{CN^-} = 2.2x10^{7}\ dm^3mol^{-1}s^{-1}$

It is worth noting that in the case of the nitrosoiminium ion Kresge and co-workers have recorded the rate constants for the reaction of the cation with various nucleophiles, including cyanide ion, of particular interest for the present work.

3.2 Results and discussion

The reactions of N-benzylidene benzylamine, N-benzylidene allylamine and N-(4-nitro-)benzylidene benzylamine with cyanide are reported. Kinetic studies of the reaction of the above mentioned imines with cyanide ions in aqueous solutions were performed. The rates of decomposition of the resulting aminonitriles were determined and the equilibrium constants corresponding to the system calculated.

The hydrolysis process was also examined for the three imines.

3.2.1 Methodology

3.2.1.1 Aminonitriles formation

Addition of trimethylsilyl cyanide (TMSCN) to the imines in damp acetonitrile afforded the α-aminonitriles. The products were not isolated and were solely used as characterisation tools.

3.2.1.2 UV/Vis spectroscopy

N-Benzylidene benzylamine and N-benzylidene allylamine absorb strongly in the 250 nm region whereas N-(4-nitro)benzylidene benzylamine displays a strong absorbance in the 280 nm region of the spectrum. Addition of cyanide resulted in the formation of aminonitriles. The products do not display a significant absorbance in the above mentioned regions. The rates of formation and decomposition can then be determined using readings at $\lambda = 250$ nm or 280 nm accordingly.

Hydrolysis of imines results in the re-formation of the parent aldehyde which absorbs in the same region of the spectrum. The difference in magnitude of the extinction coefficients is sufficiently high to follow a decrease in absorbance when completing the reaction.

3.2.1.3 NMR spectroscopy

The aminonitriles formed from the addition of TMSCN to the imines in damp acetonitrile were characterised using their NMR spectra. The spectra were recorded by diluting the solutions in deuterated acetonitrile (CD_3CN).

3.2.2 α-aminonitriles formation: Strecker reaction

3.2.2.1 2-Benzylamino-2-phenylacetonitrile

3.2.2.1.1 ^{1}H NMR characterisation

Experimental

2-Benzylamino-2-phenylacetonitrile

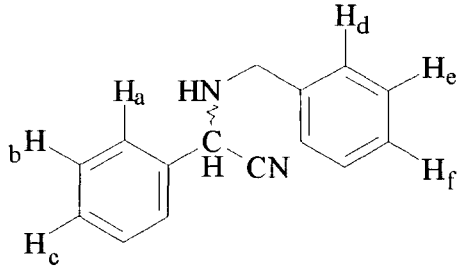

To a solution of benzylidene benzylamine (0.95 cm^3, 5.10 mmol) in damp acetonitrile (50 cm^3) was added 1.1 equivalent of TMSCN (0.748 cm^3, 5.61 mmol) at room temperature. The solution was left to react overnight. ^{1}H NMR was used to check that the reaction went to completion by monitoring the resonance of the CHN proton which is at δ_H = 8.47 ppm in the imine and shifts to δ_H = 4.80 ppm in the aminonitrile. δ_H (400 MHz, CD_3CN): 2.54 (1H, *broad m*, NH), 3.77-3.90 (2H, *2x dd*, J = 6 Hz and 13 Hz, CH_2), 4.80 (1H, *d*, J = 10 Hz, CHN), 7.22 - 7.40 (8H, *m*, H_b, $H_{b'}$, H_c, H_d, $H_{d'}$, H_e, $H_{e'}$ and H_f), 7.47 – 7.49 (2H, *m*, H_a and $H_{a'}$)

3.2.2.1.2 Kinetic measurements

Experimental procedure:

Aqueous solutions of cyanide (using potassium cyanide) were freshly prepared under a fume hood before each experiment.

The rate constants were determined by diluting benzylidene benzylamine to a $1x10^{-4}$ mol dm^{-3} concentration in aqueous buffered solutions of potassium cyanide under a fume hood.

The changes with time of the U. V. absorbance at 250 nm were used to monitor the reactions.

Typical plots are shown on Figures 3.1 and 3.2.

Figure 3.1 Absorbance versus time plots for the reaction of $1x10^{-4}$ mol dm^{-3} benzylidene benzylamine with varying cyanide concentrations at pH=9.01, 25° C, λ = 250 nm

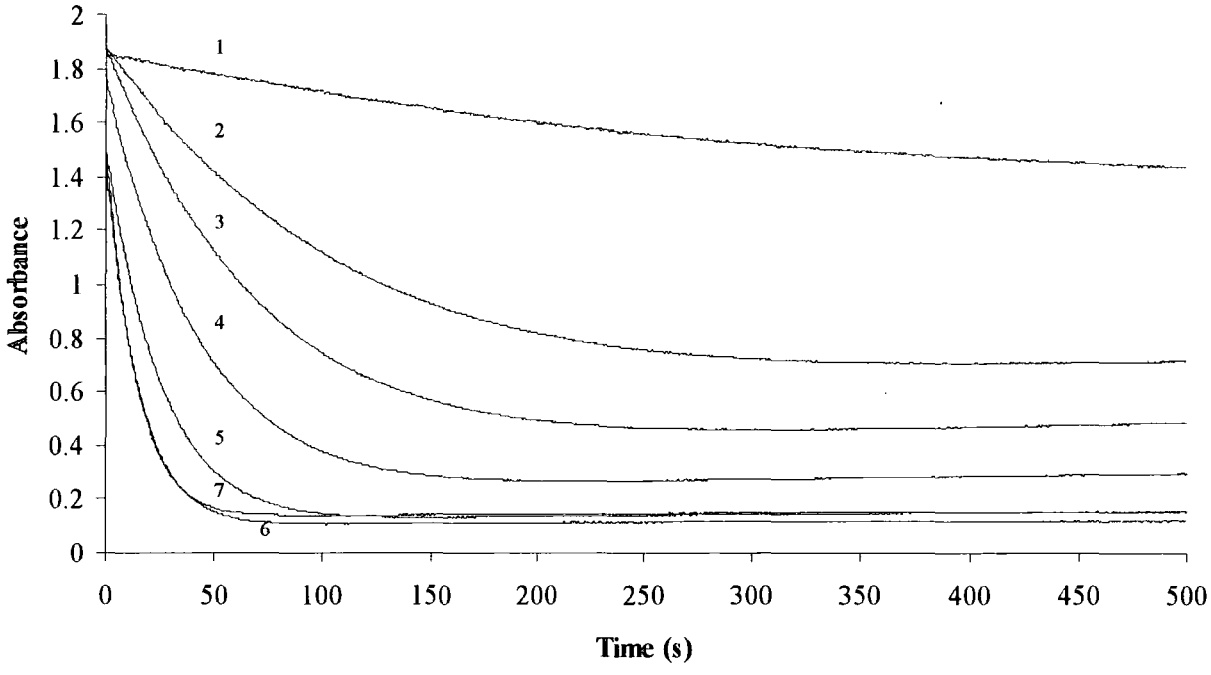

Concentrations of cyanide are: 1, 0 mol dm^{-3}; 2, $1x10^{-3}$ mol dm^{-3}; 3, $2x10^{-3}$ mol dm^{-3}; 4, $4x10^{-3}$ mol dm^{-3}; 5, $8x10^{-3}$ mol dm^{-3}; 6, $1.6x10^{-2}$ mol dm^{-3}; 7, $2x10^{-2}$ mol dm^{-3}

Figure 3.2 Absorbance versus time plots for the reaction of $1x10^{-4}$ mol dm^{-3} benzylidene benzylamine with varying cyanide concentrations at pH=9.01, 25° C, λ = 250 nm

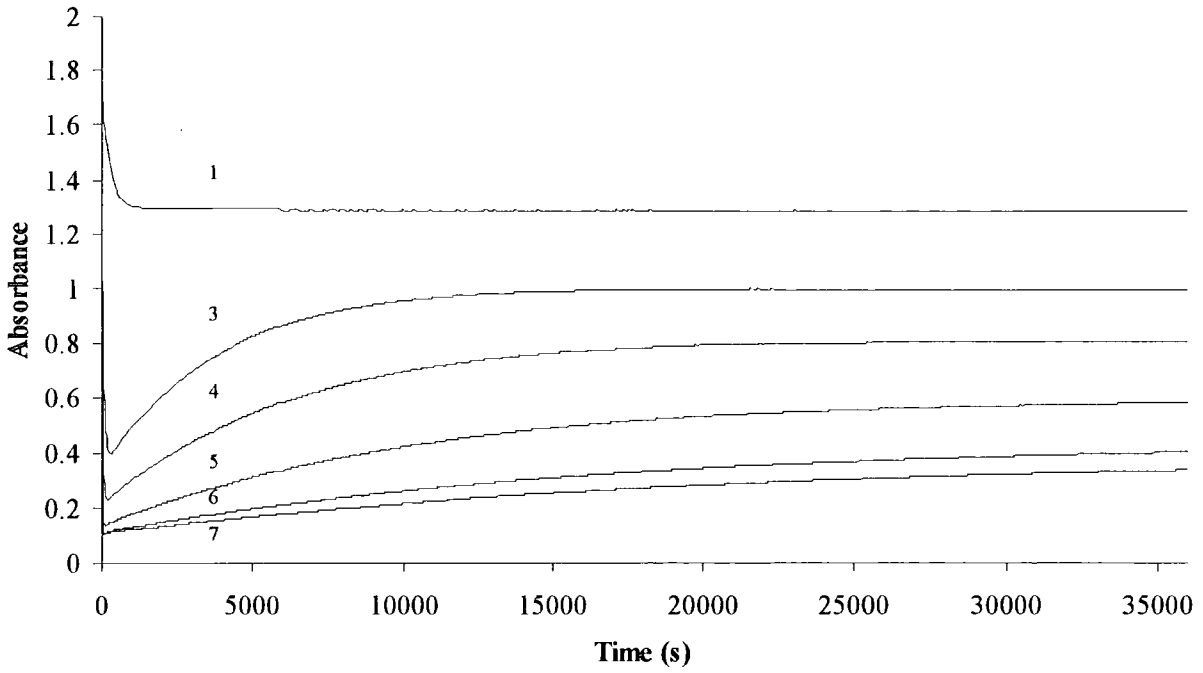

Concentrations of cyanide are: 1, 0 mol dm^{-3}; 3, $2x10^{-3}$ mol dm^{-3}; 4, $4x10^{-3}$ mol dm^{-3}; 5, $8x10^{-3}$ mol dm^{-3}; 6, $1.6x10^{-2}$ mol dm^{-3}; 7, $2x10^{-2}$ mol dm^{-3}

Results

From Figures 3.1 and 3.2 it is possible to distinguish two processes. The initial decrease in absorbance accounts for the fast reaction, k_{fast}, of the parent imine which fractionates between aminonitrile formation and hydrolysis to form benzaldehyde. The slower second process, k_{slow}, leading to an increase in absorbance is due to the decomposition of the aminonitrile.

The increase in the value of the absorbance with decreasing cyanide concentration at the end of the fast process is due to formation of benzaldehyde rather than decomposition of the aminonitrile implying that the reverse process, k_{-1}, is negligible here.

The kinetic scheme for the formation of 2-benzylamino-2-phenylacetonitrile can represented as follows:

Scheme 3.10

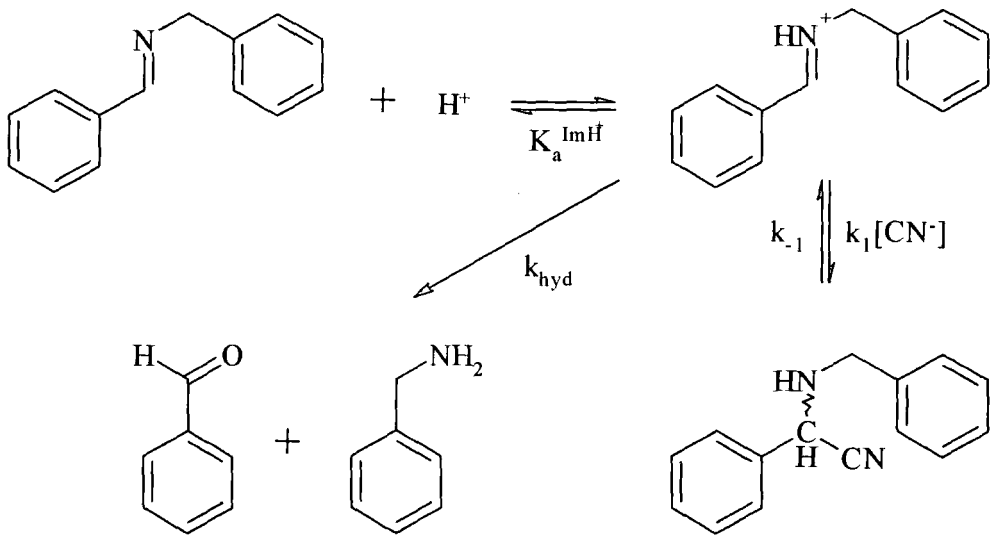

Formation of the α-aminonitrile involves reaction through the iminium ion. Hydrolysis, to give benzaldehyde and benzylamine, competes with the cyanide reaction. Since the formation of the α-aminonitrile is reversible, the eventual products in dilute aqueous solution are benzaldehyde (or its cyanohydrin derivative) and benzylamine.

The velocity for the formation of the α-aminonitrile, with reference to Scheme 3.10, is given by equation 3.1

$$\text{velocity} = k_1[\text{ImineH}^+][CN^-] + k_{hyd}[\text{Imine}]_{stoich} \qquad \textbf{(3.1)}$$

k_{hyd} is the overall rate constant for hydrolysis of the imine, in both its neutral and protonated forms, at a given pH. Here and elsewhere the subscript 'stoich' is used to represent the total, stoichiometric concentration of a species in all its ionisation states.

The proton transfers are likely to be rapid:

$$K_a^{HCN} = \frac{[H^+][CN^-]}{[HCN]} \qquad \textbf{(3.2)}$$

$$K_a^{\text{ImineH}^+} = \frac{[H^+][\text{Imine}]}{[\text{ImineH}^+]} \quad (3.3)$$

$$K_a^{\text{AdductH}^+} = \frac{[\text{Adduct}][H^+]}{[\text{AdductH}^+]} \quad (3.4)$$

According to the stoichiometry:

$$[\text{Imine}]_{\text{stoich}} = [\text{Imine}] + [\text{ImineH}^+] \quad (3.5)$$

and

$$[CN^-]_{\text{stoich}} = [CN^-] + [\text{HCN}] \quad (3.6)$$

Therefore:

$$[\text{Imine}]_{\text{stoich}} = \frac{(K_a^{\text{ImH}^+} + [H^+])}{[H^+]} \times [\text{ImineH}^+] \quad (3.7)$$

and

$$[CN^-]_{\text{stoich}} = \frac{(K_a^{\text{HCN}} + [H^+])}{K_a^{\text{HCN}}} \times [CN^-] \quad (3.8)$$

Rearranging **(3.7)** and **(3.8)** in **(3.1)**:

$$\text{velocity} = k_1[\text{Imine}]_{\text{stoich}}[CN^-]_{\text{stoich}} \times \frac{[H^+]}{(K_a^{\text{ImH}^+} + [H^+])} \times \frac{K_a^{\text{HCN}}}{([H^+] + K_a^{\text{HCN}})} + k_{\text{hyd}}[\text{Imine}]_{\text{stoich}} \quad (3.9)$$

Hence:

$$\text{velocity} = k_{\text{fast}}[\text{Imine}]_{\text{stoich}} \quad (3.10)$$

with:

$$k_{fast} = k_1[CN^-]_{stoich} \times \frac{[H^+]}{(K_a^{ImH^+} + [H^+])} \times \frac{K_a^{HCN}}{([H^+] + K_a^{HCN})} + k_{hyd} \quad (3.11)$$

Therefore plots of k_{fast} versus $[CN^-]_{stoich}$ are predicted to be linear with:

$$k_{fast} = k_f[CN^-]_{stoich} + k_{hyd} \quad (3.12)$$

where:

$$k_f = k_1 \times \frac{[H^+]}{(K_a^{ImH^+} + [H^+])} \times \frac{K_a^{HCN}}{([H^+] + K_a^{HCN})} \quad (3.13)$$

The equation predicts two linear parts for the plot of Log (k_f) against pH. For low pH values, $[H^+] >> K_a^{ImH+}$ and $[H^+] >> K_a^{HCN}$ therefore:

$$k_f = k_f \times K_a^{HCN} \times \frac{1}{[H^+]} \Leftrightarrow Log(k_f) = Log(k_1 \times K_a^{HCN}) + pH \quad (3.14)$$

At high pH, $[H^+] << K_a^{ImH+}$ and $[H^+] << K_a^{HCN}$ therefore:

$$k_f = \frac{k_1}{K_a^{ImH^+}} \times [H^+] \Leftrightarrow Log(k_f) = Log(\frac{k_1}{K_a^{ImH^+}}) - pH \quad (3.15)$$

The decrease in absorbance with time was measured in the pH range 6-10. The process followed first order kinetics and the curves were fitted using the Scientist® computer package. The rate constants k_{fast} were collected and for each pH value plotted against the stoichiometric concentration in cyanide, $[CN^-]$. Spectra are shown in Figures 3.3 to 3.9. An example of the linear plot for $k_{fast} = k_f([CN^-]$ according to equation 3.12 is shown on Figure 3.10.

Note: The legend for Figures 3.3 to 3.9 is given in Table 3.2

Figure 3.3 Absorbance versus time plots for the reaction of $1x10^{-4}$ mol dm^{-3} benzylidene benzylamine with varying cyanide concentrations at pH=5.94, 25° C, λ = 250 nm

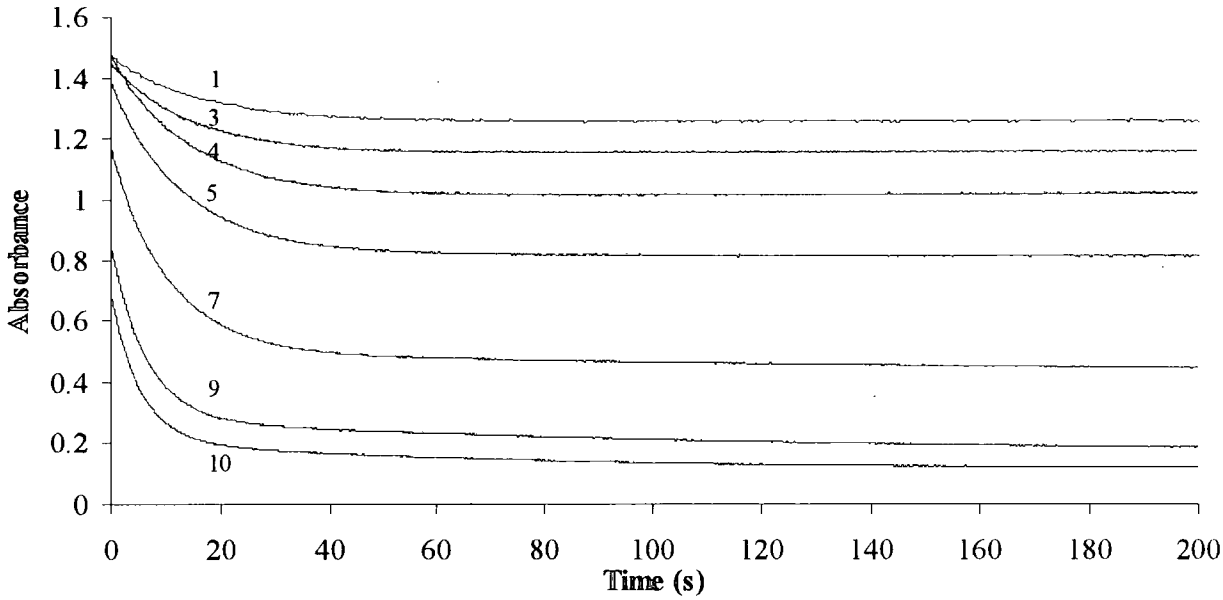

Figure 3.4 Absorbance versus time plots for the reaction of $1x10^{-4}$ mol dm^{-3} benzylidene benzylamine with varying cyanide concentrations at pH=6.40, 25° C, λ = 250 nm

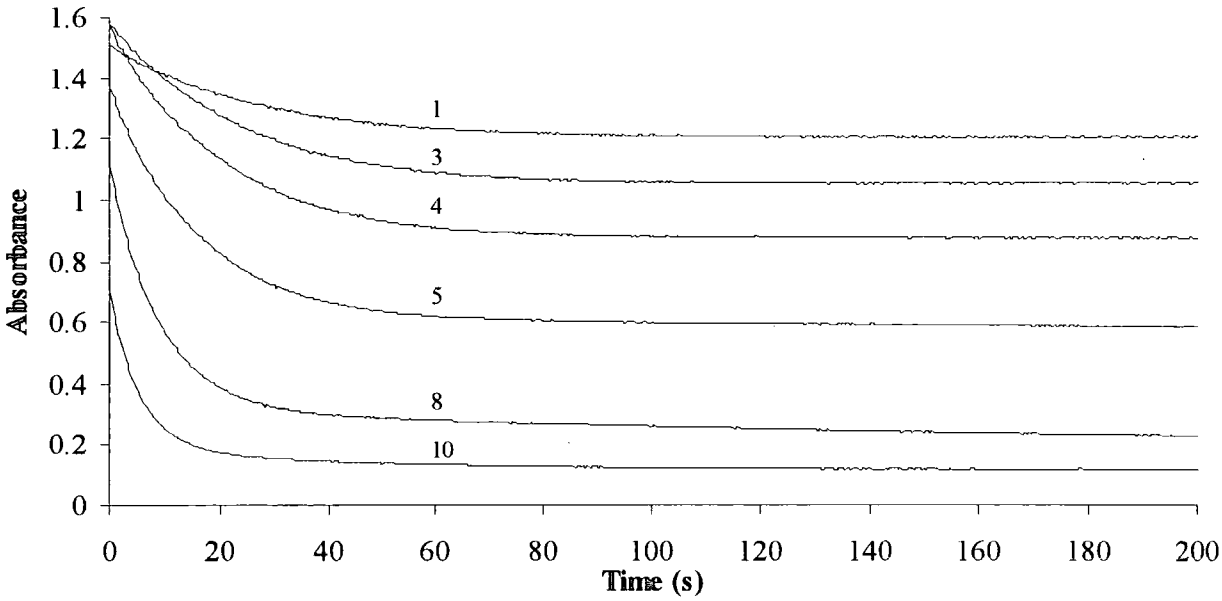

Figure 3.5 Absorbance versus time plots for the reaction of $1x10^{-4}$ mol dm^{-3} benzylidene benzylamine with varying cyanide concentrations at pH=7.28, 25° C, λ = 250 nm

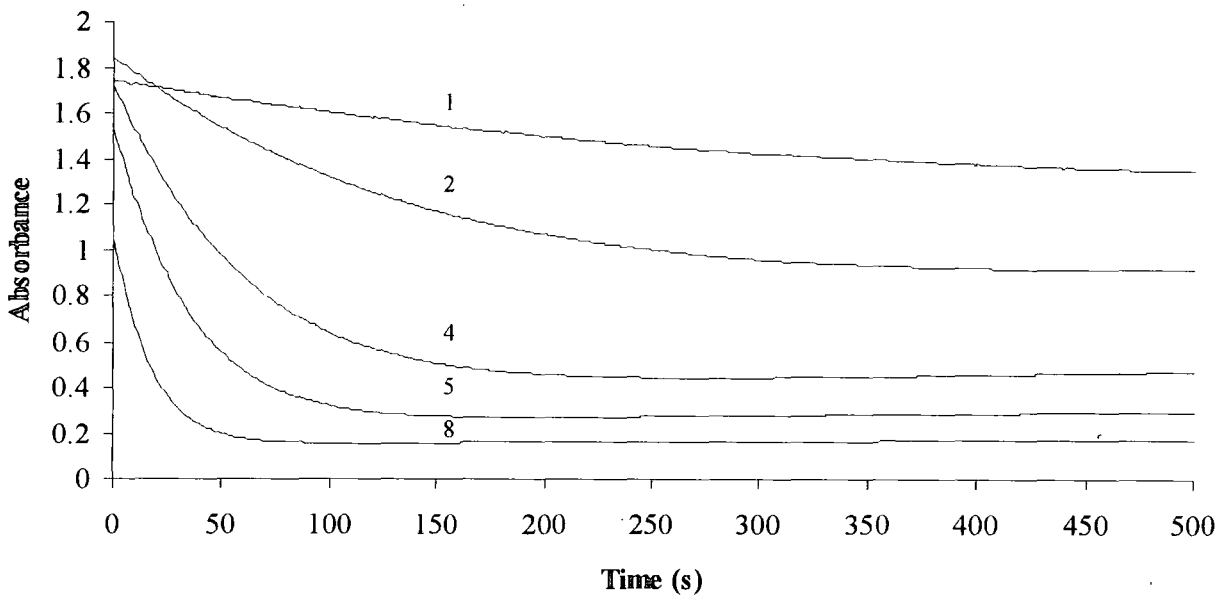

Figure 3.6 Absorbance versus time plots for the reaction of $1x10^{-4}$ mol dm^{-3} benzylidene benzylamine with varying cyanide concentrations at pH=8.55, 25° C, λ = 250 nm

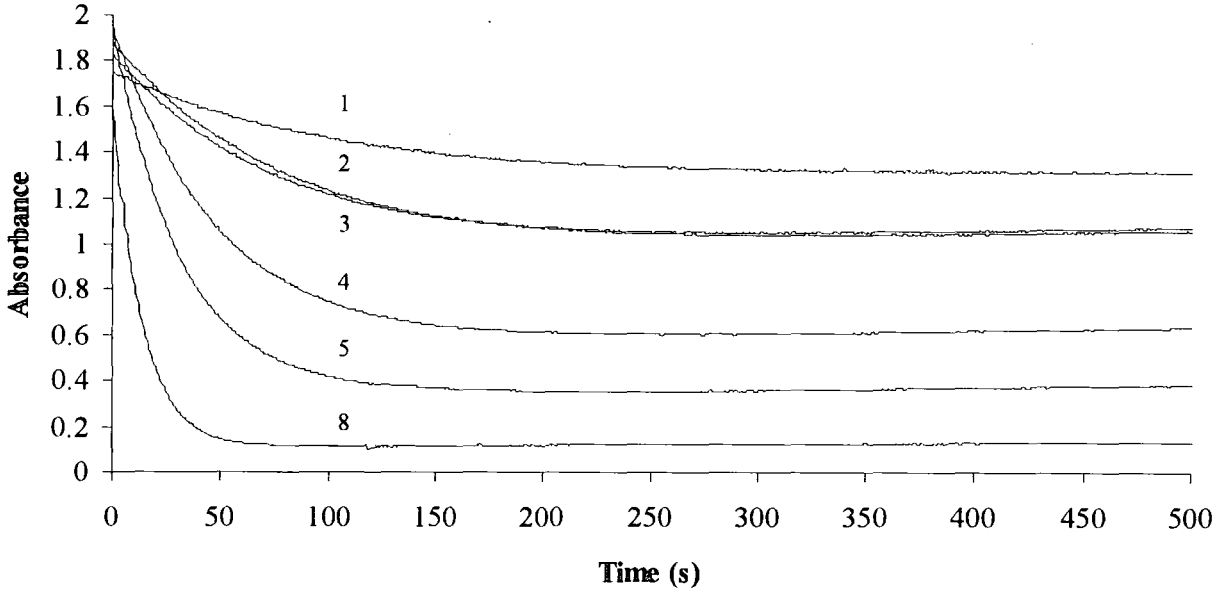

Figure 3.7 Absorbance versus time plots for the reaction of $1x10^{-4}$ mol dm^{-3} benzylidene benzylamine with varying cyanide concentrations at pH=9.01, 25° C, λ = 250 nm

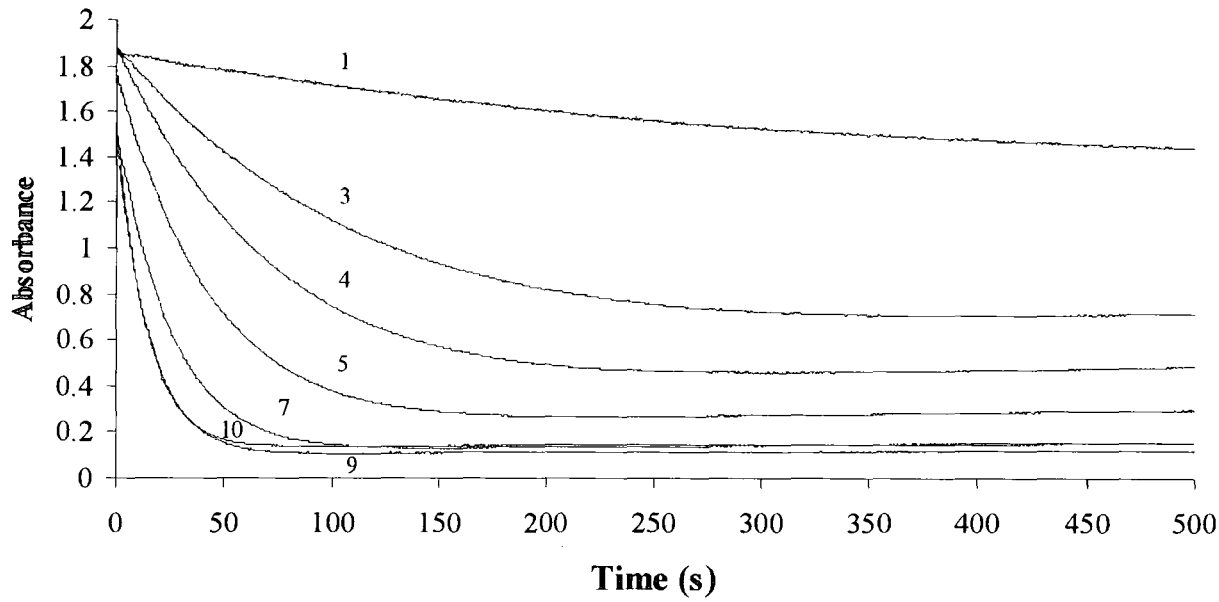

Figure 3.8 Absorbance versus time plots for the reaction of $1x10^{-4}$ mol dm^{-3} benzylidene benzylamine with varying cyanide concentrations at pH=9.85, 25° C, λ = 250 nm

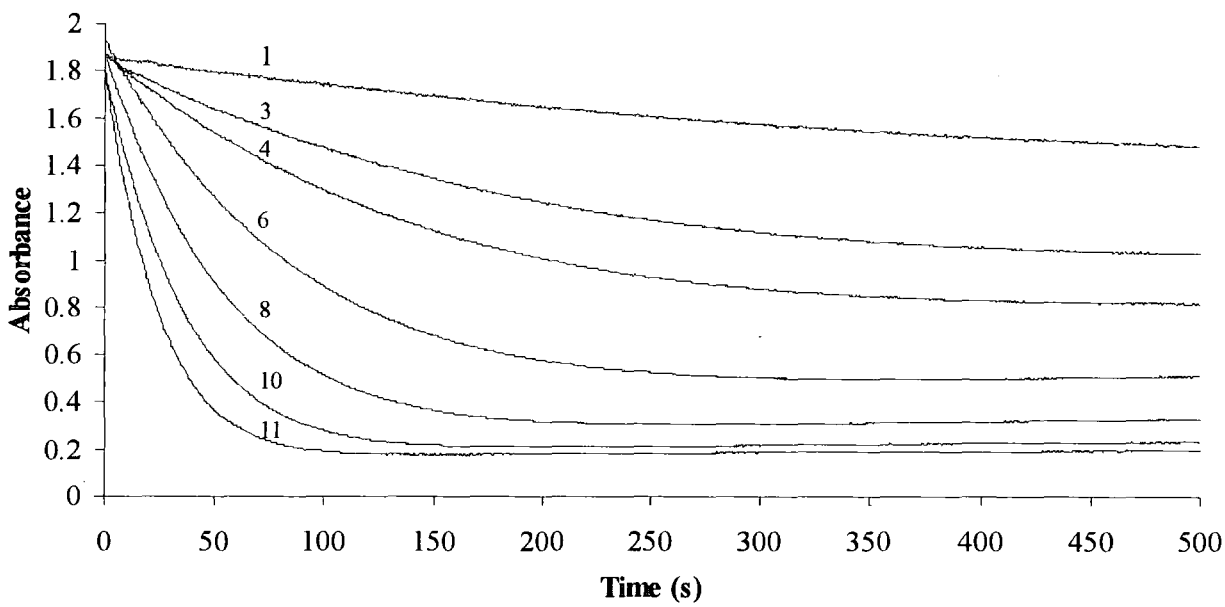

Figure 3.9 Absorbance versus time plots for the reaction of $1x10^{-4}$ mol dm^{-3} benzylidene benzylamine with varying cyanide concentrations at pH=10.4, 25° C, λ = 250 nm

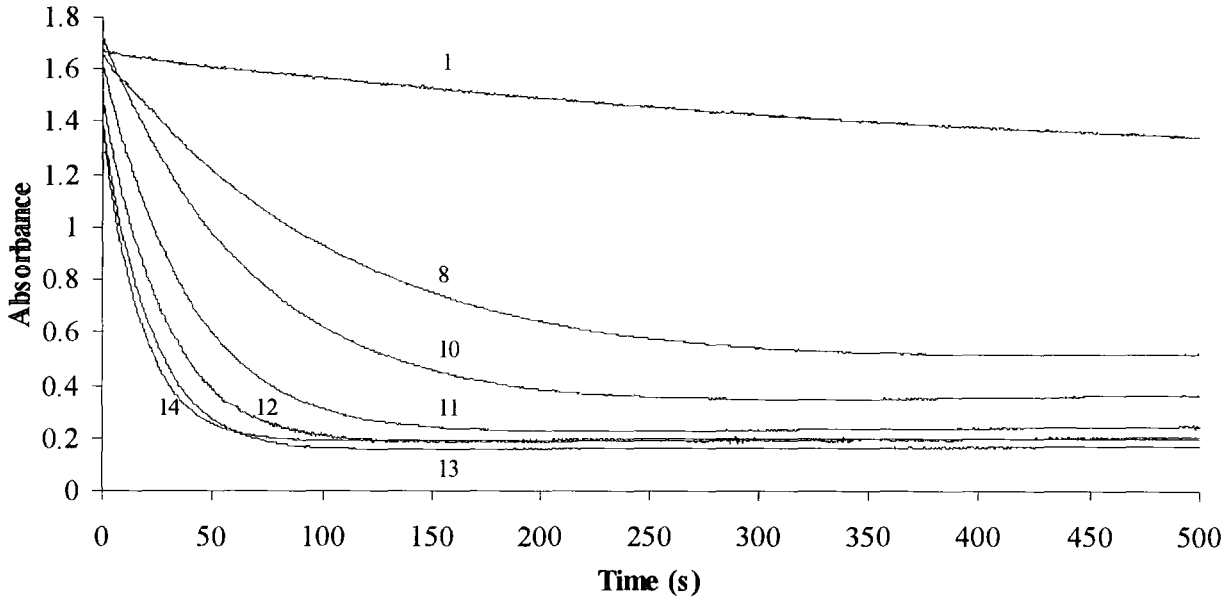

Table 3.2 Legend of Figures 3.3 – 3.9

Legend	$[CN^-]$ (dm^3 mol^{-1})
1	0
2	$5.0x10^{-4}$
3	$1.0x10^{-3}$
4	$2.0x10^{-3}$
5	$4.0x10^{-3}$
6	$5.0x10^{-3}$
7	$8.0x10^{-3}$
8	$1.0x10^{-2}$
9	$1.6x10^{-2}$
10	$2.0x10^{-2}$
11	$4.0x10^{-2}$
12	$6.0x10^{-2}$
13	$8.0x10^{-2}$
14	$1.0x10^{-1}$

Figure 3.10 Plot of k_{fast} versus [CN^-] for the reaction of $1x10^{-4}$ mol dm^{-3} benzylidene benzylamine with cyanide at pH=6.40, 25° C.

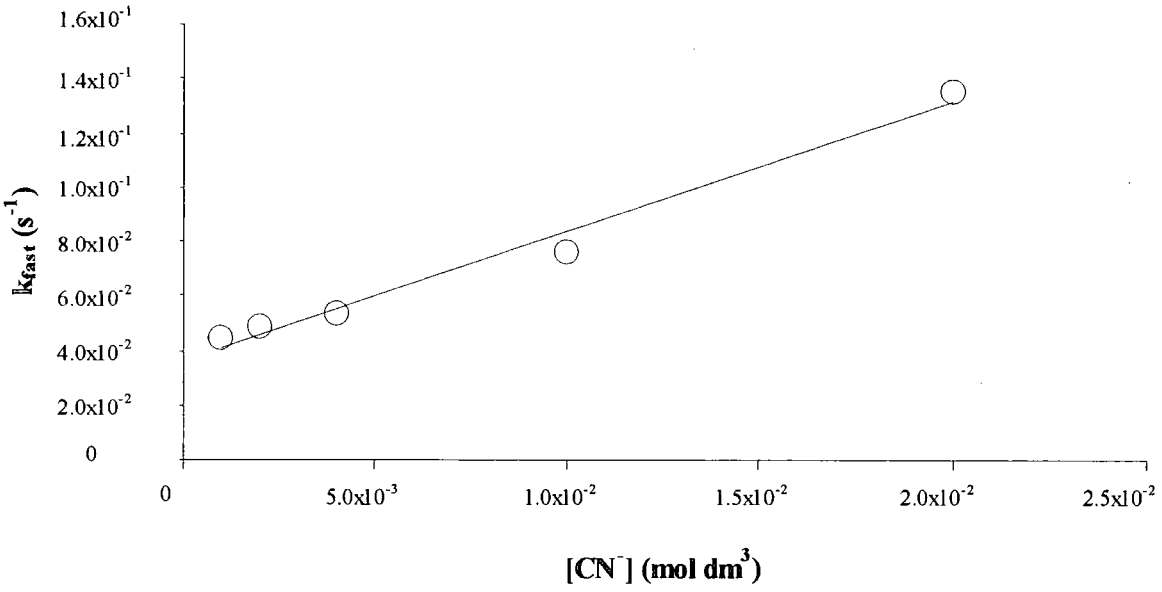

The linear regression of the above data yields the following equation:

$$k_{fast} = (4.73 \pm 0.37) \times [CN^-]_{stoich} + (0.036 \pm 0.004)$$

Hence:

$$k_f = 4.73 \pm 0.37\, dm^3 mol^{-1} s^{-1} \text{ and } k_{hyd} = 0.036 \pm 0.004 s^{-1}$$

Linear fits according to equation 3.12 have been performed for each pH and the data for k_f and k_{hyd} collected (Table 3.3). Using the Scientist® computer package the values of k_f have been plotted against pH and fitted to equation 3.13 (Figure 3.11). The value used for K_a^{HCN} was that of Ching and Kallen[14], $pK_a^{HCN} = 9.1$.

It has then been possible to determine the values for k_1 and K_a^{ImH+}.

Table 3.3 Variation of k_f and k_{hyd} with pH for the reaction of benzylidene benzylamine with cyanide

pH	k_f ($dm^3 mol^{-1} s^{-1}$)	k_{hyd} (s^{-1})
5.94	2.85	6.18×10^{-2}
6.40	4.73	3.64×10^{-2}
7.28	6.60	8.35×10^{-3}
8.55	4.89	7.80×10^{-3}
9.01	3.52	9.70×10^{-3}
9.85	1.05	8.10×10^{-3}
10.40	0.51	5.40×10^{-3}

Figure 3.11 Plot of Log (k_f) versus pH for the reaction of benzylidene benzylamine with cyanide in water

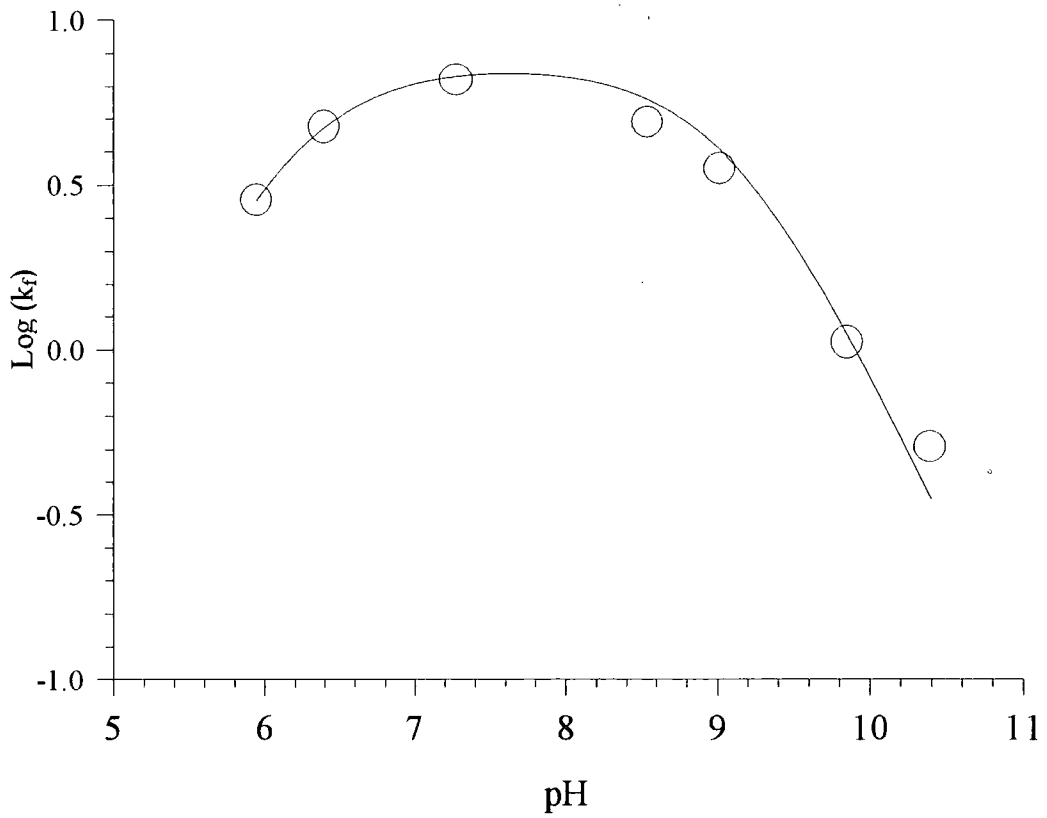

The experimental values for k_f give a good fit with values calculated with $k_1 = (6.7 \pm 1.0) \times 10^3$ $dm^3 mol^{-1} s^{-1}$ and $pK_a^{ImH+} = 6.14 \pm 0.10$.

3.2.2.2 2-Allylamino-2-phenylacetonitrile

3.2.2.2.1 ^{1}H NMR characterisation

Experimental

2-Allylamino-2-phenylacetonitrile

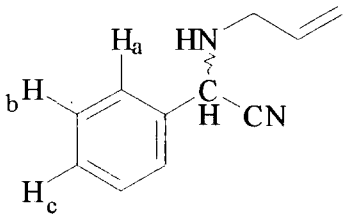

To a solution of benzylidene allylamine (0.8 cm^3, 5.1 mmol) in damp acetonitrile (50 cm^3) was added 1.1 equivalent of TMSCN (0.748 cm^3, 5.61 mmol) at room temperature. The solution was left to react overnight. ^{1}H NMR was used to check that the reaction went to completion by monitoring the resonance of the CHN proton which is at δ_H = 8.30 ppm in the imine and shifts to δ_H = 4.80 ppm in the aminonitrile. δ_H (400 MHz, CD_3CN): 2.54 (1H, *broad m*, NH), 3.77-3.90 (2H, *2x dd*, J = 6 Hz and 13 Hz, CH_2), 4.80 (1H, *d*, J = 10 Hz, CHN), 7.22 - 7.40 (8H, *m*, H_b, $H_{b'}$, H_c, H_d, $H_{d'}$, H_e, $H_{e'}$ and H_f), 7.47 – 7.49 (2H, *m*, H_a and $H_{a'}$)

3.2.2.2.2 Kinetic measurements

Experimental procedure:

This was identical to that described (3.2.2.1.2) for the corresponding benzylidene benzylamine.

Typical plots, measured at 250 nm, are in Figure 3.12.

Figure 3.12 Absorbance versus time plots for the reaction of $1x10^{-4}$ mol dm^{-3} benzylidene allylamine with varying cyanide concentrations at pH=9.07, 25° C, λ = 250 nm

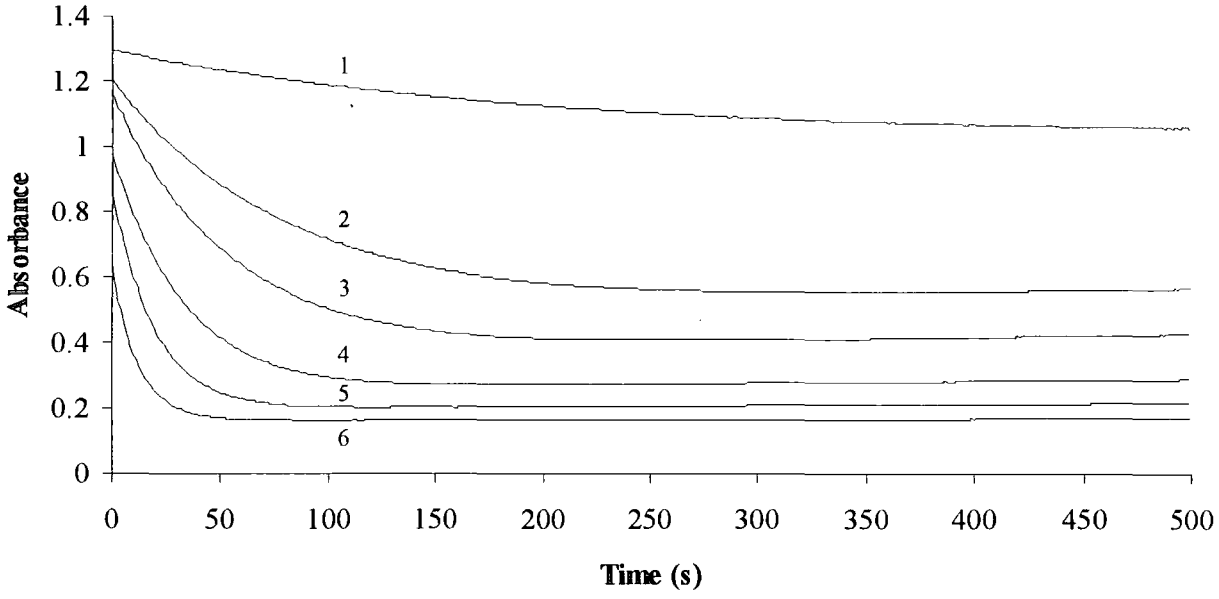

Concentrations of cyanide are: 1, 0 mol dm^{-3}; 2, $1x10^{-3}$ mol dm^{-3}; 3, $2x10^{-3}$ mol dm^{-3}; 4, $4x10^{-3}$ mol dm^{-3}; 5, $8x10^{-3}$ mol dm^{-3}; 6, $1.6x10^{-2}$ mol dm^{-3}

Similarly to the addition of cyanide to the benzylidene benzyliminium ion the fast process shown above is followed by a slow process resulting in a decrease in absorbance. Again this is characteristic of the decomposition of the aminonitrile.

Results

The kinetic scheme for the formation of 2-allylamino-2-phenylacetonitrile can represented as follows:

Scheme 3.11

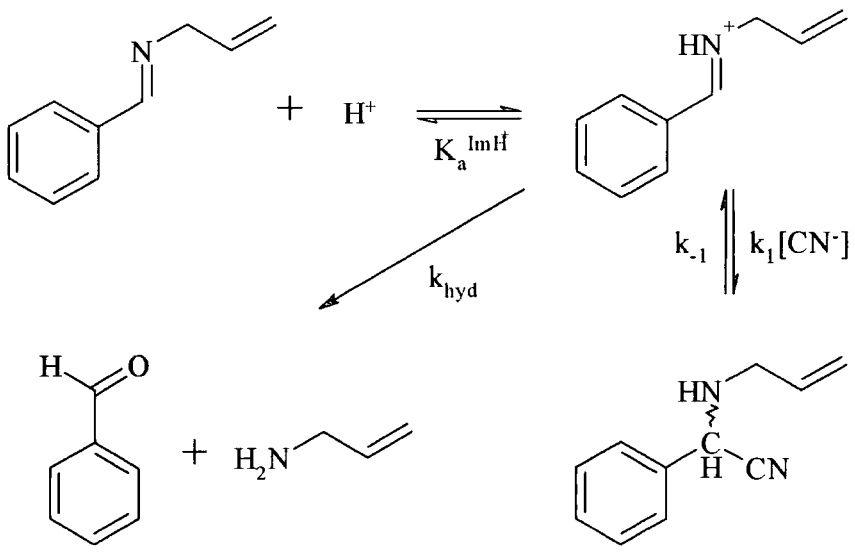

The scheme is identical to the one of addition of cyanide to benzylidene benzylamine. Consequently the kinetics are similar and the equations defined in part 3.2.2.1.2 stand for the addition of cyanide to the benzylidene allyliminium ion.

Values for k_f and k_{hyd} are tabulated below and the variation of k_f with pH represented in Figure 3.13.

Table 3.4 Variation of k_f and k_{hyd} with pH for the reaction of benzylidene allylamine with cyanide

pH	k_f ($dm^3 mol^{-1} s^{-1}$)	k_{hyd} (s^{-1})
6.10	5.21	7.16×10^{-2}
6.63	6.76	4.65×10^{-2}
7.15	7.75	2.02×10^{-2}
7.52	8.30	1.09×10^{-2}
8.17	8.41	1.00×10^{-2}
8.50	7.59	1.19×10^{-2}
9.07	4.65	1.22×10^{-2}
10.06	1.13	7.10×10^{-3}

Figure 3.13 Plot of Log (k_f) versus pH for the reaction of benzylidene allylamine with cyanide in water

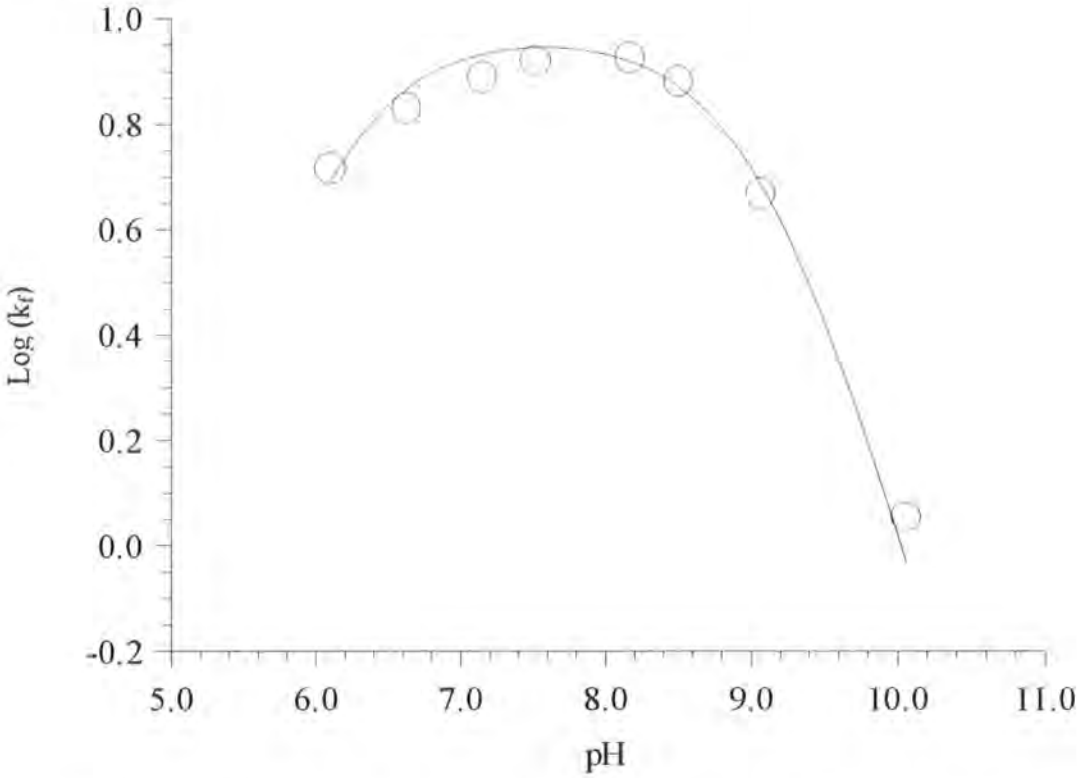

The experimental values for k_f give a good fit with values calculated with $k_l = (1.03 \pm 0.23) \times 10^4$ $dm^3 mol^{-1} s^{-1}$ and $pK_a^{lmlH+} = 6.05 \pm 0.10$.

3.2.2.3 2-Benzylamino-2-(4-nitro-)phenylacetonitrile

3.2.2.3.1 ^{1}H NMR characterisation

It has not been possible to synthesise 2-benzylamino-2-(4-nitro-)phenylacetonitrile by addition of TMSCN to the imine.

3.2.2.3.2 Kinetic measurements

Experimental procedure:

This was similar to that previously described (3.2.2.1.2), except that UV measurements were made at 286 nm. Typical plots are shown in Figure 3.14.

Figure 3.14 Absorbance versus time plots for the reaction of $1x10^{-4}$ mol dm^{-3} 4-nitro-benzylidene benzylamine with varying cyanide concentrations at pH=9.32, 25° C, λ = 286 nm

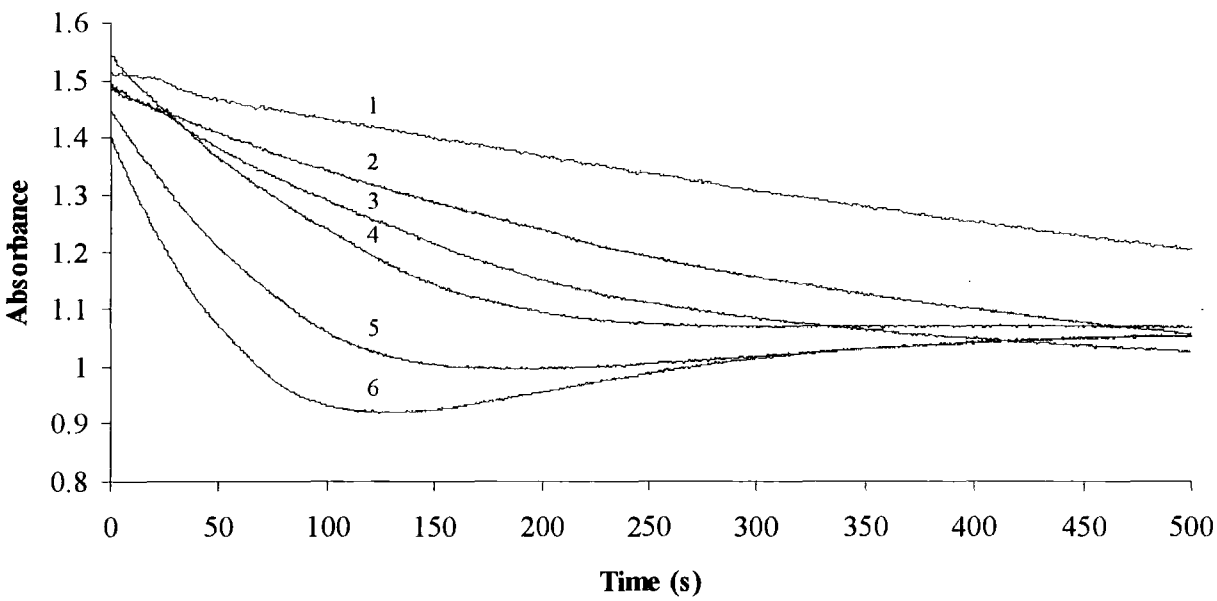

Concentrations of cyanide are: 1, 0 mol dm^{-3}; 2, $1x10^{-3}$ mol dm^{-3}; 3, $2x10^{-3}$ mol dm^{-3}; 4, $4x10^{-3}$ mol dm^{-3}; 5, $8x10^{-3}$ mol dm^{-3}; 6, $1.6x10^{-2}$ mol dm^{-3}

It is worth noting that the reaction is significantly faster with the nitro derivative than with benzylidene benzylamine itself. Consequently the decomposition of the adduct is observable in significantly shorter time interval.

Results

The kinetic scheme for the formation of 2-benzylamino-2-(4-nitro-)phenylacetonitrile can represented as Scheme 3.12

Scheme 3.12

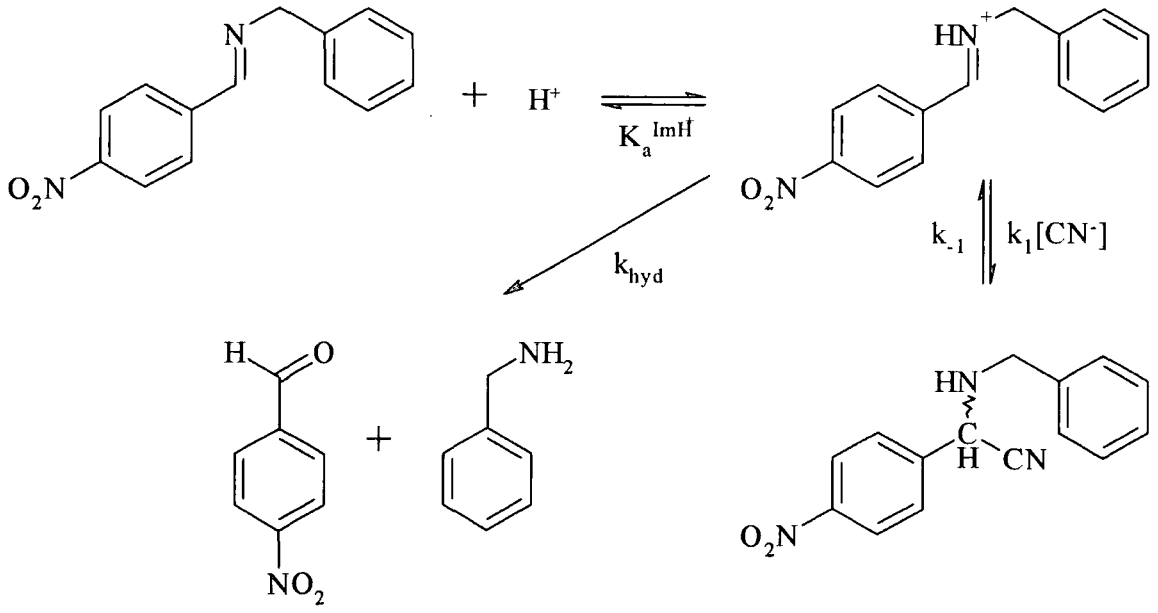

The scheme is identical to the one of addition of cyanide to benzylidene benzylamine or benzylidene allylamine. Consequently the kinetics are similar and the equations defined in part 3.2.2.1.2 stand for the addition of cyanide to the (4-nitro-)benzylidene benzyliminium ion:

Values for k_f and k_{hyd} have been recorded in the pH range 6.50 – 10. Unfortunately the reaction proved to be very fast and data for pH values below 6.5 could not be recorded (results are shown in Table 3.5 and Figure 3.15). Consequently it has not been possible to fit our data and gain values for K_a and k_1.

Nonetheless it is possible to obtain a value for the ratio of $\frac{k_l}{K_a^{ImH^+}}$ and to compare this with the corresponding value for reaction of the unsubstituted derivative.

The value for $pK_a^{ImH^+}$ for benzylidene benzylamine is 6.14, and the presence of a 4-nitro group is expected to enhance the acidity of the iminium ion and thus reduce the pK_a value. Therefore in solutions where pH>8, $K_a^{ImH^+} >> [H^+]$ will apply.

Thus equation 3.13 reduces to:

$$k_f = k_l \times \frac{[H^+]}{K_a^{ImH^+}} \times \frac{K_a^{HCN}}{[H^+] + K_a^{HCN}} \qquad \textbf{(3.16)}$$

where:

$$\frac{k_l}{K_a^{ImH^+}} = k_f \times \left(\frac{[H^+] + K_a^{HCN}}{[H^+] \times K_a^{HCN}}\right) \qquad \textbf{(3.17)}$$

Values of $\frac{k_l}{K_a^{ImH^+}}$ calculated using this expression are given in Table 3.5. These give (apart from the value at pH = 9.96, which appears to be anomalous) a value of $(2.5 \pm 0.2)\times10^9$ $dm^6mol^{-2}s^{-1}$. This compares with a corresponding value of 9.3×10^9 $dm^6mol^{-2}s^{-1}$ for the unsubstituted compound.

The presence of the nitro group is expected to acidify the iminium ion, increasing the value of K_a, and also to enhance its electrophilicity. Thus the value of k_l is also likely to be increased. The results indicate that the former effect, due to an equilibrium process, is larger than the latter which represents an energy difference between the reactant and the transition state.

Table 3.5 Variation of k_f, k_{hyd} and ($k_1 / K_a^{Im H^+}$) with pH for the reaction of (4-nitro-) benzylidene benzylamine with cyanide

pH	k_f ($dm^3\ mol^{-1}\ s^{-1}$)	k_{hyd} (s^{-1})	$\frac{k_1}{K_a^{ImH^+}}$ ($dm^6\ mol^{-2}\ s^{-1}$)
6.46	2.11	1.16×10^{-2}	/
8.08	1.90	3.40×10^{-2}	2.7×10^{9}
8.56	1.59	3.10×10^{-2}	2.6×10^{9}
9.08	0.85	3.90×10^{-2}	2.2×10^{9}
9.32	0.80	3.40×10^{-2}	2.7×10^{9}
9.96	0.65	8.00×10^{-3}	(6.7×10^{9})

Figure 3.15 Plot of Log (k_f) versus pH for the reaction of (4-nitro-)benzylidene benzylamine with cyanide in water

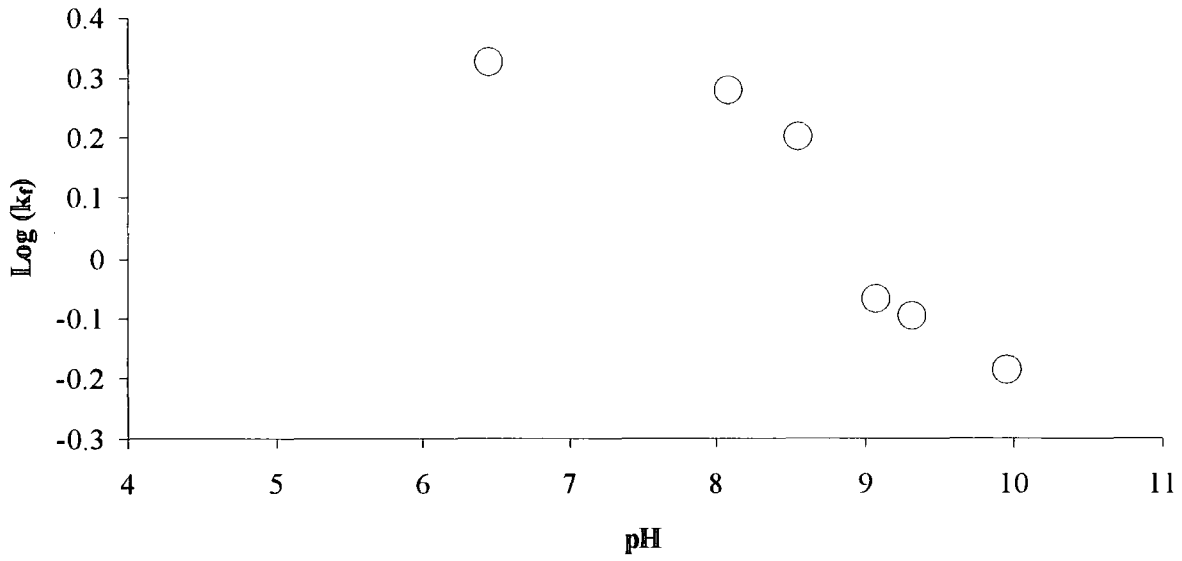

3.2.3 α-aminonitriles decomposition

The slower process observed spectrophotometrically accounts for the decomposition of the aminonitrile to benzaldehyde (Figure 3.2). Characterisation of the decomposition product was achieved. The kinetics for the process were measured for the 2-benzylamino-2-phenylacetonitrile and 2-allylamino-2-phenylacetonitrile derivatives.

3.2.3.1 Characterisation of the end product

Carbonyl compounds are known to react with hydrazines to form hydrazones. The reaction of benzaldehyde with 2,4-dinitrophenylhydrazine (DNP) yields benzaldehyde-2,4-dinitrophenylhydrazone which can be characterised[15] as crystals of melting point m.p. = 237°C.

Scheme 3.13

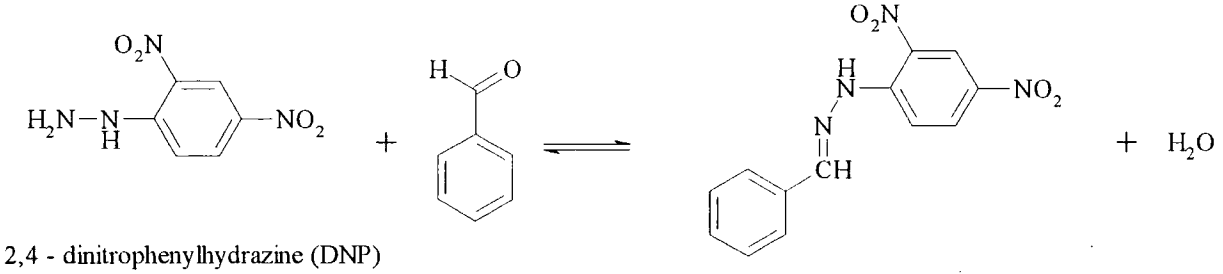

2,4 - dinitrophenylhydrazine (DNP)

benzaldehyde - 2,4 - dinitrophenylhydrazone

DNP (C = $1x10^{-2}$ mol dm^{-3}) in methanol was added to an aqueous solution of benzylidene benzylamine (C = $1x10^{-4}$ mol dm^{-3}) and left to react for an hour. A ^1H NMR spectrum of the imine was initially recorded to check the purity. No peak significant of the aldehydic proton was noted.

A crystalline structure was isolated and the melting point recorded at m.p. = 238°C confirming the decomposition of the aminonitrile to benzaldehyde.

3.2.3.2 2-Benzylamino-2-phenylacetonitrile

Aminonitriles in aqueous solutions decompose to give the parent aldehyde. However it should be noted that, in the presence of cyanide, benzaldehyde is in equilibrium with its cyanohydrin derivative[14] which does not absorb at 250 nm. Therefore the decrease in final absorbance values in Figure 3.2 with increasing cyanide concentration reflects this equilibrium.

Referring back to Scheme 3.10 (reproduced below) it is possible to define the rate as being the product of the rate of dissociation of the aminonitrile with the fractionation of the total imine concentration (imine + iminium ion), $[Im]_{stoich}$, between hydrolysis and reformation of the aminonitrile.

Scheme 3.10

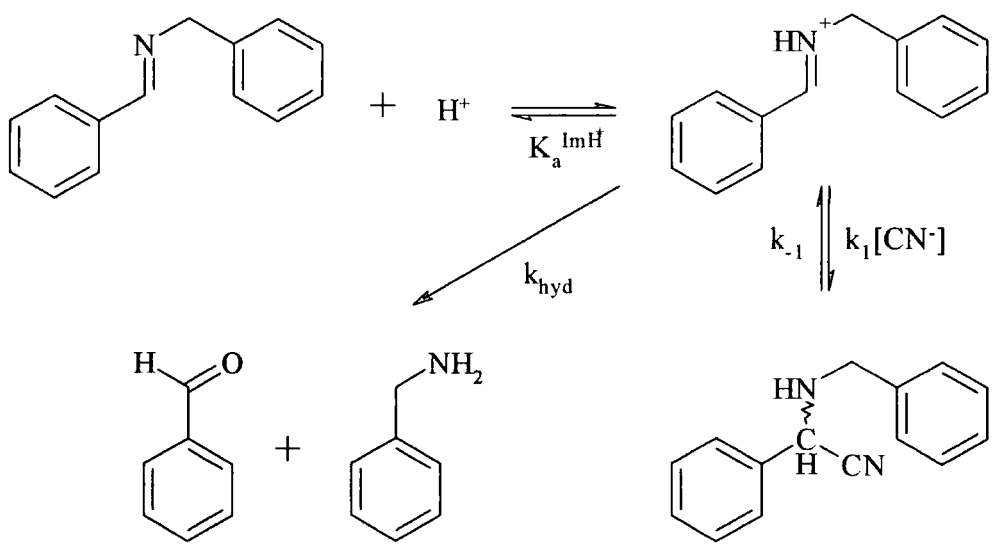

Hence:

$$\text{rate} = k_{-1}[\text{Aminonitrile}] \times \frac{k_{hyd}}{k_f[CN^-]_{stoich} + k_{hyd}} \qquad \textbf{(3.18)}$$

Since the observed kinetics are first order i.e.: rate = k_{slow}[Aminonitrile], an expression for k_{slow} is:

$$k_{slow} = k_{-1} \times \frac{k_{hyd}}{k_f[CN^-]_{stoich} + k_{hyd}} \quad (3.19)$$

Measurements were taken in the pH range 7 – 10.

Experimental procedure:

Determination of the kinetics was performed by monitoring the reaction over a longer time range allowing for the reformation of benzaldehyde.

Aqueous solutions of cyanide (using potassium cyanide) were freshly prepared under a fume hood before each experiment.

Benzylidene benzylamine was diluted to a $1x10^{-4}$ mol dm^{-3} concentration in aqueous buffered solutions of potassium cyanide under a fume hood.

Values of rate constants were determined by monitoring the changes with time of the U. V. absorbance at 250 nm were used to monitor the reactions.

Typical spectra are shown in Figure 3.16.

Figure 3.16 Absorbance versus time plots for the reaction of $1x10^{-4}$ mol dm^{-3} benzylidene benzylamine with varying cyanide concentrations at pH=10.4, 25° C, λ = 250 nm

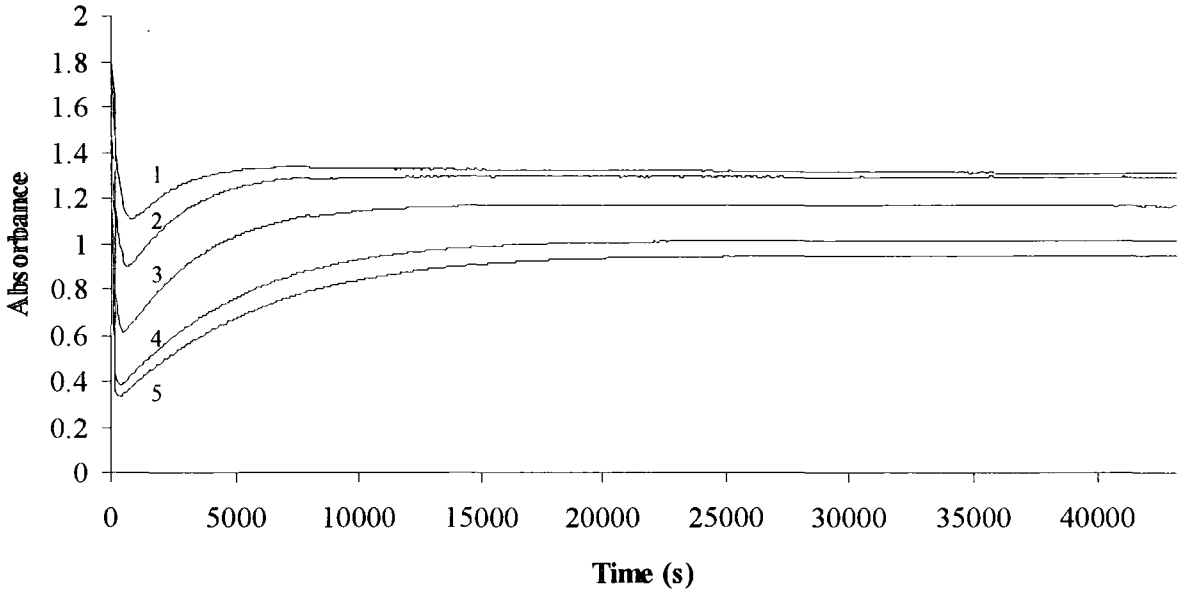

Concentrations of cyanide are: 1, $2x10^{-3}$ mol dm^{-3}; 2, $4x10^{-3}$ mol dm^{-3}; 3, $8x10^{-3}$ mol dm^{-3}; 4, $1.6x10^{-2}$ mol dm^{-3}; 5, $2x10^{-2}$ mol dm^{-3}

Results

A plot of the value obtained for k_{slow} versus the stoichiometric cyanide concentration is shown in Figure 3.17.

Figure 3.17 k_{slow} versus total cyanide concentration, $[CN^-]_{stoich}$, for the decomposition of 2-benzylamino-2-phenylacetonitrile, pH = 10.4, 25°C

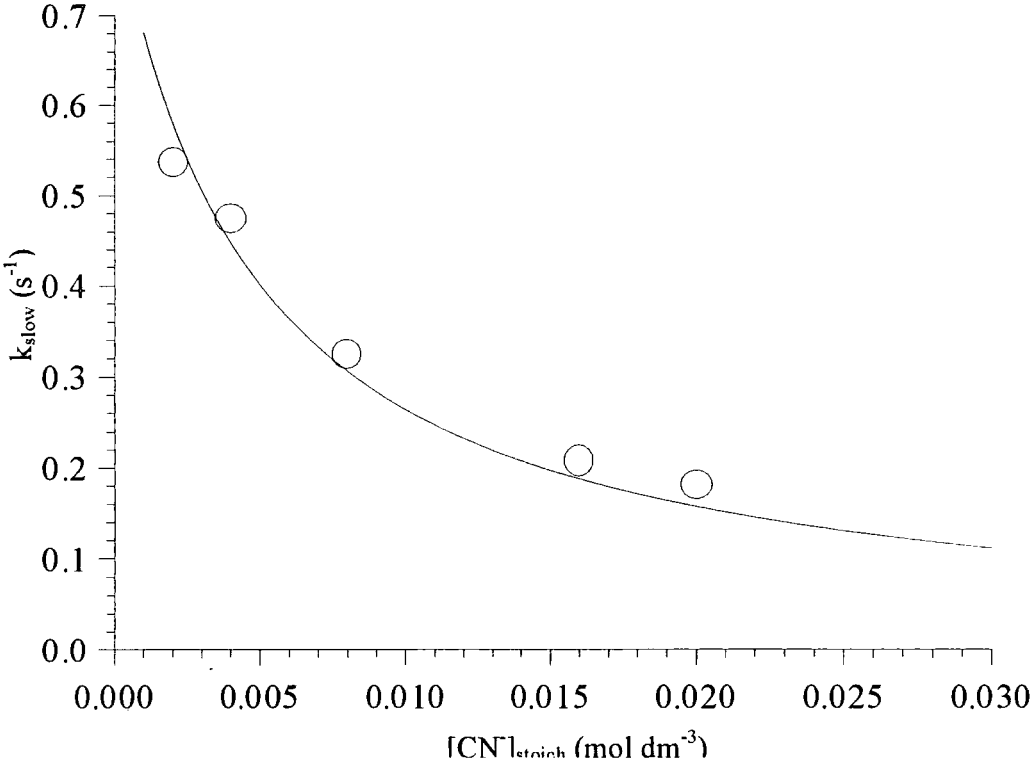

A value for k_{-1} was obtained by fitting the experimental data to equation 3.19 using known values for k_f and for k_{hyd}.

The value used for k_f is the experimental value collected at the appropriate pH value. The value used for k_{hyd} is the one calculated from a fit of the curve accounting for imine hydrolysis (i.e. $[CN^-]_{stoich}$ = 0 mol dm^{-3}). All of those values and an account for the imine hydrolysis are collected in the next part of the chapter.

The above data yielded a value for k_{-1}, at pH = 10.4, of $(8.26 \pm 0.31) \times 10^{-4}$ s^{-1}. The full line is the theoretical curve plotted using this value of k_{-1}.

Values collected at different pH values are summarised in Table 3.6.

Table 3.6 Variation of k_{-1} with pH for the decomposition of 2-benzylamino-2-phenylacetonitrile

pH	k_{-1} (s^{-1})
6.84	9.08×10^{-4}
8.21	8.67×10^{-4}
8.77	8.84×10^{-4}
9.01	8.41×10^{-4}
9.69	9.87×10^{-4}
10.4	8.26×10^{-4}

Average: 8.85×10^{-4}

Std Deviation: 5.79×10^{-5}

In the pH range under study the decomposition of the aminonitrile is pH independent. An average value for the rate constant, k_{-1}, can therefore be calculated to be $(8.85 \pm 0.58) \times 10^{-4}$ s^{-1}.

It is worth noting the influence of the solvent on the decomposition of the aminonitrile. Indeed experiments were carried out where the solvent composition was varied. The decomposition of benzylamino-2-phenylacetonitrile was monitored in various acetonitrile/water mixtures.

The increase in absorbance characteristic of the formation of benzaldehyde was recorded with time. The data are collected in Table 3.7 and typical plots are shown in Figure 3.18.

A plot of the observed rate constant against acetonitrile content (Figure 3.19) is a bell shaped curve where a maximum can be seen when the solvent composition is ca 20 vol % acetonitrile/ 80 vol % water.

It is worth noting that decomposition in pure acetonitrile is very slow and therefore it can be considered stable in this particular solvent. This confirms that all the absorbance changes monitored in water are to be related only to the aqueous medium.

Figure 3.18 Absorbance versus time plots for the decomposition of $1x10^{-4}$ mol dm^{-3} 2-benzylamino-2-phenylacetonitrile in various acetonitrile/water mixtures, 25° C, λ = 250 nm

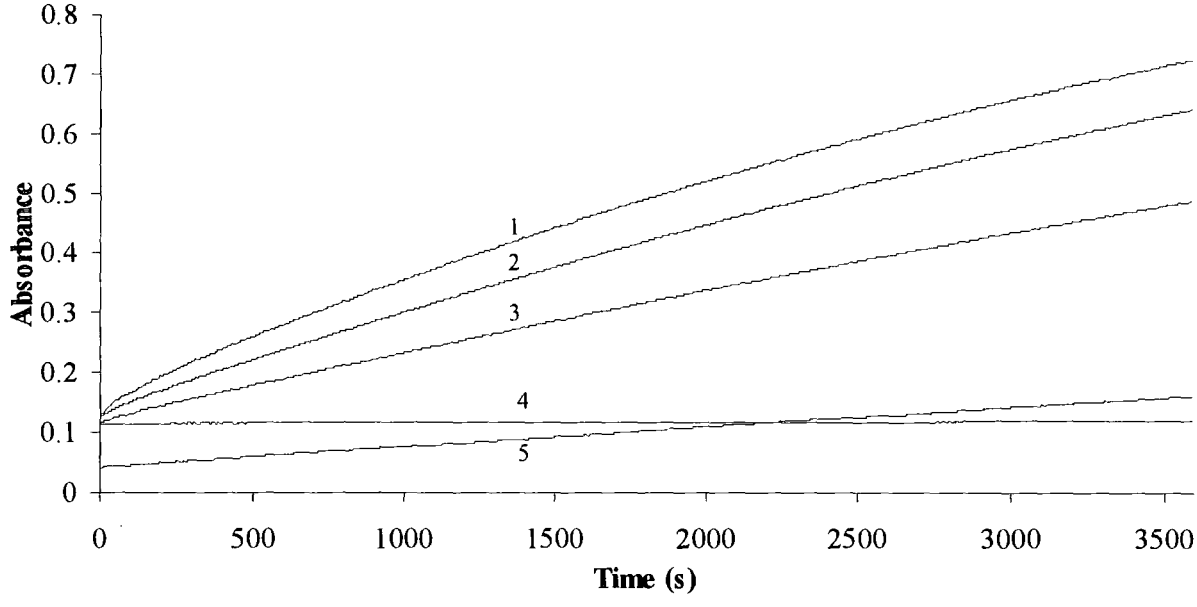

Mixtures water/acetonitrile: 1, 40/60; 2, 30/70; 3, 20/80; 4, 10/90; 5, 0/100

Table 3.7 Observed rate constants for the decomposition of 2-benzylamino-2-phenylacetonitrile in various acetonitrile/water mixtures

Acetonitrile (Vol %)	Water (Vol %)	k_{obs} (s^{-1})
0%	100%	$5.07x10^{-4}$
10%	90%	$8.57x10^{-4}$
20%	80%	$9.72x10^{-4}$
30%	70%	$9.20x10^{-4}$
40%	60%	$6.30x10^{-4}$
50%	50%	$3.97x10^{-4}$

Acetonitrile (Vol %)	Water (Vol %)	k_{obs} (s^{-1})
60%	40%	$2.21x10^{-4}$
70%	30%	$1.40x10^{-4}$
80%	20%	$7.84x10^{-5}$
90%	10%	$1.18x10^{-5}$
100%	0%	$(6.60x10^{-5})$

Figure 3.19 Plot of k_{obs} versus acetonitrile content for the decomposition of 2-

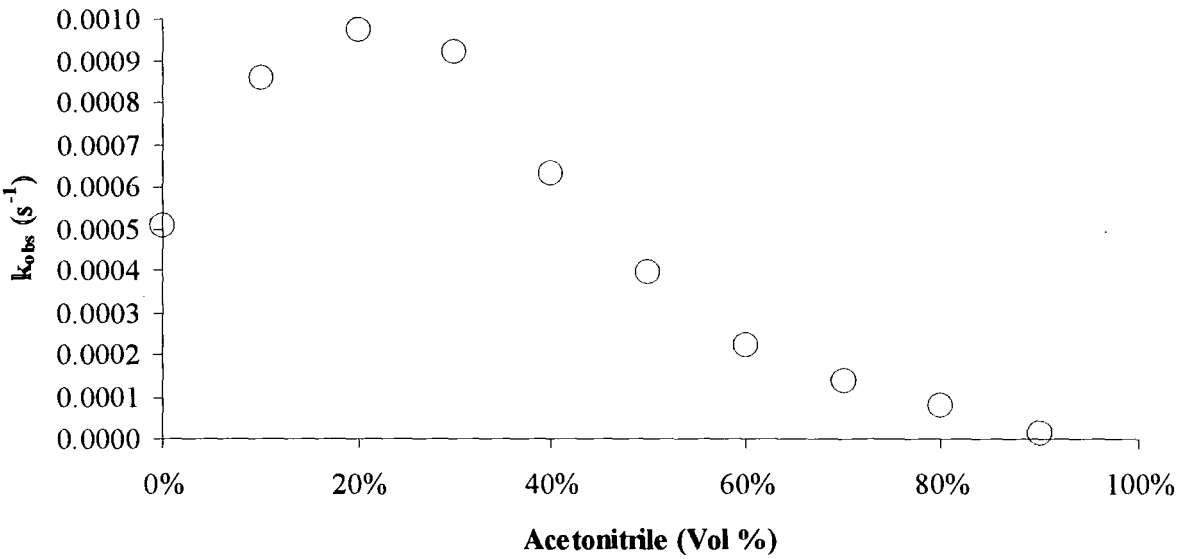

benzylamino-2-phenylacetonitrile

A detailed analysis of the solvent dependence of k_{obs} is not possible. However it is likely that a major factor will be the poorer solvation of ions in acetonitrile than in water. Thus the iminium ion and the cyanide ion will be desolvated in acetonitrile leading to a decrease in value of k_{-1} and an increase in value for k_1. Further, as the water concentration decreases the possibility of hydrolysis to give benzaldehyde is reduced. The combination of these factors results in a very low value for k_{obs} in acetonitrile rich media.

It is worth noting that a recent study of the properties of the water-acetonitrile system[16] found that the solvent basicity, based on the solvatochromism of 5-nitroindoline, went through a maximum as the acetonitrile proportion was increased.

3.2.3.3 2-Allylamino-2-phenylacetonitrile

The kinetics for the decomposition of 2-allylamino-2-phenylacetonitrile are similar to those described in the case of 2-benzylamino-2-phenylacetonitrile. The scheme defined in part 3.2.2.2 (Scheme 3.11, reproduced below) is the one of interest and the following equations have been defined accordingly.

$$\text{rate} = k_{-1}[\text{Aminonitrile}] \times \frac{k_{hyd}}{k_f[CN^-]_{stoich} + k_{hyd}} \qquad (3.18)$$

Since the observed kinetics are first order i.e.: rate = k_{slow}[Aminonitrile], an expression for k_{slow} is:

$$k_{slow} = k_{-1} \times \frac{k_{hyd}}{k_f[CN^-]_{stoich} + k_{hyd}} \qquad (3.19)$$

Scheme 3.11

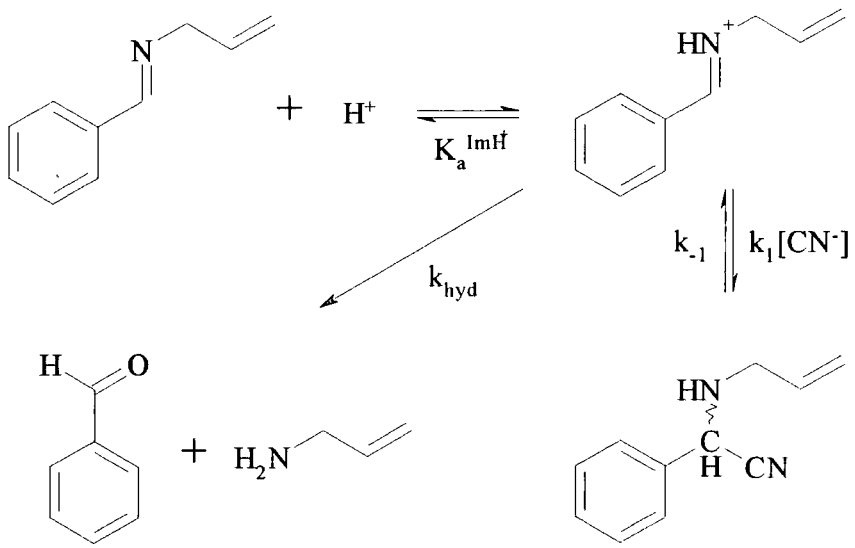

Since the conclusions of the previous part (3.2.3.2) show that the decomposition of the aminonitrile is pH independent measurements for 2-allylamino-2-phenylacetonitrile were performed at one pH value only, pH = 9.07.

Again cyanide was added to the imine and the reaction was monitored during a significant time interval so that data corresponding to the increase in absorbance could be collected.

The values collected for k_{slow} (Table 3.8) were subsequently plotted against the total cyanide concentration, $[CN^-]_{stoich}$, according to equation 3.19 to yield the value for k_{-1} as shown in Figure 3.20.

Table 3.8 Variation of k_{slow} with cyanide concentration for the decomposition of 2-allylamino-2-phenylacetonitrile

$[CN^-]$ (mol dm^{-3})	k_{slow} (s^{-1})
$1.0x10^{-3}$	$2.79x10^{-4}$
$2.0x10^{-3}$	$1.87x10^{-4}$
$4.0x10^{-3}$	$1.32x10^{-4}$
$8.0x10^{-3}$	$8.23x10^{-5}$
$1.6x10^{-2}$	$4.81x10^{-5}$

Figure 3.20 k_{slow} versus total cyanide concentration, $[CN^-]_{stoich}$, for the decomposition of 2-allylamino-2-phenylacetonitrile, pH = 9.07, 25°C

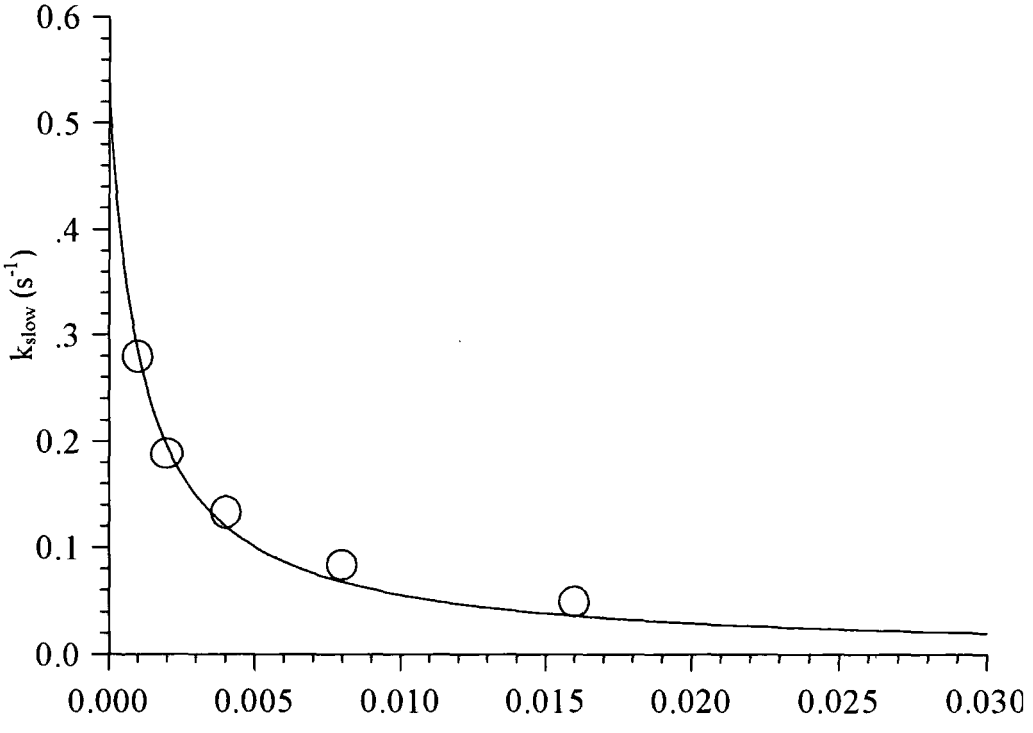

Note: $k_f = 4.65\ dm^3\ mol^{-1}\ s^{-1}$ and $k_{hyd} = 5.48 \times 10^{-3}\ s^{-1}$

The value of the rate constant for the decomposition of 2-allylamino-2-phenylacetonitrile in aqueous medium, k_{-1}, was found to be $(5.25 \pm 0.17) \times 10^{-4}\ s^{-1}$.

3.2.4 Hydrolysis of imines

3.2.4.1 Kinetics

Imines are known not to be stable in aqueous solutions. Jencks and co-workers[9] studied the hydrolysis of some imines and showed that the rate constant was pH dependent with a bell-shaped profile.

In the previous parts when following the reaction of imines (namely benzylidene benzylamine, benzylidene allylamine and 4-nitrobenzylidene benzylamine) with cyanide in aqueous buffers spectrophotometrically a decrease in absorbance was observed even in the absence of cyanide.

The process is likely to involve attack on the iminium ion by water or hydroxyl ions as shown in Scheme 3.14

Since the works of Jencks and co-workers[9] the process described below is well understood. The pH dependence of the rate of the reaction, represented by a bell-shaped curve is accounted for by changes in the rate determining step.

In alkaline condition attack of the hydroxyl ion on the iminium ion is rate determining however as the pH decreases reaction with water becomes more significant. In acidic conditions the decomposition of the carbinolamine intermediate is rate limiting. It is therefore predicted that the rate decreases with pH as the concentration in the reactive zwitterionic form of the carbinolamine decreases. Also of interest is the possible protonation of the carbinolamine yielding an unreactive cationic form.

Scheme 3.14

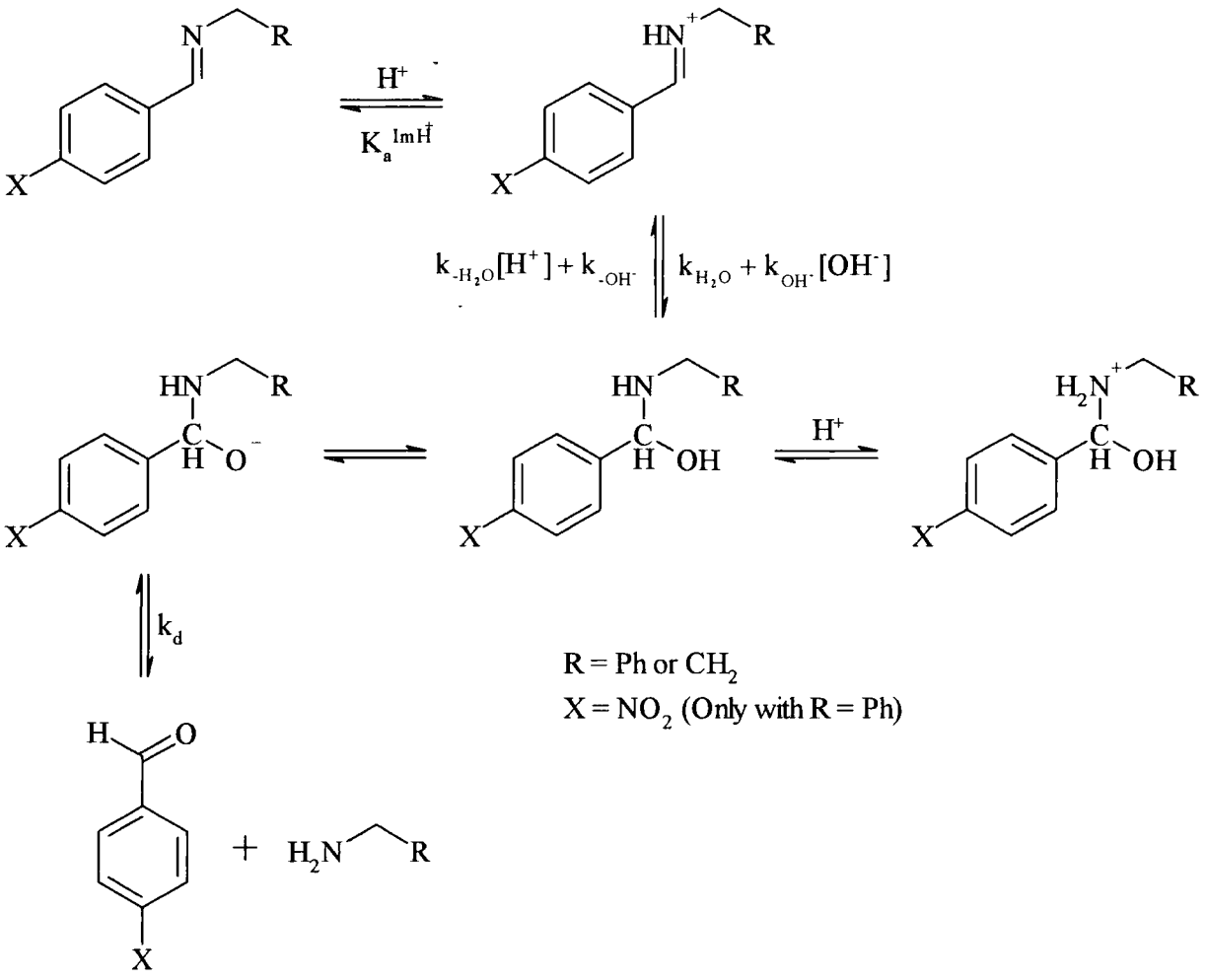

With reference to Jencks's work the different rate laws with respect to the reactant, the intermediate and the products can be expressed as:

$$\frac{-d[ImineH^+]}{dt} = k_{H_2O}[ImineH^+] - k_{-H_2O}[Carbinolamine][H^+] + k_{OH^-}[ImineH^+][OH^-] - k_{-OH^-}[Carbinolamine] \quad \textbf{(3.20)}$$

$$\frac{d[Carbinolamine]}{dt} = k_{H_2O}[ImineH^+] - k_{-H_2O}[Carbinolamine][H^+] + k_{OH^-}[ImineH^+][OH^-] - k_{-OH^-}[Carbinolamine] - k_d[Carbinolamine] \quad \textbf{(3.21)}$$

$$\frac{d[Products]}{dt} = k_d[Carbinolamine] \quad \textbf{(3.22)}$$

Under the steady-state conditions for the carbinolamine the concentration in the intermediate is constant therefore $\frac{d[\text{Carbinolamine}]}{dt} = 0$. Consequently:

$$0 = k_{H_2O}[\text{ImineH}^+] - k_{-H_2O}[\text{Carbinolamine}][H^+] + k_{OH^-}[\text{ImineH}^+][OH^-] - k_{OH^-}[\text{Carbinolamine}] - k_d[\text{Carbinolamine}] \quad \textbf{(3.23)}$$

From the expression for the acid dissociation constant of the iminium ion:

$$[\text{ImineH}^+] = \frac{[H^+]}{K_a^{\text{ImH}^+} + H^+} \times [\text{Imine}]_{\text{stoich}} \quad \textbf{(3.24)}$$

Hence combining equations 3.23 and 3.24:

$$[\text{Carbinolamine}] = \frac{k_{H_2O} + k_{OH^-}[OH^-]}{k_{-H_2O}[H^+] + k_{-OH^-} + k_d} \times \frac{[H^+]}{K_a^{\text{ImH}^+} + H^+} \times [\text{Imine}]_{\text{stoich}} \quad \textbf{(3.25)}$$

Rearranging **(3.25)** in **(3.20)** and **(3.22)**:

$$\frac{-d[\text{ImineH}^+]}{dt} = \frac{d[\text{Products}]}{dt} = \frac{k_{H_2O}k_d[H^+] + k_d k_{OH^-}Kw}{([H^+] + K_a^{\text{ImH}^+})(k_{-H_2O}[H^+] + k_{-OH^-} + k_d)} \times [\text{Imine}]_{\text{stoich}} \quad \textbf{(3.26)}$$

Since the experimental data show that the hydrolysis follows first order kinetics:

$$\frac{-d[\text{ImineH}^+]}{dt} = \frac{d[\text{Products}]}{dt} = k_{obs} \times [\text{Imine}]_{\text{stoich}} \quad \textbf{(3.27)}$$

With:

$$k_{obs} = \frac{k_{H_2O}k_d[H^+] + k_d k_{OH^-}Kw}{([H^+] + K_a^{\text{ImH}^+})(k_{-H_2O}[H^+] + k_{-OH^-} + k_d)} \quad \textbf{(3.28)}$$

It is worth noting that since in alkaline conditions the slow step is the attack of either water or the hydroxyl ion on the iminium ion it is possible to calculate the kinetics with respect to the iminium ion.

$$\frac{-d[ImineH^+]}{dt} = k_{H_2O} \times [ImineH^+] + k_{OH^-} \times [ImineH^+] \times [OH^-] \quad \textbf{(3.29)}$$

Where $k_{H_2O} \times [ImineH^+]$ corresponds to the attack of water and $k_{OH^-} \times [ImineH^+] \times [OH^-]$ to the attack of the hydroxyl ion.

Rearranging **(3.24)** in **(3.29)**

$$\frac{-d[ImineH^+]}{dt} = (k_{H_2O} + k_{OH^-} \times [OH^-]) \times \frac{[H^+]}{K_a^{ImineH^+} + [H^+]} \times [Imine]_{stoich} \quad \textbf{(3.30)}$$

Hence:

$$\frac{-d[ImineH^+]}{dt} = k_{obs} \times [Imine]_{stoich} \quad \textbf{(3.31)}$$

With:

$$k_{obs} = (k_{H_2O} + k_{OH^-} \times [OH^-]) \times \frac{[H^+]}{K_a^{ImineH^+} + [H^+]} \quad \textbf{(3.32)}$$

It is therefore possible to calculate independently the rate constants for the attack of water, k_{H_2O}, and attack of the hydroxyl ion, k_{OH^-}, as well as the acid dissociation constant for the iminium ion, $K_a^{ImineH^+}$, in alkaline conditions.

In acidic media the rate limiting step is the decomposition of the carbinolamine intermediate. Since it is not possible to determine its concentration calculation of the individual rate constants in acid conditions is not available.

3.2.4.2 Results

Experimental procedure

The rate constants were determined by diluting benzylidene benzylamine to a $1x10^{-4}$ mol dm^{-3} concentration in aqueous buffered solutions for alkaline pH values and in aqueous solutions of hydrochloric acid (HCl) for the acidic conditions.

The changes with time of the U.V. absorbance at 250 nm were used to monitor the reactions.

Typical spectra in alkaline (pH > 6) and acidic media are shown on Figures 3.21 and 3.22 respectively

It is worth noting that for pH values between 3 and 6 the reaction is too fast to be followed with conventional U.V./Vis. spectroscopy. A stopped flow spectrophotometer enables further reactions to be followed. However the apparatus requires that the two reactants are placed in two different syringes, one for the aqueous buffer or HCl solution, and another for the imine (in acetonitrile). The solvent composition in that case is then 50:50 water:acetonitrile which is not readily comparable with the other samples which relate to water.

Figure 3.21 Absorbance versus time plots for the hydrolysis of $1x10^{-4}$ mol dm^{-3} benzylidene benzylamine at pH > 6, 25° C, λ = 250 nm

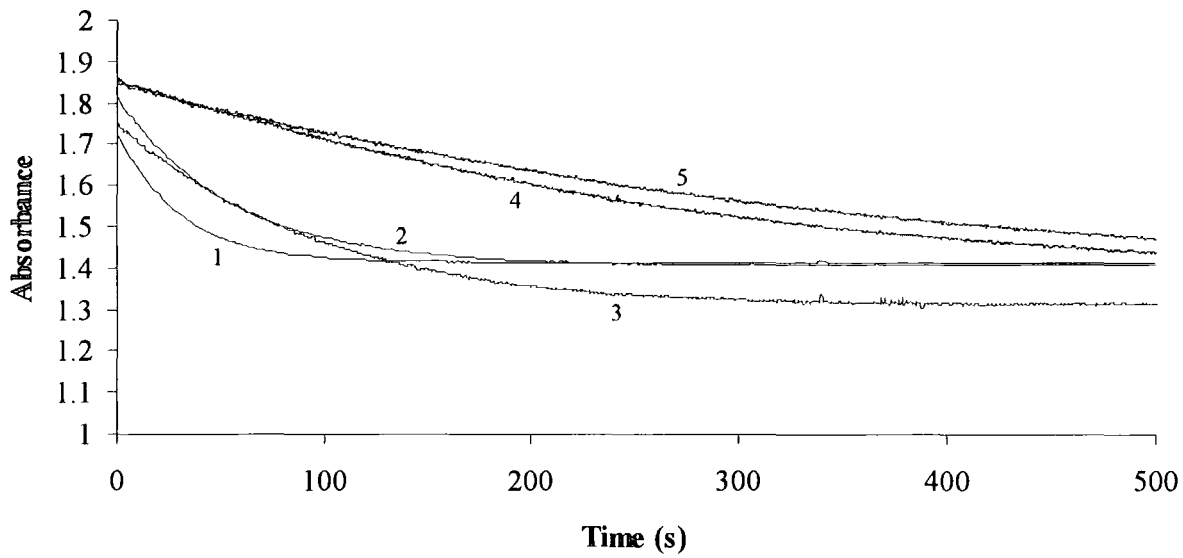

pH values: 1, pH = 6.40; 2, pH = 6.85; 3, pH = 7.28; 4, pH = 9.01; 5, pH = 9.85

Figure 3.22 Absorbance versus time plots for the hydrolysis of $1x10^{-4}$ mol dm^{-3} benzylidene benzylamine at pH < 6, 25° C, λ = 250 nm

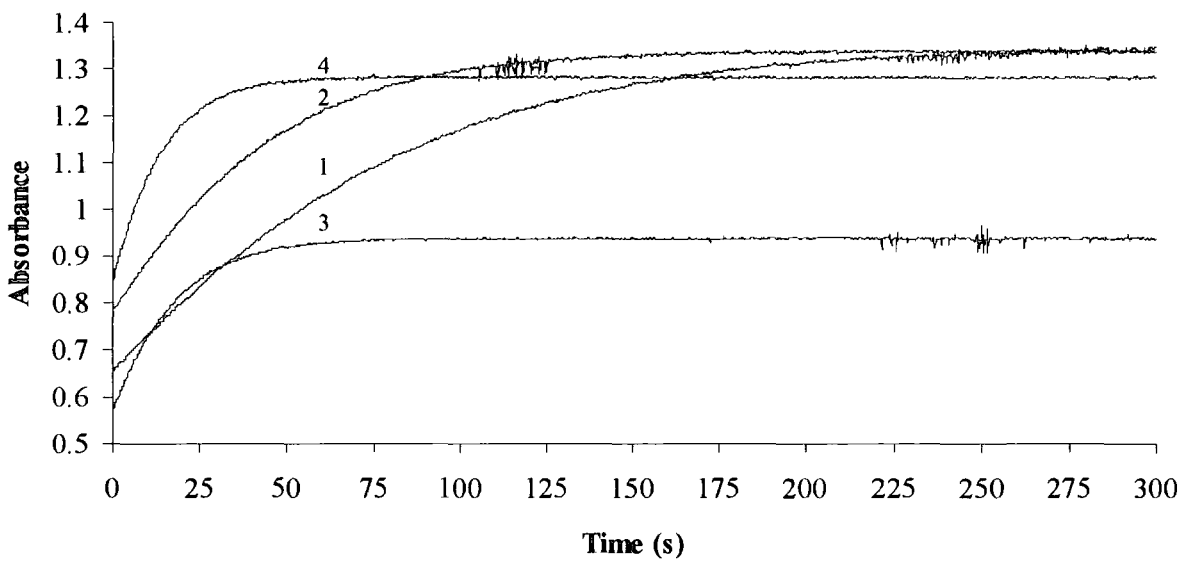

[HCl]; 1, 0.1 mol dm^{-3}; 2, 0.05 mol dm^{-3}; 3, 0.0185 mol dm^{-3}; 4, 0.01 mol dm^{-3}

3.2.4.2.1 N-Benzylidene benzylamine

3.2.4.2.1.1 Alkaline conditions (pH > 6)

The data collected for this pH range show a decrease in absorbance with time as shown in Figure 3.21. This corresponds to the rate determining attack of water and hydroxyl ion on the iminium ion. Formation of benzaldehyde induces a decrease in absorbance since it absorbs less than the imine at 250 nm.

The reaction follows first order kinetics according to equation 3.31. Values for the observed rate constant, k_{obs}, are collected in Table 3.9.

The pH dependence of the constant was fitted to equation 3.32 allowing the calculation of k_{H_2O}, k_{OH^-} and $K_a^{ImH^+}$ (Figure 3.23).

Measurements were made using dilute aqueous buffer, ca 0.05 mol dm^{-3}. The possibilities of general acid/base catalysis were not investigated since effects are likely to be small at the low buffer concentrations used[9].

Table 3.9 Variation of k_{obs} with pH for the hydrolysis reaction of benzylidene benzylamine in alkaline conditions

pH	k_{obs} (s^{-1})	Log(k_{obs})
5.94	6.32×10^{-2}	-1.20
5.99	6.27×10^{-2}	-1.20
6.15	5.52×10^{-2}	-1.26
6.40	3.31×10^{-2}	-1.48
6.85	1.84×10^{-2}	-1.74
7.28	1.14×10^{-2}	-1.94
8.10	6.33×10^{-2}	-2.20
8.55	6.97×10^{-3}	-2.40

pH	k_{obs} (s^{-1})	Log(k_{obs})
9.01	3.44×10^{-3}	-2.46
9.85	2.69×10^{-3}	-2.57
10.40	2.35×10^{-3}	-2.63
11.00	2.57×10^{-3}	-2.59
11.50	2.60×10^{-3}	-2.59
12.00	2.71×10^{-3}	-2.57
12.50	2.65×10^{-3}	-2.58

Figure 3.23 Log(k_{obs}) versus pH for the hydrolysis reaction of benzylidene benzylamine in alkaline conditions

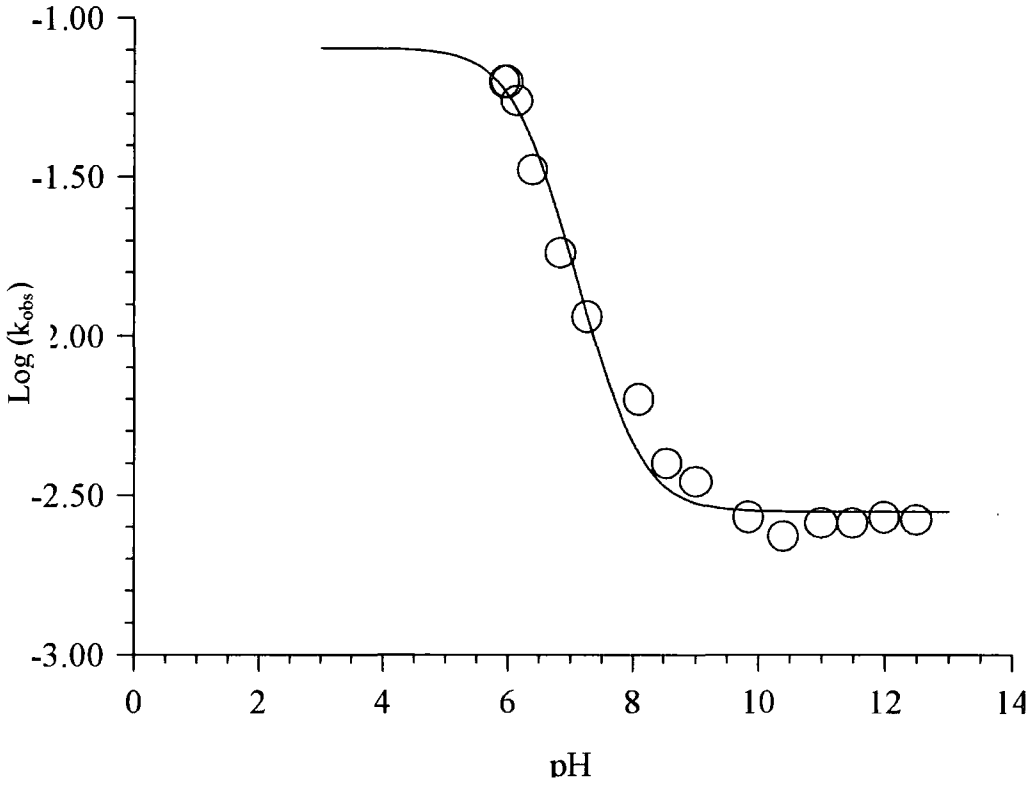

Note: the full line was calculated according to equation **3.32** using the Scientist® software package.

The curve of best fit shown above was calculated using the following constants:

Table 3.10 Rate and acid dissociation constants used to calculate the curve of best fit

$pK_a^{ImH^+}$	6.37±0.1
k_{OH^-}	$(1.19 \pm 0.43) \times 10^5 dm^3 mol^{-1} s^{-1}$
k_{H_2O}	$(8.07 \pm 1.45) \times 10^{-2} s^{-1}$

3.2.4.2.1.2 Global pH dependence

Additionally to the data summarised above, the hydrolysis reaction was also studied in acidic conditions (Table 3.11). However for reasons mentioned earlier it has not been possible to follow the reaction between pH = 3 and pH = 6.

Also worth noting is the fact that the kinetics for the acidic part of the process did not allow values of rate constants to be determined explicitly. All the data were therefore fitted to Jencks's model as described by equation 3.28 (Figure 3.24).

Table 3.11 Variation of k_{obs} with pH for the hydrolysis reaction of benzylidene benzylamine in acidic conditions

pH	k_{obs} (s^{-1})	Log (k_{obs})
0.70	6.19×10^{-3}	-2.21
0.82	9.01×10^{-3}	-2.05
1.00	1.32×10^{-2}	-1.88
1.30	2.44×10^{-2}	-1.61
1.73	5.82×10^{-2}	-1.24
2.00	7.47×10^{-2}	-1.13
2.10	9.40×10^{-2}	-1.03
2.40	1.20×10^{-1}	-0.92
2.70	1.41×10^{-1}	-0.85
3.00	1.80×10^{-1}	-0.74

Figure 3.24 pH profile for the hydrolysis of benzylidene benzylamine

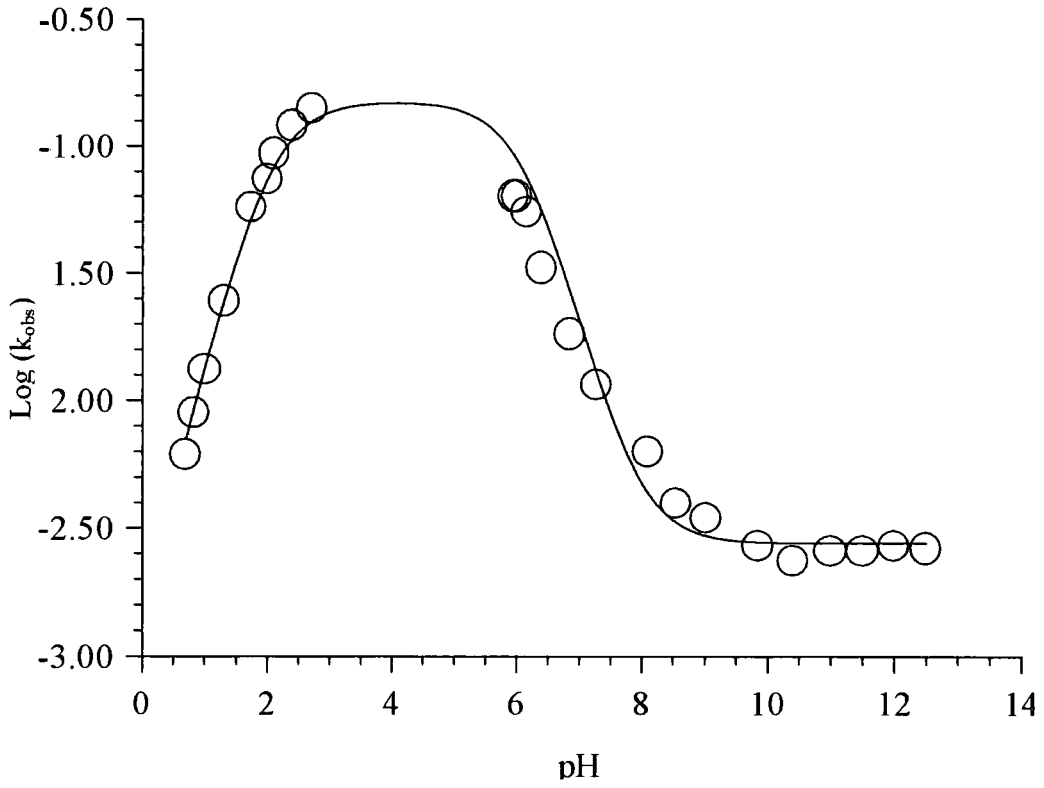

A direct fit with equation 3.28 was not possible. The number of unknown parameters combined with the lack of data in the region of the maximum meant that the software was not able to iterate the constants consistently. As a result some of the values have been fixed and a new equation defined **(3.39)**.

The value used for $pK_a^{ImH^+}$ is 6.14. It is the value gained from the kinetics on addition of cyanide to the iminium ion. This value is considered to be more reliable than the value of 6.37 given in Table 3.10, since for cyanide addition values of rate constants around the maximum are available.

Values used for other rate constants were estimated as follows:

1) k_{OH^-}

At high pH equation 3.28 can be expressed as:

$$k_{obs} = \frac{k_d k_{OH^-} Kw}{K_a^{ImH^+} \times k_d} = \frac{Kw \times k_{OH^-}}{K_a^{ImH^+}} \quad (3.33)$$

From our data in very alkaline conditions Log (k_{obs}) ≈ -2.58 hence, with $pK_a^{ImH^+}$ = 6.14:

$$k_{OH^-} = \frac{10^{-6.14} \times 10^{-2.58}}{10^{-14}} \approx 2 \times 10^5 dm^3 mol^{-1} s^{-1} \quad (3.34)$$

2) k_{H_2O}

With $pK_a^{ImH^+}$ fixed at 6.14. The best fit of the data in Table 3.9 is achieved with a value of 0.15 s^{-1} for k_{H_2O}.

3) k_{-H_2O} and k_{-OH^-}

$$\text{If } K_1 = \frac{k_{H_2O}}{k_{-H_2O}} = \frac{[Products][H^+]}{[ImineH^+]} \quad (3.35)$$

and

$$K_2 = \frac{k_{OH^-}}{k_{-OH^-}} = \frac{[Products]}{[ImineH^+][OH^-]} \quad (3.36)$$

Then:

$$\frac{K_1}{K_2} = \frac{k_{H_2O} k_{-OH^-}}{k_{-H_2O} k_{OH^-}} = Kw \quad (3.37)$$

It is then possible to express the ratio of k_{-OH^-} over k_{-H_2O} as:

$$\frac{k_{-OH^-}}{k_{-H_2O}} = 10^{-14} \times \frac{2 \times 10^5}{0.15} = 1.3 \times 10^{-8} \text{ mol dm}^{-3} \quad \textbf{(3.38)}$$

Re-writing equation 3.28:

$$k_{obs} = \frac{0.15 \times [H^+] + 2 \times 10^{-9}}{([H^+] + 7.24 \times 10^{-7})(1 + (1.3 \times 10^{-8} + [H^+]) \times \frac{k_{-H_2O}}{k_d})} \quad \textbf{(3.39)}$$

Fitting the data to the above equation allowed calculation of the ratio $\frac{k_{-H_2O}}{k_d}$. The results are collected in Table 3.12

Table 3.12 Estimated and calculated constants for the pH dependence of the hydrolysis of benzylidene benzylamine

k_{H_2O}	0.15 s^{-1}
$\frac{k_{-H_2O}}{k_d}$	101 +/- 11 dm^3mol^{-1}
k_{OH^-}	2.0 x 10^5 $dm^3mol^{-1}s^{-1}$
$pK_a^{ImH^+}$	6.14

3.2.4.2.2 N-Benzylidene allylamine

3.2.4.2.2.1 Alkaline conditions (pH > 6)

Similarly to benzylidene benzylamine the data collected for the pH range 6-12 show a decrease in absorbance with time corresponding to the rate determining attack of water or hydroxyl ion on the iminium ion.

The reaction follows first order kinetics accordingly to equation 3.31. Values for the observed rate constant, k_{obs}, were then collected (Table 3.13).

The pH dependence of the constant was fitted to equation 3.32 allowing for the calculation of k_{H_2O}, k_{OH^-} and $K_a^{ImH^+}$ (Figure 3.25).

Table 3.13 Variation of k_{obs} with pH for the hydrolysis reaction of benzylidene allylamine in alkaline conditions

pH	k_{obs} (s^{-1})	Log (k_{obs})
6.01	$8.91x10^{-2}$	-1.05
6.10	$7.75x10^{-2}$	-1.11
6.19	$7.21x10^{-2}$	-1.14
6.27	$6.04x10^{-2}$	-1.22
6.37	$5.25x10^{-2}$	-1.28
6.45	$6.19x10^{-2}$	-1.21
6.56	$4.60x10^{-2}$	-1.34
6.63	$4.72x10^{-2}$	-1.33
6.66	$3.99x10^{-2}$	-1.40
6.67	$3.33x10^{-2}$	-1.48
6.88	$2.74x10^{-2}$	-1.56
6.99	$3.02x10^{-2}$	-1.52
7.15	$2.29x10^{-2}$	-1.64
7.52	$1.21x10^{-2}$	-1.92
8.17	$5.93x10^{-3}$	-2.23
8.50	$7.48x10^{-3}$	-2.13
9.07	$5.48x10^{-3}$	-2.26
10.06	$4.58x10^{-3}$	-2.34
11.00	$4.76x10^{-3}$	-2.32
12.00	$4.46x10^{-3}$	-2.35

Figure 3.25 Log(k_{obs}) versus pH for the hydrolysis reaction of benzylidene allylamine in alkaline conditions

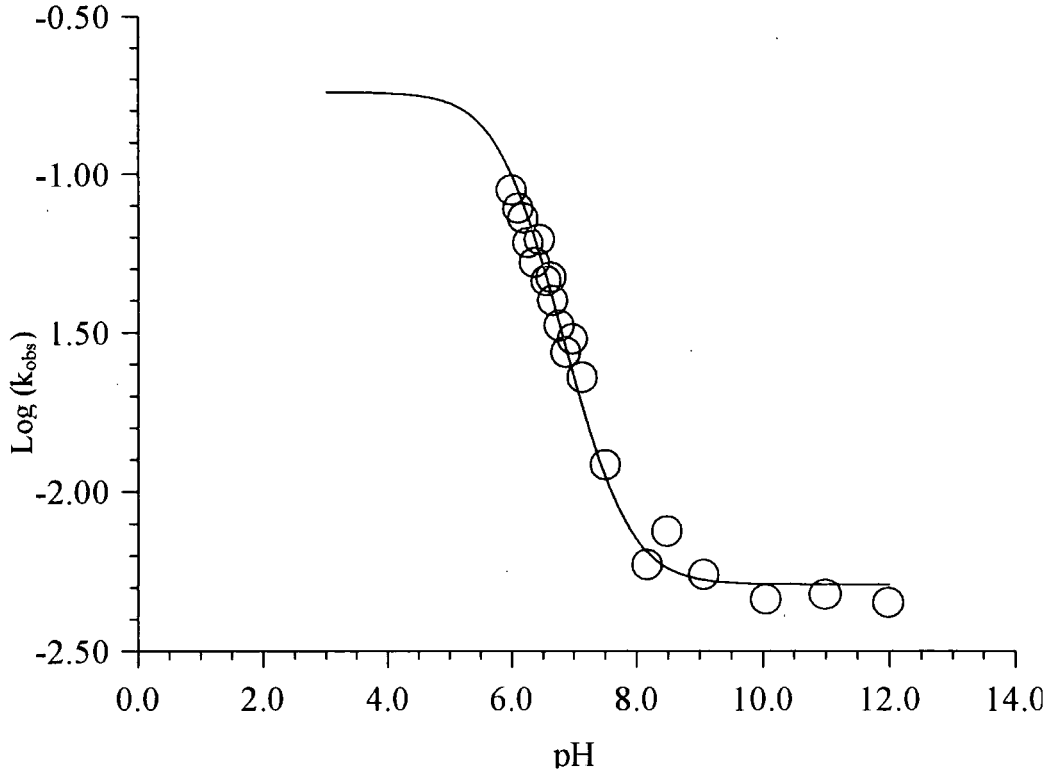

Note: the full line was calculated according to equation **3.32** using the Scientist® software package.

The curve of best fit shown above was calculated using the following constants:

Table 3.10 Rate and acid dissociation constants used to calculate the curve of best fit

$pK_a^{ImH^+}$	6.05±0.1
k_{OH^-}	$(4.58 \pm 0.28) \times 10^5 dm^3 mol^{-1} s^{-1}$
k_{H_2O}	$(1.81 \pm 0.08) \times 10^{-1} s^{-1}$

3.2.4.2.2.2 Global pH dependence

Additionally to the data summarised above, the hydrolysis reaction was also studied in acidic conditions (Table 3.14). However similarly to the study of benzylidene benzylamine and for the same reasons mentioned earlier it has not been possible to follow the reaction between pH = 3 and pH = 6.

Also worth noting is the fact that the kinetics for the acidic part of the process could not be evaluated explicitly. All the data were therefore fitted to Jencks's model as described by equation 3.28 (Figure 3.26).

Table 3.14 Variation of k_{obs} with pH for the hydrolysis reaction of benzylidene allylamine in acidic conditions

pH	k_{obs} (s^{-1})	Log(k_{obs})
0.70	$3.93x10^{-3}$	-2.41
0.82	$5.88x10^{-3}$	-2.23
1.00	$9.57x10^{-3}$	-2.01
1.30	$2.09x10^{-2}$	-1.68
1.70	$3.61x10^{-2}$	-1.44

pH	k_{obs} (s^{-1})	Log(k_{obs})
2.00	$6.42x10^{-2}$	-1.19
2.70	$1.30x10^{-1}$	-0.89
3.00	$1.50x10^{-1}$	-0.82
3.70	$2.60x10^{-1}$	-0.59
4.00	$2.40x10^{-1}$	-0.62

Figure 3.26 pH profile for the hydrolysis of benzylidene benzylamine

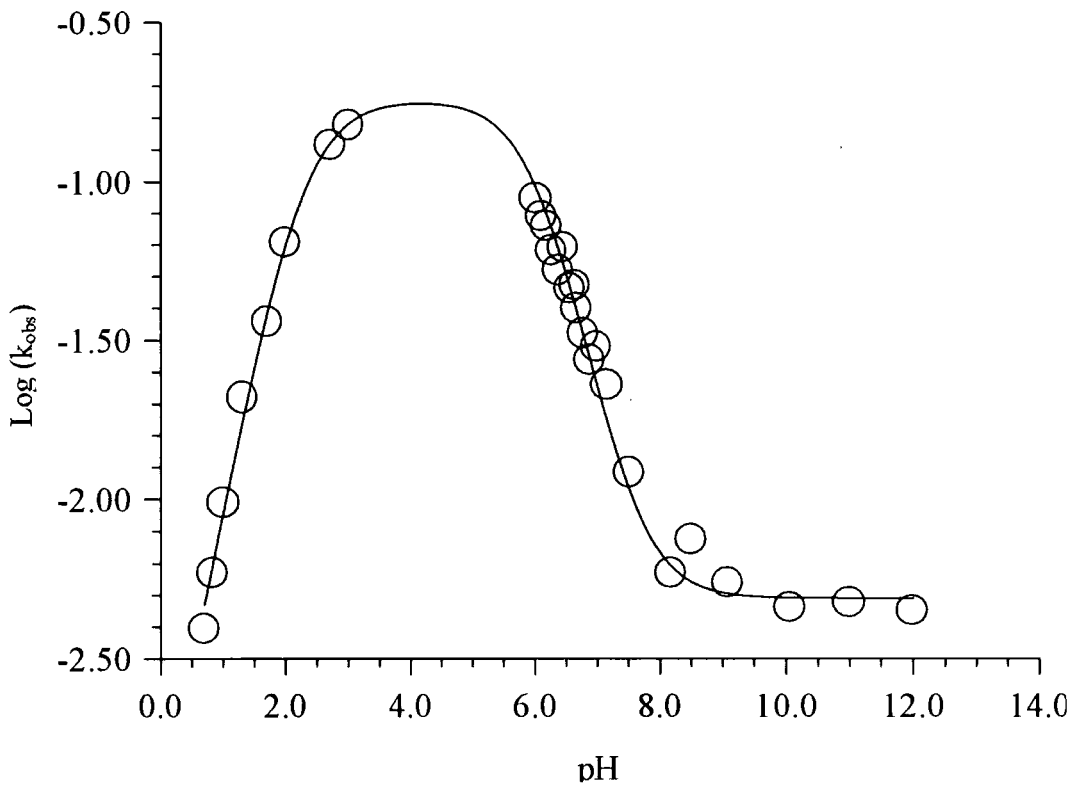

The data were fitted using an equivalent of equation 3.39. The various estimations and set parameters are summed up in Table 3.15 as well as the calculated value for $\frac{k_{-H_2O}}{k_d}$.

Table 3.15 Estimated and calculated constants for the pH dependence of the hydrolysis of benzylidene allylamine

k_{H_2O}	0.18 s^{-1}
$\frac{k_{-H_2O}}{k_d}$	188 +/- 11 dm^3mol^{-1}
k_{OH^-}	$4.4x10^5$ $dm^3mol^{-1}s^{-1}$
$pK_a^{ImH^+}$	6.05

3.2.4.2.3 N-(4-nitro)-Benzylidene benzylamine

Again a decrease in absorbance with time corresponding to the rate determining attack of water and hydroxyl ion on the iminium ion was observed.

The reaction follows first order kinetics according to equation 3.31. Values for the observed rate constant, k_{obs}, were then collected (Table 3.16).

Table 3.16 Variation of k_{obs} with pH for the hydrolysis reaction of (4-nitro)-benzylidene benzylamine in alkaline conditions

pH	k_{obs} (s^{-1})	Log (k_{obs})
6.46	$1.89x10^{-2}$	-1.72
7.00	$7.79x10^{-3}$	-2.11
8.08	$1.26x10^{-3}$	-2.90
9.08	$7.9x10^{-4}$	-3.10
9.96	$7.1x10^{-4}$	-3.15

The pH dependence of the constant was fitted to equation 3.32 allowing for the calculation of k_{H_2O}, k_{OH^-} and $K_a^{ImH^+}$ (Table 3.17 and Figure 3.27).

Table 3.17 Rate and acid dissociation constants used to calculate the curve of best fit

pKa^{ImH^+}	6.08±0.1
k_{OH^-}	$5.89 \pm 2.25 \times 10^4 dm^3 mol^{-1} s^{-1}$
k_{H_2O}	$6.41 \pm 1.91 \times 10^{-2} s^{-1}$

Figure 3.27 Log(k_{obs}) versus pH for the hydrolysis reaction of (4-nitro)-benzylidene benzylamine in alkaline conditions

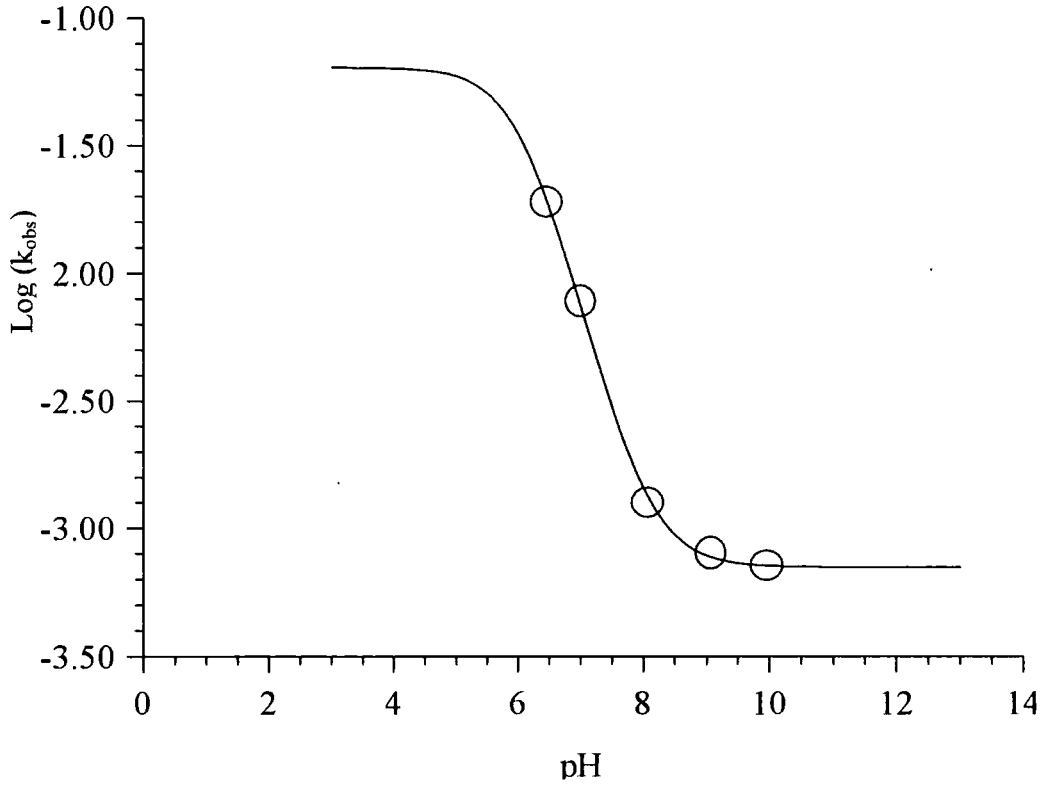

The values given in Table 3.17 produce the solid line shown in Figure 3.27. However these values should be treated with extreme caution since values of k_{obs} were not possible at pH values close to the expected $pK_a^{ImH^+}$ value. The presence of the 4-nitro substituent is expected to increase the acidity of the iminium ion, so that the true value for $pK_a^{ImH^+}$ is likely

to be < 6. Any discrepancy in the $pK_a^{ImH^+}$ value will directly affect values calculated for k_{OH^-} and k_{H_2O}.

It is worth noting that values collected in acidic conditions were neither consistent nor reproducible. Therefore it has not been possible to use Jencks's equation to determine the other constants.

3.2.5 Dissociation constant of 2-benzylamino-2-phenylacetonitrile

It is of interest to consider the process by which enantiomeric forms of the α-aminonitriles may be interconverted. Does epimerisation involve loss of cyanide to give an iminium ion which my be re-attacked by cyanide, or alternatively proton loss to give a carbanion.

Hence the acidity, in terms of carbanion formation, of the aminonitrile was investigated.

Scheme 3.15

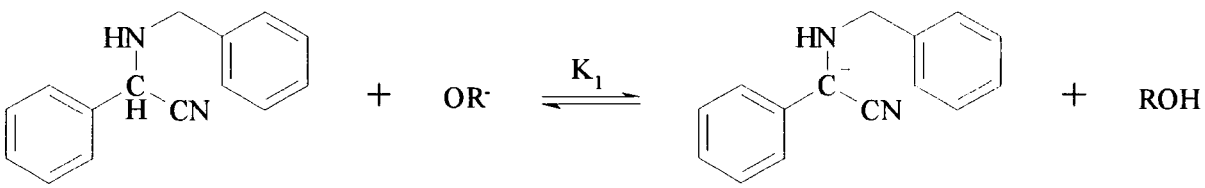

The reaction was studied using the methoxide ions in dimethyl sulfoxide (DMSO)/methanol mixtures as well as hydroxide ions in DMSO/water using tetraethylamonium hydroxide ($Et_4N^+OH^-$) as a base.

Experimental procedure

Sodium methoxide preparation:

In an oven-dried 3-necked round bottom flask (500 cm^3) clean sodium metal was added stepwise to ca 300 cm^3 of methanol under nitrogen. The solution was allowed to reach saturation. The excess metal was filtered and subsequently quenched with ethanol.

The resulting sodium methoxide (MeONa) solution was titrated using 0.1 mol dm^{-3} hydrochloric acid (commercially purchased: Aldrich) to find [MeONa] = 3.02 mol dm^{-3}.

It was then diluted to afford a 0.1 mol dm^{-3} stock solution.

DMSO/methanol/MeONa:

A range of DMSO/MeOH solutions were prepared ranging from 55 vol% to 85 vol% in DMSO. The sodium methoxide concentration was kept constant at 0.05 mol dm^{-3}.

The neutral aminonitrile shows little absorbance above 270 nm. On dilution with DMSO/MeOH without methoxide increased absorbance was noticed in that particular region. In the presence of base new absorption bands were observed with maxima at 280 and 310 nm. The formation of the anion was followed spectrophotometrically at these wavelengths.

The aminonitrile was added to the required solvent mixture in 10 cm^3 flasks so that [Aminonitrile] = $1x10^{-4}$ mol dm^{-3} and left to equilibrate. A spectrum was then recorded.

DMSO/water/$Me_4N^+OH^-$

A range of DMSO/water/$Me_4N^+OH^-$ solutions were prepared in solvents ranging from 50 vol% to 90 vol% in DMSO. The tetraethylamonium hydroxide concentration was kept constant at 0.011 mol dm^{-3}.

Similarly to the conditions described for DMSO/MeOH the formation of the anion was followed spectrophotometrically at 280 nm with [Aminonitrile] = $1x10^{-4}$ mol dm^{-3}.

The reaction was also monitored using stopped flow spectrophotometry. A solution of the aminonitrile ($2x10^{-4}$ mol dm^{-3}) in DMSO was placed in one syringe. In the other syringe tetraethylamonium hydroxide ($2.2x10^{-2}$ mol dm^{-3}) was diluted in a DMSO/water mixture.

3.2.5.1 Dissociation constant of 2-benzylamino-2-phenylacetonitrile in methanol

Scheme 3.16

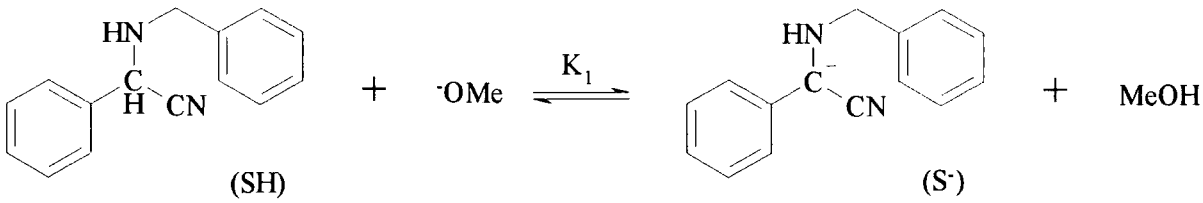

It was necessary to use strongly alkaline media in order to achieve deprotonation as shown in Scheme 3.16. The experimental spectrophotometric measurements allowed the calculation of values of the ionisation ratio (IR) defined in equation 3.40.

$$IR = \frac{[S^-]}{[SH]} \qquad \textbf{(3.40)}$$

In these media the basicity is best represented by an acidity function. In media containing methanol the appropriate function is H_M where the standard state is methanol[17,18]. The H_M function refers to the dissociation process shown in equation 3.41 and the pK_a value id given by equation 3.42.

$$SH \underset{}{\overset{K_a}{\rightleftharpoons}} S^- + H^+ \qquad \textbf{(3.41)}$$

$$pK_a = H_M - Log_{10}(IR) \qquad \textbf{(3.42)}$$

Rochester[18] quotes values of H_ for methanol/DMSO mixtures containing 0.025 mol dm^{-3} sodium methoxide. However these values refer to water as the standard state and hence must be modified to yield the appropriate H_M values.

In the present work a methoxide concentration of 0.05 mol dm^{-3} was used.

In the absence of DMSO, and at low sodium methoxide concentrations:

$$H_M = pK_{Methanol} + Log([MeONa]) \quad (3.43)$$

where $pK_{Methanol}$ refers to the autoprotolysis constant of methanol and equals 16.92.

Hence for [MeONa] = 0.05 mol dm^{-3}, H_M = 15.62

With reference to the tables H_, in the absence of DMSO, equals 12.23. Therefore a corrective factor of 3.39 must be added to the values extracted from the tables.

Accordingly the different values for IR, H_M and pK_a determined at λ = 280 and 310 nm are collected in Tables 3.18 and 3.19 respectively.

Note:

$$IR = \frac{[S^-]}{[SH]} = \frac{A - A_0}{A_\infty - A}$$

where: A_0 is the initial absorbance with $A_{0;\,280} = A_{0;\,310} = 0.01$

A_∞ is the final absorbance with $A_{\infty;\,280} = 0.68$ and $A_{\infty;\,310} = 0.33$

Table 3.18 Absorbance readings at λ = 280 nm, acidity functions, ionisation ratio and calculated pK_a values

DMSO (cm^3)	MeOH (cm^3)	DMSO (Vol %)	DMSO (mol %)	H_M	A (280 nm)	IR	Log(IR)	pK_a
5.5	4.50	55%	40%	18.23	0.048	0.06	-1.22	19.45
6.5	3.50	65%	51%	18.89	0.148	0.26	-0.59	19.47
7.0	3.00	70%	56%	19.24	0.335	0.94	-0.03	19.26
7.5	2.50	75%	63%	19.75	0.486	2.45	0.39	19.36
8.0	2.00	80%	69%	20.12	0.528	3.41	0.53	19.59
8.5	1.50	85%	76%	20.69	0.611	8.71	0.94	19.75

pK_a: Average: 19.48
Std Deviation: 0.17

Table 3.19 Absorbance readings at λ = 280 nm, acidity functions, ionisation ratio and calculated pK_a values

DMSO (cm^3)	MeOH (cm^3)	DMSO (Vol %)	DMSO (mol %)	H_M	A (310 nm)	IR	Log(IR)	pK_a
5.5	4.50	55%	40%	18.23	0.019	0.03	-1.54	19.77
6.5	3.50	65%	51%	18.89	0.058	0.18	-0.75	19.64
7.0	3.00	70%	56%	19.24	0.121	0.53	-0.27	19.51
7.5	2.50	75%	63%	19.75	0.203	1.52	0.18	19.56
8.0	2.00	80%	69%	20.12	0.231	2.23	0.35	19.78
8.5	1.50	85%	76%	20.69	0.295	8.14	0.91	19.78

pK_a: Average: 19.67
Std Deviation: 0.12

The results using measurements at two different wavelengths are self consistent and yield a value of $pK_a = 19.6 \pm 0.3$. This may be compared with values of ca 24.0 for benzyl cyanide (X) and 16.9 for 4-nitrobenzylcyanide[17].

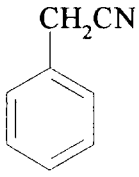

(X)

Compared to (X) the amino substituent on the α-carbon atom has the expected acidifying effect. The Taft σ^* value for the N-benzyl group is 1.68[19] indicating its electron attracting nature.

3.2.5.2 Dissociation constant of benzylamino-2-phenylacetonitrile in water

Scheme 3.17

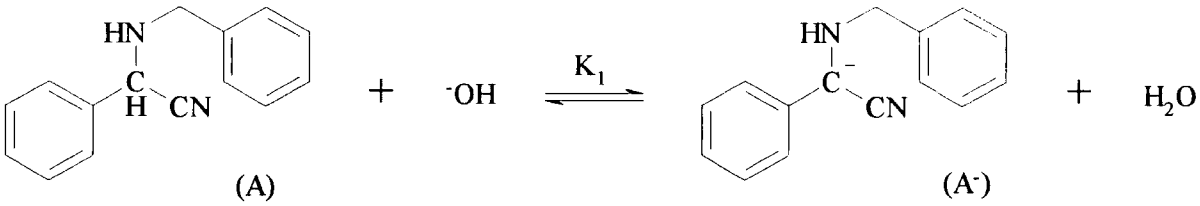

(A) (A⁻)

Similarly to the calculations carried out in methanol pK_a was calculated using equation 3.44.

$$pK_a = H_- - Log_{10}(IR) \qquad \textbf{(3.44)}$$

Values of the Hammett acidity function, H_-, corresponding to water/DMSO mixtures containing 0.011 mol dm^{-3} tetramethylammonium hydroxide have been reported by Rochester[18]. Although tetraethylammonium hydroxide was used rather than the methyl derivative the values for H_- were assumed to be similar.

Accordingly the different values for IR, H_ and pK_a determined at λ = 280 are collected in Table 3.20.

Table 3.20 Absorbance readings at λ = 280 nm, acidity functions, ionisation ratio and calculated pK_a values

DMSO (cm^3)	H_2O (cm^3)	DMSO (Vol %)	DMSO (mol %)	H_	Abs (280 nm)	IR	Log(IR)	pK_a
9	1	90%	69%	19.42	0.360	36.5	1.56	(17.86)
8	2	80%	50%	17.46	0.335	9.40	0.97	16.49
7	3	70%	37%	16.19	0.154	0.666	-0.18	16.37
6	4	60%	27%	15.24	0.019	0.027	-1.57	16.81
5	5	50%	20%	14.47	0.010	0.001	-3.26	(17.73)

pK_a:	Average:	16.56
	Std. Deviation:	0.19

Note: $A_0 = 0.01$

$A_\infty = 0.37$

The results lead to a value for pK_a in water of 16.56 ± 0.19. This value is ca 3 pK units lower than that obtained in methanol, corresponding to the difference in autoprotolysis constants for the two solvents, $pK_w = 14$, $pK_{Methanol} = 16.92$.

The value obtained in water may be used to calculate a value for K_I as defined in Scheme 3.17. The relationship is given in equation 3.45 so that $K_I = 2.5 \times 10^{-3}$ dm^3 mol^{-1}.

$$LogK_I = -pK_a + pK_w \qquad \textbf{(3.45)}$$

3.2.5.3 Rate of formation of the carbanion

Using stopped flow spectrophotometry the rate of deprotonation has been measured. A characteristic increase in absorbance with time can be seen and fits first order kinetics.

The base concentration was kept constant at 0.011 mol dm^{-3}. The ratios of DMSO to water were varied and the constants, k_{obs}, recorded as shown in Table 3.21.

According to Rochester's tables[18] for a solution containing 99% water H_ = 12.04. Hence by extrapolating a plot of Log (k_{obs}) versus H_ (Figure 3.28) it is possible to determine the value for k_{obs} in virtually pure aqueous solution.

Table 3.21 Observed rate constants for the formation reaction of the carbanion at varying Hammett acidity function values

DMSO (cm^3)	H_2O (cm^3)	DMSO (Vol %)	DMSO (mol %)	H_	k_{obs} (s^{-1})	Log (k_{obs})
7.0	3.0	70%	37%	16.19	$2.30x10^{-3}$	-2.64
7.5	2.5	75%	43%	16.80	$4.58x10^{-2}$	-1.34
8.0	2.0	80%	50%	17.46	$4.02x10^{-1}$	-0.40
8.5	1.5	85%	59%	18.39	2.39	0.38

Figure 3.28 Log(k_{obs}) versus Hammett acidity function for the formation reaction of the carbanion

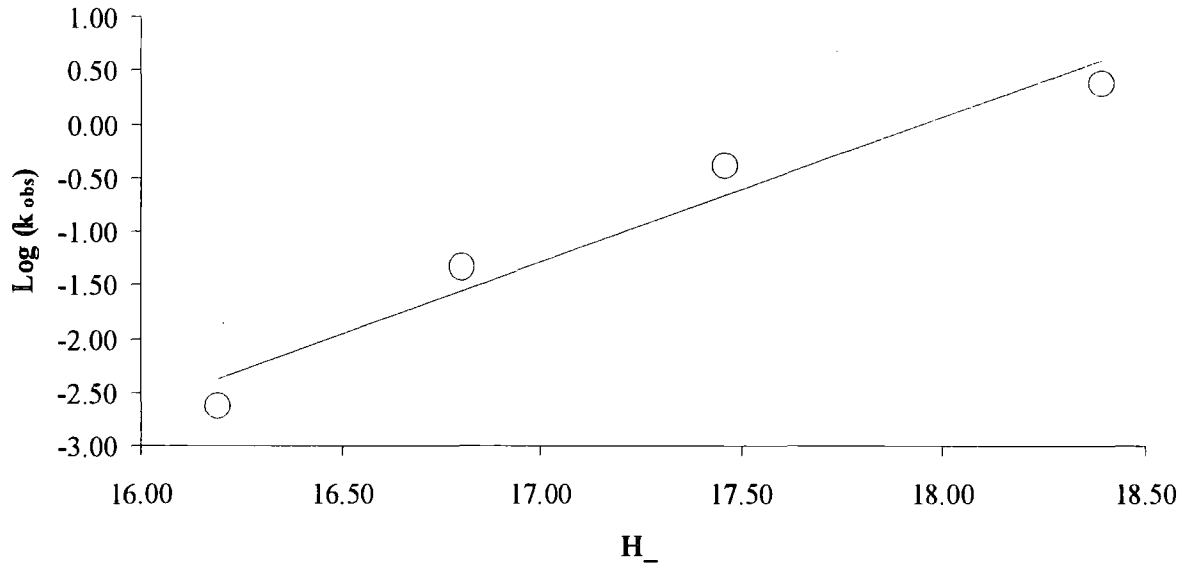

The following linear relationship was found:

$$\text{Log}(k_{obs}) = (1.35 \pm 0.21) \times H\_ - (24.2 \pm 3.6)$$

Hence for H_ = 12.04, $k_{obs} = 1.13 \times 10^{-8}\ s^{-1}$.

The plot of $\text{Log}(k_{obs})$ versus H_ is approximately linear as found for the ionisation of other carbon acids in DMSO/water mixtures[20].

At the basicities used the forward reaction in Scheme 3.17 will be dominant so that $k_{obs} = k_1[OH^-]$. Hence a value for k_1, the rate constant for reaction of the aminonitrile with hydroxide ions in water, may be estimated as $\frac{1.13 \times 10^{-8}}{1.1 \times 10^{-2}} = 1.02 \times 10^{-6}\ dm^3mol^{-1}s^{-1}$.

Since the value of K_1, the equilibrium constant, has been measured as 2.5×10^{-3} dm^3mol^{-1}, then the value for k_{-1} $(= \frac{k_1}{K_1})$ is ca $4 \times 10^{-3}\ s^{-1}$.

The processes involved in loss of cyanide from the aminonitrile and in its deprotonation are shown in Scheme 3.18, together with the corresponding rate constants in water.

Scheme 3.18

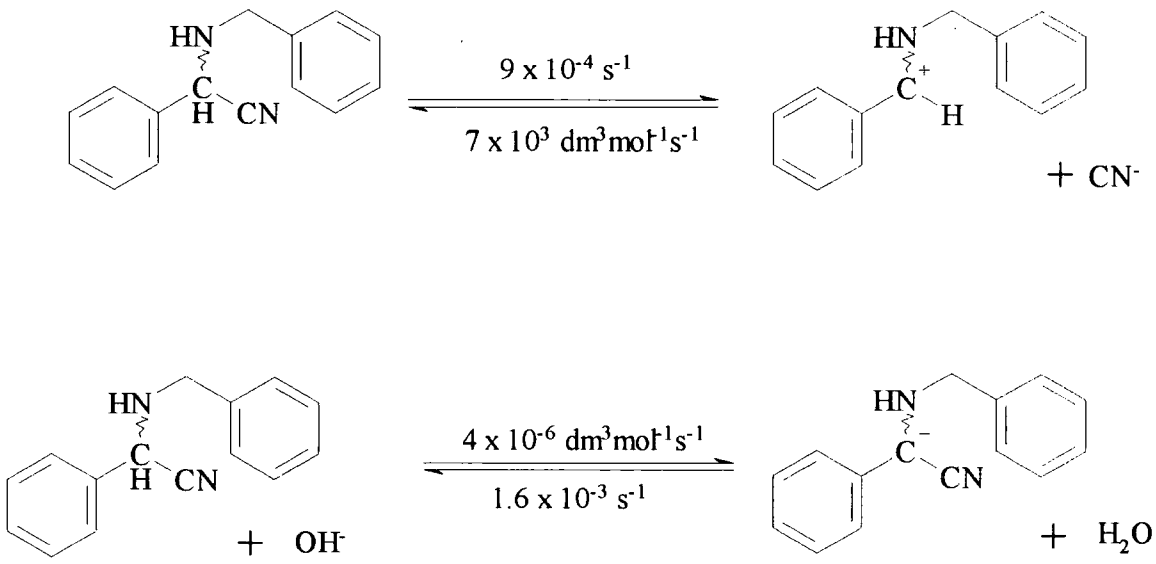

It can be seen here that in solution with pH < 14 loss of cyanide from the aminonitrile will be a considerably faster process than deprotonation. Hence epimerisation is likely to involve the former pathway.

3.3 Conclusions

The reaction of imines with cyanide leads to the formation of α-aminonitriles. The kinetics for the addition of cyanide ion (using potassium cyanide as the anion source) to N-benzylidene benzylamine, N-benzylidene allylamine and N-(4-nitro-)benzylidene benzylamine have been investigated. Commeyras and Taillades[5-8] showed when starting from the parent carbonyl compound that cyanohydrin is rapidly formed before slowly decomposing as the α-aminonitrile concentration increases. This has not been monitored on this study. However it has been possible to follow the formation of the product by measuring the decrease in absorbance of the imines (λ_{max} = 250 or 280 nm depending on the Schiff base). It is important to note that two side reactions have been characterised. First of all as mentioned in the literature imines can hydrolyse back to the starting aldehydes and amines. Furthermore α-aminonitriles slowly decompose as well.

The addition of cyanide to the imines is pH dependent. Plots of the logarithm of the observed rate constant against pH are characteristic bell-shaped curves. The plateau between pH = 6.5 and 8.5 in the plot shown in Figures 3.11 and 3.13 correspond to the regions between the pK_a values of the iminium ions and hydrogen cyanide. In this region increasing acidity increases the concentration of the iminium ions but decreases the concentration of the cyanide ions. Decreases in value of rate constant at pH > 9 result from decreases in the concentration of iminium ions when the free cyanide concentration is reaching its stoichiometric value. Correspondingly decreases in value at lower pH result from decreases in concentration of free cyanide ions when the imines are largely protonated. Rate constants for the formation of the α-aminonitriles, k_1, have been evaluated.

The rate constants for the reverse process, k_{-1}, as well as values for the acid dissociation constants of the iminium ions have also been measured as shown in Table 3.22.

Table 3.22 Acid dissociation and rate constants for the formation and dissociation of aminonitriles

Imine	k_1 ($dm^3mol^{-1}s^{-1}$)	k_{-1} (s^{-1})	pK_a
N-Benzylidene benzylamine	$(6.7 \pm 1.0)x10^3$	$(8.85 \pm 0.58)x10^{-4}$	6.14 ± 0.1
N-Benzylidene allylamine	$(1.03 \pm 0.23)x10^4$	$(5.25 \pm 0.17)x10^{-4}$	6.05 ± 0.1

In the case of the N-(4-nitro-) benzylidene benzylamine the reaction rate, k_f, is much slower and there is considerable interference from the hydrolysis reaction. Hence values of rate constants are not well-defined.

The overall equilibrium scheme for the addition of cyanide to imines and iminium ions can be represented as follows:

Scheme 3.19

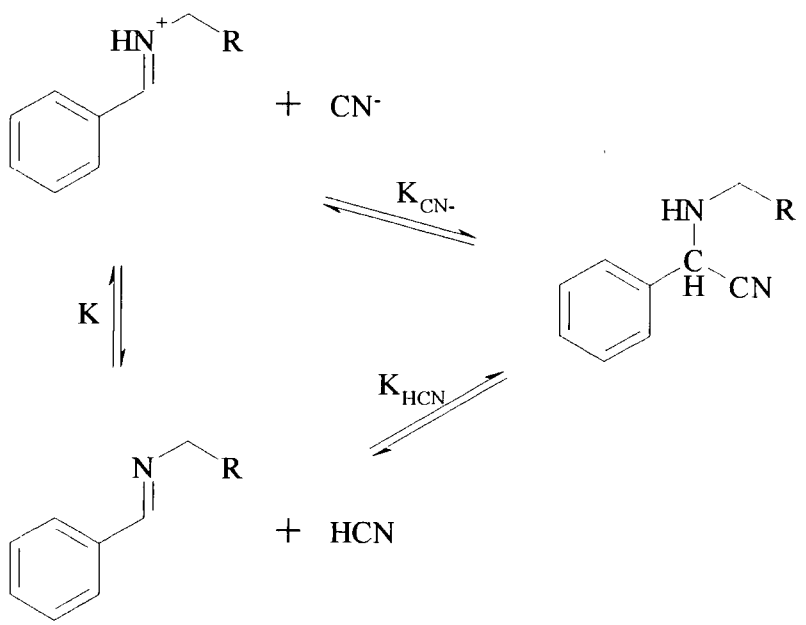

Calculations of the equilibrium constants K_{CN^-}, and K_{HCN}, according to equations 3.46 and 3.47 respectively, indicate that the addition of cyanide to the iminium ion is highly favoured (Table 3.23).

$$K_{CN^-} = \frac{k_1}{k_{-1}} \tag{3.46}$$

$$K_{HCN} = \frac{K_a^{HCN}}{K_a^{ImH^+}} \times K_{CN^-} = K \times K_{CN^-} \tag{3.47}$$

Table 3.23 Equilibrium constants for the process of cyanide addition to imines (Scheme 3.19)

Imine	K_{CN} (dm^3mol^{-1})	K	K_{HCN} (dm^3mol^{-1})
N-Benzylidene benzylamine	$7.57x10^6$	$1.10x10^{-3}$	$8.33x10^3$
N-Benzylidene allylamine	$1.96x10^7$	$8.91x10^{-4}$	$1.75x10^4$

It is worth noting that changing the R group from phenyl to $CH{=}CH_2$ has little effect on the values of the rate and equilibrium constants.

The principle of microscopic reversibility implies that hydrolysis of the imine follows the same pathway as the formation of the Schiff base. In alkaline conditions the attack of water and/or hydroxide ion on the iminium ion is rate determining corresponding to the dehydration step for the reverse reaction. Analysis of the reaction for high pH's enabled the calculation of values for the rate of addition of water, k_{H_2O}, hydroxide ion, k_{OH^-}, and the acid dissociation constant, $pK_a^{ImH^+}$ (Table 3.24)

Table 3.24 Acid dissociation and rate constants for the hydrolysis of imines

Imine	k_{H_2O} (s^{-1})	k_{OH^-} ($dm^3mol^{-1}s^{-1}$)	$pK_a^{ImH^+}$
N-Benzylidene benzylamine	$8.07x10^{-2}$	$1.19x10^5$	6.37
N-Benzylidene allylamine	$1.81x10^{-1}$	$4.58x10^5$	6.05
N-(4-nitro-)Benzylidene benzylamine	$(6.41x10^{-2})$	$(8.89x10^4)$	(6.08)

Again the change in the R group does not have a significant effect on the rate constants. However it is necessary to consider the values for the nitro derivative with care since a lack of experimental data at the lower pH values seems to indicate that the process is much faster and the pK_a value for the acid dissociation constant value lower.

Nevertheless it is worth mentioning that the values found for $pK_a^{ImH^+}$ are consistent with the ones calculated from the aminonitrile formation.

In acidic conditions the rate-determining step is the cleavage of the carbinolamine to form the amine and the aldehyde (reverse of the addition step for the formation of the Schiff base).

Using steady state conditions Jencks[9] derived a model for the hydrolysis of imines:

$$k_{obs} = \frac{k_{H_2O}k_d[H^+] + k_d k_{OH^-}Kw}{([H^+] + K_a^{ImH^+})(k_{-H_2O}[H^+] + k_{-OH^-} + k_d)} \qquad \textbf{(3.28)}$$

The equation has been applied to the data collected in both acidic and alkaline conditions for N-benzylidene benzylamine and N-benzylidene allylamine. It is important to note that, since the number of unknowns (6) was too large for the iteration to be completed

successfully, fixed values for k_{H_2O}, k_{OH^-} and $pK_a^{ImH^+}$ as well as an estimate for $\frac{k_{-OH^-}}{k_{-H_2O}}$ were used. This allowed for the calculation of $\frac{k_{-H_2O}}{k_d}$ (Table 3.25).

Table 3.25 Calculated and estimated values of the rate constants for the hydrolysis of imines

	N-Benzylidene benzylamine	N-Benzylidene allylamine
k_{H_2O} (s^{-1})	0.15	0.18
k_{OH^-} ($dm^3mol^{-1}s^{-1}$)	$2x10^5$	$4.4x10^5$
$pK_a^{ImH^+}$	6.14	6.05
$\frac{k_{-OH^-}}{k_{-H_2O}}$ (mol dm^{-3})	$1.3x10^{-8}$	$2.4x10^{-8}$
$\frac{k_{-H_2O}}{k_d}$ (dm^3mol^{-1})	101	188

All those estimations are necessary since it is not possible to record any data in the pH range 3 – 6 where the maximum of the curve lies.

Overall in terms of reactivity for the iminium ions, regardless of the R group, the order appears to be $OH^- > CN^- >> H_2O$. This order of reactivity of nucleophiles for cationic centres is that usually observed[21].

N-benzylidene benzyliminium and N-benzylidene allyliminium ions are relatively unreactive when compared with other iminium ions. Examples of reactions of iminium ions with water have been reported in the introduction and are summarised again below along with data from our study (Table 3.26).

Table 3.26 Comparison of the rate constant values for the reaction of water with iminium ions determined in the thesis with the literature

Iminium ion	k_{H_2O} (s^{-1})	Iminium ion	k_{H_2O} (s^{-1})
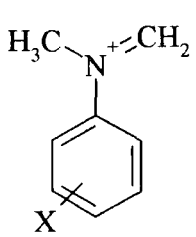	$3x10^6$ - $1x10^8$	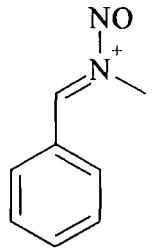	$7.6x10^5$
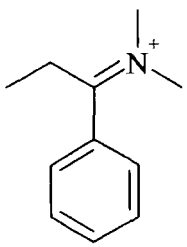	$2x10^{-3}$	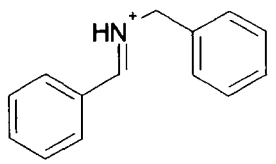	$1.5x10^{-1}$
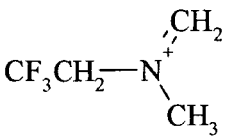	$1.8x10^7$	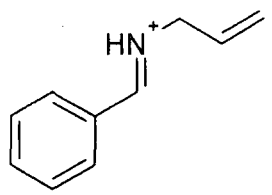	$1.8x10^{-1}$

Interestingly the reactivity of the N-nitrosoiminium ion listed in the above table has been studied with various nucleophiles including cyanide ion. A value of $2.2x10^7$ $dm^3mol^{-1}s^{-1}$ was found. This is higher than our values of $6.7x10^3$ $dm^3mol^{-1}s^{-1}$ and $1.03x10^4$ $dm^3mol^{-1}s^{-1}$ for N-benzylidene benzyliminium and N-benzylidene allyliminium ions respectively. Again the reactivity of the ions studied in this thesis is significantly lower than that of those reported in the literature.

The lower reactivity of the iminium ions herein studied can be justified by the possibility of charge delocalisation. They can be regarded as carbocations stabilised both by amino groups and by a benzene ring as shown in Scheme 3.20.

Scheme 3.20

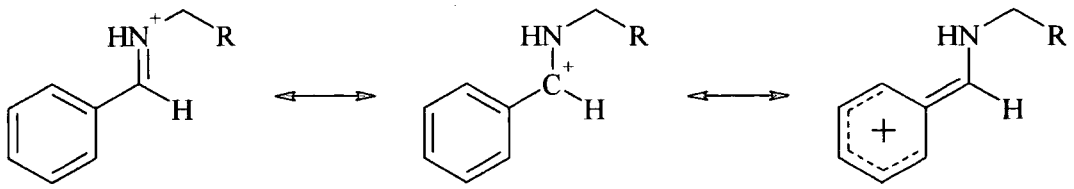

The stabilisation effect of the benzene ring has previously been reported by Sollenberger and Martin[11] who produced some iminium ions from aromatic enamines.

Other important results include the determination of the dissociation constant of 2-benzylamino-2-phenylacetonitrile, pK_a, in methanol and water presented in Table 3.27.

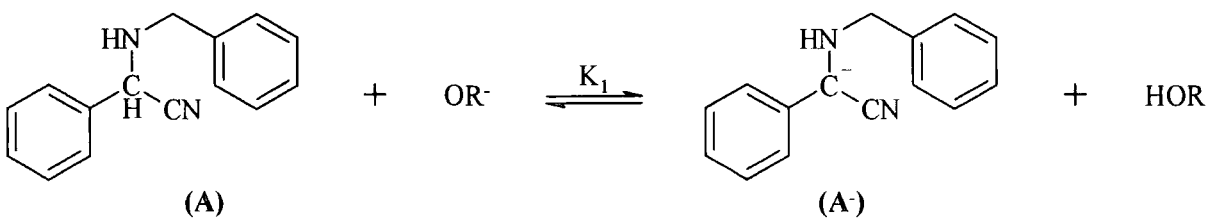

(A) **(A⁻)**

Table 3.27 Dissociation constants of benzylamino-2-phenylacetonitrile in methanol and water

Solvent	pK_a
Methanol	19.58 ± 0.29
Water	16.56 ± 0.19

Of particular interest is the rate constant for deprotonation by hydroxide ions, k_1 = 1.03×10^{-6} $dm^3mol^{-1}s^{-1}$. This can be compared to rate constant for the removal of cyanide from the aminonitrile, k = 8.85×10^{-4} s^{-1}. The former is a second order rate constant, so that the values of k_{obs} will depend on the base concentration. Nevertheless the results show that at the expected basicities involved here cyanide loss is a much faster process than deprotonation.

3.4 References

1. (a) C. Sannie, *Bull. Soc. Chim.*, 1925, **37**, 1557; (b) C. Sannie, *Bull. Soc. Chim.*, 1926, **39**, 254; (c) C. Sannie, *Bull. Soc. Chim.*, 1927, **39**, 274

2. T. D. Stewart and C. –H. Li, *J. Am. Chem. Soc.*, 1938, **60**, 2782

3. Y. Ogata and A. Kawasaki, *J. Chem. Soc. B*, 1971, 325

4. J. W. Stanley, J. G. Beasley and I. W. Mathison, *J. Org. Chem.*, 1972, **37**, 3746

5. J. Taillades and A. Commeyras, *Tetrahedron*, 1974, **30**, 127

6. J. Taillades and A. Commeyras, *Tetrahedron*, 1974, **30**, 2493

7. J. Taillades and A. Commeyras, *Tetrahedron*, 1974, **30**, 3407

8. (a) M. Béjaud, L. Mion and A. Commeyras, *Tetrahedron Lett.*, 1975, **34**, 2985; (b) M. Béjaud, L. Mion and A. Commeyras, *Bull. Soc. Chim. Fr.*, 1976, 1425; (c) A. Commeyras, J. Taillades, L. Mion and M. Béjaud, *Informations Chimie*, 1976, **158**, 199; (d) G. Moutou, J. Taillades, S. Benefice-Malouet, A. Commeyras, G. Messina and R. Mansani, *J. Phys. Org. Chem.*, 1995, **8**, 721

9. (a) E. H. Cordes and W. P. Jencks, *J. Am. Chem. Soc.*, 1962, **84**, 832; (b) E. H. Cordes and W. P. Jencks, *J. Am. Chem. Soc.*, 1963, **85**, 2843; (c) W. P. Jencks, *Progr. Phys. Org. Chem.*, 1964, **2**, 63

10. S. Eldin and W. P. Jencks, *J. Am. Chem. Soc.*, 1995, **117**, 4851

11. P. Y. Sollenberger and R. B. Martin, *J. Am. Chem. Soc.*, 1970, **92**, 4261

12. S. Eldin, J. A. Digits, S.-T. Huang and W. P. Jencks, *J. Am. Chem. Soc.*, 1995, **117**, 6631

13. A. Vigroux, A. J. Kresge and J. C. Fishbein, *J. Am. Chem. Soc.*, 1995, **117**, 4433

14. W. M. Ching and R. G. Kallen, *J. Am. Chem. Soc.*, 1978, **100**, 6119

15. A. I. Vogel, *Practical Organic Chemistry*, 5th Ed., Longman, 1989

16. J. Catalán, C. Díaz and F. García-Blanco, *Org. Biomol. Chem.*, 2003, **1**, 565

17. J. H. Atherton, M. R. Crampton, G. L. Duffield and J. A. Stevens, *J. Chem. Soc. Perkin Trans. 2*, 1995, 443

18. C. H. Rochester, *Acidity functions*, Academic Press, NY, 1970

19. M. Charton, *J. Org. Chem.*, 1964, **29**, 1222

20. J. R. Jones and R. Stewart, *J. Chem. Soc. (B)*, 1967, 1173

21. C. D. Ritchie, *Acc. Chem. Research*, 1972, **5**, 348

Chapter Four: Catalytic asymmetric synthesis of aminonitriles

Chapter four: Catalytic asymmetric synthesis of aminonitriles

4.1 Introduction

4.1.1 The Salen catalysts

As described in Chapter 1 a wide range of catalysts has been used to asymmetrically catalyse the Strecker reaction. One of the first metal-based catalysts used, and incidentally one of the most efficient, is that based on the Salen ligand shown on Scheme 4.1.

Scheme 4.1

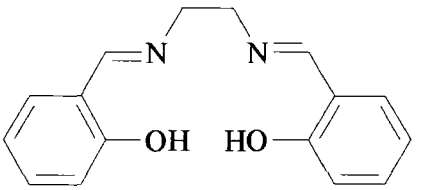

Salen (N, N' - bis (salicylaldehydo)ethylenediamine)

Salen ligands are easily prepared by the condensation of two equivalents of a salicylaldehyde derivative with a 1,2-diamine. The example shown above can be synthesised from salicylaldehyde and ethylene diamine.

The first Salen ligand and its copper complex were prepared by Combes[1] at the end of the 19th century (Scheme 4.2).

Scheme 4.2

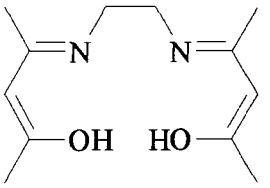

These tetradentate Schiff bases have been widely used and studied, especially during the past ten years. As Jacobsen and Larrow[2] described in a recent review on the subject of 'asymmetric processes catalysed by chiral (Salen) metal complexes' they present many attractive features.

The salicylaldehyde and the diamine are synthetically accessible materials. The metal complexes can be prepared from either first or second row transition metal salts or from main groups metals. Easy synthesis of the complexes also means that one can adapt the steric and electronic properties of the catalyst specific requirements by just modifying the metal counter ion, the chiral diamine or the salicylaldehyde moiety.

It is worth noting that a specific derivative of the ligand, namely N,N'-bis(3,5-di-*tert*-butylsalicylidene)-1,2-diaminocyclohexane, has been found to be the optimum ligand with various metal centres for a broad range of reactions (Scheme 4.3).

Scheme 4.3

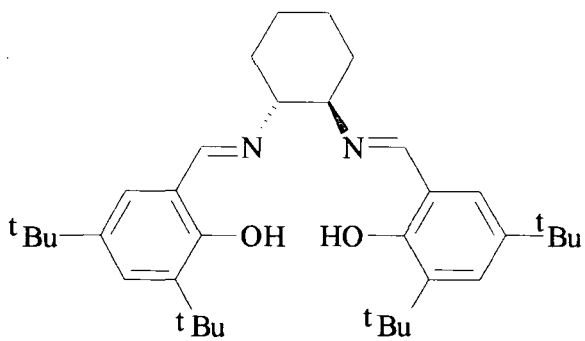

The main feature of the above ligand is the presence of the bulky tert-butyl groups which are thought to force the substrate to approach over the chiral diamine part of the molecule.

The synthesis of N,N'-bis(3,5-di-*tert*-butylsalicylidene)-1,2-diaminocyclohexane is shown below[3] (Scheme 4.4). It is worth mentioning that it is now commercially available.

Scheme 4.4

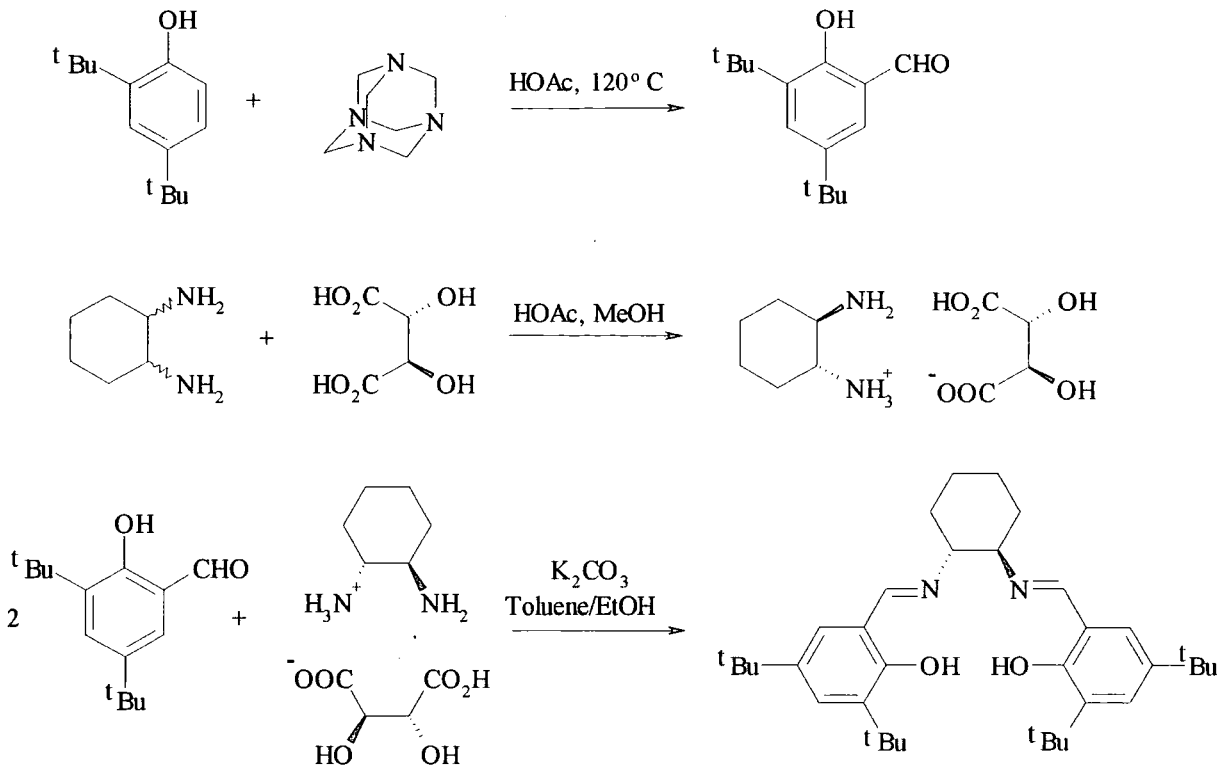

Various metals (Mn, Cr, Co, V, Al, Ti) have been used with Salen ligands to catalyse a widest range of reactions (epoxidation of alkenes, epoxide ring opening, cyclopropanation, etc...)[4].

Arguably one of the most efficient Salen catalyst is a manganese complex based on N,N'-bis(3,5-di-*tert*-butylsalicylidene)-1,2-diaminocyclohexane and commonly known as Jacobsen's catalyst since Jacobsen and co-workers designed it[5]. It is used with an oxidising agent to catalyse the enantioselective epoxidation of unfunctionalised olefins as described in Scheme 4.5.

Although truly efficient the catalytic mechanism of Jacobsen's catalyst is yet to be fully understood[6]. It is however generally agreed that the complex is oxidised to form a reactive oxo-Mn (V) Salen complex. It is worth noting that in the different mechanistic studies coordination of the alkene at the metal centre is not considered to be important.

It is thought that after the initial approach of the alkene towards the oxo oxygen atom oxygen transfer to form the epoxide directly follows. The nature of the transfer is subject to

debate and possible ways include: concerted, stepwise via a carbocation, stepwise via radical, [2+2] cycloaddition, electron transfer and charge transfer.

Scheme 4.5

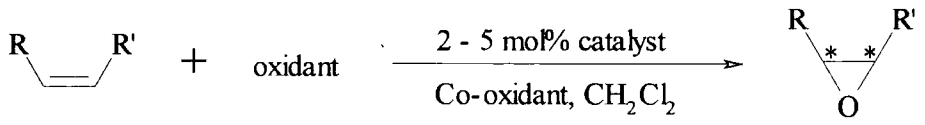

up to 98% e.e.

Jacobsen's catalyst :

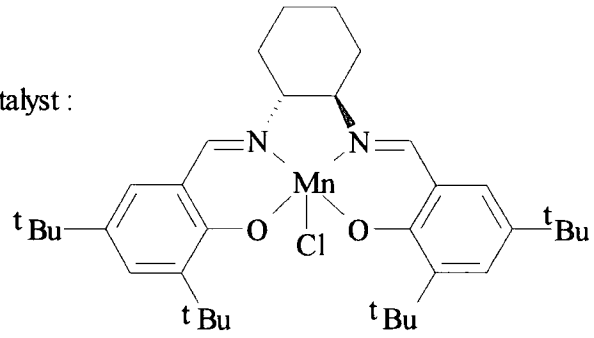

It is thought that the stereochemistry is controlled by the interaction of the alkene substituents with the ligand when the alkene approaches the Salen complex.

Of particular interest to our work are the reactions of addition of cyanide to carbonyl compounds and imines.

North and Belokon thoroughly studied the addition of trimethylsilyl cyanide (TMSCN) to aldehydes and ketones in the presence of Ti (IV) Salen catalyst. Various derivatives of the Salen ligands were compared and the optimum structure was found to be that shown in Scheme 4.3 using tert-butyl groups as R substituents on the phenyl rings[7].

It is worth noting that the catalyst produced only low levels of asymmetric induction for the reaction of highly electron deficient aromatic aldehydes. In the case of ketones no reaction was noticed.

Subsequent work[8] including full characterisation of the catalyst[9] highlighted the influence of water on the reaction. Significantly the presence of water enables the generation

of a dinuclear complex, with a central four membered ring comprising two titanium atoms and two oxygen atoms (Scheme 4.6), which exhibits better catalytic properties than the mononuclear species (Reaction time down from 20 hours to less ca an hour).

Scheme 4.6

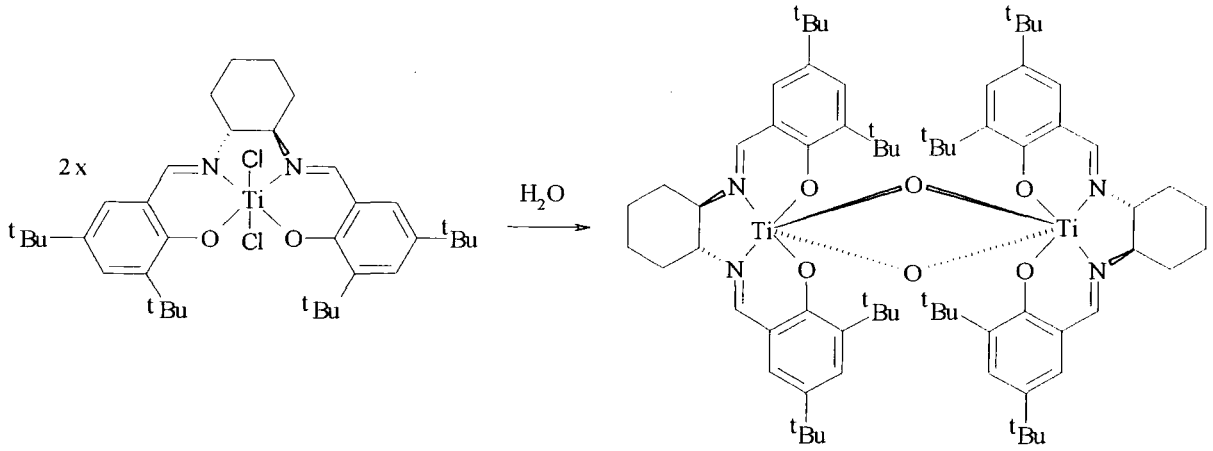

Using various analytical techniques (I.R., ^{1}H NMR spectroscopy, X-ray...) combined with kinetics, the mechanism by which the Salen dinuclear Ti complex catalyses the addition reaction of TMSCN to aldehydes was determined[10].

First it was determined that the dinuclear complex is in equilibrium with a monomeric species bearing a Ti=O group. Further, the various processes involved in the formation of the catalytic intermediates were determined.

- Formation of a **metalla- acetal** by a [2+2] cycloaddition of the Ti=O bond of the mononuclear species and the C=O bond of the carbonyl compound:

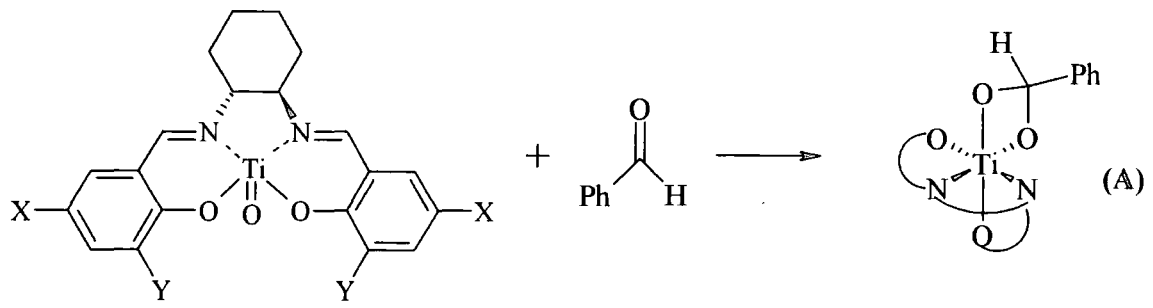

(A)

It is worth noting that detection of the above species, (A), was only possible when using electrophilic carbonyl compounds such as $(CF_3)_2CO$ or formaldehyde.

➢ In presence of excess cyanide, formation of **C_2 symmetrical structure** with the Ti moieties bridged by two OTMS groups:

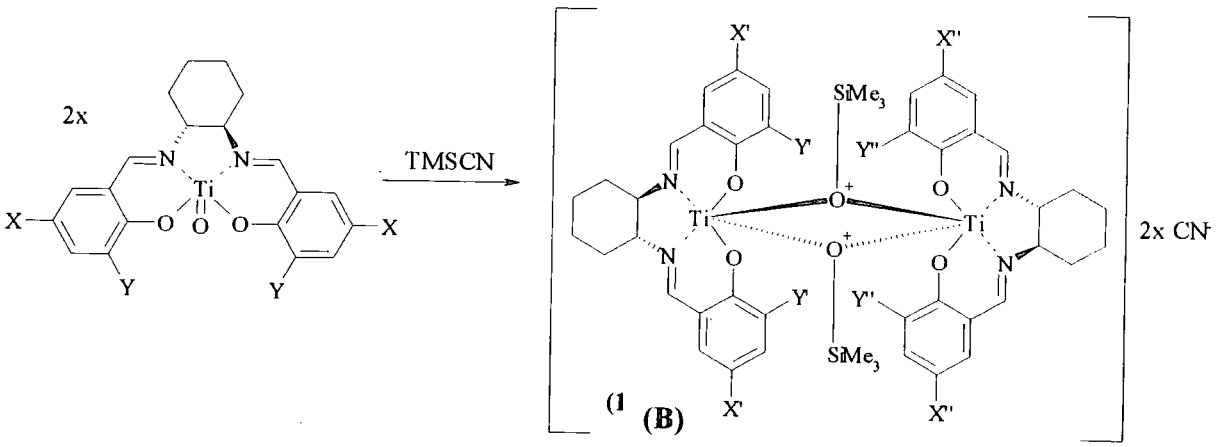

The two cyanide groups are thought to be either weakly bonded to the titanium atoms or outer-sphere anionic species.

It is worth pointing that the above species **(B)** is the predominant form in which the Ti complex exists at the end of the reaction of aldehydes with TMSCN.

➢ Decomposition of (**B**) to form a **mononuclear complex** with a planar coordination of the Salen ligand:

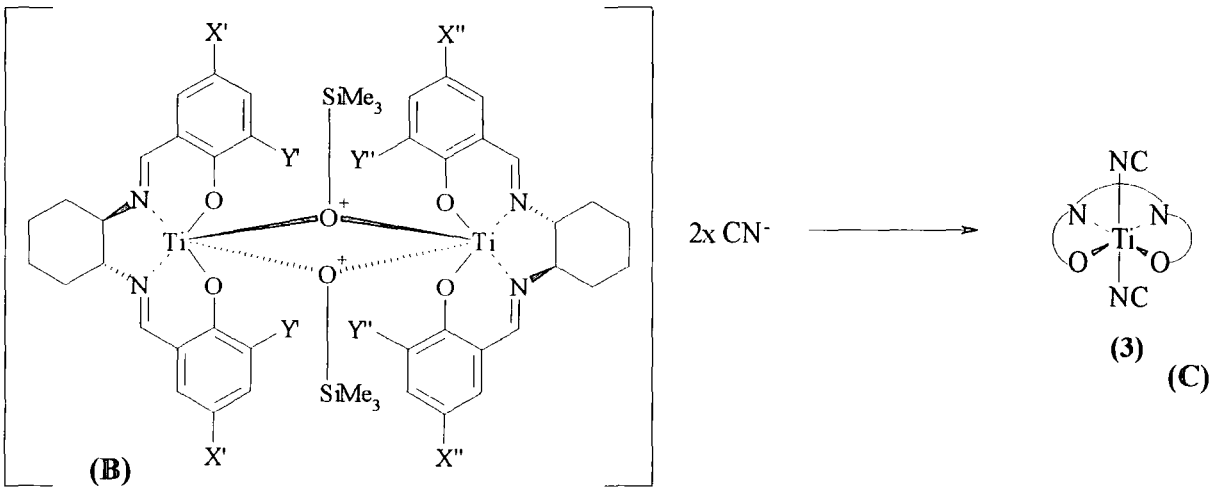

When carrying out the reaction it is necessary to add the aldehyde first since the formation of (**C**) is faster and essentially irreversible.

The association of (**B**) and (**C**) leads to a dinuclear intermediate species bearing both the aldehyde and cyanide. Coordination of the aldehyde is such that the interactions between the aldehyde substituent and the cyclohexane ring of the ligand are minimised. This effectively exposes the *re*-face of the aldehyde to intramolecular attack by the coordinated cyanide yielding the (S)-enantiomer of the product (when using the (R, R) isomer of the catalyst) as described in Scheme 4.7.

Scheme 4.7

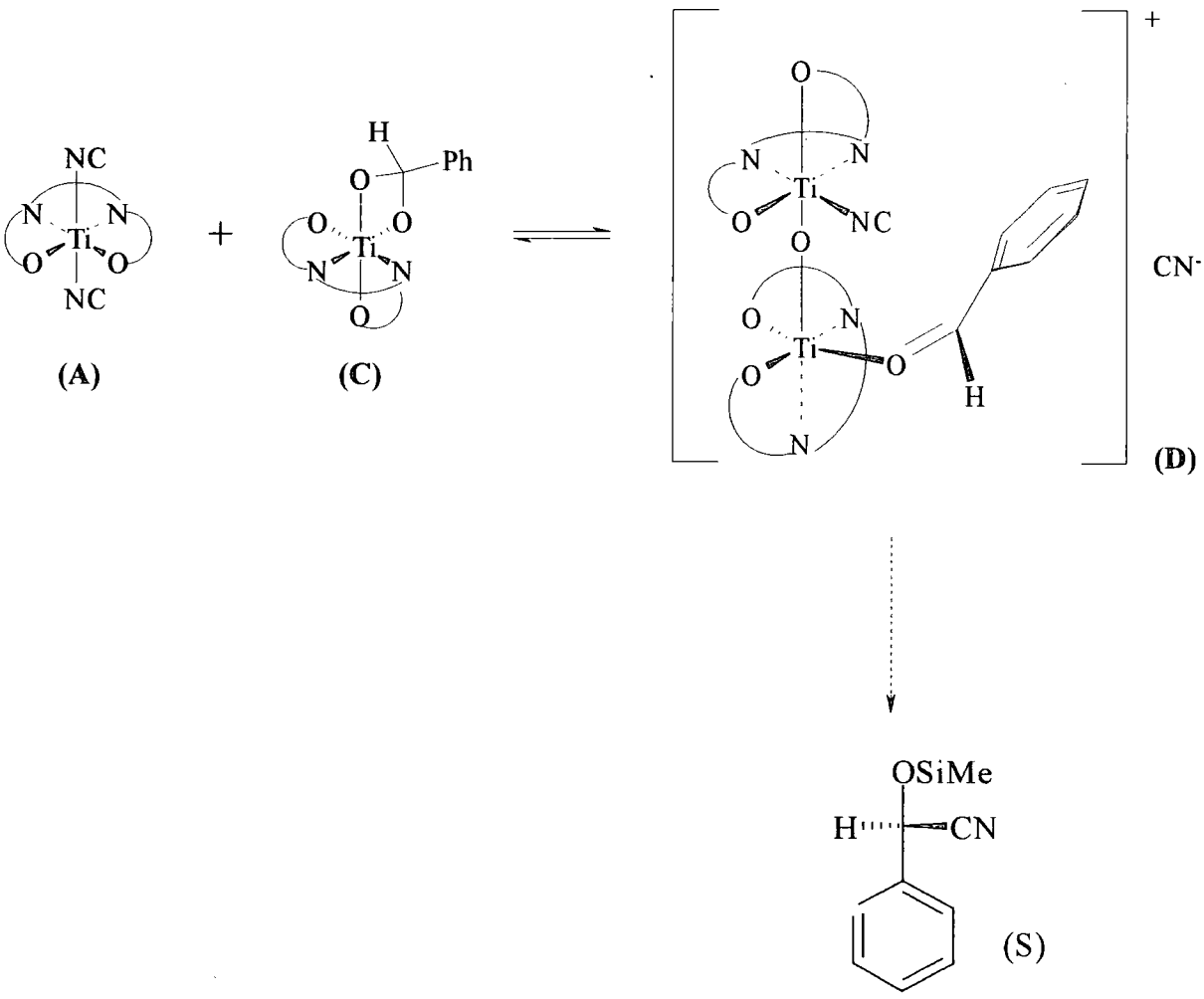

Kinetic studies showed that the dinuclear species is the catalytic form of the complex. The rate-determining step is likely to be the silylation of the coordinated cyanohydrin.

Addition of TMSCN to ketones was also investigated[11]. Although that reaction did not take place in the presence of the monomeric Ti complex, catalysis by the dinuclear species was observed. Acetophenone was converted to the corresponding cyanohydrin trimethylsilyl ether in a 93% yield with 66% enantiomeric excess (Scheme 4.8).

Scheme 4.8

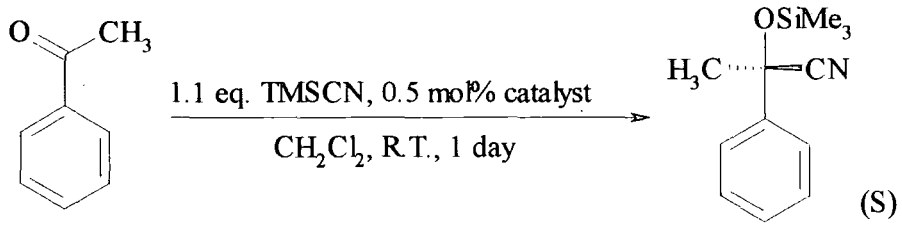

Yield: 93 %
e.e.: 66 %

Moderate to good results were also noted with other aromatic aliphatic ketones provided that the size of the aliphatic groups was not large (i.e. H or Me).

Steric and electronic effects make addition of cyanide to ketones more difficult than the corresponding reaction with aldehydes[12]. As described above, in structure **(D)** the aldehyde is coordinated to one of the Ti atom in such a way that the small hydrogen atom is located near to the cyclohexane unit and the larger substituent is significantly far off the Salen ligand.

In the case of ketones this means that the smaller substituent must be able to fit in the vicinity of the cyclohexane group of the ligand. Consequently only ketones bearing groups such as hydrogen, methyl or ethyl as the smaller substituent are suitable for catalysis by the Ti complex.

However it is worth noting that no reaction was noticed using aliphatic ketones.

A vanadium (IV) Salen complex for the addition of TMSCN to carbonyl compounds has been developed[13].

Oxo-vanadium (IV) Salen complexes have been shown to be either monometallic or polymeric[14].

Results showed that the addition of TMSCN to aldehydes and ketones was catalysed by the V (IV) Salen complex. The rates were found to be slower than with the titanium species (24 hours compared to one hour) but the enantiomeric excesses were higher (Scheme 4.9).

Scheme 4.9

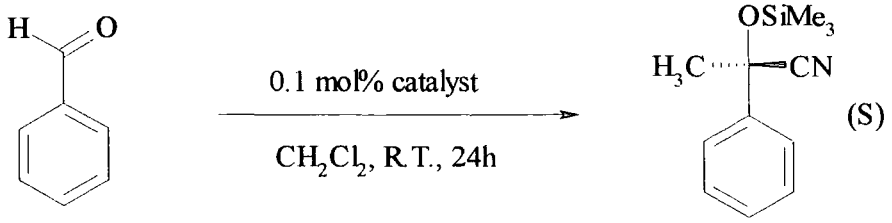

Catalyst:

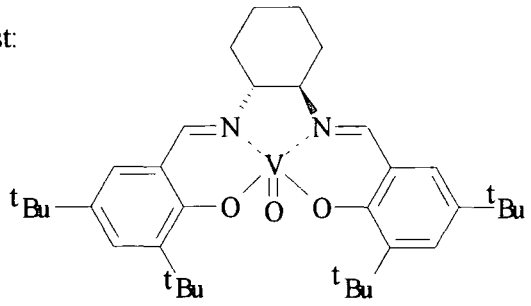

Yield:	100%
e.e.:	94%
e.e. (with Ti complex):	88%

Kinetic results indicated that in the equilibrium between the catalytically active bimetallic species and the catalytically inactive species the formation of the monometallic form was favoured consequently reducing the reactivity and therefore increasing the enantioselectivity.

When KCN is used in place of TMSCN the titanium complex proved more active than its vanadium counterpart[15].

The addition of cyanide to imines was also reported[16]. Sigman and Jacobsen used an Al (III) Salen complex to catalyse the addition of HCN to a series of imines using trifluoroacetic acid to yield the trifluoroacetamides as shown in Table 4.1. The best results were obtained using N-allyl imines.

However it is worth noting that since Jacobsen's work no further studies, neither synthetic nor mechanistic, have been carried out on the addition of cyanide to imines promoted by Salen catalysts.

Table 4.1 Recorded yields and enantiomeric excesses for the addition of HCN to a series of imine using an Al (III) salen catalyst[16]

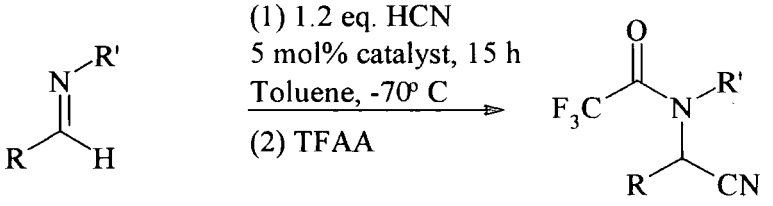

R	R'	% Yield	% e.e.
Ph	Allyl	91	95
p-$CH_3OC_6H_4$	Allyl	93	91
p-$CH_3C_6H_4$	Allyl	99	94
p-ClC_6H_4	Allyl	92	81
p-BrC_6H_4	Allyl	93	79
1-Naphtyl	Allyl	95	93
2-Naphtyl	Allyl	93	93
Cyclohexyl	Allyl	77	57
t-Butyl	Allyl	69	37
t-Butyl	Benzyl	88	49
t-Butyl	p-Methoxybenzyl	67	44
t-Butyl	o-$CH_3OC_6H_4$	74	40

4.1.2 Enantiomeric separation

4.1.2.1 Chiral gas chromatography

Although many methods are available to analytically distinguish enantiomers (chiroptical methods, NMR spectroscopy, chromatography) gas chromatography is the preferred method for quality control in many pharmaceutical and fine chemical applications.

Separation of enantiomers by chromatography can be obtained either indirectly or directly[17]. In the first case the enantiomers to be analysed are derivatised with

enantiomerically pure auxiliaries to form diastereomeric compounds that can subsequently be separated on an achiral stationary phase. With the direct method enantiomers are separated on a chiral stationary phase containing an optical auxiliary in high enantiomeric purity.

Several chiral derivatising agents are available enabling the separation of a wide range of compounds (alcohols, amines, carbonyl compounds, acids etc...). Some examples are shown in Table 4.2.

Table 4.2 Chiral derivatising agents for gas chromatography analysis and example of their use

Chiral derivatising agents	Derivative	Enantiomers
S-(+)-3-Methyl-2-butanol	Ester	N-Methyl-alpha-amino acids
R-(+)-1-Phenylethyl amine	Amide	Secondary alkylcarboxylic acids
S-(-)-Acetyl lactyl chloride	Ester	Cyanohydrins
S-(+)-Methyl-3-iodo-2-methylpropanoate	Ether	Secondary alkanols
1R,4R-(+)-Camphor-10-sulfonyl chloride	Amide	Secondary arylalkylamines

For direct separation, several chiral stationary phases are available. They can be based on amino acids and diamides, metal complexes[18], cyclodextrins[19], cyclocholates[20] or calixarenes[21].

The first chiral phases based on an amino acid derivative for chiral chromatography were developed by Gil-Av and co-workers[22]. They have used N-trifluoroacetyl-L-isoleucine lauryl ester and N-trifluoroacetyl-L-valyl-L-valine cyclohexylester to resolve N-trifluoroacetyl amino acids. The chiral recognition on those columns is based on the formation of multiple hydrogen bonds whereas for phases such as cyclodextrins or calixarenes chiral recognition is partially based on inclusion into the chiral cavities, hydrogen bondings as well as electrostatic and hydrophobic interactions[23].

4.1.2.2 NMR Spectroscopy

The resonances of enantiopic nuclei are isochronous and therefore it is not possible to separate enantiomers in an achiral medium using NMR spectroscopy. However the resonances of certain diastereotopic nuclei are anisochronous yielding a chemical shift non-equivalence[24]. Hence using chiral auxiliaries and converting a mixture of enantiomers into a diastereomeric mixture enables NMR separation[25].

Typically three types of chiral auxiliaries can be used:

- Chiral lanthanide shift reagents
- Chiral solvating agents
- Chiral derivatising agents

The first two reagents can be used directly since they form diastereomeric complexes *in situ*. Chiral derivatising agents on the other hand are used before the NMR analysis. The enantiomeric mixture is reacted with the agent and then the resulting mixture is analysed by NMR spectroscopy.

Of particular interest to our work are the chiral lanthanide shift reagents and a particular chiral derivatising agent, camphorsulfonic acid.

4.1.2.2.1 Lanthanide Shift Reagents (LSR)

The use of lanthanide based complexes to resolve enantiomeric mixtures was first discovered by Hinckley[26]. The experimental technique was later developed by Sutton and co-workers who proved that the method could be used quantitatively to determine the structures present[27].

Transition metals with an unpaired electron are strongly paramagnetic. The lanthanide (III) ions have an electronic configuration [Xe]$4f^n$. Apart from La (III) and Lu (III) that have no unpaired electrons and are diamagnetic the other ions in the series have one to seven unpaired electrons and therefore are paramagnetic[28].

The reagents associate with the non-bonding electrons of the substrate through the metal orbitals. Therefore lanthanide shifts reagents are of use only with compounds bearing non bonding electrons such as amines, alcohols, ethers, aldehydes, ketones, nitriles or epoxides.

The unpaired electron of the lanthanide f orbital associates with the non-bonding electrons of the substrate. This creates an electronic spin density at the nucleus undergoing the coupling and consequently affects the NMR resonance shift of that particular nucleus. It results in a splitting of the signal, known as pseudo-contact shift.

The affinity of the lanthanide shift reagent for the substrate is dependent on the acid character of the metal complex, the donor properties of the substrate and steric requirements[29]. Lanthanide complexes are hard Lewis acids therefore the affinity for the donor sites normally follows the order amine > alcohol > ketone > aldehyde > ester > carboxylic acid > nitrile.

Generally the importance of the shift induced by the chiral lanthanide shift reagent on a particular atom is determined by the distance between the given atom and the nucleus linked to the lanthanide ion. The way the shift is displaced is dependent on the nature of the metal. For example europium (Eu) and ytterbium (Yb) usually move signals to higher shift values (downfield) while praseodymium (Pr) usually has the opposite effect.

Since the ionic salts of the lanthanide metals are not readily soluble in NMR solvents they are derivatised by tris-complexation with enolic β-dicarbonyl compounds such as the examples shown on Scheme 4.10[28].

Scheme 4.10

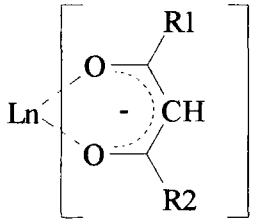

dipivaloylmethane (dpm):	R1 = R2 = ^{t}Bu
heptafluorodimethyloctanedione (fod):	R1 = ^{t}Bu; R2 = -C_3F_7
decafluoroheptanedione (fhd):	R1 = R2 = -C_2F_5

$Eu(fod)_3$ is most commonly used since it is more soluble than other complexes ($Ln(dpm)_3$ for example) and it forms adducts with higher stabilities, due to the electron withdrawing effect of the fluorine atoms[30].

4.1.2.2.2 Camphorsulfonic acid

(E)

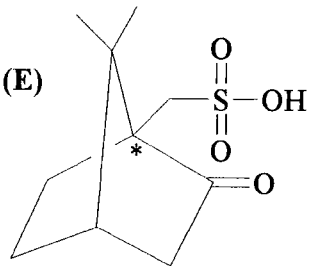

(+)-10-Camphorsulfonic acid **(E)** is used in liquid chromatography as a mobile phase additive for the optical resolution of some amino acids[31]. The amino alcohol in its protonated form combines with the camphorsulfonate by electrostatic interactions to form diastereomeric complexes.

It has also been used in electrophoretic methods to separate barbiturates[32].

However of more interest to the present work is the use of (1R) and (1S)-(-)-10-camphorsulfonic acid as a chiral derivatising agent for aminonitriles[33]. Conveniently the acid was added to the NMR solutions in $CDCl_3$ rather than in a preliminary derivatisation. It resulted in significant shift and split of the signal characteristic of the CHCN proton from one singlet at 4.69 ppm to two signals at 5.25 and 5.41 ppm.

An explanation with regards to the influence of camphorsulfonic acid to enantiomeric separation may be explained when comparing to camphanic acid **(F)**. Camphanic acid has

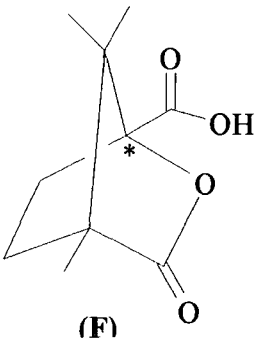

(F)

been used in the determination of the enantiomeric purity of chiral amines[34] and β-amino alcohols[35]. In this case it is the anisotropy of the carbonyl group that leads to differential shielding of the diastereotopic groups[25].

4.2 Results and discussion

Since Sigman and Jacobsen[16] reported the high catalytic activity of the Al (III) Salen complex in the addition of cyanide to imines it was decided in a first instance to reproduce their work and then investigate the mechanism by which the catalyst operates. Another Salen complex based on vanadium (V) was also synthesised and used with the system.

Note that all the syntheses (catalysts, imines and aminonitriles) are detailed in the experimental chapter (Chapter 6, section 6.8).

4.2.1 Addition of trimethylsilyl cyanide (TMSCN) to imines catalysed by Salen complexes: Sigman and Jacobsen's experiment

4.2.1.1 Al (III) Salen complex

Sigman and Jacobsen reported the highly enantioselective addition of HCN to imines in presence of an aluminium (III) salen complex **(1a)** in toluene at -70°C.

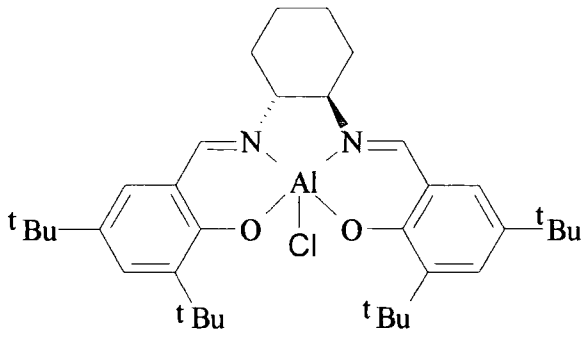

(1a)

Prior to optimisation of the reacting conditions they used **(1a)** at room temperature with TMSCN as the cyanide source to quantitatively convert N-benzylidene allylamine to the

corresponding trifluoroacetamides in a 45% enantiomeric excess (e.e.) in the additional presence of trifluoroacetic anhydride (TFAA) as shown in Scheme 4.11.

Scheme 4.11

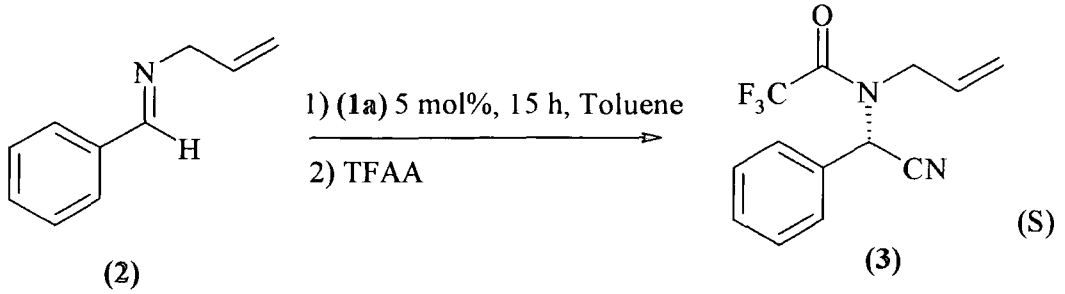

(2) (3)

+ TMSCN, R.T. 100% yield, 45% e.e.

+ 1.2 eq. HCN, -70°C 91% yield (isolated), 95% e.e

The experiment at room temperature was reproduced assuming that 1.2 equivalents of cyanide were added since the quantity is not specified in the manuscript. It is worth noting that the (S,S)- derivative (**1b**) of the salen ligand was used compared to the (R,R)- Salen complex (**1a**) used by Sigman and Jacobsen.

A 91% yield in solution was achieved. A sample was run on a chiral gas chromatography column (chiral GC) but no enantiomeric excess was recorded.

It is worth noting that a sample of the reacting mixture prior to quenching with TFAA was submitted for analysis on GC/MS. The product at that stage was identified as 2-Allylamino-2-phenylacetonitrile (m/z (EI): 171 (M^+)) and not as the TMS derivative (m/z (EI): 244 (M^+)). Although the possibility of decomposition in the column is to be considered it is thought that the aminonitrile was the actual end product.

Kobayashi and co-workers[36] used tributyltin cyanide as the cyanide source for their catalytic asymmetric Strecker synthesis because of its stability in water and the fact it does not produce HCN. According to the authors this is in contrast with TMSCN which can easily hydrolyse to form hydrogen cyanide even in the presence of a small amount of water.

Considering that the solvents used in the present work have not been dried it is reasonable to consider hydrolysis of TMSCN as a likely phenomenon and HCN as a likely reactant.

Alternatively the water present could have potentially hydrolysed the TMS adduct itself to form the aminonitrile.

Further, before the quenching stage the reaction did not go to completion. A low conversion level of 25% was reached. As the experiment was repeated over a longer reaction time (65 hours) the yields before and after quenching although higher showed the same trend as completion was only reached after addition of TFAA. Also worth noting is the fact that although it has been possible to detect the aminonitrile on the GC/MS instrument it does not appear on the chromatograms recorded using the chiral GC. It has therefore not been possible to assess the enantiopurity of the mixture at that stage (Scheme 4.12).

Scheme 4.12

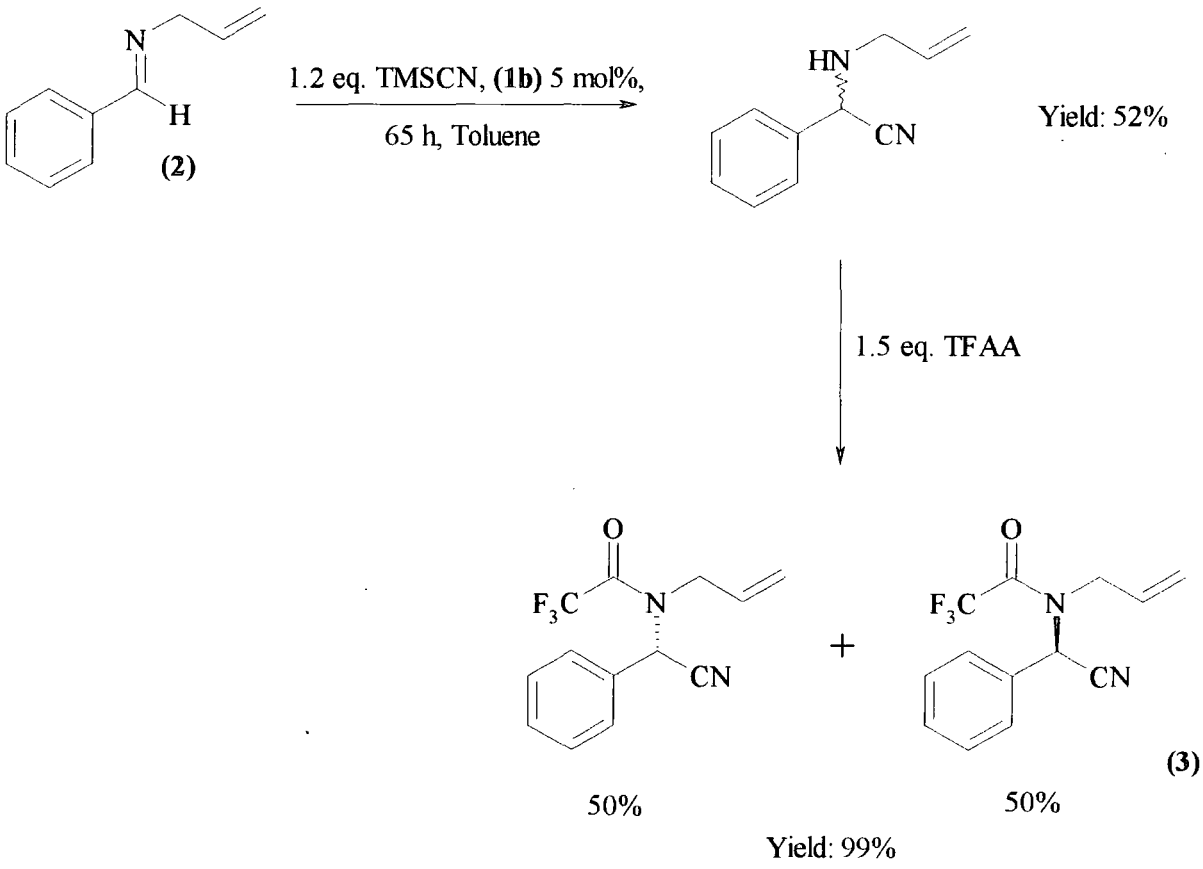

Since Sigman and Jacobsen used the isolated imine for their experiment N-benzylidene allylamine was isolated and the experiment was repeated. Also of interest is the fact the original experiment designed by the authors suggests mixing cyanide with the catalyst in the first instance and then adding the imine.

Following rigorously the above experimental conditions yielded values of 12% conversion to the aminonitrile. After addition of TFAA a conversion of 83% to the trifluoroacetamide was achieved.

In the absence of catalyst an 'intermediate' yield of 27%for the formation of the aminonitrile after 16.5 hours was recorded. After quenching with TFAA 84% of the imine had been converted to the trifluoroacetamide.

Therefore it was not possible to reproduce Sigman and Jacobsen's results. A possible explanation for this conclusion is that the catalyst has not been synthesised properly. Although the ^{1}H NMR spectrum of the product when compared to one of the ligand alone presents significant changes in the chemical shifts it has not been possible to recrystallise the catalyst and get an X-ray structure to confirm the success of the synthesis. Comparison with other ^{1}H NMR spectroscopic data of metal Salen complex (including Al Salen (Et))[37] however suggests that the catalyst was correctly identified and synthesised.

Based on the results from the reaction carried out in the absence of catalyst it appears that the addition of TMSCN to imines in toluene is not favoured. Previous experiments carried out in acetonitrile showed that the reaction goes to completion overnight (See chapter 3). This phenomenon is likely to be due to the presence of water which is less soluble in toluene than in acetonitrile.

Further the present results indicate that the addition of cyanide to the imine is promoted by trifluoroacetic anhydride. Since Sigman and Jacobsen recorded neither any yields nor enantiomeric excesses prior to the addition of TFAA it is not possible to compare these conclusions with their work. However the reaction of TFAA with imines and its possible implications on the addition of cyanide will be further examined in Chapter 5.

4.2.1.2 V (V) Salen complex

A further attempt at using Sigman and Jacobsen's method was carried out using the available vanadium oxide (V) Salen complex, (1c).

Experimentally the procedure was identical as the one used with the aluminium complex to yield (3).

The GC/MS results showed that conversion before quenching with TFAA was 32%. After addition of the anhydride 100% conversion in solution was reached.

A sample of the trifluoroacetamide was submitted on a chiral GC stationary phase. A 50% enantiomeric excess was recorded as shown in Figure 4.1.

Figure 4.1 Enantioseparation of (R) and (S) 2-allyltrifluoroacetamido-2-phenylacetonitriles using CP-Chirasil-Dex-CB (25m x 0.25mm x 0.25µm; toluene, initial T = 120°C for 30 min, final T = 200°C, 10 min ramp)

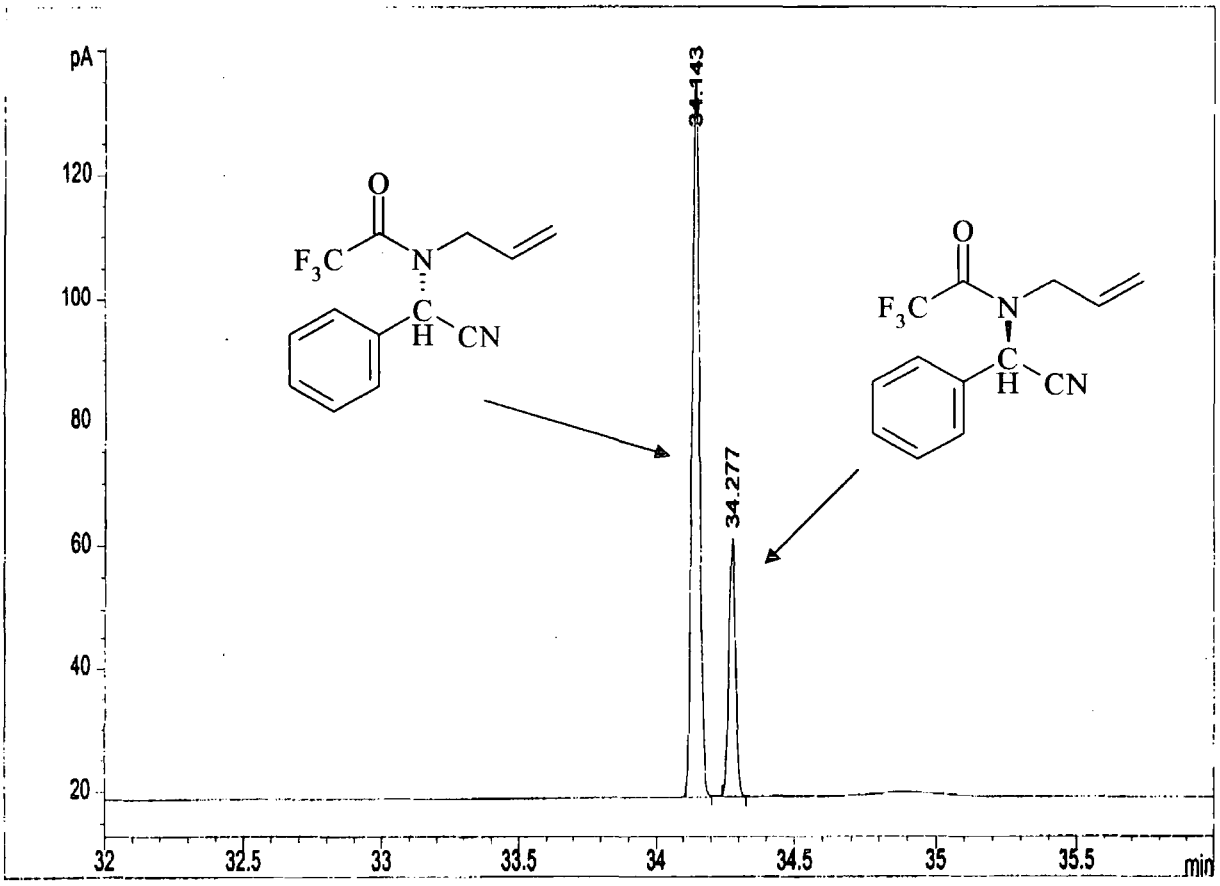

The vanadium (V) Salen catalyst proves to be enantioselective to a satisfactory level. It is worth noting that conversion before quenching again is quite low and that only on addition of the anhydride does the reaction go to completion.

Since the enantiopurity can not be measured be prior to quenching three cases are possible as whether TFAA affects the enantioselectivity of the reaction or not:

- The catalyst yields 100% enantiopure aminonitrile in the absence of TFAA. In this case 32% of the (S) enantiomer would be formed before quenching and on addition of the anhydride the enantioselectivity drops considerably.

- The catalyst is not enantioselective in the absence of TFAA.

- TFAA does not affect the enantioselectivity but increases reactivity.

Further experiments were carried out where samples were taken before completion time in an attempt to understand the influence of TFAA addition on the enantiomeric excess. Consequently three results are possible:

- If the anhydride causes the enantioselectivity to drop then e.e. should increase with time as more reaction time in the absence of TFAA will allow more enantiopure product to be formed.

- If the reaction is not enantioselective in the absence of the anhydride, the e.e. should decrease with time as more racemic product will be formed when the substrate is allowed to react for a longer period of time in the presence of the catalyst.

- If the anhydride does not affect the enantioselectivity but simply increases reactivity the e.e is not expected to evolve with time and a 50% excess should be reported for all samples.

The above described experiments were carried out in the same conditions as the previous ones. However on analysis by chiral GC it was noted that a peak characteristic of the imine (confirmed by GC/MS) was still present after quenching with the anhydride. This is in complete contradiction with the fact that TFAA promotes addition of cyanide to the imine. It was therefore decided only to record enantiomeric excesses with time and discard the

conversions data. Results measured for e.e. for five separate experiments run under the same experimental conditions are given in Table 4.3.

Table 4.3 Reaction of N-benzylidene allylamine with TMSCN (1.2 eq.) in presence of 5 mol% V(V) Salen catalyst at room temperature

1

Time (min)	e.e. %
5	30%
60	32%
1040	27%

2

5	47%
60	46%
3965	46%

3

5	48%
60	46%
120	45%
1200	48%

4

Time (min)	e.e. %
5	50%
120	47%
180	46%
240	45%
1250	45%

5

5	38%
85	47%
120	46%
1130	41%
1210	41%
1325	41%
1540	41%

From those five experiments it is possible to see that, with the exception of experiment 1, the enantiomeric excess does not vary with time, suggesting that TFAA does not have an influence on the enantioselectivity of the reaction. An average value for the e.e. generated by the vanadium (V) salen catalyst for the addition of cyanide to benzylidene allylamine (discarding experiment 1) is 45%.

It is worth noting that the results although consistent are to be considered with care since data collected for the conversion levels have proved unreliable. It therefore underpinned the quantitative use of chromatography as an analytical tool. Calculations for the level of conversion to the trifluoroacetamide using both data from chiral chromatography and GC/MS did not correlate. For the same reactions discrepancies up to 25% were found.

This also suggests that the data recorded for the conversion level before addition of TFAA are not reliable. Hence the theory by which quenching with the anhydride promotes the

reaction and does not affect the enantioselective activity of the catalyst has to be revised. Further a consistent and reproducible method for the determination of both the enantiomeric excess and the conversion levels of the reaction has to be found.

4.2.2 Enantiomeric separation using ^{1}H NMR spectroscopy

4.2.2.1 Chiral lanthanide shift reagents

The addition of TMSCN to N-benzylidene benzylamine was carried out in two NMR tubes to yield benzylamino-2-phenylacetonitrile as a racemate in $CDCl_3$. Signals accounting for the methyl groups of TMSCN, hexamethyldisiloxane (TMS-O-TMS) and trimethylsilanol (TMSOH) were observed as shown in Figure 4.2.

Figure 4.2 ^{1}H NMR spectrum in $CDCl_3$ of benzylamino-2-phenylacetonitrile

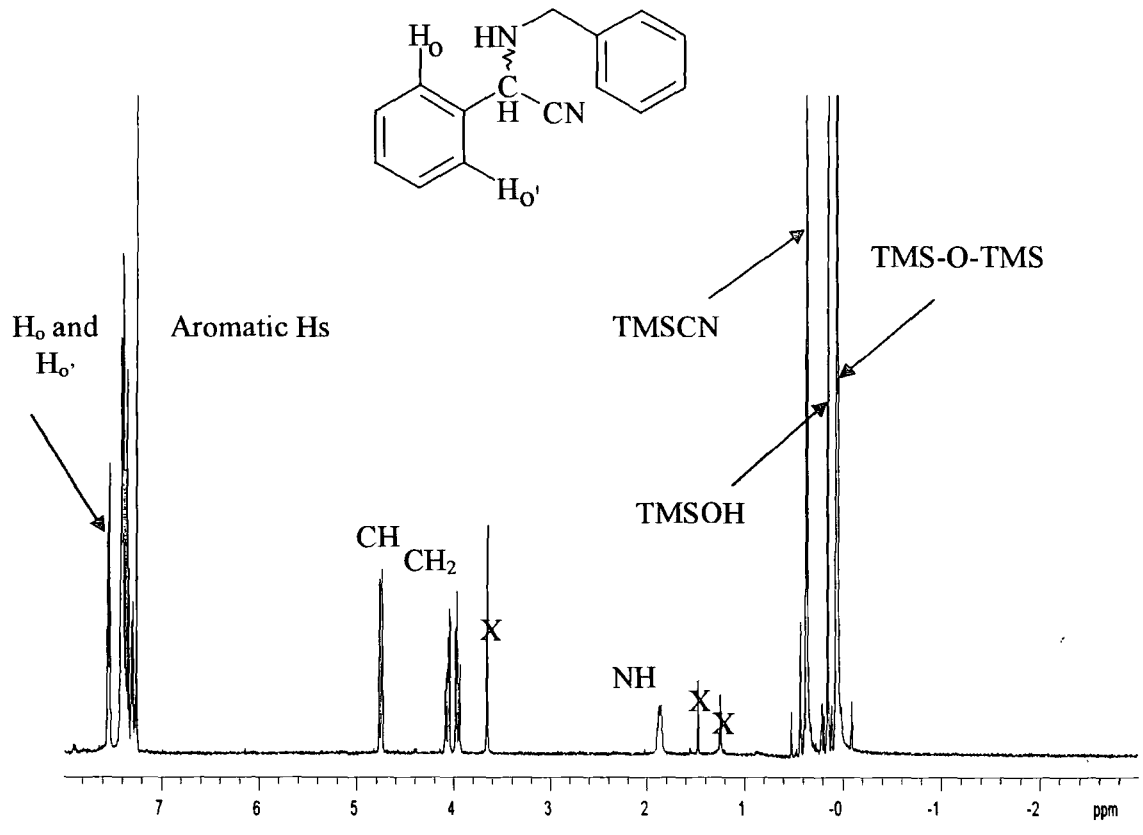

In each of the tubes a chiral lanthanide shift reagent was introduced. It is worth noting that quantitative addition of the reagent was not performed.

The addition of Praseodymiumtris[3-(heptafluoropropylhydroxymethylene)-(+)-camphorate], [Pr(hfc)$_3$], did not enable the resolution of the mixture as shown in Figure 4.3 and Table 4.4.

Figure 4.3 ^{1}H NMR spectrum in $CDCl_3$ of benzylamino-2-phenylacetonitrile with excess [Pr(hfc)$_3$]

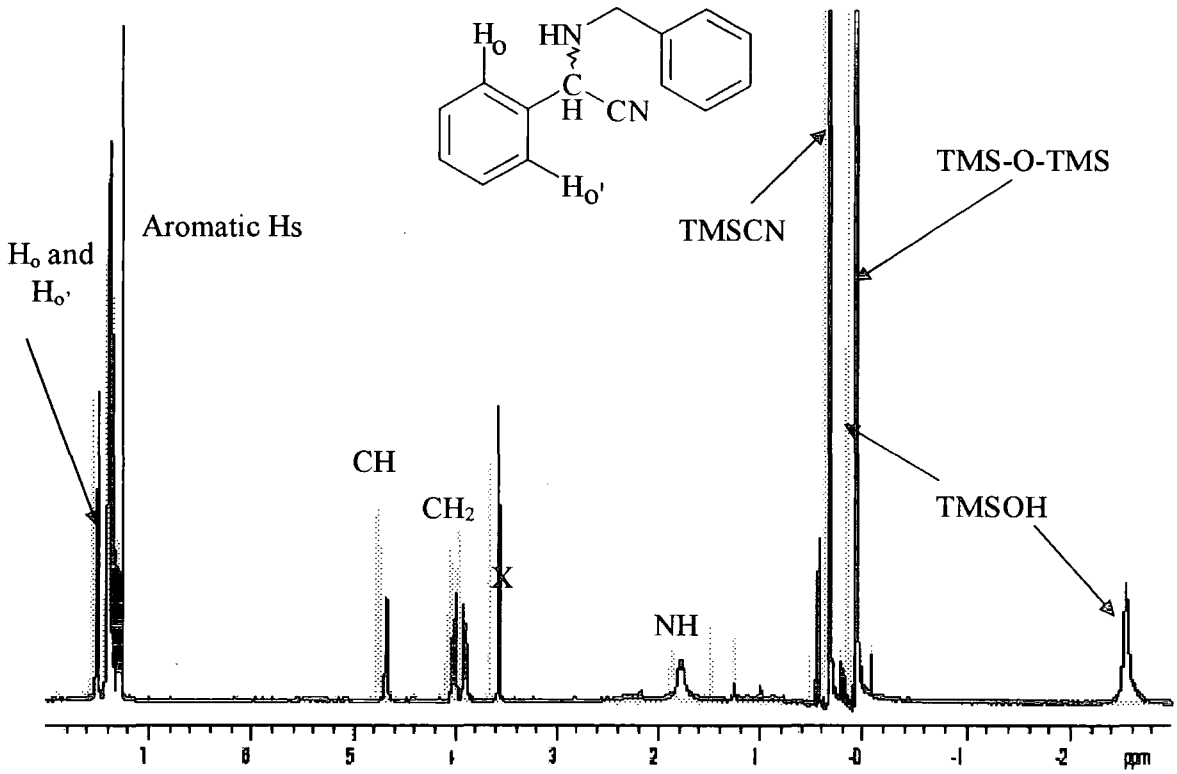

Faded lines: No Pr(hfc)$_3$ (column 1 in Table 4.4);
Black lines: high amount of Pr(hfc)$_3$ (column 4 in Table 4.4)

Interestingly a significant difference in the chemical shift of the TMSOH was noticed suggesting that the chiral lanthanide shift reagent preferably interacted with trimethylsilanol compared to the aminonitrile.

Addition of Europiumtris(6,6,7,7,8,8,8-heptafluoro-2,2-dimethyl-3,5-octanedionate), Eu(fod)$_3$, to the second tube did not provide further resolution as described in Table 4.5

Table 4.4 Evolution of the ^{1}H NMR chemical shifts of benzylamino-2-phenylacetonitrile in $CDCl_3$ with increasing amount of $Pr(hfc)_3$

	No $Pr(hfc)_3$		$Pr(hfc)_3$		More $Pr(hfc)_3$		More $Pr(hfc)_3$	
Protons	Chemical Shift (ppm)	Multiplicity	Chemical Shift (ppm)	Multiplicity	Chemical Shift (ppm)	Multiplicity	Chemical Shift (ppm)	Multiplicity
TMSOTMS	0.06	s	0.07	s	0.08	s	0.07	s
TMSOH	0.15	s	-0.36	broad s	-1.64	broad s	-2.49	broad s
TMSCN	0.37	s	0.37	s	0.35	s	0.32	s
NH	1.88	m	1.88	m	1.84	broad s	1.80	broad s
CH_2	3.96 + 4.07	2x dd	3.95 + 4.07	2x dd	3.93 + 4.05	broad d	3.90 + 4.02	broad d
CH	4.76	d	4.75	d	4.72	broad s	4.68	broad s
Aromatic Hs - (H_o + $H_{o'}$)	7.30-7.43	m	7.22-7.44	m	7.26-7.41	m	7.26-7.40	m
H_o + $H_{o'}$	7.55	d	7.53	d	7.53	d	7.50	d

Table 4.5 Evolution of the ^{1}H NMR chemical shifts of benzylamino-2-phenylacetonitrile in $CDCl_3$ with increasing amount of $Eu(fod)_3$

	No $Eu(fod)_3$		$Eu(fod)_3$		More $Eu(fod)_3$	
Protons	Chemical Shift (ppm)	Multiplicity	Chemical Shift (ppm)	Multiplicity	Chemical Shift (ppm)	Multiplicity
TMSOTMS	0.06	s	0.07	s	0.08	s
TMSOH	0.15	s	1.47	broad s	1.53	broad s
TMSCN	0.37	s	0.51	s	0.60	s
NH	1.88	m	2.05	broad s	2.15	broad s
CH_2	3.96 + 4.07	2x dd	4.09 + 4.15	2x dd	4.14 + 4.22	broad d
CH	4.76	d	4.93	d	5.03	broad s
Aromatic Hs - (H_o + $H_{o'}$)	7.30-7.43	m	7.26-7.46	m	7.26-7.48	m
H_o + $H_{o'}$	7.55	d	7.63	d	7.59	d

Again with $Eu(fod)_3$ the only significant change in terms of chemical shifts concerns the signal for the methyl groups of TMSOH which is moved downfield

Chiral lanthanide shift reagents do not prove a useful tool for the enantiomeric resolution of chiral aminonitriles.

J. C. Jochims[33] and co-workers reported the synthesis of optically active α-aminonitriles by asymmetric transformation of the second kind using a principle of Otto Dimroth. While investigating the enantiomeric purity of the products by ^1H NMR they also noted that no, or at best minor, shift difference for the resolution of racemic aminonitriles in $CDCl_3$ in the presence of chiral europium shift reagents.

The method they used to obtain enantiomeric resolution is that of derivatising the aminonitriles in solution in $CDCl_3$ with (1R)- or (1S)-camphorsulfonic acid. In the case of racemic 2-benzylamino-2-phenylacetonitrile in $CDCl_3$ two signals of equal intensities were observed for H-C-CN at 5.25 and 5.41 ppm. This compares to the signal observed at $\delta = 4.69$ ppm in the absence of the acid.

4.2.2.2 Camphorsulfonic acid

2-Benzylamino-2-phenylacetonitrile was prepared according to a literature procedure using a fast and solventless method and isolated as a chloride salt[38] as shown in Scheme 4.13.

Scheme 4.13

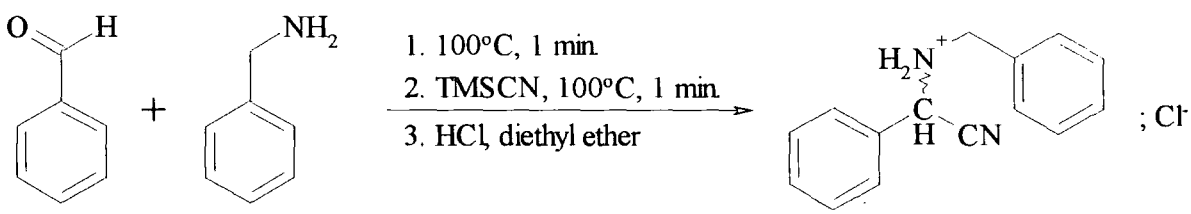

(4a), 46% yield

The product was dissolved in $CDCl_3$ (Figure 4.4) and (1R)-(-)-camphor-10-sulfonic acid added (Figure 4.5). Of particular interest is the observation that the salt does not dissolve readily in $CDCl_3$ but that addition of the camphorsulfonic acid increases solubility.

Figure 4.4 ^{1}H NMR spectrum in $CDCl_3$ of benzylamonium-2-phenylacetonitrile chloride

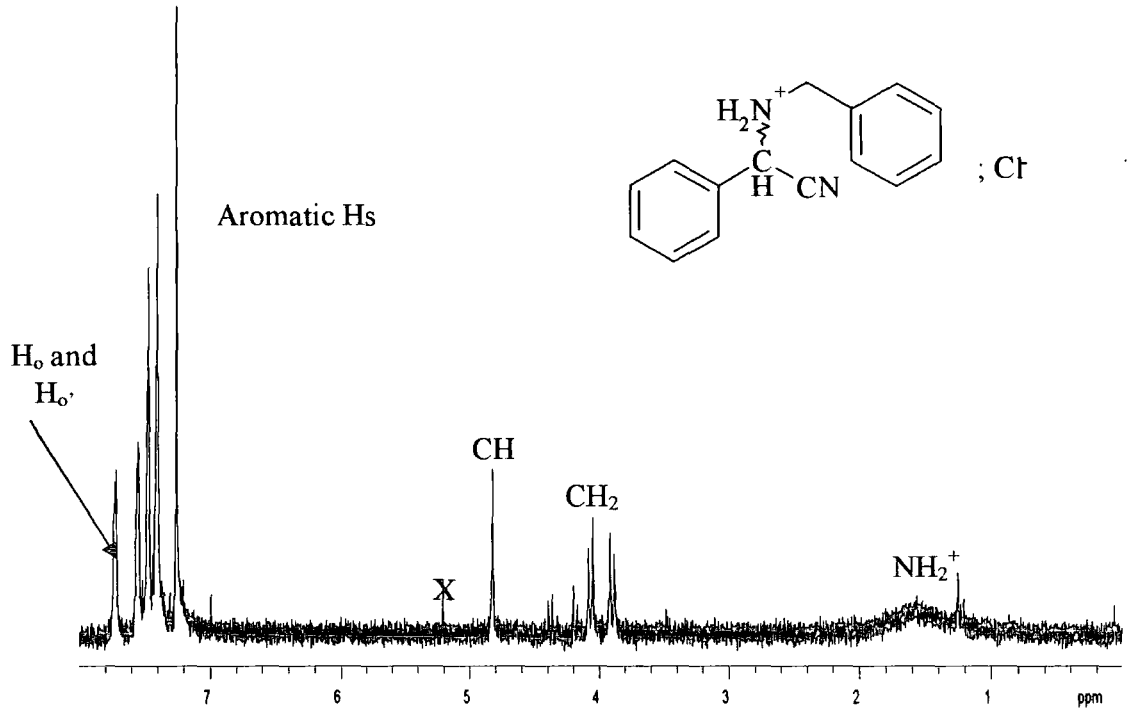

Figure 4.5 ^{1}H NMR spectrum in $CDCl_3$ of benzylamonium-2-phenylacetonitrile chloride in the presence of camphorsulfonic acid

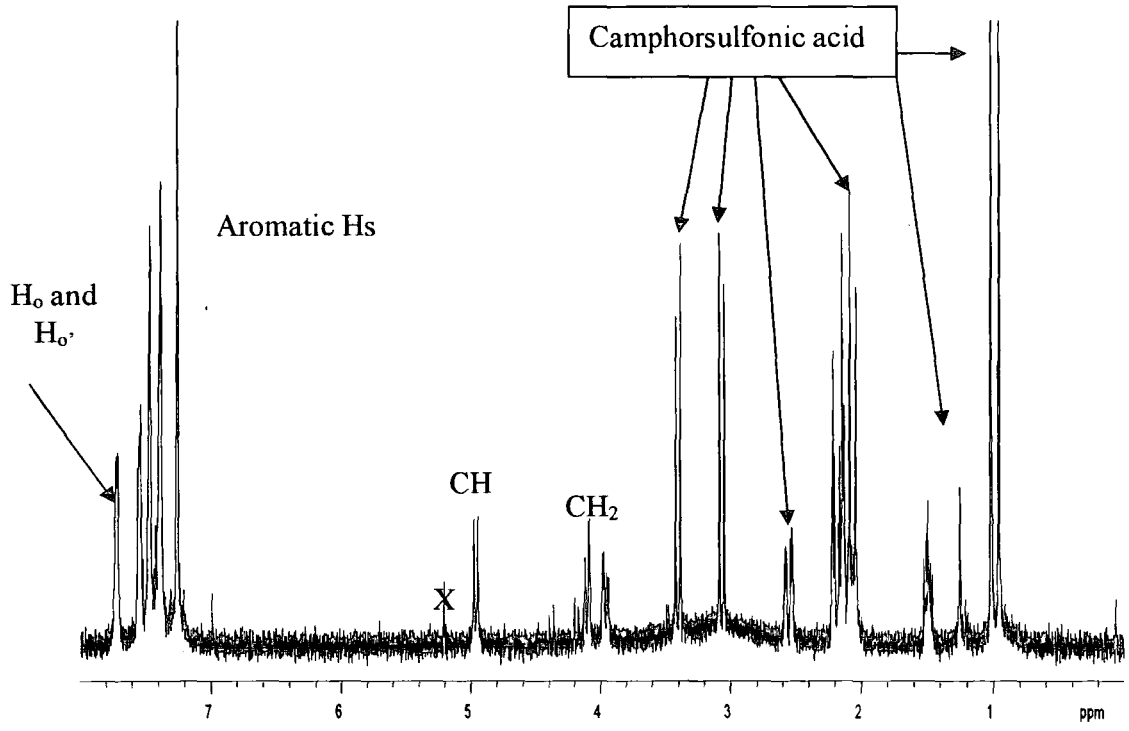

Addition of camphorsulfonic acid resulted in a significant resolution of the CHCN proton from a singlet at 4.83 ppm to two signals of equal intensity at 4.98 and 4.95 ppm as shown on Figure 4.6 where the region around $\delta = 5.00$ ppm is expanded.

Figure 4.6 ^{1}H NMR spectrum in $CDCl_3$ of benzylamonium-2-phenylacetonitrile chloride in the presence of camphorsulfonic acid, expansion of the region around $\delta = 5.00$ ppm

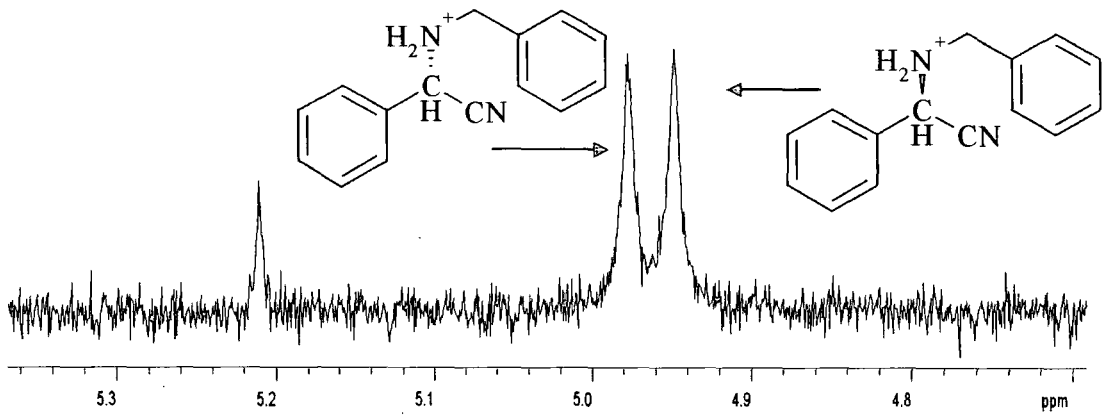

On addition of more acid an even more significant resolution was achieved with two signals observed at 5.17 and 5.10 ppm (Figure 4.7).

Figure 4.7 ^{1}H NMR spectrum in $CDCl_3$ of benzylamonium-2-phenylacetonitrile chloride in the presence of more camphorsulfonic acid, expansion of the region around $\delta = 5.00$ ppm

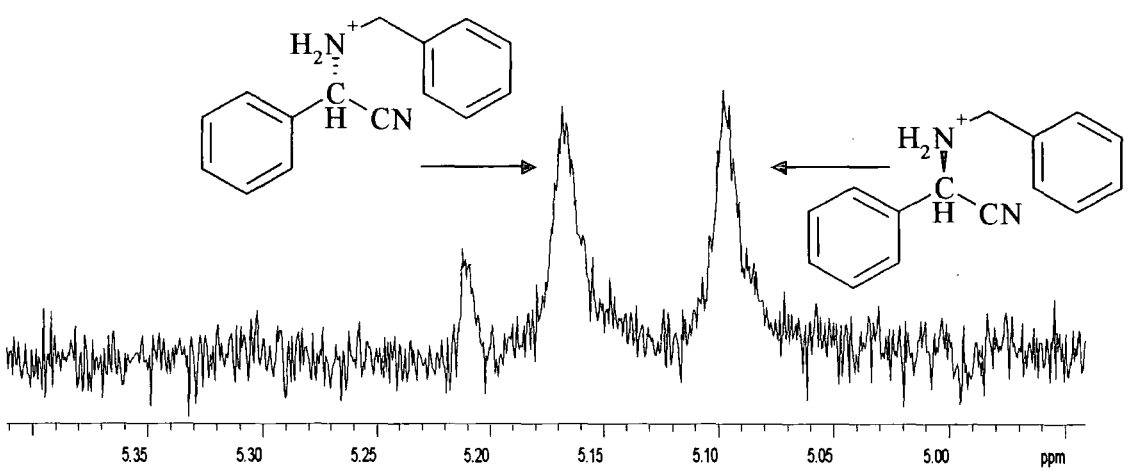

Since the reaction was carried out in the absence of any catalyst a racemic mixture was expected, hence two signals of equal intensities.

Jochims and co-workers recorded the ^1H NMR spectrum of (S)-2-Benzylamino-2-phenylacetonitrile in presence of (1R)-camphor-10-sulfonic acid and compared it to the one of a racemic mixture of (R)- and (S)- 2-benzylamino-2-phenylacetonitrile. In the racemic mixture two signals of equal intensities are observed at 5.25 and 5.41 ppm whereas the (S) derivative only gives rise to one signal at 5.40 ppm. Therefore it is possible to assign the enantiomers using ^1H NMR spectroscopy and camphorsulfonic acid since the more downfield signal can be attributed to the (S) enantiomer.

The reaction of N-benzylidene allylamine with TMSCN in toluene in the presence of the vanadium (V) salen catalyst has been studied in the previous part. Results indicated the enantioselective properties of the catalyst. However the irreproducibility of the chromatographic method did not allow for reliable calculations of the enantiomeric excess.

Furthermore attempts to use hydrogen chloride in ether and camphorsulfonic acid to resolve the enantiomeric mixture of 2-allylamino-2-phenylacetonitriles did not prove successful. Indeed the signal characteristic of the C<u>H</u>CN proton is shifted by the addition of the acid but unfortunately it overlaps with the allyl CH=C<u>H</u>$_2$ peaks and resolution is not possible. The above experiment was therefore repeated using N-benzylidene benzylamine as the substrate.

It was also noted that the addition of few drops of d_4-methanol in $CDCl_3$ increased the solubility of the chloride salt.

4.2.3 Addition of trimethylsilyl cyanide (TMSCN) to N-benzylidene benzylamine in the presence of the vanadium (V) salen catalyst

Once a reliable method for determining the e.e. of the product had been found the catalysis could be studied more quantitatively. A number of variables were examined.

a) TMSCN was added to N-benzylidene benzylamine in the presence of the vanadium (V) salen catalyst in toluene. Since Sigman and Jacobsen[16] reported that no reaction was observed under strictly anhydrous conditions the influence of added water was studied.

b) Catalysed reactions are known to give optimum results at an optimum catalyst concentration, below which the catalytic activity is reduced and above which catalyst poisoning can occur and affect both the catalysis and the enantioselectivity. Hence the influence of the catalyst concentration on the reaction was studied.

c) Since the product is isolated by acidifying the reaction medium, the only yields and enantiomeric excesses available are those of the isolated salt. A possibility exists that acidification promotes the protonation of unreacted imine and therefore addition of cyanide. In this case the enantiomeric excesses recorded could be those of the catalysed reactions added to the acid catalysed racemic additions. The evolution of enantiomeric excess with reaction time was therefore studied.

d) The influence of the temperature on the enantioselectivity is also reported.

e) Finally four other salen catalysts were used in the addition of TMSCN to N-benzylidene benzylamine. First of all the Al (III) salen complex used earlier and suggested by Sigman and Jacobsen was tried. The titanium (IV) and vanadium (IV) catalysts used by North and Belokon for the addition of TMSCN to aldehydes and ketones were also investigated.

Overall the experimental procedure for the addition of TMSCN to N-benzylidene benzylamine can be represented by Scheme 4.14:

Scheme 4.14

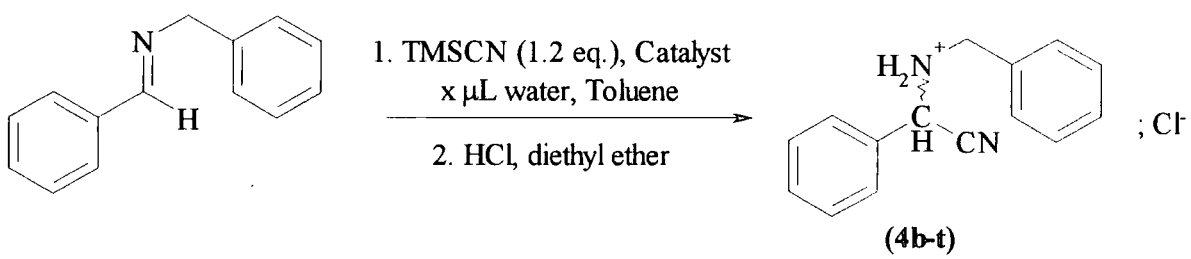

(4b-t)

It is worth noting that each of the individual experimental procedures for the syntheses of **4b-t** is reported in Section 6.8 of Chapter 6.

A specimen spectrum of the separation achieved on **4b-t** is represented on Figure 4.8.

Figure 4.8 ^{1}H NMR spectrum in $CDCl_3$ of benzylamonium-2-phenylacetonitrile chloride in the presence of camphorsulfonic acid

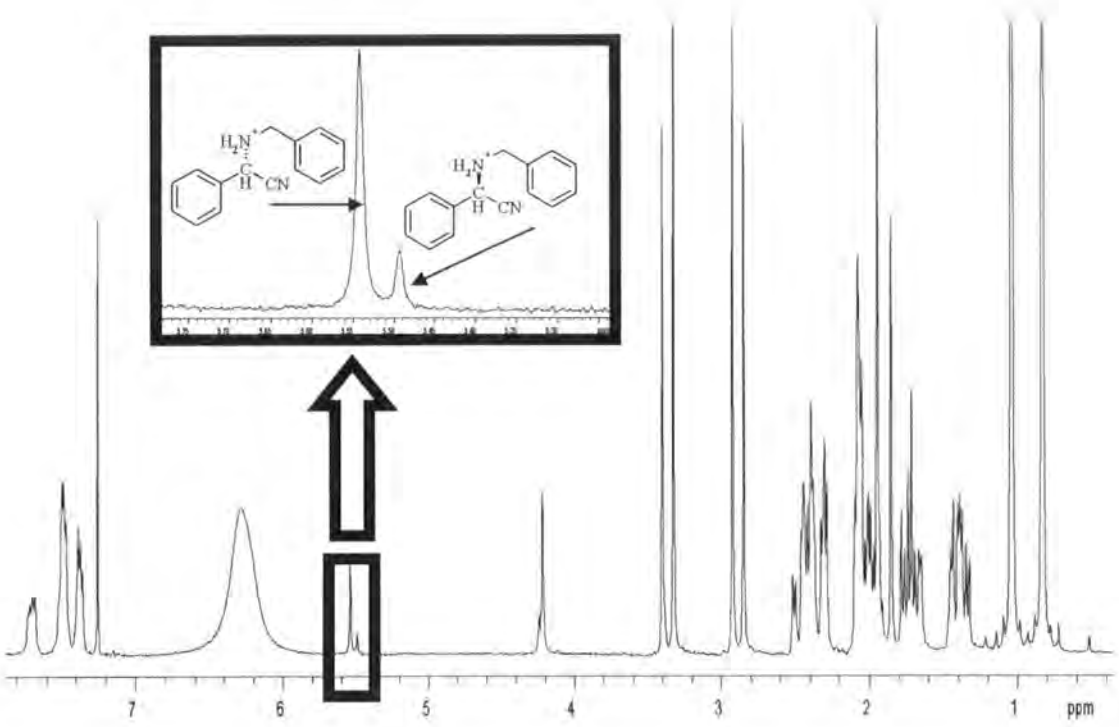

4.2.3.1 Influence of water

Scheme 4.15

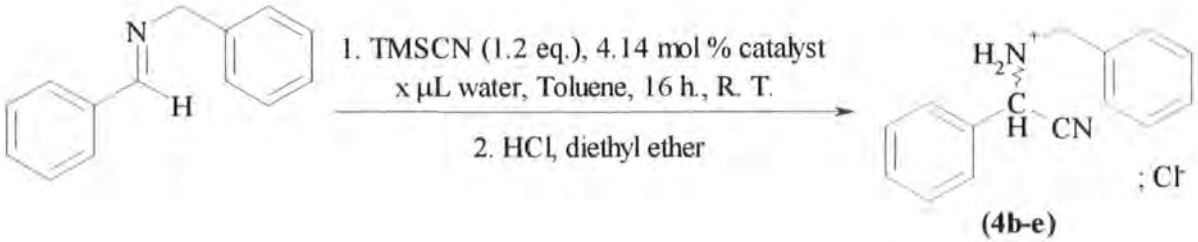

(4b-e)

The amount of water added to the reaction has been varied. However it is important to note that the solvent used has not been dried and therefore the water volumes quoted do not represent the exact amount of water present in the reaction. Furthermore the catalyst itself bears a molecule of water which can also be involved in the catalytic process.

Results are presented in Table 4.6.

Table 4.6 Evolution of the yields and enantiomeric excesses recorded for the synthesis of benzylamonium-2-phenylacetonitrile chloride (TMSCN (1.2 eq.), 4.14 mol% catalyst, toluene, 16 h, R.T.) with varying amount of water

	Water ($x10^{-3}$ cm^3)	Water (vol%)	Yield	e.e.
4b	10	0.05	74%	61%
4c	20	0.10	93%	64%
4d	30	0.15	100%	61%
4e	40	0.20	100%	62%

Addition of water increases the yield although since it is the salt which is collected no data on the actual yield of the aminonitrile is available. In terms of enantiomeric excess it appears that the optimum enantioselectivity is achieved when adding 20μL of water to the medium. However the significance of this number is to be taken carefully since the standard deviation between the enantiopurity of the four products is only 1.4%. This probably better compares with experimental errors rather than actual influence of water on the enantioselectivity. It may be noted that the solubility of water in toluene[39] is ca 0.05% at 25°C, although the presence of solutes may increase solubility.

Nevertheless in the next experiments the amount of water added has been fixed at 0.10 vol% (20 μL in 20 cm^3 of toluene).

4.2.3.2 Influence of catalyst concentration

Scheme 4.16

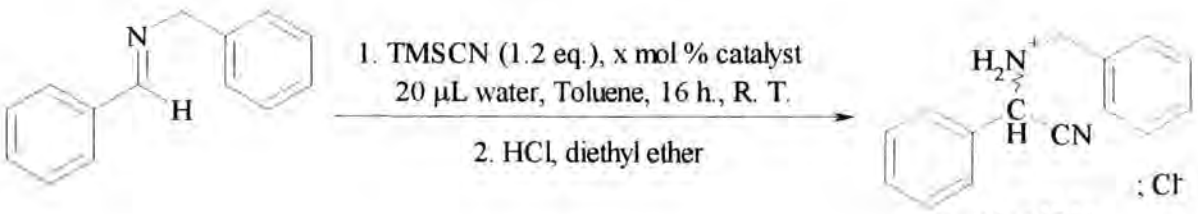

(4c+4f-h)

Variations of the yield and enantiomeric excess according to the catalyst concentration are reported in Table 4.7.

Table 4.7 Evolution of the yields and enantiomeric excesses recorded for the synthesis of benzylamonium-2-phenylacetonitrile chloride (TMSCN (1.2 eq.), 20 µL water, toluene, 16 h, R.T.) with varying amount of catalyst

	Catalyst ($x10^{-3}$ g)	Catalyst (mol %)	Yield	e.e.
4c	31.3	4.14	93%	64%
4f	36.3	4.81	104%	69%
4g	43.3	5.74	89%	62%
4h	50.8	6.73	100%	56%

Values collected for the different yields do not seem to show any dependence on the catalyst concentration. Again since the data recorded are for the salt it is not possible to account for an effect of the catalyst concentration on the aminonitrile formation. The enantiomeric excess on the other hand indicates that a concentration of 4.81 mol% in catalyst leads to more enantioselectivity. Even if considering the experimental error linked to the integration of the peaks in the NMR spectrum it seems reasonable to consider 4.81 mol% as an enantioselectively optimum concentration for the catalyst. This amount will be therefore used in the following experiments.

4.2.3.3 Influence of time

Scheme 4.17

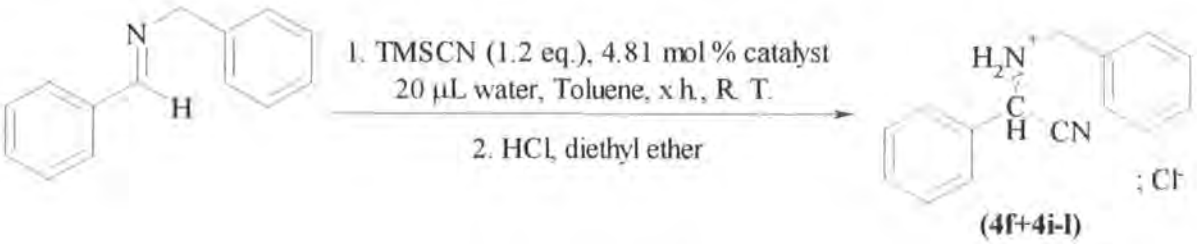

(4f+4i-l)

Rather than taking a sample after a given time and proceed through the acidification step the reactions were carried out individually for a fixed amount of time and the salt isolated. The yields and enantiomeric excesses are collected in Table 4.8.

Table 4.8 Evolution of the yields and enantiomeric excesses recorded for the synthesis of benzylamonium-2-phenylacetonitrile chloride (TMSCN (1.2 eq.), 20 µL water, 4.81 mol% catalyst, toluene, R.T.) with varying reaction time

	Time (h)	Yield	e.e.
4i	2	85%	52%
4j	3	77%	66%
4k	4	89%	69%
4l	6	77%	66%
4f	16	69%	69%

The enantiomeric excess increases with time to reach a maximal value after 3-4 hours. The value of 69% recorded after 4 hours compares to the one reported after 16 hours. Considering that acidification using HCl is likely to promote the racemic background reaction it is possible to confirm that the reaction goes to completion after 3 to 4 hours. Indeed the overall enantiomeric excess of a reaction is a consequence of the competition between the catalysed and uncatalysed reaction. If the reaction has not reached completion before HCl is added then the acid will racemically catalyse the addition of TMSCN to the unreacted imine,

therefore decreasing the enantiomeric excess. A stable value on the other hand indicates that the acid only reacts with the aminonitrile to form the salt without affecting the e.e..

The optimum reaction time for the addition of TMSCN to N-benzylidene benzylamine at room temperature using 4.81 mol% catalyst and 20μL of water in toluene is 4 hours.

4.2.3.4 Influence of temperature

Scheme 4.18

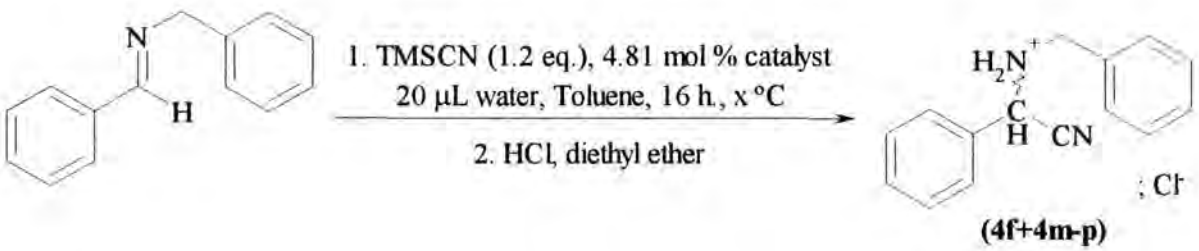

(4f+4m-p)

In the results summarised below (Table 4.9) the reaction time is 16 hours for all but one sample, 4m. The reaction at 0°C was run for 10 hours.

Table 4.9 Evolution of the yields and enantiomeric excesses recorded for the synthesis of benzylamonium-2-phenylacetonitrile chloride (TMSCN (1.2 eq.), 20 μL water, 4.81 mol% catalyst, toluene, 16 h) with varying temperature

	Temperature (°C)	Yield	e.e.
4f	25	69%	69%
4m	0	89%	73%
4n	-10	74%	76%
4o	-20	77%	79%
4p	-30	85%	80%

Lowering the temperature clearly enhances the enantioselectivity. It appears from the results above that at temperatures of -20°C and -30°C 80% enantiopure aminonitriles can be obtained. Since lowering the temperature also affects the rate of the reaction it is however

possible that both those values could be higher had the reaction not reached completion when acidified. This obviously applies to all the experiments carried out at 0°C and below.

4.2.3.5 Other Salen catalysts

Scheme 4.19

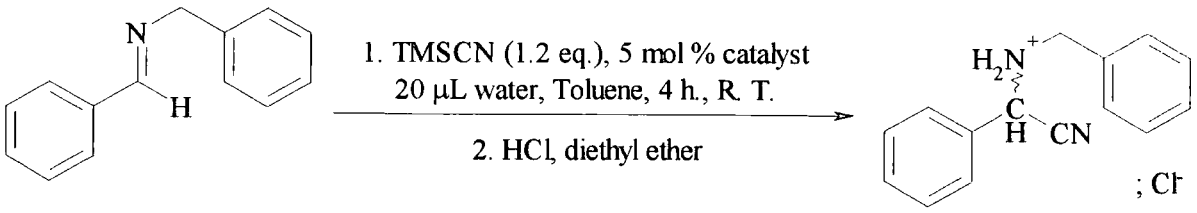

(4k+4q-t)

The reaction was performed using 5 mol% of four different catalysts (Scheme 4.20) and compared to the results gained with 4.81 mol% of the vanadium (V) catalyst (Table 4.10).

Scheme 4.20

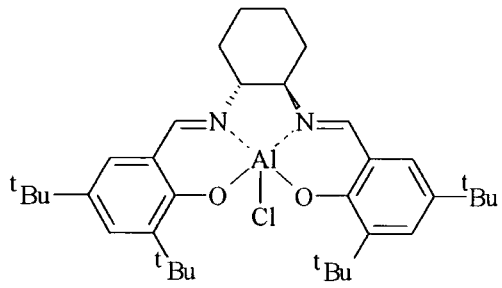

q

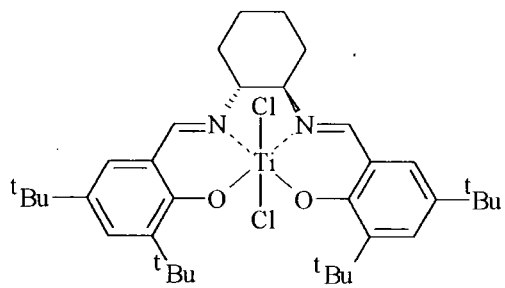

r

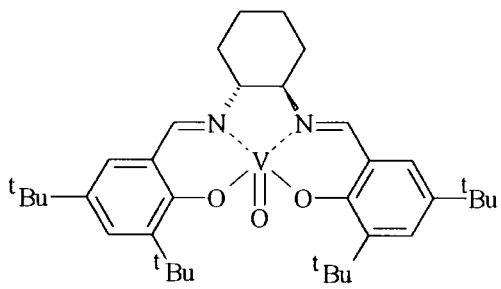

s

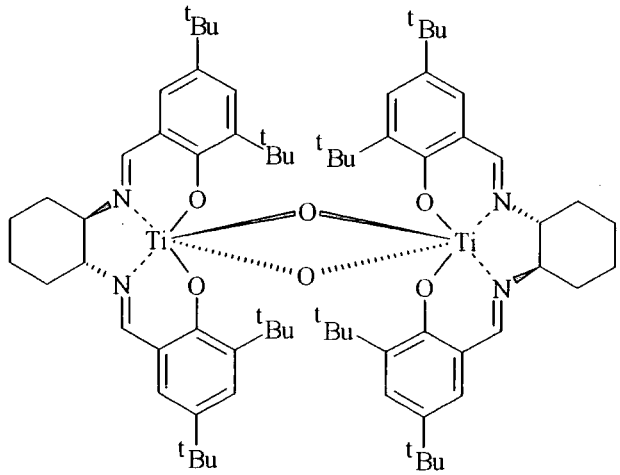

t

Table 4.10 Evolution of the yields and enantiomeric excesses recorded for the synthesis of benzylamonium-2-phenylacetonitrile chloride (TMSCN (1.2 eq.), 20 µL water, 5 mol% catalyst, toluene, 16 h, R.T.) with varying catalysts

	Catalyst	Yield	e.e.
4k	V(V)	89%	66%
4q	Al(III)	27%	< 5%
4r	Ti (monomer)	93%	43%
4s	V(IV)	81%	< 5%
4t	Ti (dimer)	89%	54%

Of all the catalysts used the V (V) salen complex is the most enantioselective. The results gained using the Al (III) salen complex confirms the previous data collected using chiral chromatography as the mixture is virtually racemic. The other catalysts have been reported[7-13, 15] to be particularly enantioselective in the addition of TMSCN to carbonyl compounds with the dimeric titanium salen complex being the more active form of the catalyst when titanium was chosen as a metal core. According to our results although presenting enantioselective properties the titanium complexes yield a lower e.e. than when using the vanadium (V) complex. A moderately higher enantiopurity was recorded when using the dimeric species compared to the monomeric one. As for the vanadium (IV) complex although it proved to be a very enantioselective catalyst for the reaction of cyanide with carbonyl compounds, in the case of imines no significant enantioselectivity was gained.

4.3 Conclusions

Catalysts based on Salen ligands have been used for a wide range of reactions. Notably, North and Belokon[7-13, 15] used titanium and vanadium derivatives to asymmetrically catalyse the addition of cyanide to carbonyl compounds. Later Sigman and Jacobsen[16] reported the enantioselective formation of aminonitriles from imines using an aluminium (III) salen complex.

Addition of cyanide (from TMSCN) to N-benzylidene allylamine using (S,S)-N,N'-bis(3,5-di-*tert*-butylsalicylidene)-1,2-diaminocyclohexane-aluminium (III) chloride was performed since Sigman and Jacobsen reported complete conversion to the corresponding trifluoroacetamide, after quenching with trifluoroacetic anhydride (TFAA) and a 45% e.e. at room temperature. The experiments carried out were analysed by chiral chromatography and GC/MS.

The results did not confirm Sigman and Jacobsen's data and only racemic mixtures of 2-allyltrifluoroacetamido-2-phenylacetonitrile were identified.

It has not been possible to fully explain the difference between our results and those published. The only sensible explanation seems to be that the synthesis of our catalyst did not meet the require end product. Data from elemental analysis indicate a discrepancy between the calculated percentages and the ones found as shown in Table 4.11.

Table 4.11 Found and calculated elemental analysis results for the aluminium catalyst

	Percentage			
Element	Monomer (**1a**) Calculated	Dimer (**H**) Calculated	Dichloride (**I**) Calculated	Found
C	71.2%	69.3%	67.3%	67.4%
H	8.6%	8.5%	8.1%	8.5%
N	4.6%	4.5%	4.4%	4.3%
Cl	5.9%	5.7%	11.0%	7.3%
Al	4.5%	4.3%	4.2%	4.7%

Other likely structures have been included in the table. Since the ^{1}H NMR spectrum analysis appears to confirm that the Al (III) salen has been synthesised and that all signals are assigned, the only possibilities for another structures must be similar to that of (S,S)-N,N'-bis(3,5-di-*tert*-butylsalicylidene)-1,2-diaminocyclohexane-aluminium (III) chloride. Therefore the dimeric species and the dichloride complex can be considered (Scheme 4.21).

Scheme 4.21

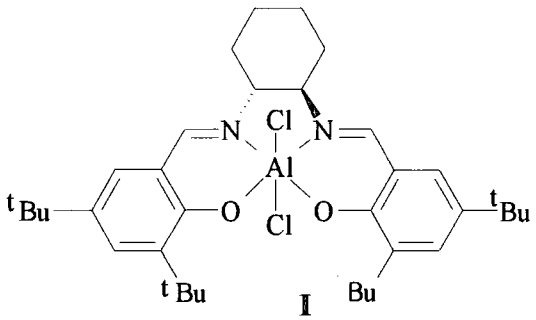

I

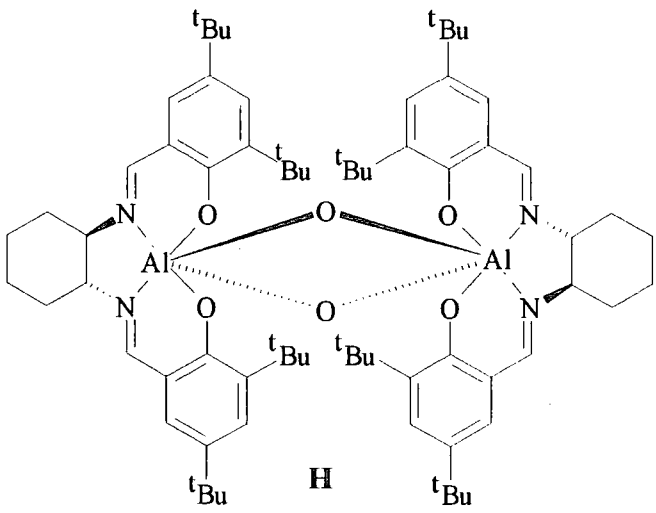

II

Data from the elemental analysis seem to indicate that the dichloride is more likely although the calculated chlorine content is lower.

Unfortunately it has not been possible to recrystallise our sample therefore a determination of the exact structure by X-ray crystallography could not be performed.

Therefore it is only possible to account for the difference between our results and those of Sigman and Jacobsen by assuming that the dichloride structure depicted above has been wrongly synthesised. Moreover, if it is the case this complex does not result in any enantioselective separation.

Changing the catalyst to the (R,R)-vanadium (V) salen complex proved to generate an enantiomeric excess of the (S)- 2-Allyltrifluoroacetamido-2-phenylacetonitrile. However analysis using chiral GC and GC/MS proved unreliable since reproducibility could not be achieved. Even though a value of 45% e.e. was gained using the method the discrepancies between the conversion data suggest that the number is to be considered with care.

Furthermore derivatisation using TFAA appeared to affect the conversion level. Extended investigation of the reaction of the anhydride with imines will be carried out in the next chapter.

An alternative method for enantiopurity determination is the use of chiral lanthanide shift reagents. $Pr(hfc)_3$ and $Eu(fod)_3$ have been used with 2-benzylamino-2-phenylacetonitrile in $CDCl_3$. The use of those two reagents did not provide resolution of the mixture. Noteworthy is the fact that the lanthanide reagent induced a significant displacement of the signal accounting for TMSOH. It appears that the reagent has more affinity for trimethylsilanol than for the aminonitriles. This is in good agreement with the affinity order (amine > alcohol > ketone > aldehyde > ester > carboxylic acid > nitrile) reported in the literature[29].

Jochims and co-workers[33] additionally reported on the inability of $Eu(fod)_3$ of separating 2-benzylamino-2-phenylacetonitrile and used instead (1R)- or (1S)-camphorsulfonic acid. Addition in situ of the acid provides for a displacement of the C<u>H</u>CN proton as well as the formation of a pseudo contact shift (splitting of the signal).

Also a solventless method[38] for the synthesis of aminonitriles was reproduced. The experimental procedure proved dangerous and could not be reproduced in its entirety. However it allowed the isolation of the product as a salt. Subsequent dissolution of the salt in $CDCl_3$ (promoted by MeOD) and addition of camphorsulfonic acid enabled chiral resolution.

Nevertheless attempts to use the above described procedure to characterise the product of reaction between TMSCN and N-benzylidene allylamine could not be achieved. Indeed the displacement caused by the addition of camphorsulfonic acid caused the proton of interest (C<u>H</u>CN) to be overlapped by another signal. N-benzylidene benzylamine was used and an account of the enantioselectivity generated by the vanadium (V) salen catalyst could be given.

The vanadium (V) salen catalyst is significantly enantioselective. At room temperature an e.e. of 69% has been recorded.

Optimal conditions proved to be ones using 4.81 mol% catalyst in the presence of 20μL water. No further enantioselectivity was gained after 4 hours of reaction. The reaction is represented in Scheme 4.22.

Scheme 4.22

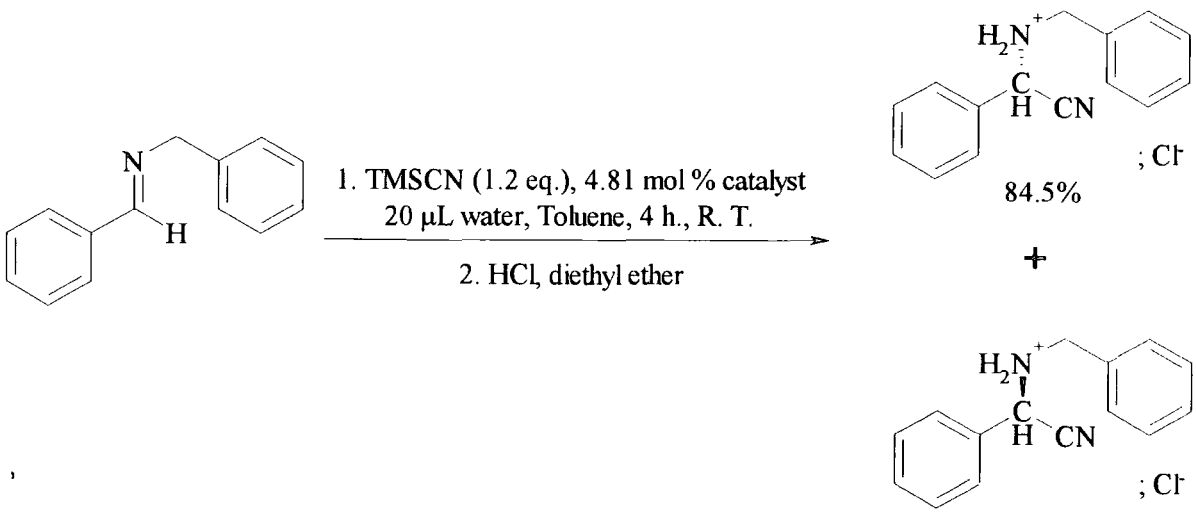

(4k)

After 16 hours at –20 and -30°C an e.e. of 80% was recorded. At lower temperatures the background reaction is reduced allowing for the catalysed reaction to be favoured hence increasing the enantioselectivity.

Further the enantiomeric excess is expected to increase with decrease in temperature on purely thermodynamic grounds. Thus from transition state theory the relationship between the rate constant, k, for a reaction and the standard Gibbs free energy of activation, $\Delta^{\ddagger}G^{\circ}$, is:

$$k = \frac{k_B T}{h} \exp(-\Delta^{\ddagger}G^{\circ} / RT)$$

where k_B is Boltzmann's constant and h is Planck's constant

Hence for the formation of two enantiomers with rate constants k_1 and k_2 respectively:

$$\frac{k_1}{k_2} = \exp(-\Delta(\Delta^{\ddagger}G^{\circ}) / RT)$$

where $\Delta(\Delta^{\ddagger}G^{\circ})$ is the difference in Gibbs free energies of activation for the two enantiomers. This shows that the ratio of rate constants will increase with decrease in temperature.

When compared to other salen catalysts vanadium (V) appears to be the more enantioselective. The complexes from titanium (IV) also provided reasonable enantiopurity, 43 and 54% e.e. for the monomer and the dimer respectively. However the aluminium (III) and vanadium (IV) yielded racemic mixtures. The aluminium catalyst was the same as the one used with the chromatographic method therefore the same justification for not being enantioselective stands.

Mechanistically it is not possible to draw definite conclusions for the asymmetric catalysis of the addition of TMSCN to N-benzylidene benzylamine by the vanadium (V) salen complex.

In the case of addition of TMSCN to carbonyl compounds (namely aldehydes and ketones) in the presence of the salen titanium complex North and Belokon[7-13, 15] suggested that the active catalyst is a dimeric species. The intermediacy of monomeric species produced from the interaction of TMSCN and the carbonyl compound with the mononuclear titanium complex has also been reported. Applying this theory to N-benzylidene benzylamine implies the formation of the two structures shown in Scheme 4.23 as possible interaction products between the catalyst and the imine.

Scheme 4.23

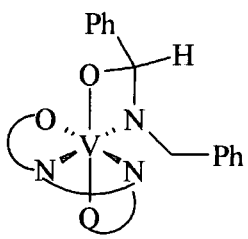

(A)

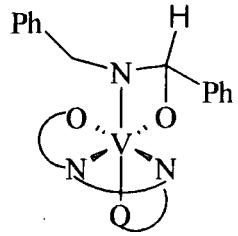

(B)

The geometry of the complexes should be dictated both by the configuration of the imine (trans) and the bulkiness of the phenyl and benzyl groups that are likely to be as far away as possible from the bulky ter-butyl groups of the ligand.

Combination with the dicyano form of the catalyst might lead to a binuclear species bearing both the imine and a cyanide moiety similar to structure (**D**) pictured in Scheme 4.7.

However it may seem unlikely that the structure is actually formed given the bulkiness of the aromatic groups of the imine. Steric over-crowding due to the presence of the ter butyl groups will almost certainly cause the imine to dissociate from the metal centre.

This is comparable with North and Belokon's assumption that only ketones having methyl or ethyl as the smallest substituent can undergo catalysis with the salen complex.

Further, Jacobsen[4a] reported the addition of TMSCN to imines using the Al(III) Salen complex to be first order in catalyst suggesting that the possibility of a cooperative bimetallic mechanism is unlikely.

4.4 References

1. A. Combes, *C. R. Acad. Fr.*, 1889, **108**, 1252

2. J. F. Larrow and E. N. Jacobsen, *Topics Organomet. Chem.*, 2004, **6**, 123

3. (a) J. F. Larrow, E. N. Jacobsen, Y. Gao, Y. P. Hong, X. Y. Nie and C. M. Zepp, *J. Org. Chem.*, 1994, **59**, 1939; (b) J. F. Larrow and E. N. Jacobsen, *Org. Syn.*, 1997, **75**, 1

4. (a) J. F. Larrow and E. N. Jacobsen, *Topics Organomet. Chem.*, 2004, **6**, 123; (b) L. Canali and D. C. Sherrington, *Chem. Soc. Rev.*, 1999, **28**, 85

5. E. N. Jacobsen, *Comprehensive Organometallic Chemistry II*, Ed. E. W. Abel, F. G. A. Stone and E. Willinson, Pergamon, New York, 1995, vol. 12, p. 1097

6. C. T. Dalton, K. M. Ryan, V. M. Wall, C. D. Bousquet and G. Gilheany, *Top. Catal.*, 1998, **5**, 75

7. Y. Belokon, M. Flego, N. Ikonnikov, M. Moscalenko, M. North, C. Orizu, V. Tararov and M. Tasinazzo, *J. Chem. Soc., Perkin Trans. 1*, 1997, 1293

8. Y. N. Belokon, S. Caveda-Cepas, B. Green, N. S. Ikonnikov, V. N. Krustalev, V. S. Larichev, M. A. Moscalenko, M. North, C. Orizu, V. I. Tararov, M. Tasinazzo, G. I. Timofeeva and L. V. Yashkina, *J. Am. Chem. Soc.*, 1999, **121**, 3968

9. V. I. Tararov, D. E. Hibbs, M. B. Hursthouse, N. S. Ikonnikov, K. M. A. Malik, M. North, C. Orizu and Y. Belokon, *Chem. Commun.*, 1998, 387

10. Y. Belokon, B. Green, N. S. Ikonnikov, V. S. Larichev, B. V. Lokshin, M. A. Moscalenko, M. North, C. Orizu, A. S. Peregudov and G. I. Timofeeva, *Eur. J. Org. Chem.*, 2000, 2655

11. Y. N. Belokon, B. Green, N. S. Ikonnikov, M. North and V. I. Tararov, *Tetrahedron Lett.*, 1999, **40**, 8147

12. Y. Belokon, B. Green, N. S. Ikonnikov, M. North, T. Parsons and V. I. Tararov, *Tetrahedron*, 2001, **57**, 771

13. (a) Y. N. Belokon, M. North and T. Parsons, *Org. Lett.*, 2000, **2**, 1617; (b) Ref 12

14. (a) K. Nakajima et al., *Bull. Chem. Soc. Jpn.*, 1996, **69**, 3207; (b) H. Schmidt and D. Rehder, *Inorg. Chim. Acta*, 1998, **267**, 229; (c) M. Mathew, A. J. Carty and G. J. Palenik, *J. Am. Chem. Soc.*, 1970, **92**, 3197

15. Y. Belokon, P. Carta, A. V. Gutnov, V. Maleev, M. A. Moskalenko, L. V. Yashkina, N. S. Ikonnikov, N. V. Voskoboev, V. N. Khrustalev and M. North, *Helvetica Chim. Acta.*, 2002, **85**, 3301

16. M. S. Sigman and E. N. Jacobsen, *J. Am. Chem. Soc.*, 1998, **120**, 5315

17. (a) P. Schreier, A. Bernreuther and M. Huffer, *Analysis of Chiral Organic Molecules*, Walter de Gruyter (Ed.), Berlin – New York, 1995; (b) E. J. Gil-Av, *J. Mol. Evol.*, 1975, **6**, 131; (c) J. Gal in *Drug stereochemistry. Analytical Methods and Pharmacology*, I. W. Wainer (Ed.), 2nd Ed., Dekker: New York, 1992, p.65

18. (a) V. Schurig, *Angew. Chem. Int. Ed. Engl.*, 1977, **16**, 110; (b) V. Schurig, W. Burkle, K. Hintzer and R. Weber, *J. Chromatogr.*, 1989, **475**, 23; (c) V. Schurig, D. Schmalzing and M. Schleimer, *Angew. Chem. Int. Ed. Engl.*, 1991, **30**, 987

19. (a) V. Schurig and H.-P. Novotny, *J. Chromatogr.*, 1988, **441**, 155; (b) W. A. König, S. Lutz and G. Wenz, *Angew. Chem. Int. Ed. Engl.*, 1988, **27**, 979; (c) W. A. König, S. Lutz and P. Mischnick-Lubbecke, *J. Chromatogr.*, 1988, **447**, 193; (d) Ref 18c

20. N. Bucaille, L. Vaton-Chanvrier, Y. Combret and J. C. Combret, *J. High Resol. Chromatogr.*, 1999, **22**, 671

21. (a) J. Pfeiffer and V. Schurig, *J. Chromatogr. A*, 1999, **840**, 145; (b) F. Narumi, N. Iki, T. Suzuki, T. Onodera and S. Miyano, *Enantiomer*, 2000, **5**, 83

22. (a) E. Gil-Av, B. Feibush and R. Charles-Sigler, *Tetrahedron Lett.*, 1966, **8**, 1009; (b) E. Gil-Av and B. Feibush, *Tetrahedron Lett.*, 1967, **9**, 3345

23. G. Gübitz and M. G. Schmid, *Biopharm. Drug Dispos.*, 2001, **22**, 291

24. D. J. Cram and J. L. Mateos, *J. Am. Chem. Soc.*, 1959, **81**, 5150

25. D. Parker, *Chem. Rev.*, 1991, **91**, 1441

26. C. C. Hinckley, *J. Am. Chem. Soc.*, 1969, **91**, 5160

27. D. J. Raber, M. D. Johnston, Jr., C. M. Campbell, C. M. Jancks and P. Sutton, *Org. Magn. Res.*, 1978, **11**, 323

28. (a) J. A. Peters, J. Huskens and D. J. Raber, *Progr. Nuc. Magn. Res. Spectr.*, 1996, **28**, 283; (b) W. Kemp, *NMR in Chemistry, A Multinuclear Introduction*, Mc Millan Edition Ltd, Handmills, Basingstoke, Hampshire, 1986

29. (a) W. D. Horrocks, J. Sipe and D. Sudnick, *NMR Shifts Reagents*, Ed. R. E. Sievers, Academic Press, New York, 1973; (b) L. Ernst and A. Mannschreck, *Tetrahedron Lett.*, 1971, **13**, 3023; (c) T. C. Morrill, R. J. Opitz and R. Mozzer, *Tetrahedron Lett.*, 1973, **15**, 3715; (d) S. P. Sinha, *J. Mol. Struct.*, 1973, **19**, 387

30. (a) R. E. Rondeau and R. E. Sievers, *J. Am. Chem. Soc.*, 1971, **93**, 1522; (b) T. C. Morrill, *Lanthanide Shift Reagents in Stereochemical Analysis*, VCH Publishers Inc., New York, 1986, Chapter 1

31. C. Pettersson and G. Schill, *J. Chromatogr.*, 1981, **204**, 179

32. H. Nishi and S. Terabe, *J. Pharm. Biomed. Anal.*, 1993, **11**, 1277

33. N. A. Hassan, E. Bayer and J. C. Jochims , *J. Chem. Soc., Perkin Trans. 1*, 1998, 3747

34. D. Parker, *J. Chem. Soc., Perkin Trans. 2*, 1983, 83

35. R. M. Williams, P. J. Sinclair, D. Ahari and D. Chen, *J. Am. Chem. Soc.*, 1988, **110**, 1547

36. H. Ishitani, S. Komiyama, Y. Hasegawa and S. Kobayashi., *J. Am. Chem. Soc.*, 2000, **122**, 762

37. W. –H. Leung, E. Y. Y. Chan, E. K. F. Chow, I. D. Williams and S. –M. Peng, *J. Chem. Soc., Dalton Trans.*, 1996, 1229

38. K. Mai and G. Patil, *Synthetic Comm.*, 1985, **15**, 157

39. H. Stephen and T. Stephen, *Solubilities of Inorganic and Organic Compounds*, Pergamon Press, 1963, Vol. 1, 477

Chapter Five: The reaction of imines with trifluoroacetic anhydride

Chapter five: The reaction of imines with trifluoroacetic anhydride (TFAA)

5.1 Introduction

In their account of the asymmetric addition of trimethylsilyl cyanide (TMSCN) to a series of imines Sigman and Jacobsen[1] quenched the reaction using trifluoroacetic anhydride as shown in Scheme 5.1.

Scheme 5.1

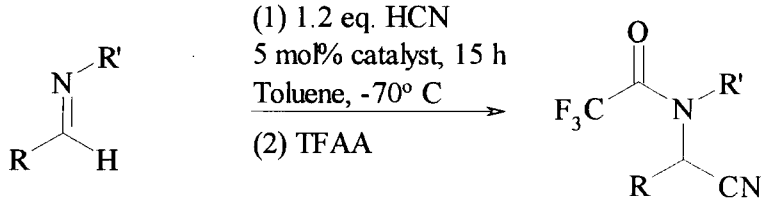

The experiments carried out in chapter four have been based on the above example and trifluoroacetic anhydride was used as described.

In a first set of experiments, using chiral gas chromatography (GC) to assess the enantiomeric excess, the addition of TFAA seemed to affect the conversion level of the reaction. Indeed quenching with the anhydride appeared to result in a significant increase in the yield. However further experiments indicated the unreliability of those results since a peak accountable for the imine was observed on the chromatograms.

It is of interest to question whether TFAA interacts with the imine to promote addition of cyanide or if it is only acetylating the aminonitrile to yield a trifluoroacetamide.

The reaction of trifluoroacetic anhydride with imines is not one that has been thoroughly studied. However in 1928 Kalkin[2] accounted for the reaction of N-benzylidene aniline with acetic anhydride in the presence of potassium carbonate. He managed to isolate 4.3% of cinnamic acid (Scheme 5.2).

Scheme 5.2

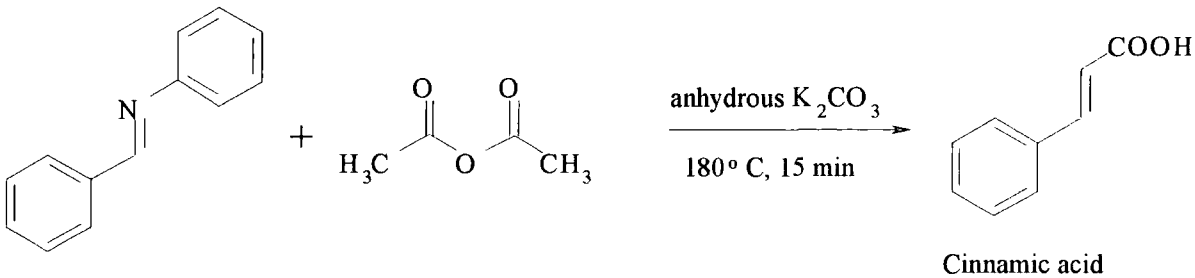

Cinnamic acid

4.3 % yield

The same year Passerini and Mancetelli[3] also reported the reaction of acetic anhydride with N-benzylidene aniline. After heating up the mixture for several hours they isolated a product which they assumed to be one described in Scheme 5.3.

Scheme 5.3

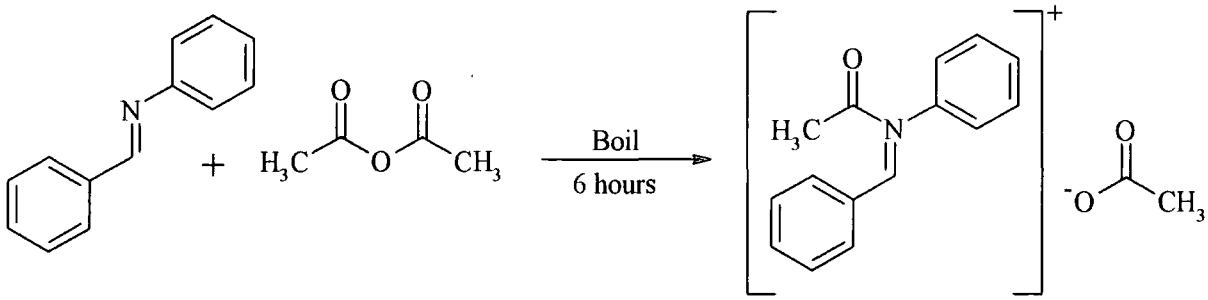

[A]

The structure, **[A]**, was proposed since the isolated compound hydrolyses to form N-benzylidene aniline, benzaldehyde and acetic acid.

Later Johnson and co-workers[4] suggested that the product is in fact best represented by structure **[B]** (Scheme 5.4).

Scheme 5.4

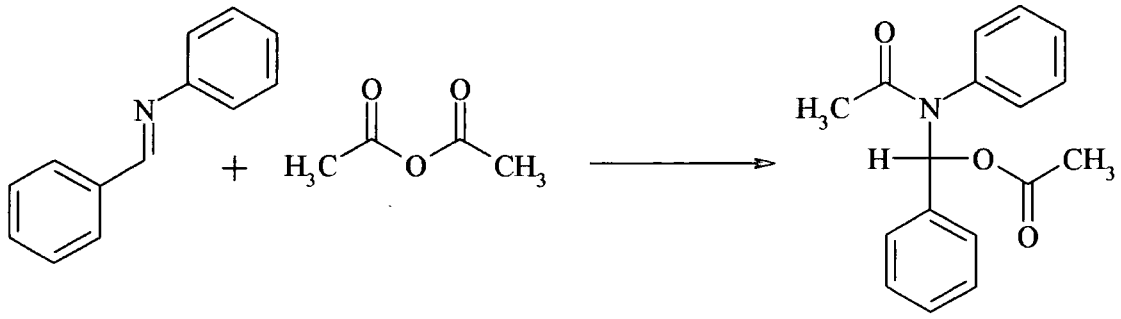

[B]

A mechanism for the formation of **[B]** was subsequently proposed by Wiley and co-workers[5]. They found that the reaction was catalysed by acetic acid and suggested that the addition of the acid is the first step of the reaction. Acetylation by acetic anhydride occurs in a second step regenerating acetic acid (Scheme 5.5).

Scheme 5.5

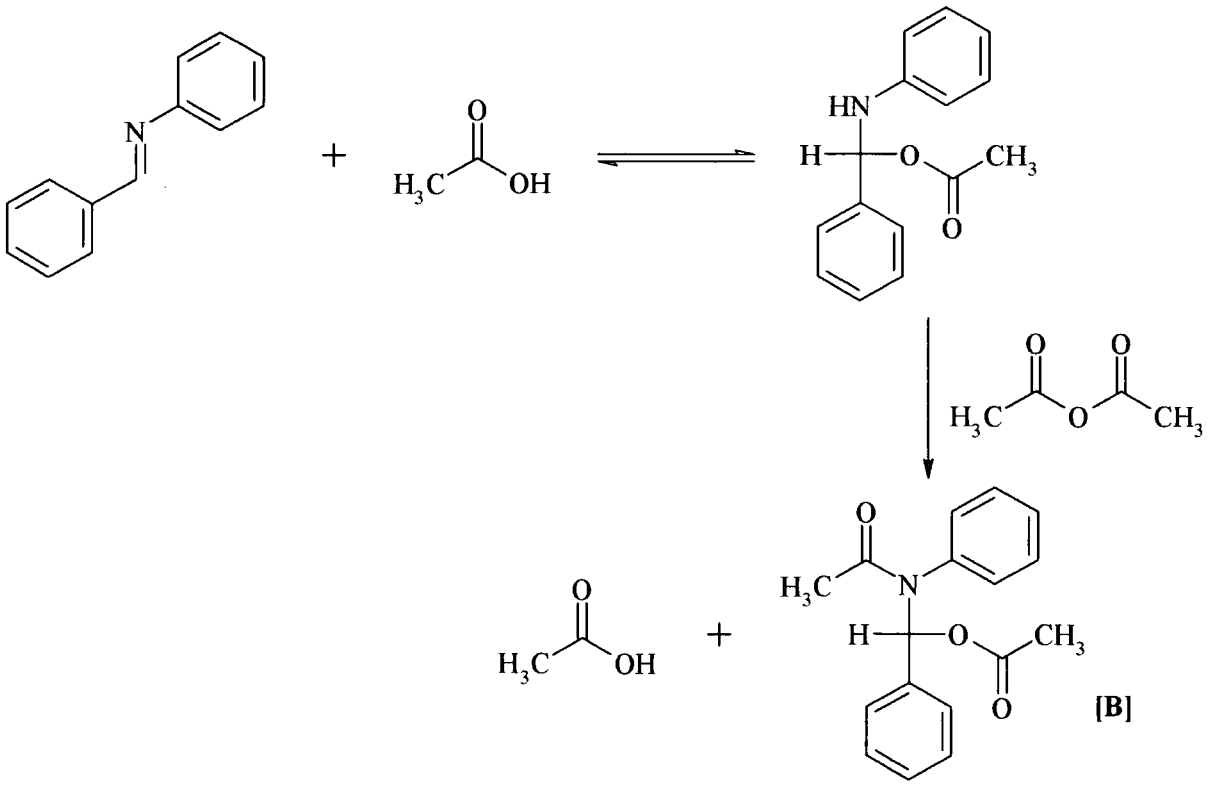

Angel and Day[6] offered an alternative product for the reaction, [C], following a Perkin type reaction.

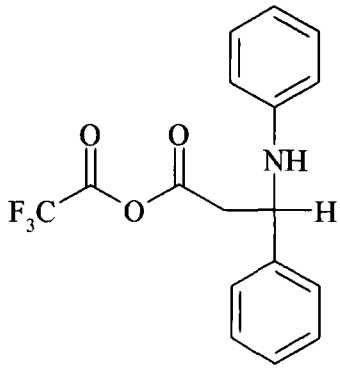

[C]

However Burgstahler[7] showed the mechanism leading to the above was unlikely and indicated that structure [B] was more probable with an alternative mechanism (Scheme 5.6) to that of Wiley and co-workers shown above (Scheme 5.5).

Scheme 5.6

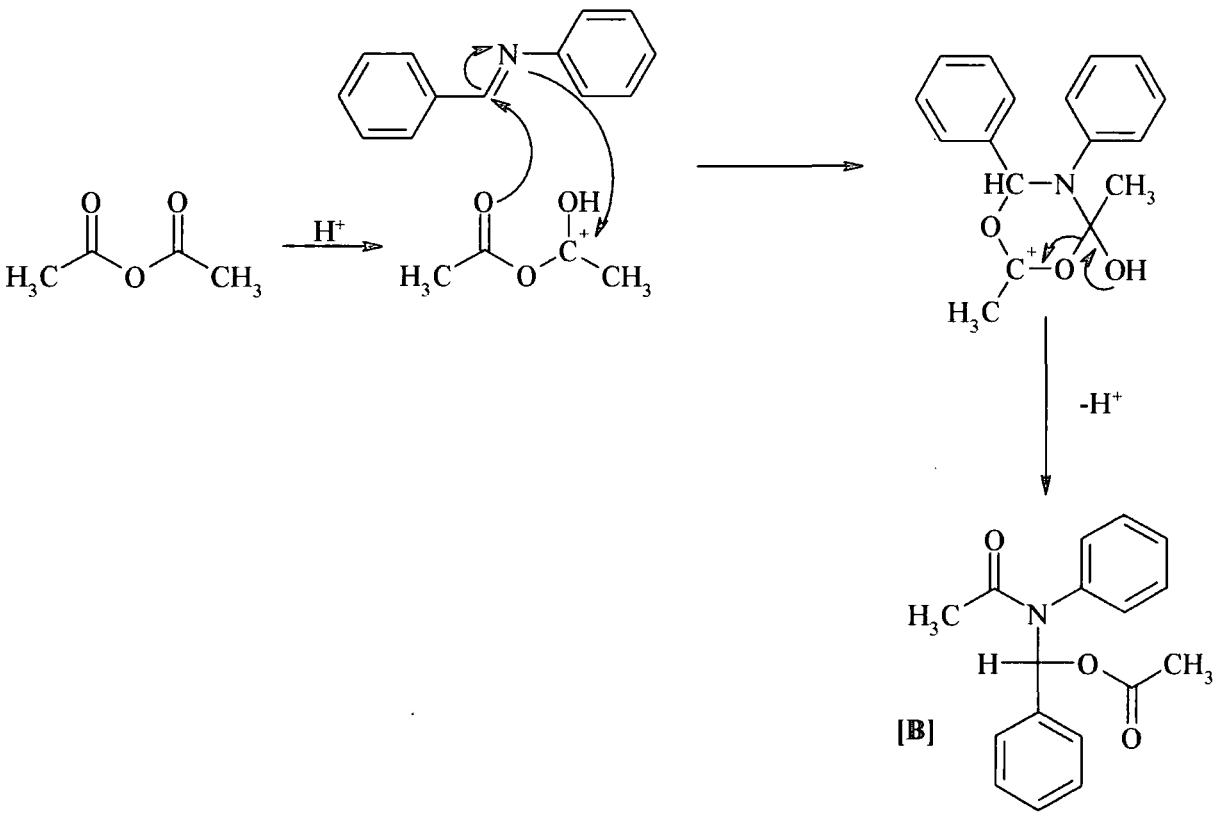

In 1975 Sekiya and Morimoto[8] showed that the reaction of trichloroacetic anhydride with N-benzylidene aniline in 1:1 molar proportion in solution at room temperature yielded the trichloro-derivative of **[B]** as described in Scheme 5.7.

Scheme 5.7

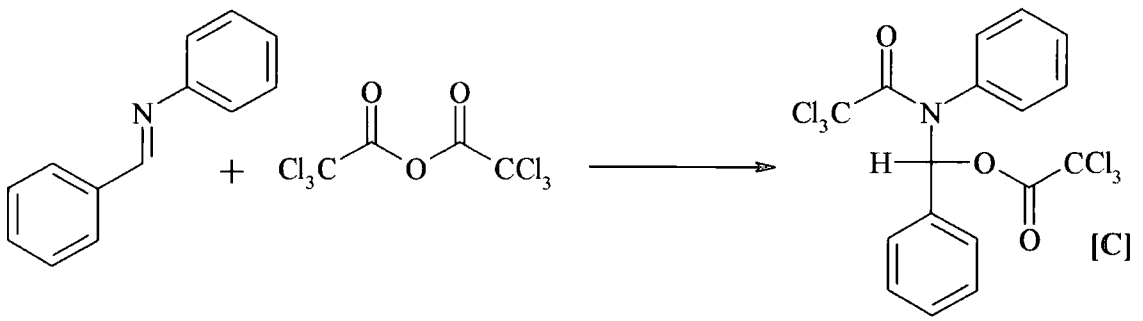

It is worth noting that, upon heating, the addition of trichloroacetic anhydride to N-benzylidene aniline yields 3,3-dichloro-1,4-diphenyl-2-azetidinone. Sekiya and Morimoto suggested that N-(α-trichloroacetoxybenzyl)trichloroacetanilide, **[C]** is an intermediate in the process.

Scheme 5.8

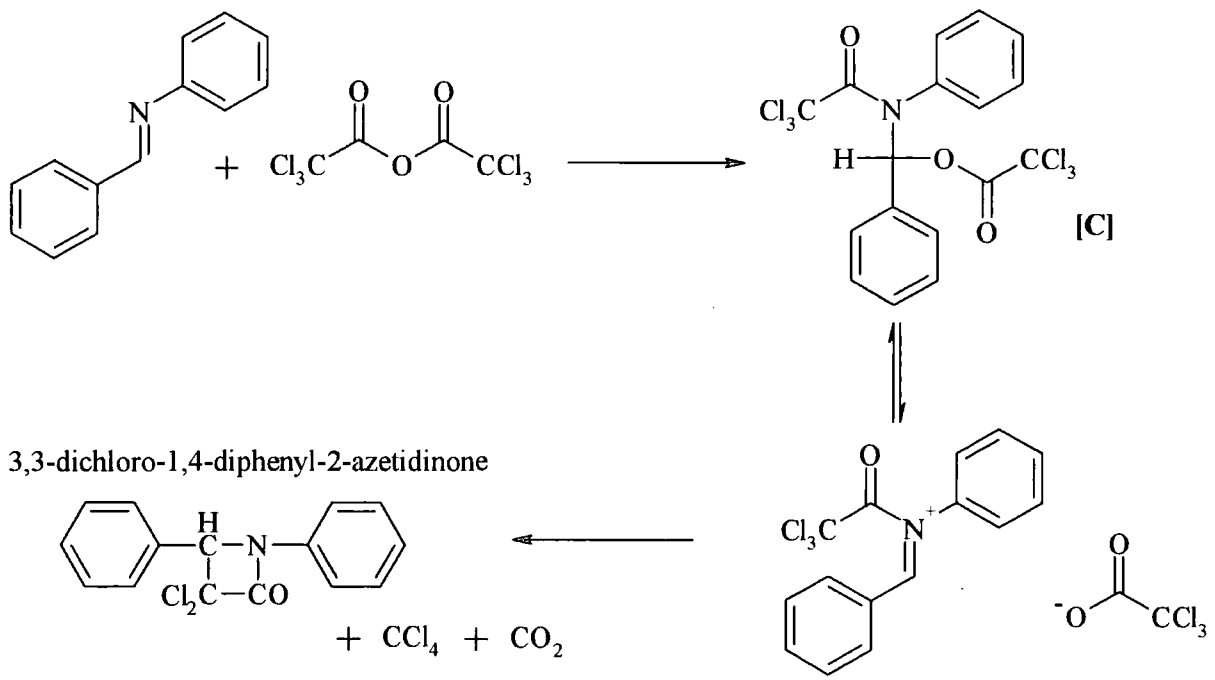

It should be noted that trifluoroacetic acid is a considerably stronger acid[9] in water ($pK_a = 0.22$) than is acetic acid ($pK_a = 4.76$).

The electron-withdrawing influence of the trifluoromethyl group is expected to greatly enhance the electrophilicity of the trifluoroacetyl cation, [D], relative to the acetyl group while reducing the nucleophilicity of the trifluoroacetate anion, [E], relative to that of the acetate ion.

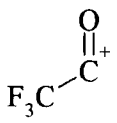

[D]

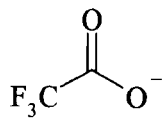

[E]

5.2 Results and discussion

5.2.1 UV/Vis spectroscopic monitoring of the reaction in acetonitrile

The imines of interest, namely N-benzylidene benzylamine and N-benzylidene allylamine show a strong absorbance at 250nm. Trifluoroacetic anhydride, in the concentration used ($1x10^{-4}$ mol dm^{-3}) shows negligible absorbance in this region of the UV/Vis spectrum.

A stock solution ($1x10^{-2}$ mol dm^{-3}) of trifluoroacetic anhydride (14.1 μL, 0.1 mmol) in acetonitrile (10 cm^3) was prepared.

A solution of the required imine ($1x10^{-4}$ mol dm^{-3}) in acetonitrile (2.5 cm^3) was placed in a UV cell. An equivalent of TFAA (2.5 μL stock solution) was added to the solution and the spectrum recorded immediately. Repeat scans were performed at 1 minute intervals.

Typical spectra are shown in Figure 5.1.

Figure 5.1 UV/Vis spectra for the reaction of $1x10^{-4}$ mol dm^{-3} benzylidene benzylamine with $1x10^{-4}$ mol dm^{-3} TFAA in acetonitrile. Total reaction time = 30 min

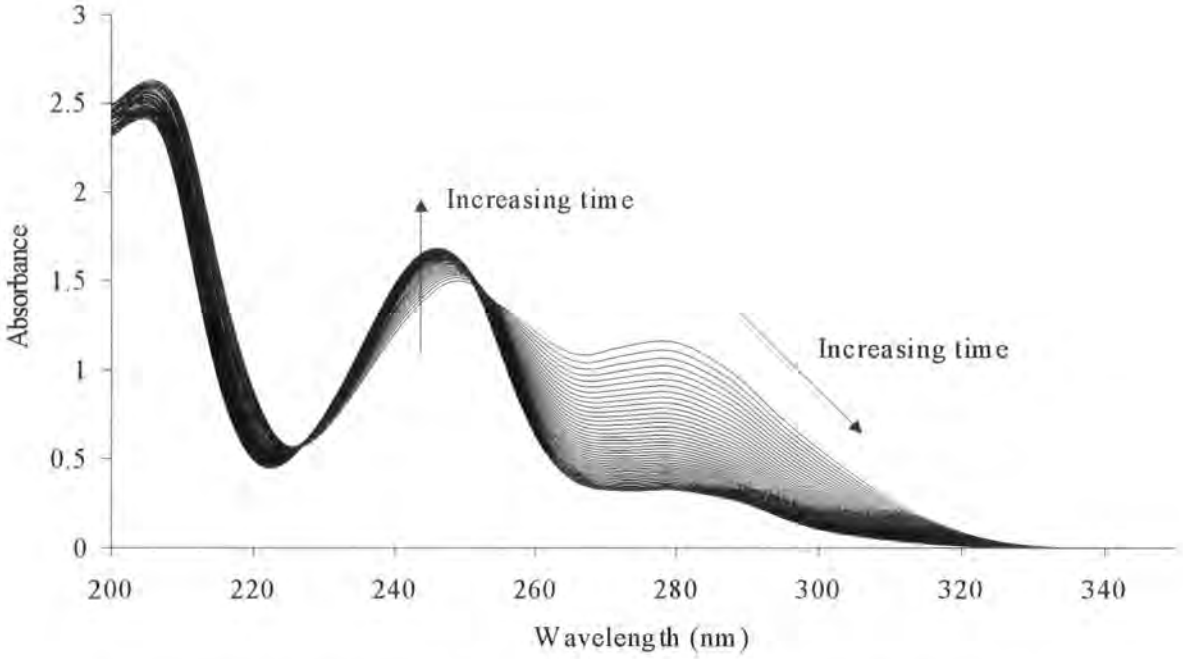

The reaction with either of the imines (N-benzylidene benzylamine or N-benzylidene allylamine) yields the same spectrum indicating similar behaviour. The two observed isobestic points are characteristic of one compound disappearing while another is forming.

To allow for comparison the UV spectrum of N-benzylidene benzylamine in acetonitrile is displayed in Figure 5.2

Figure 5.2 UV/Vis spectrum for $1x10^{-4}$ mol dm^{-3} benzylidene benzylamine in acetonitrile

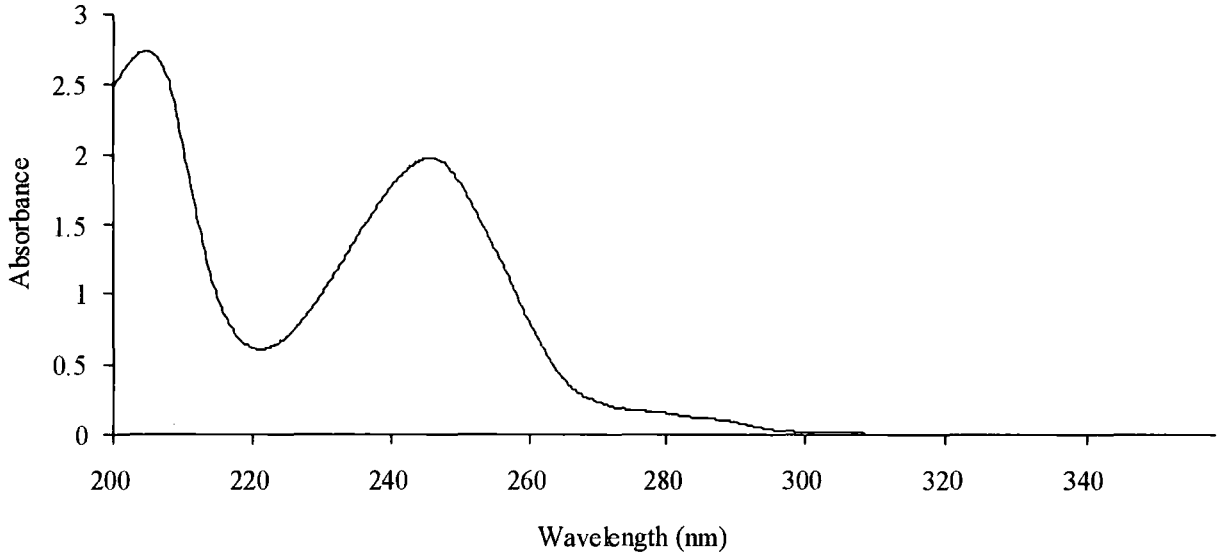

It is possible to distinguish two successive phenomena in the reaction of the imines with TFAA. First of all a fast process by which absorbance at 250 nm is decreased and absorbance at 280 nm increases can be identified. Secondly a slower process is observed with absorbance at 280 nm decreasing and the absorbance at 245 nm increasing.

The fact that the absorbance in the 250 nm region decreases indicates reaction at the carbon nitrogen double bond. Nevertheless subsequent increase in absorbance in the similar region but with λ_{max} = 245 nm shows that the imine is not re-formed. It is worth noting that benzaldehyde in acetonitrile absorbs in the same region with λ_{max} = 245 nm.

The presence of the absorption band at λ_{max} = 280 nm suggests that N-(α-trifluoroacetoxybenzyl)trifluoroacetanilide is not formed, since negligible absorbance is expected for this compound in the given region. Thus the corresponding aminonitrile does not absorb in this region. However the species may be in equilibrium with an ionic form as described by Sekiya and Morimoto[8] (Scheme 5.9).

Scheme 5.9

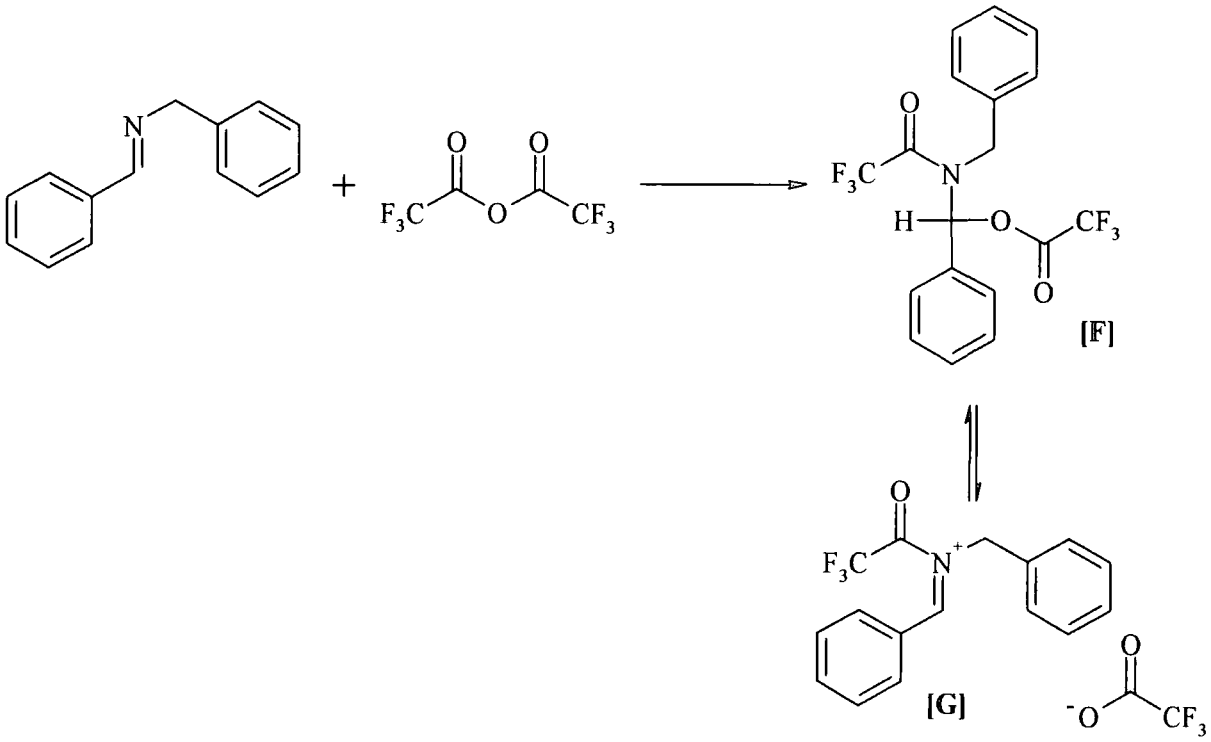

Delocalisation of the positive charge within the benzene ring is likely to account for the absorbance observed at 280 nm (Scheme 5.10).

Scheme 5.10

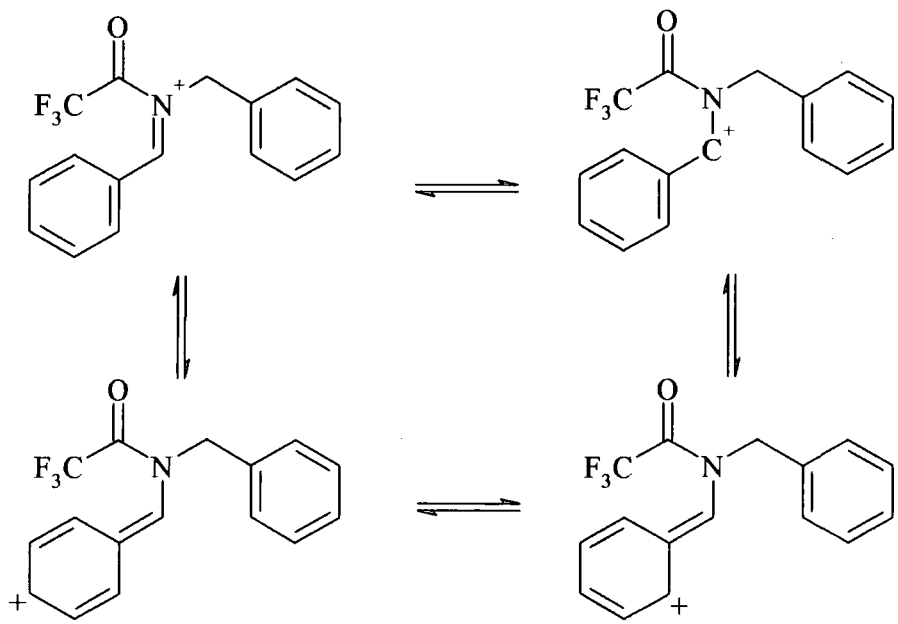

The behaviour was qualitatively similar in the presence of excess TFAA. Measurements of the initial absorbance at 280 nm, and the rate constant for the decomposition reaction are in Table 5.0. They show that the initial equilibrium is essentially complete with a small excess of TFAA and that the rate constant fro the decomposition reaction shows little dependence on the excess.

One conclusion is that the initial reaction is likely to form ionic species as shown in Scheme 5.9 with a high value for the equilibrium constant. The independence of k_{decomp} on excess TFAA is compatible with decomposition of the trifluoroacetylated cation probably by reaction with adventitious water. Since water content was not strictly controlled the variations of k_{decomp} in Table 5.0 probably reflect the amount of water in the solvent.

Table 5.0 Variation of absorbance at 280 nm and k_{decomp} with TFAA concentration in acetonitrile[a]

[TFAA] 10^{-4} mol dm^{-3}	Abs 280 nm[b]	k_{decomp}[c] 10^{-3} s^{-1}
1	0.85	1.9
4	1.35	1.9
8	1.38	1.8
12	1.28	3.8
20	1.43	3.4

a. The concentration of N-benzylidene allylamine is $1x10^{-4}$ mol dm^{-3}
b. Initially after mixing
c. Measured at 280 nm

In the presence of added water the cationic species can be hydrolysed to yield benzaldehyde. This is confirmed by the shift in the λ_{max} value from 250 to 245 nm along with the decrease in absorbance at 280 nm.

It is worth noting that addition of acetic anhydride to either of the imines caused no change in UV spectrum, indicating the absence of reaction.

5.2.2 NMR spectroscopy

NMR spectra of the imines in presence of TFAA were recorded in deuterated acetonitrile (CD_3CN) and deuterated benzene (C_6D_6). In each case addition of the anhydride to the imine was performed immediately prior to the insertion of the sample in the instrument. A time lag of 3 minutes is expected before the first spectrum is recorded.

5.2.2.1 N-Benzylidene allylamine

Trifluoroacetic anhydride was added to N-benzylidene allylamine in CD_3CN. Scans were repeated at an interval of 3 minutes for the first 6 scans. A further 30 minutes was allowed before taking the last (seventh) scan. A specimen spectrum, the seventh scan, is shown on Figure 5.3.

Figure 5.3 ^1H NMR spectrum in CD_3CN for the observed reaction of benzylidene allylamine with TFAA (1 eq.) after 48 minutes

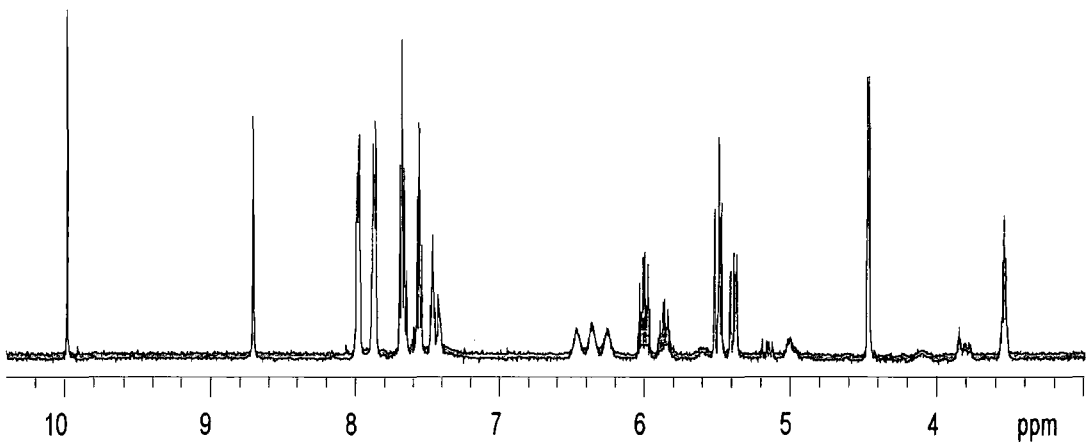

Initially bands are observed which can be ascribed to [H] the trifluoroacetylated cation of the allyl imine. With time these decrease in intensity and bands due to benzaldehyde and protonated allylamine increase. In Figure 5.3 the band at $\delta = 8.71$ ppm is due to the methine hydrogen of [H] while that at $\delta = 9.98$ ppm is due to benzaldehyde.

The detailed analysis of the spectra is given below in Tables 5.1, 5.2 and 5.3.

Table 5.1 ^{1}H NMR chemical shifts of benzaldehyde in CD_3CN

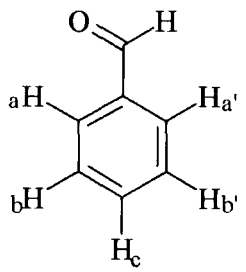

	Chemical shifts (ppm)	
Protons	Standard	Reaction mixture
H_b, $H_{b'}$ & H_c	7.63	7.57
H_a & $H_{a'}$	7.90	7.88
CHO	10.0	9.98

When assigning the peaks corresponding to the amine, in Table 5.2, it is possible to see that the relative intensity of the signal accounting for the amino protons is 3 compared to the other signals for the allylamine. It is therefore the allylammonium species which is formed rather the neutral allylamine. Allylammonium was synthesised in CD_3CN by adding hydrochloric acid to allylamine. Interestingly coupling of the ammonium protons to the ^{14}N quadrupole is observed with the expected coupling constant of J = 54 Hz. The chemical shift of this band is at δ = 7.42 ppm in the synthesised ammonium ion and at δ = 6.36 in the reaction mixture. This difference can be attributed to the presence of some amine in rapid equilibrium with the ammonium ion.

Table 5.2 ^{1}H NMR chemical shifts of allylamine and allylammonium in CD_3CN

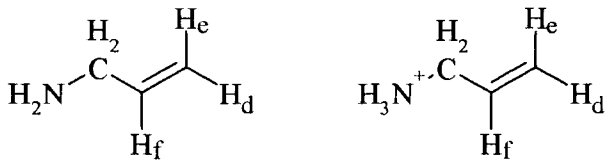

	Chemical shifts (ppm)		
Protons	Standard	Allyl ammonium	Reaction mixture
NH_2	1.10	7.42	6.36
CH_2	3.20	3.57	3.54
H_d	4.98	5.37	5.38
H_e	5.13	5.44	5.41
H_f	5.95	5.95	5.86

Table 5.3 ^{1}H NMR chemical shifts of N-benzylidene allylamine in CD_3CN

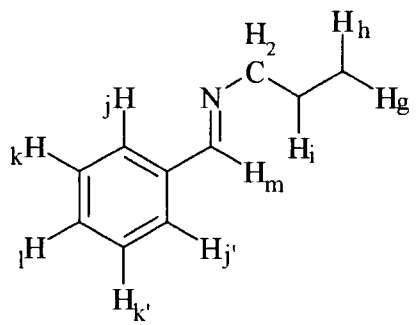

	Chemical shifts (ppm)	
Protons	Standard	Reaction mixture†
CH_2	4.19	4.47
H_g	5.09	5.48
H_h	5.19	5.51
H_i	6.10	6.00
H_l	7.38	7.88
H_k & $H_{k'}$	7.39	7.69
H_j & $H_{j'}$	7.74	7.98
H_m	8.30	8.71

†. Corresponds to the trifluoroacetylated imine, **[H]**.

From the UV/Vis results it is assumed that an ionic species is formed (band at λ_{max} = 280 nm). This is consistent with the chemical shifts shown above where the effect of a lower electron density in the ionic species deshields the protons. This is translated on the spectrum by a downfield shift of the signals and especially the one accounting for the methine proton since it is bound to the carbon bearing the positive charge. The effect is also quite strong for the aromatic protons because of the possible delocalisation responsible for the increase in absorbance at 280 nm.

The reaction can then be written as Scheme 5.11.

Scheme 5.11

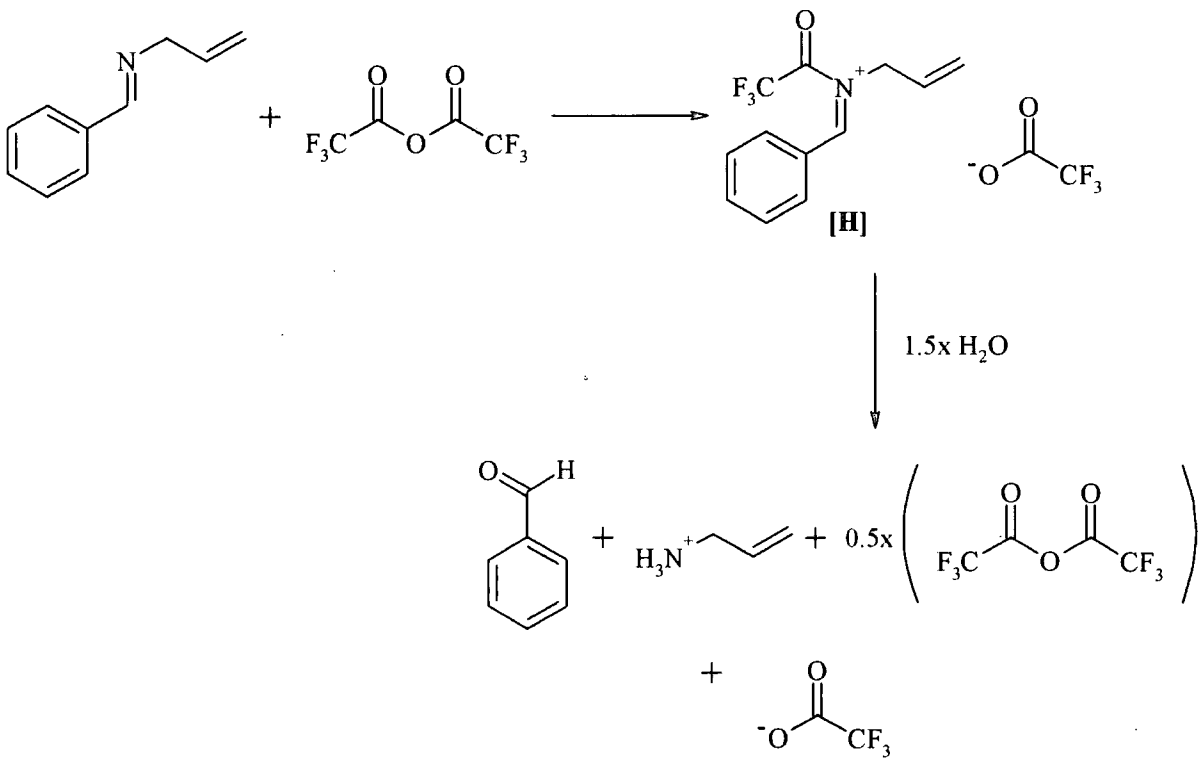

It is worth noting that according to the NMR data the imine is fully converted to the trifluoroacetamide adduct. Also that the decomposition process requires 1.5 molecules of water for completion.

It is possible to record the relative intensities corresponding to the methine and aldehydic protons with time. Since one molecule of the cation decomposes to give one molecule of benzaldehyde the ratio of the two intensities corresponds to the conversion level. Knowing the initial concentration of imine and assuming that it is fully converted to the adduct it is then possible to calculate concentrations in the ion and benzaldehyde as shown in Table 5.4. The hydrolysis reaction clearly does not go to completion indicating that there is insufficient water present for this to happen.

Table 5.4 Evolution with time of the relative intensities of the methane and aldehydic protons in the ^{1}H NMR spectrum

Time (min)	Time (s)	Relative intensities		Conversion level	Concentrations / 10^{-3} mol dm^{-3}	
		CHN	PhCHO		Adduct	Benzaldehyde
3	180	7.51	0.9	11%	8.92	1.07
6	360	7.47	0.86	10%	8.97	1.03
9	540	7.2	1.47	17%	8.30	1.70
12	720	6.76	1.96	22%	7.75	2.25
15	900	5.40	1.87	26%	7.43	2.57
18	1080	4.84	2.04	30%	7.03	2.97
48	2880	4.26	2.63	38%	6.18	3.82

Figure 5.4 Evolution of the benzaldehyde concentration with time for the reaction of benzylidene allylamine with TFAA

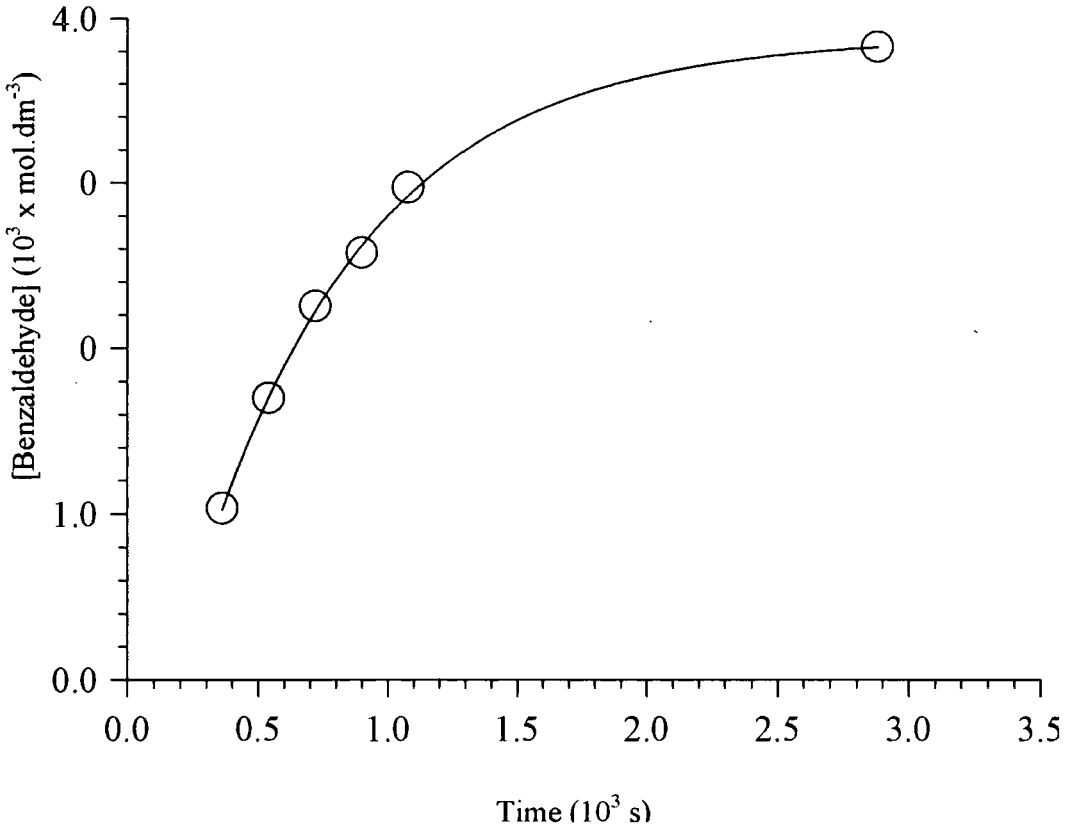

5.2.2.2 N-Benzylidene benzylamine

5.2.2.2.1 Reaction in CD_3CN

The procedure was repeated using N-benzylidene benzylamine. Thus trifluoroacetic anhydride was added to N-benzylidene benzylamine in CD_3CN. Scans were repeated at an interval of 3 minutes for the first 6 samples. 30 minutes were allowed before taking the last (seventh) scan. A specimen spectrum is shown on Figure 5.5.

Figure 5.5 ^{1}H NMR spectrum in CD_3CN for the observed reaction of benzylidene benzylamine with TFAA (1 eq.) after 48 minutes

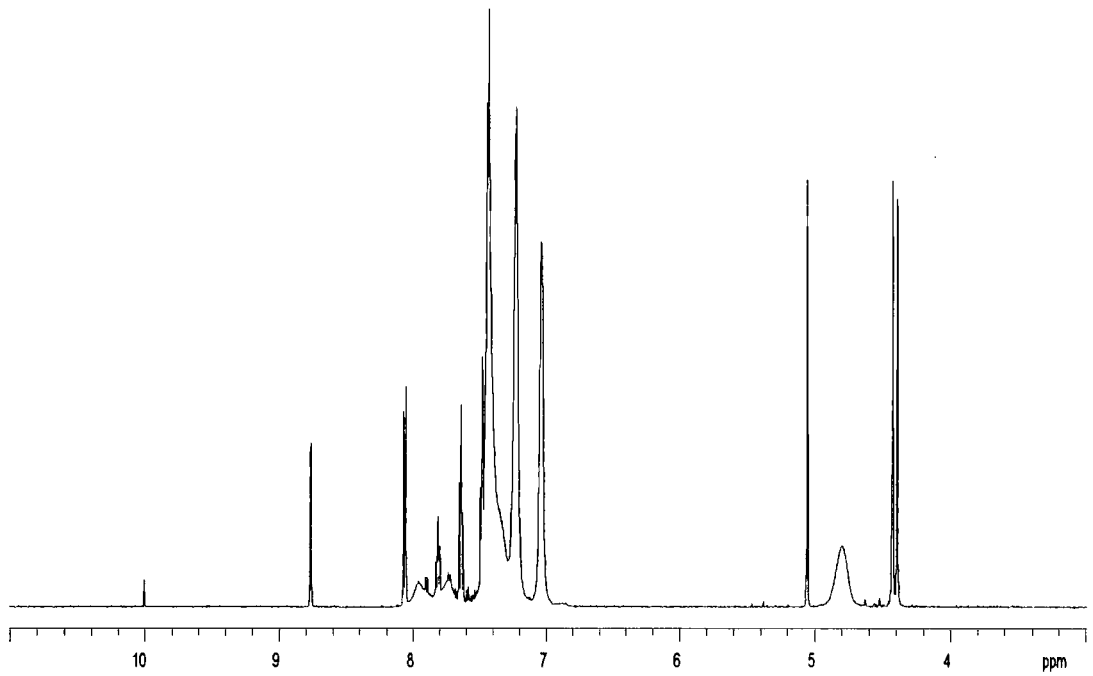

In the case of N-benzylidene benzylamine again a downfield shift of the signals is observed. However, no evolution with time was observed. The spectrum shown above is that observed over a 30 minutes time period. Although decomposition to benzaldehyde and benzylamine is observed it is to a relatively low level and does not increase with time. It is not possible to assign any of the peaks to the parent aldehyde and amine apart from the signal at 10.01 ppm representative of the aldehydic proton of benzaldehyde.

Further the spectrum indicates the presence of a mixture. Also, several broad peaks (namely at 4.80, 7.73 and 7.97 ppm) indicate possible conformational changes within the molecule(s). A possible justification for the features displayed in Figure 5.5 is a 5:1 mixture between N-(α-trifluoroacetoxybenzyl)trifluoroacetobenzylamide and the ionic species (Scheme 5.12).

Scheme 5.12

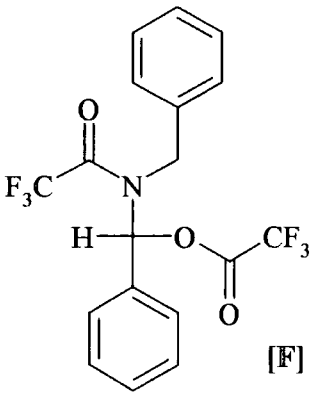

[F]

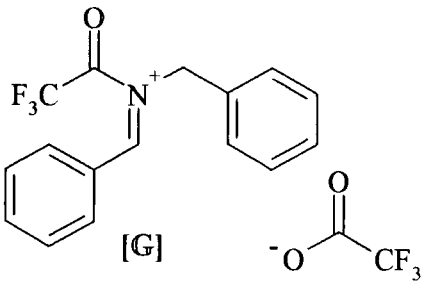

[G]

5 : 1

The relative intensities recorded indicate the above ratio. Three signals are observable in the upfield part of the spectrum. Since the only resonance expected in this region is that of the CH_2 moiety of the benzyl group three signals it indicates the presence of at least two compounds in the mixture. Possibilities are that four species can be present: the two structures represented above, N-benzylidene benzylamine and benzylamine. Benzylamine is a decomposition product of the system and is formed in a 1:1 ratio with benzaldehyde. The relative intensity of benzaldehyde is about 34 times lower than that of the signal of lowest intensity therefore it is not possible to consider the occurrence of the amine. N-benzylidene benzylamine gives rise to a signal for the methine proton at $\delta = 8.47$ ppm. Such a resonance is not observed on the spectrum therefore the imine is not present either. Hence the three signals are a consequence of the two structures proposed above. It is indeed possible to account for the ionic species. A resonance peak at $\delta = 8.77$ ppm is observable and compatible with a methine proton in an environment of low electron density. Comparing the relative intensity of the signal with that of the peaks of interest in the upfield region it is possible to assign one of them to the CH_2 moiety. The remaining two peaks must therefore be two distinct signals accounting for each of the protons on N-(α-trifluoroacetoxybenzyl)trifluoroacetobenzylamide. All those considerations enable the calculation of a 5:1 ratio between the cation and the neutral species respectively. Chemical shifts are summarised in Tables 5.5 and 5.6.

Table 5.5 ^{1}H NMR chemical shifts of N-(α-trifluoroacetoxybenzyl) trifluoroacetobenzylamide in CD_3CN

	N-(α-trifluoroacetoxybenzyl) trifluoroacetobenzylamide
Protons	Chemical shifts (ppm)
CH_2	4.41 & 4.80
H_e & $H_{e'}$	7.04
H_d, $H_{d'}$ & H_f	7.23
H_i, $H_{i'}$, H_h, $H_{h'}$ and H_g	7.25-7.46
CHN	7.70-8.00

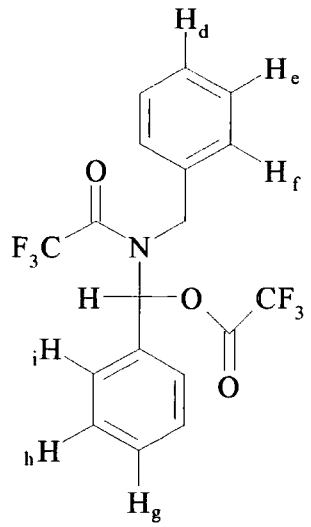

[F]

Table 5.6 ^{1}H NMR chemical shifts of the ionic species in CD_3CN

	Ionic species
Protons	Chemical shifts (ppm)
CH_2	5.06
H_d, $H_{d'}$, H_e, $H_{e'}$ & H_f	7.25-7.40
H_h & $H_{h'}$	7.64
H_g	7.91
H_i & $H_{i'}$	8.07
CHN	8.77

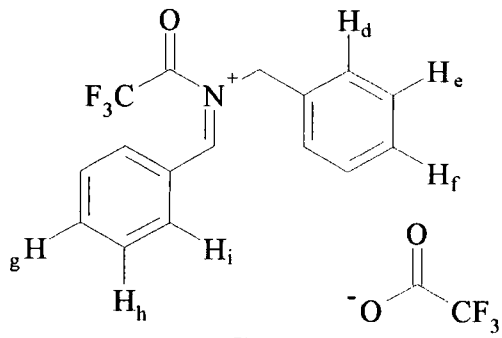

[G]

It is worth noting that although the above assignments account for the presence of a mixture of the two species the signals accounting for the CH_2 moiety in N-(α-trifluoroacetoxybenzyl) trifluoroacetobenzylamide are significantly distinct. One is a well-defined doublet whereas the other one appears as a broad singlet. Only the relative intensities enable the assignment. The behaviour seems to indicate an exchange phenomenon affecting one hydrogen more than the other.

It is difficult to account for the difference in behaviour of the adduct of the allyl and benzyl imines in the presence of TFAA. The allyl imine gives a single species whose spectra accord with the ionic structure **[H]**, while the benzyl imine gives a mixture. The minor component has a spectrum comparable with that of **[H]** and can be attributed to the corresponding ionic form **[G]**. The major component may represent the covalently bound adduct **[F]**.

It is possible that the energy separation of the ionic and covalent forms is very small so that changing from the allyl to the benzyl group is sufficient to affect the identity of the thermodynamically favoured form. A further difference is the partial decomposition with time of the allyl product **[H]**, but the stability of the benzyl products **[G]** and **[F]**. Since water is required for the decomposition process this may simply reflect the presence or absence of some adventitious water in the NMR samples measured.

It is notable that sharp bands are observed from the signals attributed to the ionic forms **[H]** and **[G]** while broadened bands are observed due to the covalent form **[F]**. The broadness of the bands may reflect different chemical environments for hydrogen resulting from restricted bond rotations. It is known that the C-N bond in amides has partial double bond character, so that it is possible that **[F]** may exist as a mixture of two rotational isomers, **[F']** and **[F'']**.

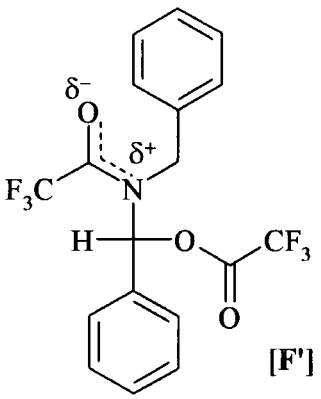

[F']

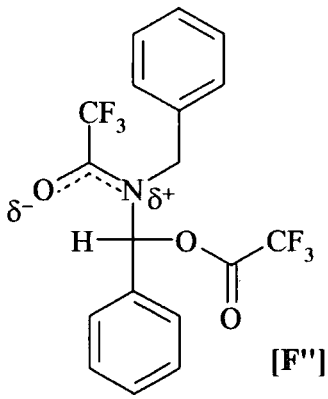

[F'']

Since the ionic form **[G]** already carries positive charge, rotation about the C-N bond should be relatively unrestricted leading to sharp signals.

5.2.2.2.2 Reaction in C_6D_6

TFAA was used in the catalysed asymmetric addition of TMSCN to imines to quench the reaction. Then the solvent used was toluene. Since deuterated toluene is not readily available C_6D_6 benzene was used here as a substitute; the solvating and polar properties of benzene being close to those of toluene.

A spectrum of N-benzylidene benzylamine in C_6D_6 is shown on Figure 5.6.

The signals and their chemical shifts are assigned in Table 5.8.

Figure 5.6 ^{1}H NMR spectrum in C_6D_6 of benzylidene benzylamine

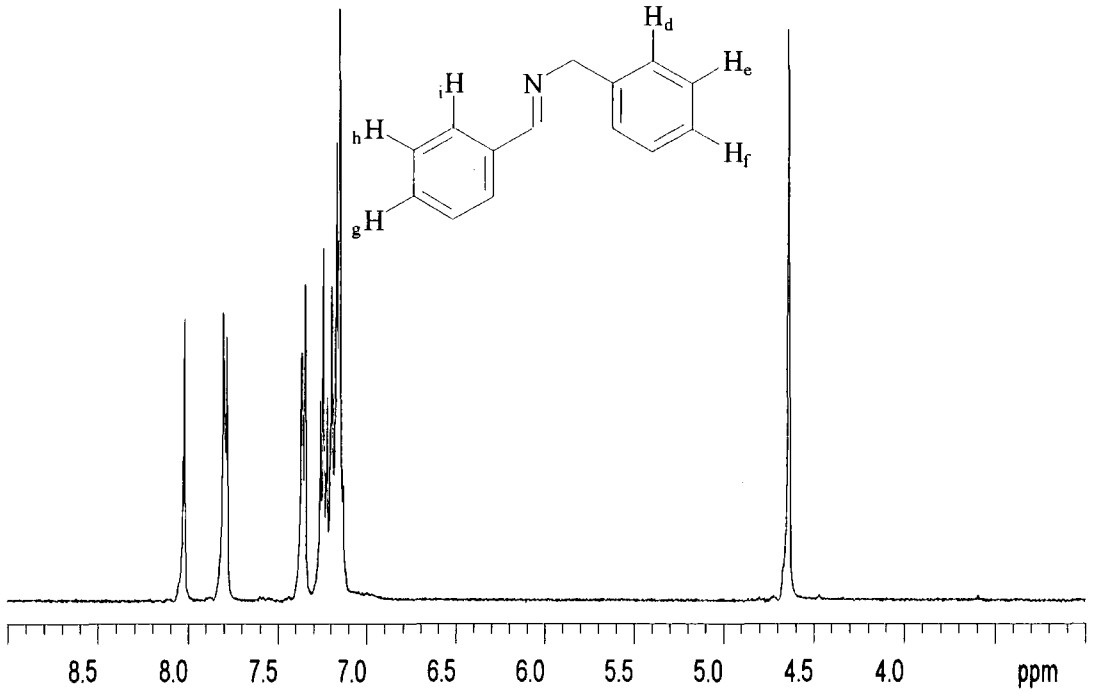

Table 5.8 ^{1}H NMR chemical shifts of benzylamine in C_6D_6

Protons	Chemical shift (ppm)	Multiplicity
CH_2	4.64	s
H_d, $H_{d'}$, H_e, $H_{e'}$, H_f & H_g	7.18-7.26	m
H_h & $H_{h'}$	7.36	d
H_i & $H_{i'}$	7.79	d
CHN	8.04	s

On addition of TFAA a spectrum was recorded. Further scans were recorded at regular time intervals (every 3 minutes between the first 6 records and 30 minutes between the sixth and the last one).

The specimen spectrum displayed in Figure 5.7 is that of the first recording. However, similarly to the experiment carried out in CD_3CN no evolution with time was noted. Again benzaldehyde (δ = 9.46 ppm for CHO) is formed at very low level.

Two pairs of broad signals are observable. Firstly in the upfield region (where signals for CH_2 moieties are expected to be seen) two resonance signals are noted at δ = 3.90 and δ = 4.38 ppm. Secondly in the downfield region of the spectrum (where signals for the methine protons are expected to be seen) two resonance signals are observed at δ = 7.66 and δ = 8.06 ppm. The sum of the intensities of the later peaks represents a single hydrogen. The broadness of the signals indicates a slow exchange process.

Figure 5.7 ^{1}H NMR spectrum in C_6D_6 for the observed reaction of benzylidene benzylamine with TFAA (1 eq.) after 3 minutes

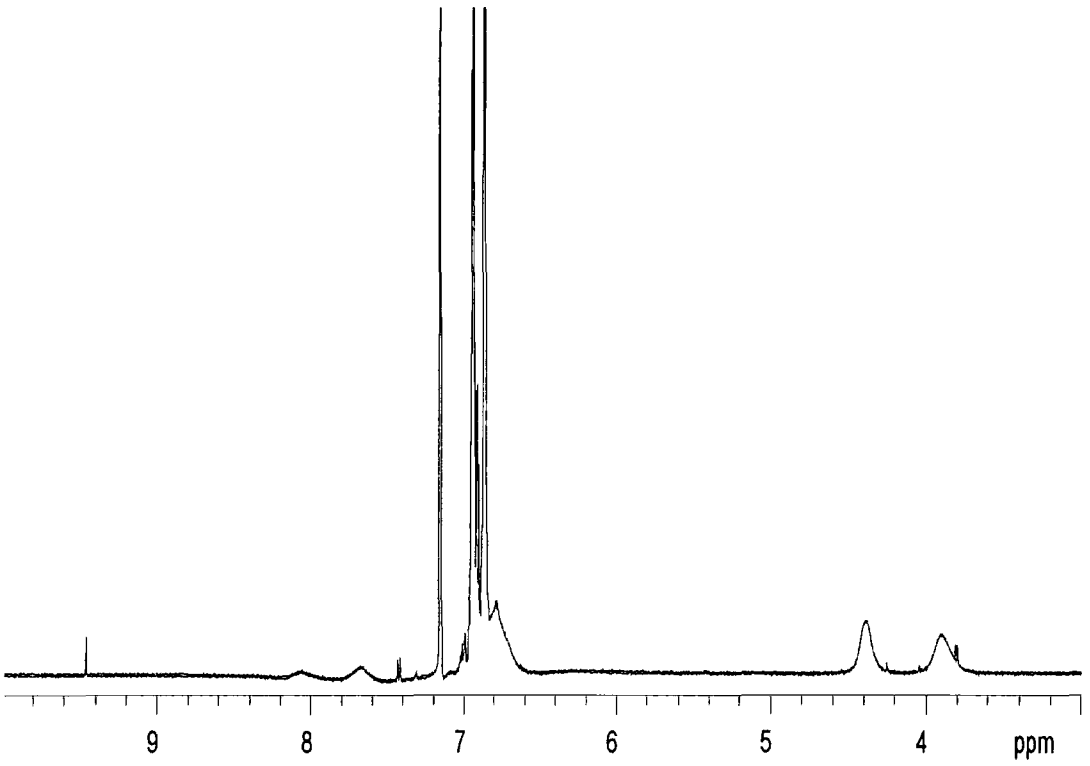

In order to investigate the exchange process the temperature variation of the spectrum was examined. Increasing the temperature accelerate the process and therefore sharpened the signals. An experiment was carried out where the temperature was increased gradually from room temperature to 50°C. A spectrum was recorded every 5°C.

Upon heating the two signals in the upfield region sharpened to yield two doublets. In the downfield region however the two broad peaks merged into one similarly broad signal.

It is also worth noting the shifting of some signals with temperature. This a known phenomenon and methanol is often used in NMR spectroscopy to calibrate temperature probes since the variation in frequency between the fixed signal for the methyl group and the hydroxyl moiety is a function of temperature. In this case the aldehydic proton of benzaldehyde is shifted from δ = 9.46 ppm at room temperature to 9.58 ppm at 50°C. More significantly, a resonance peak, originally present in the broad multiplet of the aromatic region

is significantly shifted form 6.79 ppm at room temperature to 6.39 ppm at 50°C. The spectrum of the reaction mixture at 50°C is displayed on Figure 5.8.

Figure 5.8 ^{1}H NMR spectrum in C_6D_6 for the observed reaction of benzylidene benzylamine with TFAA (1 eq.), T = 50°C

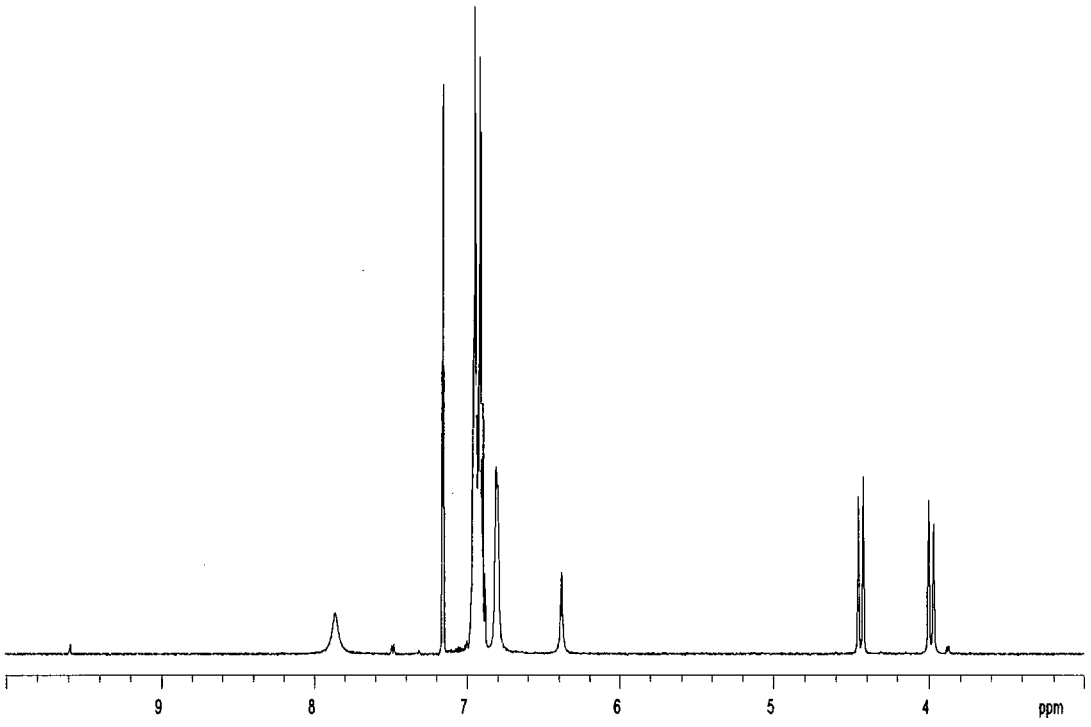

Although some features remain unexplained, some speculations may be made. First, the spectrum is more compatible with the covalently bound species [F] than the ionic one [G]. Thus the shift of the methine hydrogen is at ca $\delta = 7.8$ ppm, and the broad signals represent the presence of an exchange process. It is to be expected that a covalently bound form will be favoured over the ionic form in a non-polar solvent such as benzene. As the temperature is raised and rotation about the C-N bond of the trifluoroacetamide group increases the non equivalence of the methine hydrogens in structures [F'] and [F''] is removed. Similarly the normal AB coupling pattern of the two non-equivalent methylene hydrogens is observable.

The identity of the band representing ca 0.5 H, which shifts from $\delta = 6.79$ ppm to 6.39 ppm is unknown. It may represent water (or partially protonated water).

5.3 Conclusions

The reactions of two imines, N-benzylidene benzylamine and N-benzylidene allylamine, with trifluoroacetic anhydride have been reported.

The UV/Vis data suggest a rapid conversion to an ionic trifluoroacetamide which decomposes with time to give benzaldehyde and the parent amine as shown in Scheme 5.14.

Scheme 5.14

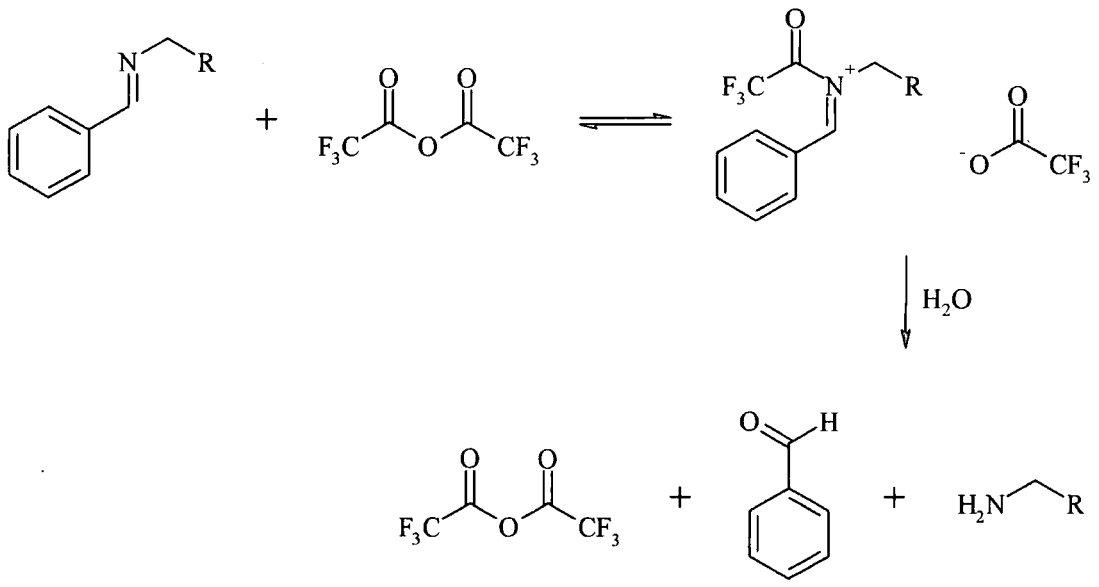

It is worth noting that when using acetic anhydride no reaction was observed. Previous work on the reaction of N-benzylidene aniline with acetic anhydride report the formation of the ionic acetamide[3] and N-(α-acetoxybenzyl) acetoanilide[4,5,7] upon heating. Later Sekiya and Morimoto[8] reported the reaction at room temperature of trichloroacetic anhydride with N-benzylidene aniline to form the corresponding N-(α-trichloroacetoxybenzyl) trichloroacetanilide. As expected at room temperature the reaction of acid anhydrides with imines is promoted by the presence of electron withdrawing groups, such as fluorine or chlorine atoms, in the α position.

The NMR data for the reaction of TFAA with N-benzylidene allylamine in CD_3CN confirmed the above result but indicated that the amine is actually in the protonated form as shown previously in Scheme 5.11.

The reaction of N-benzylidene benzylamine in CD_3CN on the other hand suggested the presence of two structures, the ionic species and N-(α-trifluoroacetoxybenzyl) trifluoroacetobenzylamide in a 1:5 ratio.

If the solvent is changed to C_6D_6 covalently bound adduct is favoured.

The addition of cyanide (TMSCN) to an equilibrated solution of imine and TFAA did not yield the trifluoroaminonitrile. This is compatible with the presence of the covalently bound N-(α-trifluoroacetoxybenzyl)trifluoroacetamide which will not be expected to react with cyanide.

Clearly some anomalies remain in the interpretation of the results reported in this section. More work could be done to clarify the nature of the initial interactions and the effects of added water could be investigated. Conductivity measurements of the solutions, particularly in acetonitrile, could be used to confirm the presence of ionic species.

The results indicate that while in aromatic solvents, benzene and toluene, the addition of TFAA will trifluoroacetylate the formed aminonitrile, it will not facilitate aminonitrile formation. Thus reaction of the imines with TFAA will render them unreactive.

5.4 References

1. M. S. Sigman and E. N. Jacobsen, *J. Am. Chem. Soc.*, 1998, **120**, 5315

2. P. Kalkin, Helv. Chim. Acta, 1928, **11**, 977

3. M. Passerini and M. Pia. Macentelli, *Gazz. Chim. Ital.*, 1928, **58**, 64

4. J. B. Ekeley, M. C. Swisher and C. C. Johnson, *Gazz. Chim. Ital.*, 1932, **62**, 81

5. H. R. Snyder, R. H. Levin and P. F. Wiley, *J. Am. Chem. Soc.*, 1938, **60**, 2025

6. H. S. Angel and A. R. Day, *J. Am. Chem. Soc.*, 1950, **72**, 3874

7. A. W. Burgstahler, *J. Am. Chem. Soc.*, 1951, **73**, 3021

8. M. Sekiya and T. Morimoto, *Chemical and Pharmaceutical Bulletin*, 1975, **23**, 2353

9. L Eberson, *The Chemistry of carboxylic acids and esters*, Ed. S. Patai, Wiley-Interscience, 1969, 211

Chapter Six: Experimental

Chapter six: Experimental

6.1 Materials

All materials used to prepare the buffer solutions were purchased commercially. Subsequent dilutions were made in highly purified water. Full dissolution of the solid compounds was achieved using a Sonomathic ultrasonic bath.

Chemicals used for the synthesis of imines, aminonitriles and catalysts were purchased commercially with the exception of the salen ligands, (S,S)-(-)-N,N'-bis(3,5-di-*tert*-butylsalicylidene)-1,2-diaminocyclohexane and (R,R)-(-)-N,N'-bis(3,5-di-*tert*-butylsalicylidene)-1,2-diaminocyclohexane, as well as the vanadium (IV) and the two titanium catalysts which were provided by Avecia (industrial sponsors).

Cited reaction temperatures refer to the external bath temperatures.

All reactions involving cyanide use were performed in a fume cupboard where all the necessary safety procedures were taken.

General purpose methanol was used for washing all apparatus. The cyanide contaminated equipment was quenched with commercially purchased 30% bleach solutions containing sodium hypochlorite. Thorough washing with more bleach was then performed followed by methanol.

6.2 Experimental measurements

For volumes smaller than 5 cm^3 Gilson Pipettman dispensing pipettes were used. The pipettes were calibrated prior to each measurement by weighing the volume of water dispensed at a particular setting, assuming a density for water of 1 g cm^{-3}, and adjusting the volume setting accordingly. All other volumes were measured using glass pipettes.

6.3 UV/Vis Spectrophotometry

6.3.1 'Conventional' UV/Vis spectrophotometry

UV/Vis spectral measurements were carried out on a Shimadzu UV-2101PC spectrophotometer. Time course runs were performed on Perkin Elmer λ12 or λ2 instruments.

All measurements were carried out at 25°C in stoppered, quartz cuvettes with a 1 cm path length. A reference cell containing the appropriate solvent/buffer was used to zero the instrument prior to each experiment. In the case of spectral scans the reference cell was used to perform a baseline correction.

6.3.2 Stopped–flow spectrophotometry

Fast reactions were followed using an Applied Photophysics Biosequential DX-17MV stopped flow spectrophotometer as represented diagrammatically in Figure 6.1[1].

Figure 6.1 Stopped-flow spectrophotometer

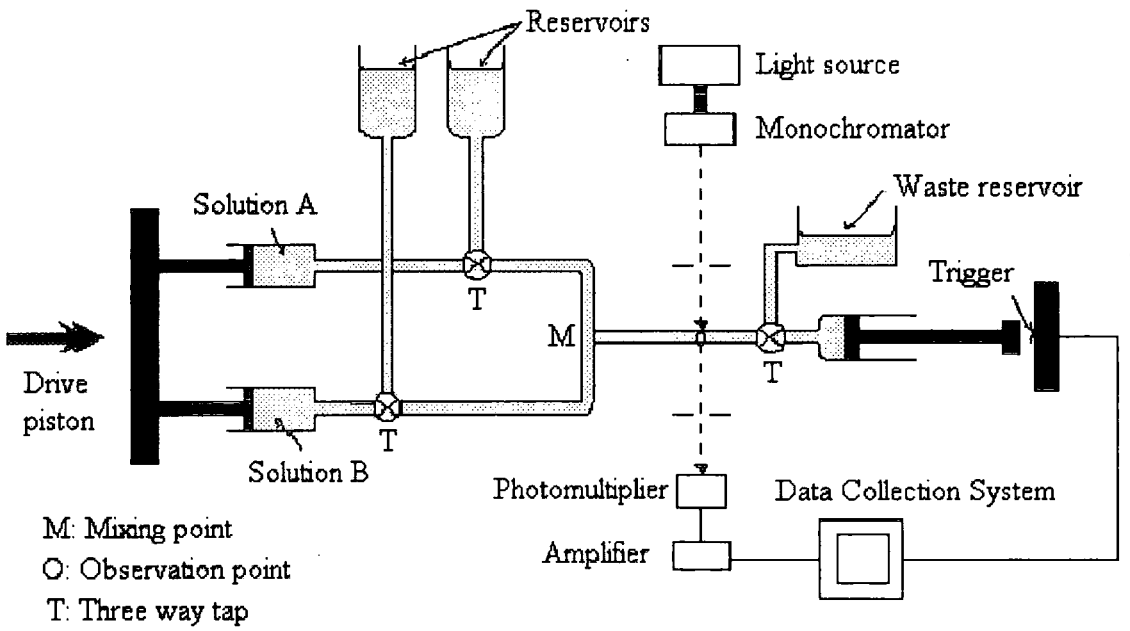

The reaction solutions were placed in two identical syringes ensuring equal volume delivery. The reaction was initiated using the computer controlled automated drive which ensured simultaneous delivery of the reagents through the automated mixing chamber into the observation cell (1 cm path length) within 5 ms. On entry to the observation cell the solution causes a third syringe to load and trigger the acquisition of the absorbance time data.

The syringes, delivery tubes and the observation cell were thermostated (24.8 – 25.2 °C) using a circulating water bath.

UV/Vis measurements are made by the means of a fibre optic cable that directs a beam of monochromatic light, of the set wavelength, into the observation cell. After the light passes through the reaction solution it reaches a photolmultiplier. The recorded change in voltage with time is then converted to absorbance change with time by the computer software. The software also provides for data fitting options allowing calculation of the rate constants.

Prior to each experiment the apparatus was washed thoroughly with highly purified water as well as with the two solutions to be mixed. Several runs on a short time-base were carried out prior to the actual recorded experiments to ensure that previous solutions had been expelled.

6.3.3 Data fitting and errors in measurements

All UV/Vis and stopped flow experiments were carried out under pseudo first order conditions. The rate constants were obtained by fitting the data to a single exponential model using the Scientist® computer package[2] in the case of conventional UV/Vis measurements or by using the stopped flow software for the measurements taken on the apparatus. Data collected from conventional spectrophotometers were converted to an ASCII format and processed using Microsoft Excel® prior to rate constant determination.

For reactions at equilibria, such as that represented in Scheme 6.1, when one reactant, B, is in excess to the other, A, the reaction becomes pseudo first order and the rate is defined by equation 6.1.

Scheme 6.1

$$A + B \underset{k_b}{\overset{k_f}{\rightleftharpoons}} C$$

$$-\frac{d[A]}{dt} = k'_f[A] - k_b[C] \quad \textbf{(6.1)}$$

where:

$$k'_f = k_f[B] \quad \textbf{(6.2)}$$

Considering $[A]_e$ and $[C]_e$, the concentrations of A and C at equilibrium respectively, and x, the distance of these concentrations from equilibrium:

$$[A] = [A]_e + x \quad \textbf{(6.3)}$$

$$[C] = [C]_e - x \quad \textbf{(6.4)}$$

where:

$$x = [A] - [A]_e = [C]_e - [C] \quad \textbf{(6.5)}$$

Hence substitution in equation (6.1) gives:

$$-\frac{d[A]}{dt} = (k'_f + k_b)x + (k'_f[A]_e - k_b[C]_e) \quad \textbf{(6.6)}$$

At equilibrium the rates of the forward, $k'_f[A]_e$, and reverse reactions, $k_b[C]_e$, are equal thus equation (6.6) can be expressed as:

$$-\frac{d[A]}{dt} = (k'_f + k_b)x \quad \textbf{(6.7)}$$

Hence the pseudo first order rate constant, k_{obs}, can be expressed as equation (6.8).

$$k_{obs} = k'_f + k_b \quad \textbf{(6.8)}$$

Thus the relation between [B] and k_{obs} is:

$$k_{obs} = k_f[B] + k_b \quad (6.9)$$

Hence plots of k_{obs} versus [B] are linear with k_f corresponding to the slope and k_b to the intercept.

Such plots were fitted using the linear regression tool of the data analysis function built into Microsoft Excel®. The software allowed calculation for both the gradient and the intercept as well as errors.

6.4 NMR spectroscopy

^{1}H, ^{13}C and ^{19}F spectra were recorded using Varian spectrometers (200, 400 or 500 MHz). The peaks accounting for the appropriate solvents were taken as references. Indeed trimethylsilyl cyanide has been used as a reagent and addition of tetramethylsilane (TMS) would have resulted in an unnecessary complication of the spectrum in the upfield region.

Repeat scans and variable temperature measurements were taken immediately after mixing of the reagents so that the first spectra would account for a reaction time of ca 2-3 minutes.

6.5 Mass spectrometry

Mass spectrometry was used coupled to gas chromatography (GC/MS) using electron ionisation (EI) or chemical ionisation (CI) with in the latter case methane being used as the ion source.

6.6 Chiral chromatography

Chromatograms were obtained using a CP-Chirasil-Dex-CB column. The temperature was held constant at 120°C for 30 minutes. This was followed by a 10 minutes regular increase in temperature up to 200°C.

The samples were automatically injected by the instrument with injection volume being 2 μL.

6.7 Buffers solutions and pH measurements

The buffer solutions used throughout have been prepared with reference to the CRC Handbook[3]. The different buffer systems used were: potassium dihydrogen phosphate/sodium hydroxide, borax/sodium hydroxide or hydrochloric acid, sodium bicarbonate/sodium hydroxide, and tris(hydroxymethyl)aminomethane/hydrochloric acid.

The pH values of the solutions was measured using a Jenway 3020 pH meter, calibrated using pH 7 and pH 10 buffers for alkaline solutions and pH 7 and pH 4 buffers for acidic solutions. All the solutions were thermostated at 25° C prior to measurement.

6.8 Synthetic procedures (with reference to Chapter 4)

(S,S)-N,N'-bis(3,5-di-*tert*-butylsalicylidene)-1,2-diaminocyclohexane-aluminium (III) chloride[4]

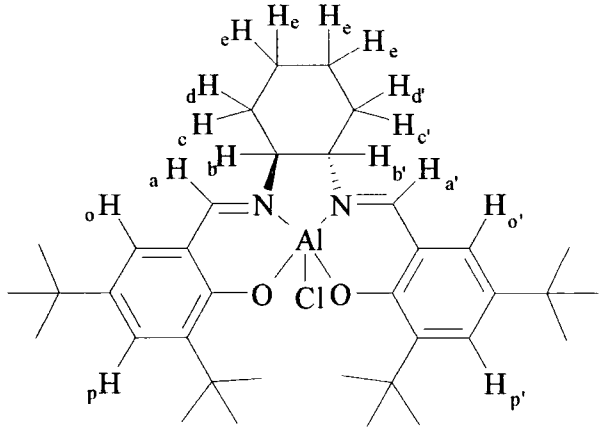

(1b)

In an oven dried 100 cm^3 round bottom flask equipped with a stir bar and under nitrogen (S,S)-(-)-N,N'-bis(3,5-di-*tert*-butylsalicylidene)-1,2-diaminocyclohexane (1.52g., 2.78 mmol) and 20 cm^3 of anhydrous dichloromethane were combined and stirred.

At ambient temperature diethylaluminium chloride (2.78 cm^3 (0.1 dm^3mol^{-1} solution in hexane), 2.78 mmol) was added slowly to the stirring solution.

After stirring for 2 hours the solvents were removed in vacuo and the resulting yellow solid was rinsed with 50 cm^3 of hexanes. The solid was dried in vacuo to yield **1b** (1.52g., 90% yield). δ_H (400 MHz, $CDCl_3$): 1.26 - 1.60 (40H, *m*, ^tBu and H_e), 2.09 (2H, *m*, H_c and $H_{c'}$), 2.54 (2H, *m*, H_d and $H_{d'}$), 3.18 and 3.92 (2H, 2x *broad s*, H_b and $H_{b'}$), 7.08 (2H, *s*, H_o and $H_{o'}$), 7.56 (2H, *s*, H_p and $H_{p'}$), 8.18 and 8.38 (2H, *2x broad s*, H_a and $H_{a'}$)

N-Benzylidene allylamine, $5x10^{-2}$ mol dm^{-3} in toluene

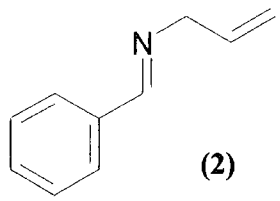

(2)

To a solution of benzaldehyde (0.51 cm^3, 5.00 mmol) in toluene (100 cm^3) was added allylamine (0.37 cm^3, 5.00 mmol) at room temperature. The solution was left to react for 3 hours. (2) was identified as a 100% conversion product in solution by mass spectrometry. m/z (EI): 145 (M^+, 30%), 144 (M^+ - H, 100%), 117 (M^+ - CH_2=CH_2, 30%), 104 (M^+ - CH_2-CH=CH_2, 24%), 91 (M^+ - N= ; m/z (CI): 146 (MH^+)

2-Allyltrifluoroacetamido-2-phenylacetonitrile

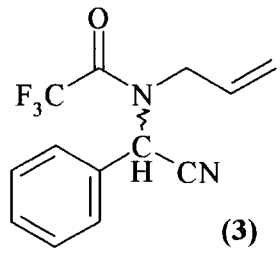

(3)

In an oven dried 100 cm^3 round bottom flask **(1b)** (30 mg, 0.05 mmol, 5 mol%) and **(2)** (20 cm^3, 1 mmol) were stirred until **(1b)** dissolved. 1.2 equivalent of TMSCN was then added (0.16 cm^3, 1.20 mmol). After 16.5 hours the reaction was quenched using 1.5 equivalents of trifluoroacetic anhydride (0.212 cm^3, 1.5 mmol) to yield **(3)** as a 91% conversion product in

solution. m/z (EI): 268 (M^+; 11%), 227 (M^+ - CH_2-CH=CH_2, 98%), 200 (M^+ - CH_2-CH=CH_2 – HCN, 100%)

(ℝ,ℝ)-ℕ,ℕ'-bis(3,5-di-*tert*-butylsalicylidene)-1,2-diaminocyclohexane-vanadium (𝕍) oxide

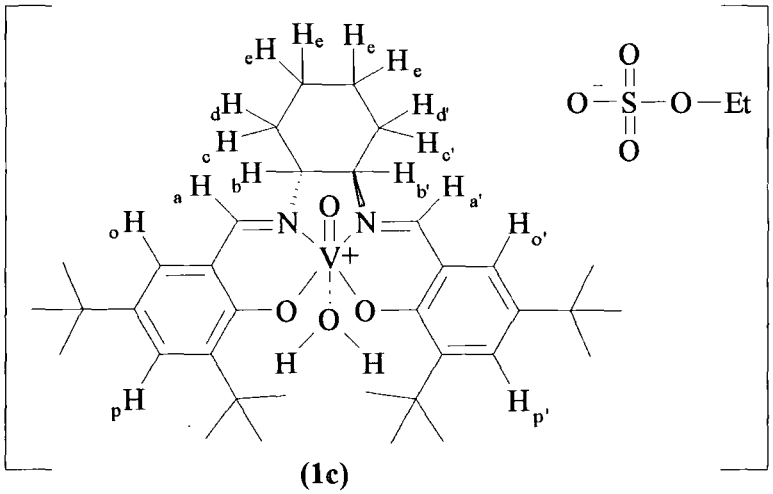

(1c)

In an oven dried 100 cm^3 round bottom flask equipped with a stir bar and placed under nitrogen (R,R)-(-)-N,N'-bis(3,5-di-*tert*-butylsalicylidene)-1,2-diaminocyclohexane (1.0g., 1.8 mmol) in THF (20 cm^3)and vanadyl sulfate hydrate (0.55g, 2.0 mmol) in hot ethanol (32 cm^3) were mixed and stirred under reflux for 2 hours.

The solvents were removed under vacuo. The residue was dissolved in dichloromethane (DCM) and absorbed onto a plug of silica. Two successive elutions, first with DCM, to elute the excess ligand and then with ethylacetate:methanol (2:1), to elute the complex, were performed.

The solvent was removed by evaporation under vacuo to give a dark green crystalline solid **1c** (0.79g, 58% yield). δ_H (400 MHz, $CDCl_3$): 0.87 (3H, *t*, J = 7.2 Hz, $C\underline{H}_3CH_2OSO_3^-$), 1.36 (9H, *s*, ^{t}Bu), 1.38 (9H, *s*, ^{t}Bu), 1.53 (18H, *s*, ^{t}Bu), 1.7 - 2.2 (6H, *m*, H_c, $H_{c'}$ and 4x H_e), 2.52 and 2.80 (2H, 2x *d*, J = 11.8 Hz, H_d and $H_{d'}$), 3.47 (2H, *q*, J = 7.2 Hz, $CH_3C\underline{H}_2OSO_3^-$), 3.80 and 4.26 (2H, *2x t*, J = 11 Hz, H_b and $H_{b'}$), 7.51 and 7.56 (2H, *2x d*, J = 2.4 Hz, H_o and $H_{o'}$), 7.71 and 7.76 (2H, *2x d*, J = 2.4 Hz, H_p and $H_{p'}$), 8.55 and 8.76 (2H, *2x s*, H_a and $H_{a'}$)

2-Benzylamonium-2-phenylacetonitrile chloride[5]

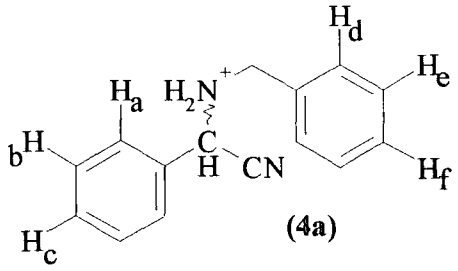

; Cl^-

(4a)

A neat mixture of benzaldehyde (2.04 cm^3, 20 mmol) and benzylamine (1.09 cm^3, 10 mmol) was heated at 100°C for 1 minute and cooled to room temperature. TMSCN (2.67 cm^3, 20 mmol) was added. The mixture was then heated at 100°C for 30 seconds and cooled to room temperature. Ether was added and the reacting medium acidified with hydrogen chloride. The solution was then filtered and the product, **4a**, isolated as a white solid (1.03g, 38% yield). δ_H (400 MHz, $CDCl_3$): 1.50 (2H, *broad s*, NH_2^+), 3.90 + 4.07 (2H, *2x d*, J = 13.2 Hz, CH_2), 4.83 (1H, *s*, CHCN), 7.40 (3H, *broad m*, H_e, $H_{e'}$ and H_f), 7.48 (3H, *broad m*, H_b, $H_{b'}$ and H_c), 7.55 (2H, *broad m*, H_d and $H_{d'}$), 7.72 (2H, *broad m*, H_a and $H_{a'}$); Anal. calculated for $C_{15}H_{15}N_2Cl$: C, 69.63; H, 5.80; N, 10.83; Cl, 13.73. Found: C, 67.65; H, 5.79; N, 10.48; Cl, 13.68.

Note: It is worth noting that Mai and Patil recommend that after addition of TMSCN the reaction vial is tightly capped in order to minimise the lost of HCN. This was not followed. However after 30 seconds at 100°C the pressure created inside the flask by the formation of HCN expelled the stopper violently and it was not possible to complete the 1 minute heating period.

Still it was decided to isolate the product according to the method.

2-Benzylamonium-2-phenylacetonitrile chloride: experiment 4b

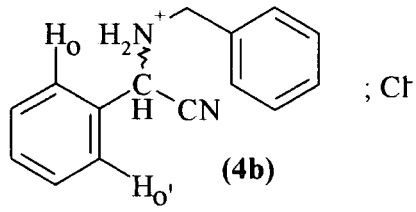

(4b)

In an oven dried 50 cm^3 round bottom flask **(1c)** (31.25 mg, 0.0414 mmol, 4.14 mol%) and N-benzylidene benzylamine (0.19 cm^3, 1 mmol) were mixed in toluene (20 cm^3) with 10 μL water and stirred until dissolution of **(1c)**. 1.2 equivalent of TMSCN were then added (0.16 cm^3, 1.20 mmol). After 16 hours the reaction medium was acidified using hydrogen chloride in ether (1 cm^3, 1.0 mol dm^{-3} solution, 1 mmol). The solution was filtered under reduced pressure to yield **(4b)** as a white solid (0.19g, 74% yield). δ_H (200 MHz, $CDCl_3$): 2.33 (2H, *broad s*, NH_2^+), 4.15 (2H, *s*, CH_2), 5.37 (1H, *s*, CH), 7.40-7.51 (8H, *m*, aromatic Hs – (H_o and $H_{o'}$)), 7.71 (2H, *broad m*, H_o and $H_{o'}$)

Experiment 4b was repeated using different amounts of added water. The results are given in Table 6.1.

Table 6.1 Recorded yields for the synthesis of benzylamonium-2-phenylacetonitrile chloride (TMSCN (1.2 eq.), 4.14 mol% catalyst, toluene, 16 h, R.T.) with varying amount of water

Experiment	Volume of water in 20 cm^3 toluene (μL)	Yield
4b	10	74%
4c	20	93%
4d	30	100%
4e	40	100%

2-Benzylamonium-2-phenylacetonitrile chloride: experiment 4f

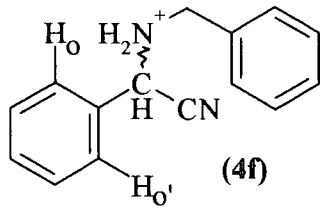

; Cl⁻

(4f)

In an oven dried 50 cm^3 round bottom flask (**1c**) (21.75 mg, 0.0288 mmol, 2.88 mol%) and N-benzylidene benzylamine (0.19 cm^3, 1 mmol) were mixed in toluene (20 cm^3) with 20 µL water and stirred until dissolution of (**1c**). 1.2 equivalent of TMSCN were then added (0.16 cm^3, 1.20 mmol). After 16 hours the reaction medium was acidified using hydrogen chloride in ether (1 cm^3, 1.0 mol dm^{-3} solution, 1 mmol). The solution was filtered under reduced pressure to yield (**4f**) as a white solid (0.27g, 104% yield). δ_H (200 MHz, $CDCl_3$): 2.33 (2H, *broad s*, NH_2^+), 4.12 (2H, *s*, CH_2), 5.22 (1H, *s*, CH), 7.37-7.49 (8H, *m*, aromatic Hs – (H_o and $H_{o'}$)), 7.65 (2H, *broad m*, H_o and $H_{o'}$)

Experiment 4f was repeated using different amounts of vanadium catalyst. The results are given in Table 6.2.

Table 6.2 Recorded yields for the synthesis of benzylamonium-2-phenylacetonitrile chloride (TMSCN (1.2 eq.), 20 µL, catalyst, toluene, 16 h, R.T.) with varying amount of catalyst

Experiment	Amount of catalyst	Yield
4f	4.81 mol%	104%
4g	5.74 mol%	89%
4h	6.73 mol%	100%

2-Benzylamonium-2-phenylacetonitrile chloride: experiment 4i

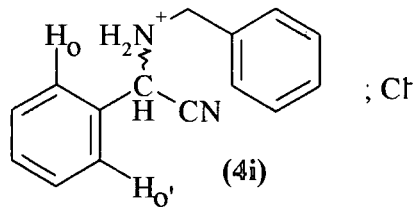

(4i)

In an oven dried 50 cm^3 round bottom flask (**1c**) (43.25 mg, 0.0574 mmol, 5.74 mol%) and N-benzylidene benzylamine (0.19 cm^3, 1 mmol) were mixed in toluene (20 cm^3) with 20 μL water and stirred until dissolution of (**1c**). 1.2 equivalent of TMSCN were then added (0.16 cm^3, 1.20 mmol). After 2 hours the reaction medium was acidified using hydrogen chloride in ether (1 cm^3, 1.0 mol dm^{-3} solution, 1 mmol). The solution was filtered under reduced pressure to yield (**4i**) as a white solid (0.22g, 85% yield). δ_H (200 MHz, $CDCl_3$): 2.32 (2H, *broad s*, NH_2^+), 4.15 (2H, *s*, CH_2), 5.40 (1H, *broad s*, CH), 7.41-7.50 (8H, *m*, aromatic Hs – (H_o and $H_{o'}$)), 7.70 (2H, *broad m*, H_o and $H_{o'}$)

Experiment 4i was repeated allowing different reaction time before acidification. The results are given in Table 6.3.

Table 6.3 Recorded yields for the synthesis of benzylamonium-2-phenylacetonitrile chloride (TMSCN (1.2 eq.), 20μL water, 5.74 mol% catalyst, toluene, R.T.) with varying time

Experiment	Reaction time (hours)	Yield
4i	2	85%
4j	3	77%
4k	4	89%
4l	6	77%

2-Benzylamonium-2-phenylacetonitrile chloride: experiment 4m

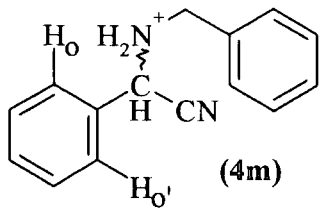

; Cl⁻

(4m)

In an oven dried 50 cm^3 round bottom flask **(1c)** (43.25 mg, 0.0574 mmol, 5.74 mol%) and N-benzylidene benzylamine (0.19 cm^3, 1 mmol) were mixed in toluene (20 cm^3) with 20 μL water at 0°C and stirred until dissolution of **(1c)**. 1.2 equivalent of TMSCN were then added (0.16 cm^3, 1.20 mmol). The reaction was kept at 0°C using an ice bath. After 10 hours the reaction medium was acidified using hydrogen chloride in ether (1 cm^3, 1.0 mol dm^{-3} solution, 1 mmol). The solution was filtered under reduced pressure to yield **(4m)** as a white solid (0.23g, 89% yield). δ_H (200 MHz, $CDCl_3$): 2.27 (2H, *broad s*, NH_2^+), 4.15 (2H, *s*, CH_2), 5.38 (1H, *s*, CH), 7.40-7.50 (8H, *m*, aromatic Hs – (H_o and $H_{o'}$)), 7.70 (2H, *broad m*, H_o and $H_{o'}$)

Experiment 4m was repeated at different reaction temperature before acidification. The results are given in Table 6.4.

Table 6.4 Recorded yields for the synthesis of benzylamonium-2-phenylacetonitrile chloride (TMSCN (1.2 eq.), 20 μL, 5.74 mol% catalyst, toluene, 16 h) with varying temperature

Experiment	Temperature (°C)	Yield
4m	0	89%
4n	-10	74%
4o	-20	77%
4p	-30	85%

2-Benzylamonium-2-phenylacetonitrile chloride

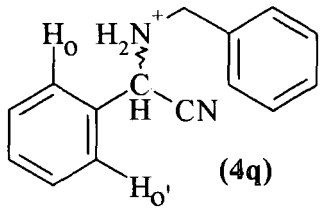

(4q)

In an oven dried 50 cm^3 round bottom flask **(1b)** (30.33 mg, 0.05 mmol, 5 mol%) and N-benzylidene benzylamine (0.19 cm^3, 1 mmol) were mixed in toluene (20 cm^3) with 20 μL water and stirred until dissolution of **(1b)**. 1.2 equivalent of TMSCN were then added (0.16 cm^3, 1.20 mmol). After 4 hours the reaction medium was acidified using hydrogen chloride in ether (1 cm^3, 1.0 mol dm^{-3} solution, 1 mmol). The solution was filtered under reduced pressure to yield **(4q)** as a white solid (0.07g, 27% yield). δ_H (200 MHz, $CDCl_3$): 1.67 (2H, *broad s*, NH_2^+), 4.09 (2H, *s*, CH_2), 5.11 (1H, *s*, CH), 7.39-7.49 (8H, *m*, aromatic Hs – (H_o and $H_{o'}$)), 7.68 (2H, *broad m*, H_o and $H_{o'}$)

2-Benzylamonium-2-phenylacetonitrile chloride

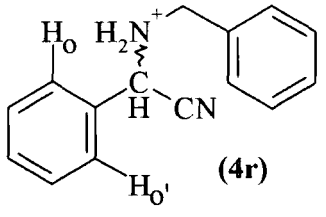

(4r)

In an oven dried 50 cm^3 round bottom flask (S,S)-N,N'-bis(3,5-di-*tert*-butylsalicylidene)-1,2-diaminocyclohexane-titanium (IV) dichloride (33.15 mg, 0.05 mmol, 5 mol%) and N-benzylidene benzylamine (0.19 cm^3, 1 mmol) were mixed in toluene (20 cm^3) with 20 μL water and stirred until dissolution of (S,S)-N,N'-bis(3,5-di-*tert*-butylsalicylidene)-1,2-diaminocyclohexane-titanium (IV) dichloride. 1.2 equivalent of TMSCN were then added (0.16 cm^3, 1.20 mmol). After 4 hours the reaction medium was acidified using hydrogen chloride in ether (1 cm^3, 1.0 mol dm^{-3} solution, 1 mmol). The solution was filtered under reduced pressure to yield **(4r)** as a white solid (0.24g, 93% yield). δ_H (200 MHz, $CDCl_3$): 1.67 (2H, *broad s*, NH_2^+), 4.07 (2H, *s*, CH_2), 5.06 (1H, *s*, CH), 7.38-7.48 (8H, *m*, aromatic Hs – (H_o and $H_{o'}$)), 7.66 (2H, *broad m*, H_o and $H_{o'}$)

2-Benzylamonium-2-phenylacetonitrile chloride

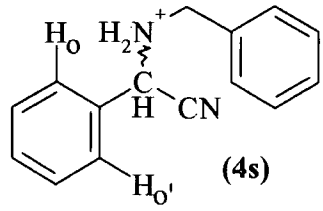

; Cl⁻

(4s)

In an oven dried 50 cm^3 round bottom flask (S,S)-N,N'-bis(3,5-di-*tert*-butylsalicylidene)-1,2-diaminocyclohexane-vanadium (IV) oxide (30.55 mg, 0.05 mmol, 5 mol%) and N-benzylidene benzylamine (0.19 cm^3, 1 mmol) were mixed in toluene (20 cm^3) with 20 μL water and stirred until dissolution of (S,S)-N,N'-bis(3,5-di-*tert*-butylsalicylidene)-1,2-diaminocyclohexane-vanadium (IV) oxide. 1.2 equivalent of TMSCN were then added (0.16 cm^3, 1.20 mmol). After 4 hours the reaction medium was acidified using hydrogen chloride in ether (1 cm^3, 1.0 mol dm^{-3} solution, 1 mmol). The solution was filtered under reduced pressure to yield **(4s)** as a white solid (0.21g, 81% yield). δ_H (200 MHz, $CDCl_3$): 1.68 (2H, *broad s*, NH_2^+), 4.11 (2H, *s*, CH_2), 5.21 (1H, *s*, CH), 7.33-7.47 (8H, *m*, aromatic Hs – (H_o and $H_{o'}$)), 7.75 (2H, *broad m*, H_o and $H_{o'}$)

2-Benzylamonium-2-phenylacetonitrile chloride

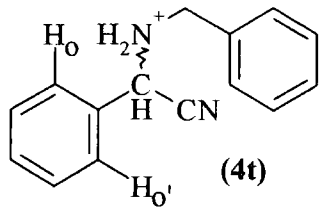

; Cl⁻

(4t)

In an oven dried 50 cm^3 round bottom flask [(S,S)-N,N'-bis(3,5-di-*tert*-butylsalicylidene)-1,2-diaminocyclohexane-titanium (IV) dioxide]$_2$ (60.8 mg, 0.05 mmol, 5 mol%) and N-benzylidene benzylamine (0.19 cm^3, 1 mmol) were mixed in toluene (20 cm^3) with 20 μL water and stirred until dissolution of[(S,S)-N,N'-bis(3,5-di-*tert*-butylsalicylidene)-1,2-diaminocyclohexane-titanium (IV) dioxide]$_2$. 1.2 equivalent of TMSCN were then added (0.16 cm^3, 1.20 mmol). After 4 hours the reaction medium was acidified using hydrogen chloride in ether (1 cm^3, 1.0 mol dm^{-3} solution, 1 mmol). The solution was filtered under reduced pressure to yield **(4t)** as a white solid (0.23g, 89% yield). δ_H (200 MHz, $CDCl_3$): 1.69

(2H, *broad s*, NH_2^+), 4.09 (2H, *s*, CH_2), 5.08 (1H, *s*, CH), 7.38-7.49 (8H, *m*, aromatic Hs – (H_o and $H_{o'}$)), 7.67 (2H, *broad m*, H_o and $H_{o'}$)

6.9 References

1. B. G. Cox, *Modern Liquid Phase Kinetics*, Oxford Chemistry Primers, 1996

2. Micromath® Scientist® for Windows®, Version 2.02

3. *CRC Handbook of Chemistry and Physics*, R. C. Weat, CRC Press, Florida, 63rd Ed., 1982-1983

4. M. S. Sigman and E. N. Jacobsen, *J. Am. Chem. Soc.*, 1998, **120**, 5315

5. K. Mai and G. Patil, *Synthetic Comm.*, 1985, **15**, 157

Appendix

Appendix

Conferences attended during the course of the PhD:

PERKIN NORTH EAST DIVISION MEETING 8th April 2002

University of York

ORGANIC REACTIVITY 20th September 2002

Royal Society of Chemistry: Organic Reaction Mechanism Group

Astra Zeneca, Loughborough

Poster: "*Kinetic and Equilibrium Studies of the Strecker Reaction*"

POSTGRADUATE WINTER SCHOOL ON ORGANIC REACTIVITY – WISOR XII 6th-13th January 2003

Bressanone, ITALY

Poster: "*Kinetic and Equilibrium Studies of the Strecker Reaction*"

9th EUROPEAN SYMPOSIUM ON ORGANIC REACTIVITY – ESOR IX 12th-17th July 2003

Oslo, NORWAY

Poster: "*Kinetic and Equilibrium Studies of the Strecker Reaction*"

ORGANIC REACTIVITY 19th September 2003

Royal Society of Chemistry: Organic Reaction Mechanism Group

Avecia, Huddersfield

Oral presentation: "*Kinetic and Equilibrium Studies of the Strecker Reaction*"

REACTION MECHANISMS VII — 4th-8th July 2004

University College Dublin

Dublin, IRELAND

Poster: "*Kinetic and Equilibrium Studies of the Strecker Reaction*"

ORGANIC REACTIVITY — 20th September 2004

Royal Society of Chemistry: Organic Reaction Mechanism Group

Syngenta, Huddersfield

Poster: "*Kinetic and Equilibrium Studies of the Strecker Reaction*"

Publication:

The Strecker reaction: kinetic and equilibrium studies of cyanide addition to iminium ions

John H. Atherton, John Blacker, Michael R. Crampton and Christophe Grosjean, *Org. Biomol. Chem.*, 2004, 2, 2567